Coarsening and Osmotic Stabilisation of Emulsions and Foams

Anthony James Webster

Thesis submitted for the degree of Doctor of Philosophy

Department of Physics and Astronomy

University of Edinburgh

2000

Abstract

The coarsening of emulsions and foams due to a diffusive flux of dissolved disperse phase between droplets and bubbles is considered, and the effects of trapping an extra species within droplets/bubbles are studied. It is demonstrated that the extra species may provide an osmotic pressure to counteract the effects of surface tension and "osmotically stabilise" an emulsion/foam. For dilute emulsions a rigorous condition to prevent coarsening by a diffusive flux of disperse phase is derived, which remains valid with polydispersity in droplet size and number of trapped species. The coarsening of dilute, insufficiently stabilised emulsions was found to proceed as when no trapped species were present, but with a reduction in the volume fraction of the growing droplets due to the volume fraction now residing in stable, shrunken droplets. Foams are studied by considering the osmotic compression of previously dilute foam bubbles by an osmotic pressure Π. Careful arguments are given for the dependence of bubble pressure on Π, which are confirmed for a monodisperse 2D model. The arguments are believed to be valid for sufficiently dry and monodisperse foams, for which the stability requirement is shown to be of the same order of magnitude as for dilute foam bubbles, regardless of the magnitude of Π. In the absence of bubble rearrangements, the elastic energy from the necessary deformation of surrounding bubbles is also found to stabilise a foam. Sources of dissipation in coarsening nondilute foams are considered, and for given parameters enable prediction of the rate limiting mechanism and the associated coarsening rate. Since an osmotically stabilised emulsion may be destabilised by a rapid transport of the trapped species between droplets, the extent to which micelles may affect the rate of coarsening by transporting oil between droplets is considered. Different mechanisms of micelle–mediated exchange are considered, and the applicability of the different mechanisms indicated. Various applications are suggested.

Declaration

This thesis has been written entirely by me and has not been submitted in any previous application for a degree. Except where stated, all the work detailed in this thesis was carried out by me.

A. J. Webster.

Acknowledgements

Grateful thanks to my supervisor Mike Cates, without whom I would not have embarked on this thesis. It is important to acknowledge his careful reading of the thesis, his quick appreciation of the physical principles underlying phenomena, and many interesting discussions which I will greatly miss. His generosity in "The Old Bell", on Friday evenings where he regularly supplied more than one round of beer to an understandably large group of students, postdocs, and lecturers, should also not be forgotten.

Discussions with Alex Lips, Marcel Penders, and Wilson Poon, which initiated the work on emulsions should be thankfully acknowledged. Thanks also to Alexey Kabalnov for suggesting additional references, and for discussions about the instability of metastable emulsions. I gratefully acknowledge EPSRC (U.K.) for providing me with a research studentship, and in particular for the increase in grant after 1998 which greatly improved the standard of student life.

I would like to express my heartfelt appreciation for the support and understanding of my parents who not only gave me a wonderful childhood but even now remain a source of help, advice and inspiration; and also the rest of my family and friends, in particular Roisin, Michelle, Jane Morris, Kenny Dawe, and Alison Barker, all of which have provided a friendly ear and advice when needed most.

Finally, thanks for the friendship and tolerance of my various flatmates: Laura Starrs, Andy Robinson, Mark Buchanan (at ICTP), Nick Arini, Richard Blythe, Morgan Hankins, and Katrina Niederndorfer. Thanks also to my landlord Pete Bell for enabling me to complete my PhD without moving flat.

Contents

1 Introduction **1**

1.1 General Overview 1

1.2 Outline 3

2 Emulsions **7**

2.1 Introduction to Emulsions 7

2.2 A Brief History of Ostwald Ripening 9

2.2.1 Ostwald Ripening 9

2.2.2 Theoretical Improvements 10

2.2.3 Ostwald Ripening of Emulsions 11

2.2.4 Effects of Ostwald Ripening in Meteorology 12

2.2.5 Effects of Ostwald Ripening in Metallurgy 12

2.2.6 The Stabilising Effect of Trapped Particles 12

2.3 Free Energy of Dilute Emulsions 14

2.3.1 Free Energy Without Trapped Species 15

2.3.2 Free Energy With Trapped Species 17

2.3.3 Concentration of Dissolved Disperse Phase 17

2.4 Kinetics of droplet growth 18

2.4.1 Droplet growth rate 20

2.4.2 Characteristic Length Scales and Droplet Growth 21

3 Formation of Stable Emulsions **25**

3.1 Equilibrium at Fixed Droplet Number 25

3.2 Stability Criterion for Monodisperse Emulsions 28

3.3 Kinetic Interpretation of Metastability 30

3.4 Metastability at Fixed Initial Concentration 32

3.5 Laplace and Osmotic Pressure Balance 36

3.6 Stability of Polydisperse Emulsions 37

3.7 The Metastable Regime (II) 40

3.8 Other Equations of State 42

3.9 Slightly Soluble "Trapped" Species 44

3.10 Conclusions 47

4 Coarsening of Unstable Emulsions **49**

4.1 Overview 49

4.2 The Physics of Coarsening 50

4.3 Asymptotic Analysis 52

4.3.1 Determination of A_T and A_L 53

4.3.2 Determination of n_T 54

4.3.3 Determination of n_L 56

4.4 Polydispersity in Trapped Species 58

4.5 Conclusions 61

5 Applications of Osmotic Stabilisation **63**

5.1 Optimal Sizing of Emulsions 63

5.1.1 Orders of Magnitude 64

5.2 Reversing the Coarsening Process 65

5.3 Formation of Mini-emulsions by Shrinking 66

6 Effects of Micelles on Emulsion Stability **69**

6.1 Introduction 69

6.2 Mechanisms for Solubilisation 71

6.3 Diffusion Limited Coarsening:
A Simple Model 73

6.3.1 Droplet Growth Rate 76

6.3.2 Droplet Size Distribution 78

6.3.3 Effect on Ostwald Ripening 79

6.4 Rate of Solubilisation 79

6.4.1 Solubilisation Time ($x_0 > 1$) 81

6.4.2 Saturation Time ($x_0 < 1$) 83

6.4.3 Consistency of Steady State Assumption 84

6.4.4 Transient Phenomena 84

6.5 Exchange of Molecules Between Micelles 87

6.5.1 Calculating Oil and Surfactant Flux 87

6.5.2 Steady State Droplet Growth Rate 90

6.6 Reaction–Limited Coarsening 93

6.6.1 Reaction Limited Droplet Size Distribution 95

6.7 Reaction Limited Solubilisation 95

6.7.1 Solubilisation Time 96

6.7.2 Saturation Time 98

6.8 Micelle–Mediated Coarsening? 98

6.9 Conclusions 100

6.9.1 Micelle–Mediated Coarsening 101

6.9.2 Solubilisation by Micelles 102

6.9.3 Can Micelles Destabilise an Emulsion? 102

7 Foams **103**

7.1 A Brief History of Osmotic Stabilisation of Foams 105

7.2 Foam Equilibria 108

7.3 The Helmholtz Free Energy of Dilute Ideal Gases 110

7.4 Gibbs Free Energy of a Bulk Gas Phase 111

7.5 Gibbs Free Energy of Dilute (Spherical) Bubbles 112

8 Non–Dilute Foams **115**

8.1 Role of the Disjoining Pressure 117

8.2 'Softness Simplifies' 120

8.3 Case Study: *Dry* 2D Foam 122

8.4 A Simple 2D Model 125

8.4.1 The Geometric Pressure of a Nearly Hexagonal Bubble . . 127

8.4.2 Exact Calculation of the Osmotic Pressure 129

8.5 Polydisperse systems 131

8.6 Alternate Approach: Force Balance 134

8.7 Definition and Estimation of P^G 137

8.8 Relationship to Von Neumann's Law 140

8.9 Bubble Rearrangements 142

8.9.1 A Mechanism for Bubble Rearrangements 143

8.10 Conclusions 144

9 Stabilisation of Foams **147**

9.1 Coexistence Size/Composition 148

9.2 A Condition for Stability 149

9.3 Dilute Bubbles 151

9.4 Monodisperse, 2D Model 152

9.5 Sufficiently Dry Foams 153

9.5.1 Requirements for Stability 153

9.6 A Lower Bound on Stability Requirements 155

9.7 Compressed Emulsions 157

9.8 Conclusions 158

10 Coarsening of Unstable Foams **161**

10.1 Coarsening of Foams: Qualitative Behaviour 161

10.1.1 The Excess Volume Fraction of Disperse Phase 162

10.1.2 Rate of Bubble Rearrangements 164

10.2 A Simple Mean-Field Model 166

10.2.1 System Studied 166

10.2.2 Mean-Field Model 167

10.3 Rate-Limiting Mechanisms 170

10.3.1 LSW Coarsening of Bubbles 171

10.3.2 Inviscid Rearrangements 173

10.3.3 Viscous Rearrangements 173

10.3.4 Viscous or Diffusion Limited Growth? 176

10.4 No Rearrangements: Elastic Energy 178

10.4.1 Small Deformations 178

10.4.2 Larger Deformations 181

10.5 Finite Yield Strain 183

10.6 Higher Volume Fractions 185

10.6.1 High Excess Volume Fractions 186

10.6.2 Intermediate Volume Fractions 186

10.7 Conclusions 187

11 Conclusions **191**

11.1 Stabilisation Against Ostwald Ripening 191

11.2 Coarsening of Foams and Emulsions 193

11.3 Effect of Micelles 194

11.4 Possible Applications 195

A Table of Notation **197**

B Solubilisation of Oil by Non-Ionic Micelles 211

C Geometry of Monodisperse, 2D Bubbles 213

D Osmotic Pressure: Princen's Calculation 215

E Slightly Soluble 'Trapped' Species 217

F Calculating the Diffusion Constant K 219

G Foam Constants 221

G.1 Solubility of CO_2 222

G.2 Molar Volume of CO_2 at Atmospheric Pressure 222

H Publications 223

Bibliography 224

Chapter 1

Introduction

1.1 General Overview

The subjects encountered in this thesis are emulsions, foams, and micelles; the behaviour of which knowingly or unknowingly, is of great interest and importance to society as a whole. Emulsions are important to: [1–3] the food industry (eg. mayonnaise, milk), the oil industry (eg. oil extraction), biology (eg. blood substitutes, food digestion/emulsification), the cosmetics industry (eg. creams and shampoos), and are also similar to many structures encountered in metallurgy. The most general description of a foam includes all sponge and gel–like structures [4], and all cellular structures such as: [4, 5] plant and animal tissue, insulating foam, shaving cream, whipped cream, extinguisher foam, and even the head on a beer. The ability of micelles to solubilise matter and then subsequently transport it through a second (typically aqueous) medium, is of great importance to: [2, 6] the formulation of detergents, drug carriers, petroleum recovery, froth flotation, and the adsorption of pesticides and chemicals into plant and animal tissues. Hence a greater understanding of the behaviour of foams and emulsions, and a greater knowledge of the effects of micelles on emulsions, is both desirable

and beneficial.

The main obstacle to understanding the behaviour of emulsions and foams is that they *age*, that is their properties change with time. In particular both emulsions and foams have a tendency for their bubbles/droplets to *coarsen*, by competitively growing/shrinking until the continuous phase coexists with only a single bulk (previously dispersed) phase. The mechanism by which the coarsening mainly occurs will generally depend on the type and formulation of a particular foam or emulsion. However, typically coarsening occurs either by: [2, 4, 5] coalescence or flocculation of droplets/bubbles, a diffusive flux of disperse phase from smaller to larger droplets/bubbles, or gravitational segregation of the disperse and continuous phase (ie, *creaming/sedimentation* of emulsion droplets, or *drainage* of foams). Note that gravitational segregation often occurs as a result of previous coarsening of droplets/bubbles.

If the disperse and continuous phase have similar densities, then gravitational segregation may be prevented simply by making droplets sufficiently small that Brownian motion will dominate, and so prevent creaming/sedimentation. Similarly, since the gravitational segregation of concentrated foams may only occur via narrow channels formed where 3 or more bubbles meet (Plateau borders), drainage may occur at an acceptable rate. Modern surfactants are able to prevent both coalescence and flocculation of droplets/bubbles, and may also reduce the rate of foam drainage. Hence recent attention has focused on coarsening by a diffusive flux of disperse phase between droplets/bubbles, and ways of preventing or slowing the process.

This thesis considers the coarsening of foams and emulsions by diffusive flux of disperse phase between droplets/bubbles, via the continuous phase. In particular it focuses on the effects of trapping an additional species within droplets/bubbles, so that they may no longer shrink and entirely disappear. The trapped species provides an osmotic pressure which opposes the increase in pressure due to inter-

facial tension, and hence may slow or even prevent coarsening. Previous work has indicated the possibility of using a trapped species to stabilise emulsions [7–14], and theoretical work based on the analysis of monodisperse systems has described conditions to ensure the formation of stable emulsions [12, 14]. However emulsions are generally polydisperse, and it was unknown whether results based on the analysis of a monodisperse system would be applicable to a typical polydisperse emulsion. This lack of understanding of such common and important systems as polydisperse emulsions, was the initial stimulation for the work contained in this thesis.

By clarifying and extending our knowledge on the coarsening of foams and emulsions, along with the role that micelles may have for solubilisation and transport of substances, this thesis hopes to further improve our knowledge and understanding of emulsions, foams and micelle–mediated processes. Hopefully such knowledge will enable better and easier formulation of products which will continue to enhance our everyday lives.

1.2 Outline

We begin in chapter 2 with a brief introduction to emulsions, and a review of previous work related to their coarsening by a diffusive flux of disperse phase and its prevention by trapped species within droplets. We then carefully consider the free energy of a dilute system of emulsion droplets, and the free energy of an individual droplet. The growth rate of individual drops (both with and without a trapped species) are derived, and used to emphasise how the presence of trapped species suggests the possibility of forming stabilised emulsions. The chapter is mainly concerned with setting up the necessary background, ideas, and formalism required for later chapters.

Next in chapter 3 we carefully consider stabilisation of dilute emulsions. By analogy with the conditions for phase equilibrium in a binary system, we proceed to derive a condition to ensure stability of a monodisperse emulsion; this condition corrects the work of previous authors. By a different method, the results are then generalised to systems in which there is arbitrary polydispersity in particle size and in the number of particles of trapped species within emulsion droplets. Finally we consider the "trapped" species being slightly soluble, deriving a condition which ensures that the coarsening rate would be limited by the rate of transport of the slightly soluble species. These results are amongst the most important in the thesis.

The unstable coarsening of an emulsion containing trapped species is considered in chapter 4. Coarsening is shown to result in a bimodal distribution consisting of a population of small droplets with an approximately constant size, and a coexisting distribution of larger droplets which is evolving with time. It is found that the rate of coarsening and the distribution function of the larger drops are unchanged from those of droplets coarsening without trapped species, but with a reduction in the volume fraction of the larger drops to account for that present in the coexisting, smaller droplets. A corollary to the calculations is the stability condition Eq. 3.28, previously calculated by a different method in chapter 3.

In chapter 5 we suggest some possible applications of the physical mechanisms discussed in the previous chapters. These include methods for reversing the coarsening process, and for shrinking emulsion drops to form "miniemulsions".

The possibility of micelles disrupting the stabilising mechanism by transporting the previously trapped material between droplets is considered in chapter 6. A number of regimes are considered depending on the ease with which oil is solubilised into and exchanged between micelles. The work on micelles attempts to provide a framework for describing the qualitatively different types of coarsening which may occur, and also attempts to map out when each scenario would be

applicable. Although primarily directed towards the effects of micelles on coarsening of emulsions, the work is of interest in its own right, since the solubilisation and transport of substances in micelles is highly important to: [2] detergency, oil extraction, removal of contaminants, and biological processes (eg. penetration of pesticides or chemicals into plant or body tissues).

Chapter 7 introduces and reviews related work on stabilisation of foams, before deriving the free energy and chemical potential of soluble gas within dilute (spherical), compressible foam bubbles. Then chapter 8 considers the pressures within bubbles in non–dilute foams in which bubbles press on one another. By careful argument and examination of existing experimental results, an equation for the pressure within bubbles in a sufficiently compressed foam is proposed. The arguments are confirmed for a model of a monodisperse 2D foam in which the bubble pressure is exactly calculable. Von Neumann's law for bubble growth is related to our expression for bubble pressure, and a mechanism for bubble rearrangements is suggested to explain observed experimental results.

Using the results of chapters 7 and 8, chapter 9 considers the requirements for bubble stability. Exact stability conditions are calculated for dilute foams and the monodisperse model of 2D foams, and a requirement for *instability* is given. The stability requirements for sufficiently compressed foams are considered, and results suggest that stabilisation should not only be possible, but the *stability* requirements will be similar to those of dilute foams (with well separated spherical bubbles).

The penultimate chapter considers the coarsening of insufficiently stabilised foams. Expected morphologies and behaviour are suggested, and possible rate limiting mechanisms discussed. A simple mean–field argument and a number of order of magnitude arguments are given to determine growth rates and foam behaviour. By considering the rates of dissipation due to coarsening by different mechanisms, a dominant rate limiting mechanism is found, enabling foam behaviour to

be predicted.

Finally in chapter 11 we conclude with a brief summary of the thesis, and an indication of important open questions.

Appendix A contains tables of notation for chapters 2–11. Each chapter has its own table of notation in Appendix A, which contains a brief definition and explanation of the symbols (notation) used in the chapter.

Much of the work on emulsions is published in "Stabilisation of Emulsions by Trapped Species" [15], and much of the work on foams has been submitted for publication in a paper entitled "Coarsening and Osmotic Stabilisation of (Polydisperse) Foams and Dense Emulsions" [16].

Chapter 2

Emulsions

2.1 Introduction to Emulsions

An emulsion is a mixture of two or more liquids, with droplets of a disperse phase suspended in a second continuous phase. Common examples of emulsions include milk, ketchup, mayonnaise and paint (hence the term "emulsion paint"). Emulsions are often characterised as being either a "macroemulsion" or a "microemulsion". Macroemulsions tend to consist of droplets of $\sim 10^{-6}$m in size, where as microemulsions contain drops which may be as small as [2] $\sim 10^{-9}$m in size. The main reason for this difference in droplet size is the way in which the different emulsion types form. A microemulsion will spontaneously form as the ingredients are added, producing a thermodynamically stable, long lived emulsion. Macroemulsions do not form spontaneously, instead requiring some kind of mechanical agitation to break up the liquids and form droplets. An example of the formation of a macroemulsion is the shaking of an oil and vinegar salad dressing to mix the oil and water prior to use. The mechanical way in which macroemulsions are formed limits the smallest size of droplets which may be produced (which is typically far larger than that of a microemulsion). In all that

follows we will consider only macroemulsions.

Macroemulsions are thermodynamically unstable, requiring energy for their formation and evolving over time until entirely phase separated into their constituent liquids. Their instability is due to the interfacial energy between the different liquid phases, with the emulsions evolution and phase separation being driven by a desire to reduce this interfacial energy. As mentioned previously, emulsions may coarsen by flocculation, aggregation, diffusive exchange of disperse phase from small to large droplets, or gravitational segregation. Typically, droplets will coarsen until they're sufficiently large that gravitational segregation will occur, resulting in separate bulk phases with the phase of lowest density rising to the top of the sample.

The desire to produce stable macroemulsions has led to the use of surfactants which are able to prevent both flocculation and aggregation of droplets, limiting their coarsening rates so as to prevent their eventual phase separation by gravitational segregation (for sufficiently small droplets Brownian motion will prevent gravitational segregation). Surfactant will also increase emulsion stability by reducing interfacial surface tension. For a surfactant concentration in excess of its CMC (critical micelle concentration [2]), then if the rate of surfactant equilibration between the interface and continuous phase is much faster than droplet growth, the interfacial tension will be reduced by a constant amount. We will assume here that surfactant may equilibrate much more rapidly than droplets grow, so that surface tension is reduced by a constant amount. We will also restrict ourselves to macroemulsions which are stabilised against aggregation or flocculation of droplets.

In the absence of aggregation or flocculation, emulsions can still coarsen by the disperse phase diffusing through the continuous phase between droplets. The coarsening of droplets by a diffusive flux of disperse phase through a continuous phase, is an example of a class of phenomena referred to as "Ostwald ripening",

and which includes the coarsening of precipitates in solution, water droplets in air, and alloyed components in metals. Ostwald ripening has been studied in the context of Emulsions, Meteorology, Metallurgy, and Physical Chemistry. In the next section we will briefly review work on Ostwald ripening, and its applications in Meteorology, Metallurgy and Emulsions. We will also review work on the effect of "trapping" an additional species within droplets.

2.2 A Brief History of Ostwald Ripening

2.2.1 Ostwald Ripening

Ostwald ripening is the name given to the coarsening of droplets or precipitates of disperse phase, due to diffusion of disperse phase through a continuous phase. It was first observed by Ostwald in 1900 [17]. The diffusion is a result of different vapour pressures* above different sized droplets. The differences in vapour pressure are due to the *Kelvin effect* (1871) [18], which refers to an increase in vapour pressure as a droplets radius is decreased. The reality of the Kelvin effect was verified by La Mer and Gruen (1951) [19].

By assuming a vanishingly small volume fraction of disperse phase ϕ, Lifshitz–Slyozov (1961) [20] and Wagner (1961) [21] determined the kinetics of Ostwald ripening. They derived growth laws for the average particle size along with the droplet size distribution. Experimental verification of the kinetics for the Ostwald ripening of a small volume fraction of emulsion droplets was given by Kabalnov et al (1987) [11,13].

A clear exposition of the main theoretical ideas may be found in a review by

*If the continuous phase is a liquid (as for emulsions), it arises from a differing concentration of dissolved disperse phase above a droplets surface.

Bray [22], and a fairly recent review of Ostwald ripening is given by Voorhees [23].

2.2.2 Theoretical Improvements

The Lifshitz–Slyozov & Wagner solution (here after referred to as LSW), determines the evolution of the size distribution function with time, a physical situation in which the supersaturation will decrease as the system tends to equilibrium. Marqusee and Ross [24] pointed out that the method used by LSW assumed the supersaturation to be exactly zero, an assumption which is approximately true but physically incorrect. To overcome this difficulty they assumed the supersaturation to obey a power law of time, and then considered a more general form of scaling function for the droplet size distribution than that obtained by LSW. The results they obtained were to the lowest order identical to those of LSW, and the next lowest order of results were found to depend upon the initial conditions.

The assumption of vanishing volume fraction allows droplets to be treated independently from one another in an homogeneous and isotropic environment. A non–zero volume fraction, which would occur in a real situation, prevents droplets from being treated independently since the diffusion fields surrounding droplets would now start to overlap. Approaches to Ostwald ripening at low volume fractions with $\phi \ll 1$ have proceeded by treating the drops as monopole sources/sinks and then employing various different averaging procedures so as to obtain averaged growth rates. These approaches were extensively reviewed by Voorhees [25] who summarised that the effect of the non–zero volume fraction was to alter the amplitudes of coarsening rates by a factor of $\phi^{1/2}$. A careful investigation by Fradkov et al [26] demonstrated that sometimes the coarsening rates could vary as $\phi^{1/3}$. Marsh [27] also considered volume fractions with $\phi \sim 1$. He did this by *constructing* the medium such that certain properties remained invariant under scaling of the average particle radius. The results obtained were found to be in

close agreement with experiment.

The variation in Ostwald ripening during fluid flow is treated by Ratke and Host (a review of this and related work is given by Ratke [3]). They derive results, which hold for arbitrary Peclet number, by considering the particles as being surrounded by a boundary layer. Flux within the boundary layer was treated as diffusive, with flux to the edge of the boundary layer being due to convection.

2.2.3 Ostwald Ripening of Emulsions

The possibility of coarsening in emulsions due to Ostwald ripening was theoretically analysed by Higuchi and Misra in 1962 [7]. The effect was later observed by Hallworth and Carless (1976) [8] and Davis and Smith (1976) [9], who studied O/W emulsions made from either hexane or hexadecane. They found that where as the hexadecane emulsions were stable, the hexane emulsions were not. Furthermore they found that if a small quantity of hexadecane was added to the hexane prior to the emulsions formation, then the resulting emulsion would be stable.

Renewed interest in the effects of Ostwald ripening in emulsions was initiated by the work of Kabalnov et al (1987) [11,13]. They studied coarsening of emulsions, finding it to be due to Ostwald ripening as opposed to flocculation as was traditionally assumed. They also confirmed the predictions of LSW [20,21] for the average droplet size, and the droplet size distribution of well separated droplets.

Recent reviews include "Thermodynamic and theoretical aspects of emulsions and their stability", by Kabalnov [28], and "Ostwald ripening in emulsions", by Taylor [29].

2.2.4 Effects of Ostwald Ripening in Meteorology

Ostwald ripening is considered to be the mechanism by which cloud droplets grow from a supersaturated water vapour. Kohler (1931) [30–32] considered the effect of dissolved salt on a droplets stability, and discovered the possibility of forming stable water droplets with a fixed size. The ability of salt water to form stable dispersions was then used to account for the stability of sea fogs and mists. Kulmala et al (1997) [33, 34] describe how pollution would have a similar effect to salt in stabilising droplets. This increased droplet stability was then used to account for the stability of *large droplet smogs*, which occur in heavily polluted areas such as near the exits of chimneys and in the plumes of volcanos.

2.2.5 Effects of Ostwald Ripening in Metallurgy

The phenomenon of Ostwald ripening is important in Metallurgy because it affects the strengths of alloys and steels [35]. It occurs primarily whenever the metals are at a high temperature, for example during their formation, or in turbine blades [36]. The Ostwald ripening alters both the size and number of precipitates of alloyed components within the metal, which in turn affects the materials strength. The effects of Ostwald ripening within ternary alloys has been theoretically investigated by Kuehmann and Voorhees [37], and represents the most rigorous study of Ostwald ripening in a two–component disperse–phase system.

2.2.6 The Stabilising Effect of Trapped Particles

It has been found that if an extra species has a sufficiently low solubility that it is effectively trapped in droplets, then Ostwald ripening may be prevented. The stabilising effect of trapping particles of an additional species within droplets, was first emphasised in the context of Meteorology, by Kohler in (1936) [30–32]. The

effect was mentioned in the context of emulsions by Higuchi and Misra (1962) [7]. Observations of increased emulsion stability, resulting from the addition of a less soluble component, were reported by Hallworth and Carless (1976) [8] and Davis and Smith (1976) [9]. The possibility that the less soluble component was stabilising the emulsion by forming a *complex film* was considered. Experiments by Buscall et al (1979) [38], concluded that a complex film was not always the cause of increased stability, providing evidence for the existence of another stabilising mechanism. Davis et al (1980) [10] gave a qualitative explanation for the increase in emulsion stability as a result of the *Raoult effect*.

Kabalnov (1987) [12] provided quantitative criteria for the stabilisation of an emulsion against Ostwald ripening, by considering emulsion droplets as composed of an ideal mixture of trapped and soluble components. Reiss and Koper (1995) [14] provided a systematic study of the Gibbs free energy of a system consisting of a single droplet of a non–ideal binary fluid in a continuous phase. They considered one of the two components to be trapped within the droplet and re–affirmed that a range of compositions existed where the drop would be stable. By considering the disperse phases as regular liquids, they emphasised that although non–ideal liquids may have a range of stable compositions, droplets would become unstable at both low and very high concentrations of the trapped component. It was noted that a nucleation process involving the more soluble component could de–stabilise a drop, but their estimations of fluctuations suggest this would be unlikely. It was also pointed out that if the second component was partially soluble, then its slow flux would eventually result in the droplet becoming unstable.

To understand the kinetics of the coarsening process (Ostwald ripening) and the stabilising effect of a trapped phase, it is necessary to consider the free energy of emulsions and the chemical potentials of emulsion droplets. The free energy of dilute emulsions (with low volume fractions), and the chemical potentials of their droplets are derived in section 2.3, before we consider droplet growth rates

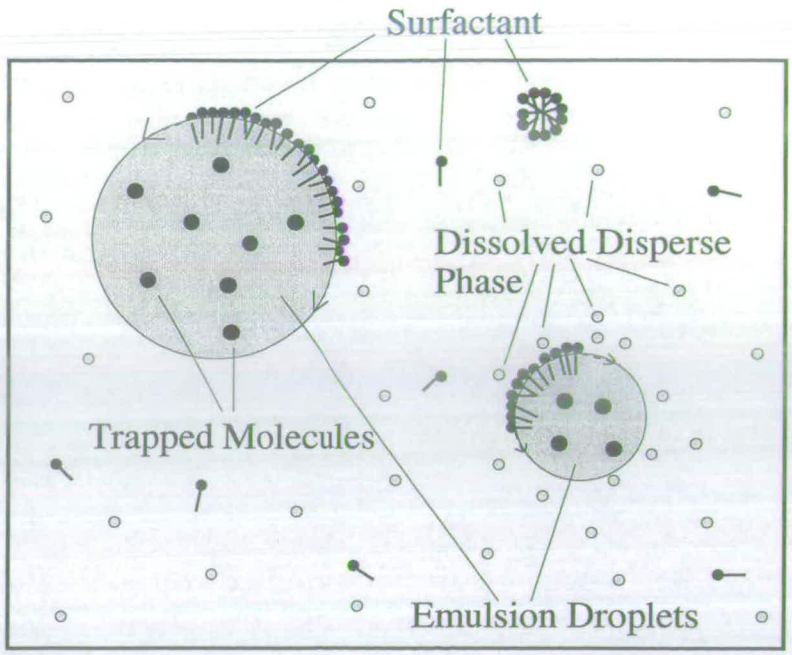

Figure 2.1: A schematic diagram of an emulsion with surfactant and a disperse phase containing trapped species.

in section 2.4.

2.3 Free Energy of Dilute Emulsions

Although a system of emulsion droplets containing trapped species and stabilised by surfactant only contains 3 components, the free energy includes contributions from the interfacial tension and from components dissolving and mixing in one another. Fortunately many of these contributions to the free energy may be neglected, as is outlined in the following sections. A schematic picture of an emulsion is given in figure 2.1.

2.3.1 Free Energy Without Trapped Species

We will firstly consider the free energy of an incompressible two component emulsion without trapped species, with a single disperse phase component. We consider emulsions with a small volume fraction of disperse phase, in which droplets are well separated from one another. We assume the emulsion to be homogeneous and isotropic, and neglect contributions to the free energy from:

- Continuous phase which has dissolved in the disperse phase (since the continuous phase is taken to have negligible solubility in the disperse phase).
- Surfactant dissolved in either of the phases.[†]
- Bending energy terms due to the surfactant at the disperse–continuous phase interface (since the droplet radii are considered as much greater than the surfactant molecules length).
- Entropy of mixing of the emulsion droplets (since the droplets are taken as macroscopic, typically measuring a few micrometres in diameter).

We neglect changes in the free energy of the continuous phase due to changes in the concentration of dissolved disperse phase, treating the free energy of the continuous phase as approximately constant. Since we assume that surfactant can redistribute itself sufficiently rapidly, we may treat the disperse–continuous phase interfacial energy σ as constant and equal for all droplets. Then we may

[†]This could have a significant effect on emulsion stability. For example, if the surfactant was preferentially soluble in the disperse phase, then the surfactant could play the role of the trapped species, providing an osmotic pressure which opposes the effects of surface tension. However if the surfactant is not preferentially oil soluble then micelles and dissolved surfactant molecules exert a net osmotic pressure on droplets. Since this osmotic pressure is independent of droplet size it results in an increase in the chemical potential of all droplets by a fixed amount, and has no effect on our following results.

treat the free energy of a droplet and its interface as composed of a sum of the free energy of a volume of disperse phase with bulk properties, and an interfacial energy. So for a spherical droplet of radius R we may write a droplet's free energy as

$$f(R) = \frac{(4\pi/3)R^3}{v_b} f_b + 4\pi R^2 \sigma \tag{2.1}$$

where f_b is the contribution per molecule to the Helmholtz free energy due to local molecular interactions of molecules of disperse phase, and v_b is the volume per molecule of bulk disperse phase. The system's free energy will be given by

$$F = F_c + \sum_i \frac{(4\pi/3)R_i^3}{v_b} f_b + 4\pi R_i^2 \sigma \tag{2.2}$$

where F_c is the free energy density of the continuous phase, and the sum is over the droplets in a unit volume of the system.

To find a droplet's chemical potential we first consider its internal pressure. We may find a droplet's internal pressure from Eq. 2.1 and $P = -(\partial f/\partial V)_{N,T}$, which gives

$$P = P_b + \frac{2\sigma}{R} \tag{2.3}$$

where P_b is the pressure of a bulk quantity of disperse phase. We note that the increase in pressure within a droplet $\frac{2\sigma}{R}$ due to surface tension, is the well known Laplace pressure [39]. The Gibbs–Duhem relation at fixed temperature has that [39] $Nd\mu = VdP$, where N is the number of molecules, V is the volume, and μ is the chemical potential. For an incompressible system we may take v_b as constant, and integrate the Gibbs–Duhem equation to get

$$\mu - \mu_b = (P - P_b)\, v_b \tag{2.4}$$

where μ_b is the chemical potential of a bulk volume of disperse phase. So writing $\Delta\mu \equiv \mu - \mu_b$ and using Eq. 2.3, we have the difference in chemical potential between a droplet and a bulk quantity of disperse phase $\Delta\mu$, given by

$$\Delta\mu = \frac{2\sigma}{R} v_b \tag{2.5}$$

2.3.2 Free Energy With Trapped Species

We now consider dilute emulsions which contain trapped species. We assume the trapped species is both dilute and ideal within the droplet, obtaining the free energy of a droplet containing η trapped species as

$$f(R,\eta) = \frac{(4\pi/3)R^3}{v_b} f_b + 4\pi R^2\sigma + kT\eta\left(\ln\left(\frac{\eta v_b^\eta}{(4\pi/3)R^3}\right) - 1\right) \tag{2.6}$$

where v_b^η is the volume per molecule of trapped species, V is the volume of a droplet ($V \equiv \frac{4\pi}{3}R^3$), k is Boltzmann's constant, and T is the temperature. The system's free energy now becomes

$$F = F_c + \sum_i \left[\frac{(4\pi/3)R_i^3}{v_b} f_b + 4\pi R_i^2\sigma + kT\eta\left(\ln\left(\frac{\eta v_b^\eta}{(4\pi/3)R_i^3}\right) - 1\right)\right] \tag{2.7}$$

To obtain $\Delta\mu$ we follow the approach of the previous section 2.3.1, to firstly obtain

$$P = P_b + \frac{2\sigma}{R} - \frac{\eta kT}{(4\pi/3)R^3} \tag{2.8}$$

where we note that there is now an additional osmotic pressure from the trapped species, which opposes the Laplace pressure. We then use the assumption of the trapped species being ideal, noting that since the volume occupied by the soluble species is Nv_b the Gibbs–Duhem equation for the soluble component at fixed T remains as $d\mu = v_b dP$. So integrating the Gibbs–Duhem equation for the soluble component at fixed T we get,

$$\Delta\mu = (P - P_b)v_b \tag{2.9}$$

as before. So for $\Delta\mu$ with trapped species we now obtain,

$$\Delta\mu = \left(\frac{2\sigma}{R} - \frac{\eta kT}{(4\pi/3)R^3}\right) v_b \tag{2.10}$$

2.3.3 Concentration of Dissolved Disperse Phase

We now consider the molecules of disperse phase that are dissolved in the continuous phase, and assume these are dilute and ideal. Then the chemical potential

of dissolved disperse phase at concentration C is given by

$$\mu_c = \mu_{c0} + kT \ln C \tag{2.11}$$

where μ_{c0} is a reference value. We now assume that each droplet is in equilibrium with the disperse phase dissolved above its surface. Then adjacent to a droplet's surface we will have $\mu = \mu_c$, and the concentration $C(R)$ will satisfy,

$$kT \ln C(R) = \mu_b + \left(\frac{2\sigma}{R} - \frac{\eta kT}{(4\pi/3)R^3} \right) v_b - \mu_{c0} \tag{2.12}$$

At a flat interface we have $R \to \infty$, and $kT \ln C(\infty) = \mu_b - \mu_{c0}$. So we may write

$$C(R) = C(\infty) \exp\left(\frac{\Delta\mu}{kT} \right) \tag{2.13}$$

Since we consider systems with small values of $\frac{\Delta\mu}{kT}$, we may expand Eq.2.13 to obtain,

$$C(R) \simeq C(\infty) \left(1 + \frac{\Delta\mu}{kT} \right) \tag{2.14}$$

So we obtain the concentration of dissolved disperse phase above the surface of a droplet of radius R as

$$C(R) \simeq C(\infty) \left(1 + \frac{2\sigma v_b}{kTR} - \frac{\eta v_b}{(4\pi/3)R^3} \right) \tag{2.15}$$

We will often refer to the dissolved concentration of disperse phase as the 'supersaturation', since in the absence of trapped species $C(R)$ is greater than that above a bulk liquid $C(\infty)$.

2.4 Kinetics of droplet growth

When considering droplet growth and coarsening of emulsions, we will consider a vanishingly small volume fraction of disperse phase, and make the following assumptions:

- Droplets are in equilibrium with their local spatial environments (as in section 2.3.3).

- Droplet interaction is by diffusion of disperse phase through the continuous medium, with the rate of diffusion being much less than the rate with which disperse phase may be adsorped/desorped from droplets, and hence that droplet growth is diffusion limited.

- The rate of diffusive flux to a droplet is determined by the difference between the concentration of dissolved disperse phase adjacent to a droplets surface, and the average far–field concentration of dissolved disperse phase.

These assumptions reduce the problem to two tasks

1. A single body equilibrium problem to determine the growth rate of a droplet in terms of its radius and the ambient saturation (far–field concentration of dissolved disperse phase). We will consider this next in section 2.4.1.

2. A many–body problem to determine the droplet size distribution as a function of time.

Since in task 2 droplets interact with each other only via the ambient supersaturation, the problem is tractable. This is the subject of chapter 4; first we solve task 2.4.1 (sections 2.4.1 to 2.4.2), and in chapter 3 obtain stability criteria that allow task 2 to be bypassed in certain cases.

The method and assumptions so far described, are basically the same as those of LSW [20, 21]. Although subsequent methods have further improved those of LSW (see section 2.2.2), the resultant corrections are small and the asymptotic solutions essentially the same.

2.4.1 Droplet growth rate

As described above, a droplet's growth rate is determined by the diffusive flux of solubilised disperse phase between its surface and the ambient far–field supersaturation. We will denote the average concentration of disperse-phase species in the continuous phase as $\bar{c}$, which under the conditions studied here will be close to $C(\infty)$. Then the reduced supersaturation ϵ, defined as

$$\epsilon = \frac{\bar{c} - C(\infty)}{C(\infty)} \tag{2.16}$$

will be small. Since the variations of the diffusion field are small, the diffusion field will relax quickly on the time scale of droplet growth. Hence we may make a steady state approximation to the diffusion profile around a droplet, replacing the diffusion equation $\partial c/\partial t = D\nabla^2 c$, by $\nabla^2 c = 0$. We then take boundary conditions of $c(R) = C(R)$, and $c(\infty) = \bar{c}$ (the mean far–field supersaturation). So solving in spherical co–ordinates we obtain the steady state profile $c(r)$ for the concentration $c(r)$ of solubilised disperse phase at distance r from the centre of a drop as

$$c(r) = R\left(\frac{C(R) - \bar{c}}{r}\right) + \bar{c} \tag{2.17}$$

Since we have assumed the process to be diffusion limited, the droplet growth rate is determined by the flux adjacent to a droplets surface. Hence we obtain the droplets growth rate as

$$\frac{dR}{dt} = v_b D \left.\frac{\partial c}{\partial r}\right|_R = v_b D \left(\frac{\bar{c} - C(R)}{R}\right) \tag{2.18}$$

Then using Eq. 2.15 for $C(R)$, we obtain

$$\frac{dR}{dt} = \frac{v_b D C(\infty)}{R}\left(\epsilon - \frac{2\sigma v_b}{kTR} + \frac{\eta v_b}{(4\pi/3)R^3}\right) \tag{2.19}$$

2.4.2 Characteristic Length Scales and Droplet Growth

Examination of Eq. 2.19 shows that when $\eta = 0$ we may define a characteristic length scale R_ϵ by

$$R_\epsilon \equiv \frac{2\sigma v_b}{\epsilon kT} \tag{2.20}$$

which gives a critical size above which droplets will grow in size and below which droplets will shrink. When $\eta \neq 0$ we may define another characteristic length scale R_B as that at which the Laplace pressure due to surface tension $\frac{2\sigma}{R}$, and the osmotic pressure due to the trapped species $\frac{\eta kT}{(4\pi/3)R^3}$, are equal. R_B is given by

$$R_B \equiv \left(\frac{3\eta kT}{8\pi\sigma}\right)^{1/2} \tag{2.21}$$

at which size a droplets osmotic and Laplace pressures will balance one another. Hence the growth rate may be written in the more informative manner as,

$$\frac{dR}{dt} = \frac{Dv_b^2 C(\infty)2\sigma}{RkT}\left(\frac{1}{R_\epsilon} - \frac{1}{R} + \frac{R_B^2}{R^3}\right) \tag{2.22}$$

As shown in figure 2.2, when $\eta > 0$ a second zero in the growth rate is introduced when $R \sim R_B$, in addition to the zero at $R \sim R_\epsilon$. We note that the fixed point at $R \sim R_B$ is stable, unlike the fixed point at $R \sim R_\epsilon$. The stability of the fixed point at $R \sim R_B$ suggests the possibility of forming stable emulsions; but since the growth rates also depend on ϵ, which is time dependent and need not even tend to zero at late times, the ultimate behaviour of the system is unclear and is considered in later sections.

It is possible to define a growth velocity $U(R', \epsilon)$ in terms of dimensionless variables, as

$$U(R', \epsilon) = \frac{\epsilon}{R'} - \frac{1}{R'^2} + \frac{{R'_B}^2}{R'^4} \tag{2.23}$$

where $R' \equiv RkT/(2\sigma v_b)$, $t' \equiv tDC(\infty)k^2T^2/(4v_b\sigma^2)$, and ${R'_B}^2 \equiv 3\eta k^3T^3/\left(32\pi\sigma^3 v_b^2\right)$. This form of the growth rate is used in chapter 4 when considering the dynamics of unstable, coarsening emulsions.

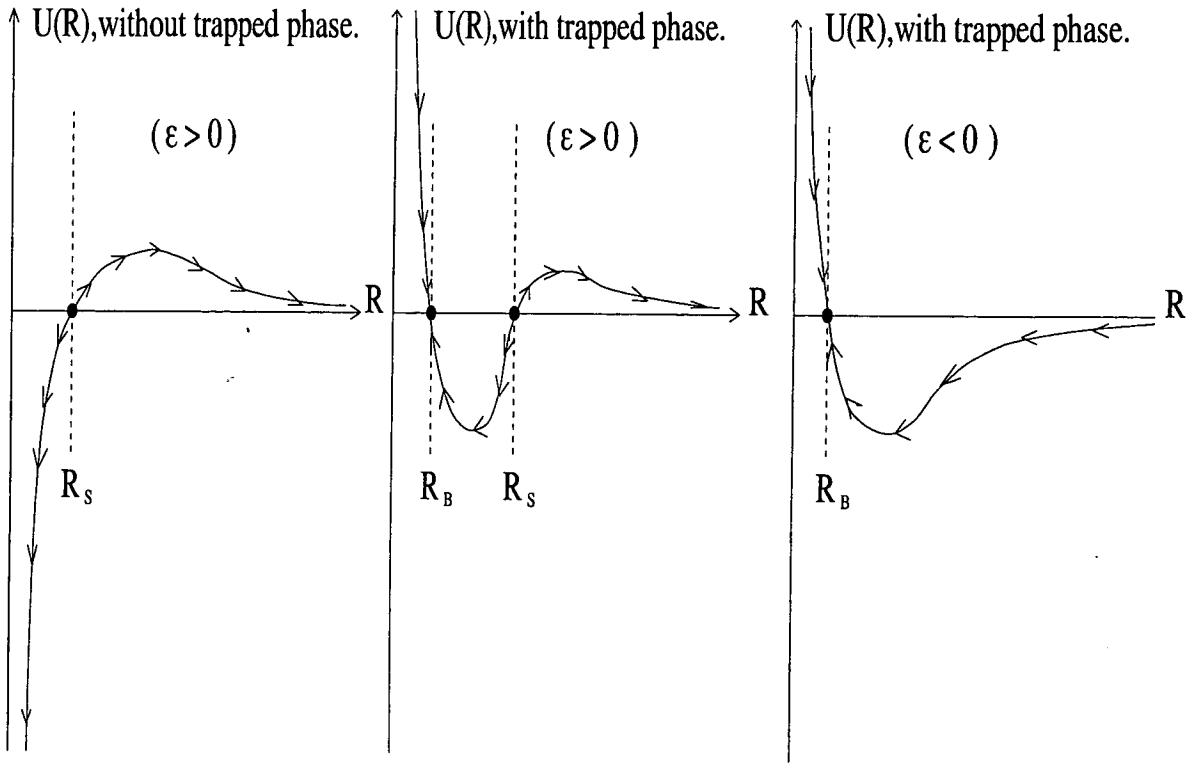

Figure 2.2: A schematic diagram representing how the presence of a trapped phase introduces a stable droplet size. Droplets of a given size move in the direction shown by the arrows. Without trapped species a new, stable, fixed point appears at R_B due to the competition between Laplace and osmotic pressure. If there are sufficient trapped species that ϵ is negative, then there is again only one fixed point, but it is the stable one at R_B. Expressions for R_S and R_B are given in section 2.4.2, $U(R)$ is defined in Eq. 2.23.

In the absence of trapped species we recover

$$U(R', \epsilon) = \frac{\epsilon}{R'} - \frac{1}{R'^2} \tag{2.24}$$

which was solved by Bray [22] in the study of the LSW model.

Having placed the coarsening of emulsions in context, and having set up the necessary formalism, the next chapter will proceed to use the formalism to derive rigorous results concerning the formulation of stable emulsions by addition of a trapped species.

Chapter 3

Formation of Stable Emulsions

The present chapter considers the possibility of using trapped species to osmotically stabilise an emulsion against coarsening (Ostwald ripening). Other coarsening mechanisms such as coalescence, are presumed negligible. We start by considering a monodisperse emulsion with an equal number of trapped species η per droplet, and a trapped species which may be treated as both dilute and ideal. These assumptions are relaxed in sections 3.6 and 3.8, and in section 3.9 we consider the previously "trapped" species as slightly soluble. In all the above cases we derive conditions to prevent coarsening, or limit its rate (when the trapped species is considered to be slightly soluble in the continuous phase). These conditions offer guidelines for the formulation of stable emulsions using the least possible amount of trapped species.

3.1 Equilibrium at Fixed Droplet Number

We consider an initially monodisperse emulsion in which the number of trapped particles η is identical in each droplet. We take the free energy of the system as given by Eq. 2.7, and write $n(V)$ as the number density of droplets of volume V.

Then the total free energy density of the system may be written

$$F = F_c + \int dV\, n(V) f(V,\eta) \tag{3.1}$$

with $f(V,\eta)$ as given by Eq. 2.6 but rewritten in terms of droplet volume V as

$$f(V,\eta) = (V/v_b) f_b + 4\pi\sigma \left(\frac{3V}{4\pi}\right)^{2/3} + kT\eta \left(\ln\left(\frac{\eta v_b^{\eta}}{V}\right) - 1\right) \tag{3.2}$$

In what will follow we will need only consider those terms in the free energies which are not constant or linear in V*. Ignoring constant terms and terms linear in V, $f(V,\eta)$ takes the form

$$f'(V,\eta) = 4\pi\sigma(3V/4\pi)^{2/3} - \eta kT \ln V \tag{3.3}$$

f' is shown in figure 3.1. Similarly for the systems free energy, we obtain

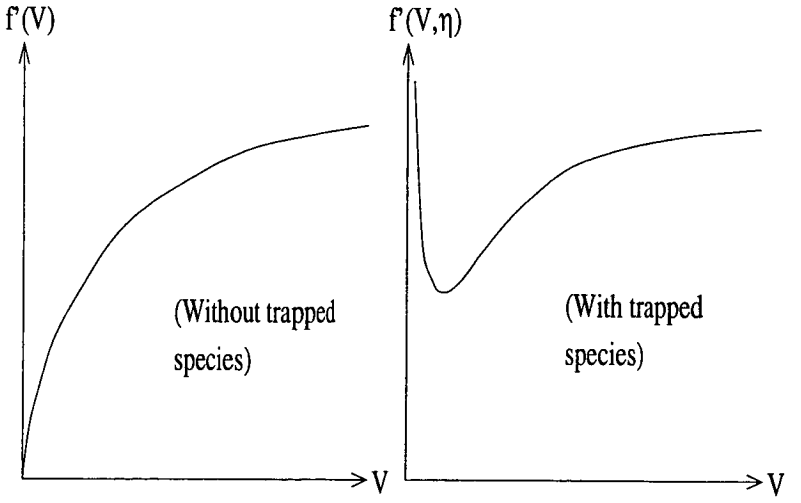

Figure 3.1: Comparison of curves of f' without (left) and with (right) trapped species.

$$F' = \int dV\, n(V) f'(V,\eta) \tag{3.4}$$

The free energy density F' is to be minimised subject to the constraints that the initial number density n_0 of droplets remains constant (since the trapped species

*Since the total number and volume of droplets are both conserved, such terms are constant when summed over the entire system.

prevents any droplets from disappearing),

$$\int dV\, n(V) = n_0 \tag{3.5}$$

and that the total volume fraction ϕ of disperse phase is constant[†]

$$\int dV\, Vn(V) = \phi = n_0 \overline{V} \tag{3.6}$$

The latter ignores a contribution from the dispersed-phase species that is solubilised in the continuous phase; for emulsions of low solubility, prepared by mechanical dispersion (rather than by quenching from a homogeneous mixture at high temperatures) the latter is always negligible.

These rules are precisely analogous to those for constructing the equilibrium state of a system whose free energy $f(\lambda)$ depends on a composition variable λ. Such a system can separate into volumes $v(\lambda)$ of phases with different compositions λ; in that case, $F = \sum_\lambda v(\lambda) f(\lambda)$ is minimised subject to the constraints $\sum_\lambda v(\lambda) = v_0$ (the total volume of the system is fixed) and $\sum_\lambda v(\lambda)\lambda = v_0\lambda_0$ (the total amount of species λ is conserved). Here the subscripts 0 describe a hypothetical homogeneous state.

In the analogy, if we replace droplet size V with composition λ, and the number of droplets $n(V)$ with the volume of phase $v(\lambda)$, then we find the determination of emulsion equilibria to be mathematically equivalent to determination of phase equilibria. Physically, since η is taken to be the same for each droplet, a droplets composition (phase) will be determined by its volume V, with V adopting the role of compositional variable λ. Similarly the quantity of droplets $n(V)$ with composition (phase) determined by V, corresponds to the quantity $v(\lambda)$ of phase with composition determined by λ. For example, a quantity n_0 of monodisperse droplets with volume V_0 corresponds to a quantity v_0 of a single phase with composition λ_0.

[†]This assumes that the volume occupied by a given amount of trapped species is independent of its concentration.

The minimisation of F' is therefore exactly as one would perform to find phase equilibrium in a binary fluid but with the function $f(\lambda)$ replaced by $f'(V,\eta)$. The usual minimisation procedure is to seek common tangencies whereby F can be lowered by phase separation. In this analogy, phase separation would correspond to the formation of droplets of more than one size, and hence composition. The volumes $v(\lambda)$ are determined by the lever rule [40], and for monodisperse η the same rule can be applied here to enable calculation of $n(V)$. Notice that the correspondence works only for the curve $f'(V,\eta)$; no similar construction applies to $f'(R,\eta)$, which is the form more usually considered in the literature [12, 14]. Also, note that any prediction of a "single phase" (*i.e.*, a monodisperse emulsion) is, in principle, subject to a small spreading of the size distribution arising from the entropy of mixing of the emulsion droplets themselves (rather than of the contents within one droplet), which we have neglected.

3.2 Stability Criterion for Monodisperse Emulsions

According to the above argument, if η is the same for all droplets (as will usually be nearly true for emulsions formed at fixed concentration of trapped species, with a nearly monodisperse initial droplet size distribution) the equilibrium state of the system at fixed droplet number can be found by inspection of the $f'(V)$ curve. A monodisperse emulsion can be stable only if the corresponding V lies in a part of the curve of positive curvature; if this is not the case then the free energy may be reduced (at fixed total number of droplets and fixed η in each drop) by the monodisperse distribution becoming polydisperse, and coarsening will occur. However, although positive curvature is necessary for stabilisation it is not sufficient, since even when the curvature is positive at a point $V = V_0$, it may be possible to find a lower free energy by constructing a common tangent on the $F'(V)$ curve which lies below $f'(V_0)$. The shape of the $f'(V)$ curve shown

in figure 3.1 dictates that any such tangency must connect the point at $V \to \infty$ to the absolute minimum of f'; the latter arises at $V = V_B(\eta)$ and is discussed further below.

The weaker of the two stability conditions (positive curvature) is precisely that given by Kabalnov et al [12]:

$$V \leq V_S(\eta) = \left(\frac{3\eta k_B T}{2\sigma}\right)^{3/2} \sqrt{\frac{3}{4\pi}} \tag{3.7}$$

Hence Kabalnov et al [12] reasoned that a sufficiently monodisperse initial distribution with droplet size $V_0 < V_S \equiv 4\pi R_S^3/3$ would be stable. However, the above argument shows this is actually a criterion for metastability. In other words, the criterion of Ref. [12] actually separates initial distributions which coarsen immediately, from those which may be stable for extended periods of time and may require some fluctuation to induce coarsening. Such fluctuations are invariably present, particularly at non–negligible volume fractions, though they are not included within the theory of Lifshitz and Slyozov. The kinetic mechanisms for the coarsening of emulsions of this 'metastable' type, are discussed in the section 3.3. The extent of the metastable region, and the likelihood of a metastable emulsion coarsening are discussed in section 3.7.

The above thermodynamic analogy shows that full stability in fact arises for initially monodisperse emulsions if and only if

$$V_0 \leq V_B(\eta) = \left(\frac{\eta k_B T}{2\sigma}\right)^{3/2} \sqrt{\frac{3}{4\pi}} \tag{3.8}$$

This corresponds to the requirement that the initial state lies to the left of the absolute minimum in the function f'. Everywhere to the right of this minimum, a lower global free energy can be constructed by a common tangency between V_B and (formally) $V = \infty$. This corresponds to a final coarsened state consisting of a monodisperse emulsion of droplet size $V_B = 4\pi R_B^3/3$ with droplet number density n_0, which coexists with an "infinite droplet", which can be interpreted as a bulk volume of the dispersed-phase species.

The subscripts B, S for $V_{B,S}$ and $R_{B,S}$ can be taken to denote "balance" (between osmotic and Laplace pressures in a drop) and "stability" (in the sense of Kabalnov et al [12]). However, in view of the thermodynamic discussion, it might be better to interpret them as "binodal" and "spinodal". Indeed, depending upon the value of V_0, any monodisperse distribution lies in one of three possible regimes: see figure 3.2. In regime I, the emulsion is fully stable under coarsening dynamics (provided droplet number is conserved). In regime II it is metastable. In regime III it is locally unstable and will coarsen immediately. The metastable region II is both mathematically and physically analogous to that between the binodal and the spinodal lines governing phase coexistence in a binary fluid.

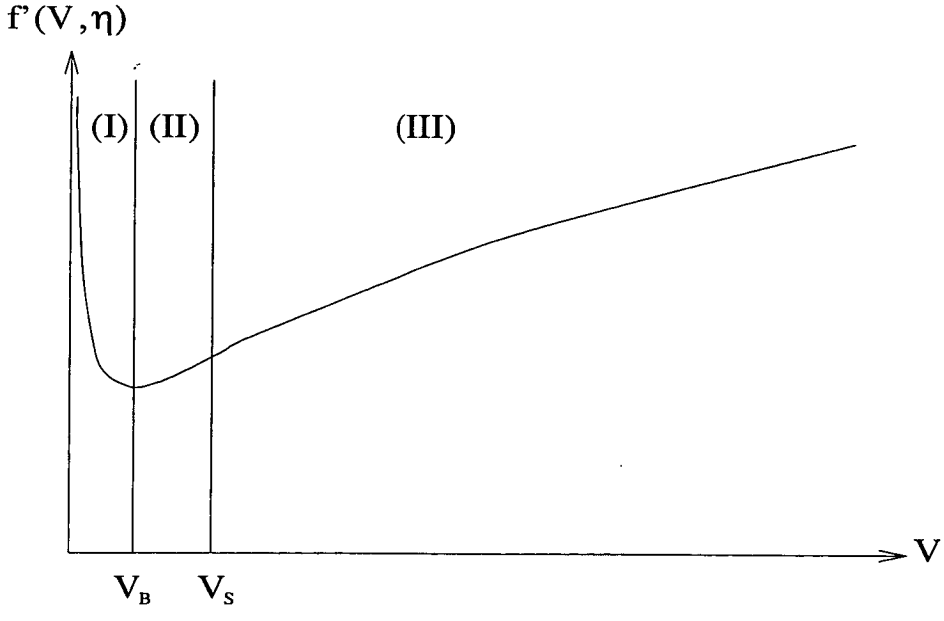

Figure 3.2: The three different stability regimes.

3.3 Kinetic Interpretation of Metastability

The above thermodynamic argument is quite formal, so it is useful to interpret it in kinetic terms. Consider a monodisperse distribution which is in equilibrium

with its "vapour" (*i.e.*, the dissolved fraction of the dispersed-phase species), and with η the same for all droplets. Let the radius of all but one droplet be (say) $R_0 < R_S$, but suppose a single larger droplet is present, of radius R. The growth of this droplet is determined by whether $C(R, \eta)$ is larger or smaller than $\bar{c}$. Since the remaining droplets are in equilibrium, $\bar{c}$ will be equal to $C(R_0, \eta)$. Now consider the concentration of dispersed-phase species $C(R, \eta)$ at the surface of the anomalously large droplet (see figure 3.3).

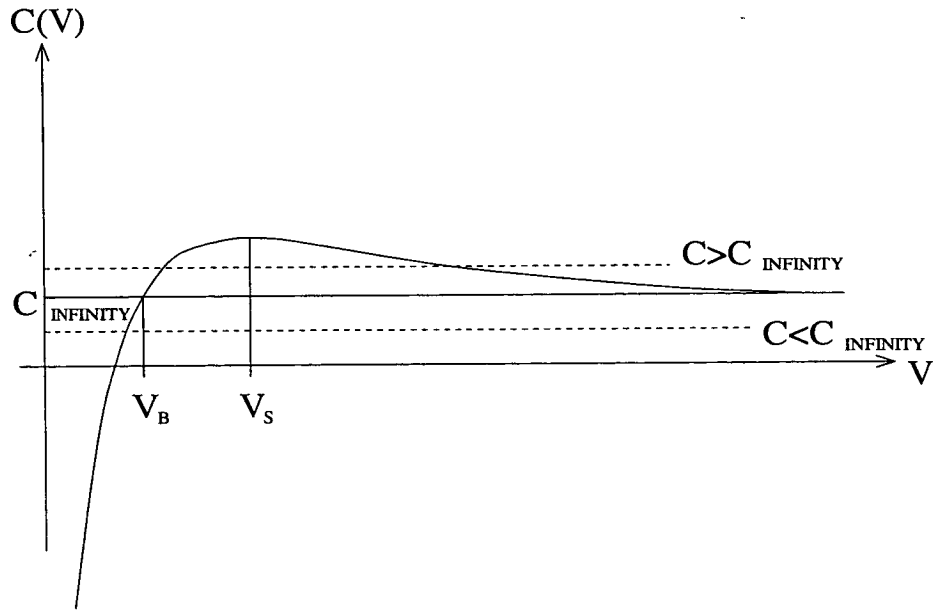

Figure 3.3: Variation in concentration of disperse phase at a droplets surface as a function of droplet volume.

Distributions in regime II have $R_B < R_0 < R_S$ and an average concentration of disperse phase $\bar{c}(R_0, \eta) > C(\infty, 0)$. Hence if a droplet is sufficiently large (perhaps due to polydispersity in the initial size distribution, or correlations in the diffusion field for example), its surface concentration will be below the ambient level and the droplet will grow at the expense of smaller droplets, by a diffusive flux through the continuous phase. Distributions in regime I ($R_0 < R_B$) have $\bar{c} < C(\infty, 0)$ and there is no size of droplet larger than R_0 for which sustained growth is possible. Such a droplet will instead redissolve to rejoin the equilibrium droplets at size

R_0.

Returning now to metastable distributions in regime II ($R_B < R_0 < R_S$), the critical size R_C above which a droplet will become unstable and start to grow is given by the larger root of $dR/dt = 0$, where dR/dt is given by Eq. 2.22. This gives

$$R_C = R_\epsilon \left(1 - \left(\frac{R_B}{R_\epsilon}\right) - 2\left(\frac{R_B}{R_\epsilon}\right)^2 - \ldots\right) \tag{3.9}$$

where R_ϵ is as in Eq. 2.20 and depends upon the supersaturation ϵ. Since the initial distribution of droplets is considered to be monodisperse with size R_0 and in equilibrium, then $dR/dt|_{R_0} = 0$ and R_ϵ may be determined as

$$R_\epsilon = \left(\frac{R_0^3}{R_0^2 - R_B^2}\right) \tag{3.10}$$

This suggests that, for a monodisperse initial state, the nucleation time for the coarsening process to begin (requiring nucleation of a droplet of size R_C) can become very large as R_0 approaches R_B. On the other hand, nucleation can occur immediately if there is any slight tail to the initial size distribution, extending beyond R_C.

The distinction between nucleation due to the existence of a tail in the initial size distribution which extends to abnormally large droplets, and nucleation resulting from fluctuations in growth rates, is similar to that between heterogeneous and homogeneous nucleation in conventional phase equilibrium. In this analogy the tail of the droplet size distribution (which may be negligible for thermodynamic purposes), provides "nucleation centres" which allow coarsening to begin.

3.4 Metastability at Fixed Initial Concentration

The above argument was for emulsions formed with a fixed number of trapped species η per droplet. We now consider emulsions formed from a fixed concentra-

tion of trapped species, with a polydispersity in η arising from polydispersity in droplet size[‡].

Consider the idealised scenario of a metastable emulsion formed from a fixed concentration of trapped species, and in which all but one droplet have radius R_0, and a single large droplet has radius R. Initially both the small and the large drops will have the same initial concentration of trapped phase c. We may then assume the following

- The many monodisperse droplets determine the supersaturation ϵ
- Until the *large* droplet becomes macroscopic in size, there are no constraints of volume fraction imposed upon the growth of the larger droplet, which grows as a result of a flux from the average supersaturation ϵ
- Throughout the initial stages of its growth (while the droplet remains mesoscopic in size), the larger drop has a negligible effect on the total volume fraction so the smaller drops will possess an effectively constant radius. Hence during the initial stages of growth (which will determine whether the large droplet will grow to a size in excess of its spinodal size R_S), the larger droplet will grow from an effectively constant supersaturation ϵ.

Equilibrium between the large drop and the small drops requires both to have the same chemical potential. At fixed initial concentration of trapped species

[‡]The motivation for the following arguments is explained below. Following a series of private communications with Dr Alexey Kabalnov, it became clear that a quantitative description of how a single large drop may destabilise an emulsion formed from a fixed concentration of trapped species, was required. Dr Kabalnov agreed that the destabilisation mechanism would apply when there was an equal number of trapped species in each droplet, but initially believed that a metastable emulsion ($\overline{V_B} < \overline{V} < \overline{V_S}$) formed from a fixed initial concentration would (in a practical situation) effectively be stable. The following uses an argument which arose following discussions with Dr Kabalnov, in which he subsequently agreed that polydispersity in the initial droplet size distribution *would* be able to nucleate coarsening in metastable emulsions.

the smaller radius of the small drops results in their having a higher chemical potential than the larger drop, which at equilibrium the larger drop must attain. However the maximum chemical potential of the larger drop is at its spinodal size R_S. So whether a larger drop can come to equilibrium with the smaller drops (as opposed to growing without bound), is determined by whether its maximum chemical potential $\Delta\mu_R(R_S)$ is in excess of that of the smaller drops. Noting that R_S is related to R_B by $R_S = \sqrt{3}R_B$, then the maximum chemical potential of the larger drop is

$$\Delta\mu_R(R_S) = 2\sigma v_b \left(\frac{1}{R_S} - \frac{R_B^2}{R_S^3}\right) = 2\sigma v_b \left(\frac{2}{3^{3/2}R_B}\right) \tag{3.11}$$

with R_B given by Eq. 2.21 in section 2.4.2.

Defining $\Delta\mu_r$ as the small drops chemical potential, and setting $\Delta\mu_r = \mathrm{Max}(\Delta\mu_R)$, we obtain the maximum value of the larger droplets R_B at which the large and small droplets may coexist in a metastable equilibrium. This gives

$$R_B = \frac{2}{3^{3/2}} \left(\frac{1}{\frac{1}{R_0} - \frac{R_{0B}^2}{R_0^3}}\right) = \frac{2}{3^{3/2}} \left(\frac{R_0^3}{R_0^2 - R_{0B}^2}\right) \tag{3.12}$$

where R_{0B} is the size at which small drops may coexist with a bulk phase.

Since the initial size of the larger drop is R, then noting that the number of trapped species in the larger drop $\eta_R = c\frac{4\pi}{3}R^3$, and using Eq. 2.21 we find

$$R_B = \left(\frac{3c(4/3)\pi R^3 kT}{8\pi\sigma}\right)^{1/2} \tag{3.13}$$

If we express the concentration c in terms of R_0 and R_{0B}, then we obtain

$$R_B = R_{0B}\left(\frac{R^3}{R_0^3}\right)^{1/2} \tag{3.14}$$

Hence we may now solve Eqs. 3.12 and 3.14 to obtain a critical initial size R_C beyond which the large drop will destabilise the emulsion. Working in terms of R_C/R_0 we have

$$\frac{R_C}{R_0} = \frac{2^{2/3}}{3}\frac{1}{R_{0B}^{2/3}} \left(\frac{R_0^3}{R_0^2 - R_{0B}^2}\right)^{2/3} \tag{3.15}$$

So as $R_0 \to R_{0B}$ the size of drop R_C, required to destabilise the emulsion $\to \infty$.

Rewriting Eq.3.15 in terms of the spinodal size of the small drops ($R_{0S} = \sqrt{3}R_{0B}$), we obtain

$$\frac{R_C}{R_0} = \left(\frac{2(R_0/R_{0S})^3}{3(R_0/R_{0S})^2 - 1} \right)^{2/3} \tag{3.16}$$

Hence, given a value of R_C/R_0 (which may be taken as a measure of polydispersity in the initial droplet size distribution), we may determine how close R_0 must be to R_{0S} if the emulsion is to be destabilised, by computing the value of R_0 for which $R = R_C$ (see figure 3.4). For example, taking $R_C/R_0 = 1.1$, we see that if

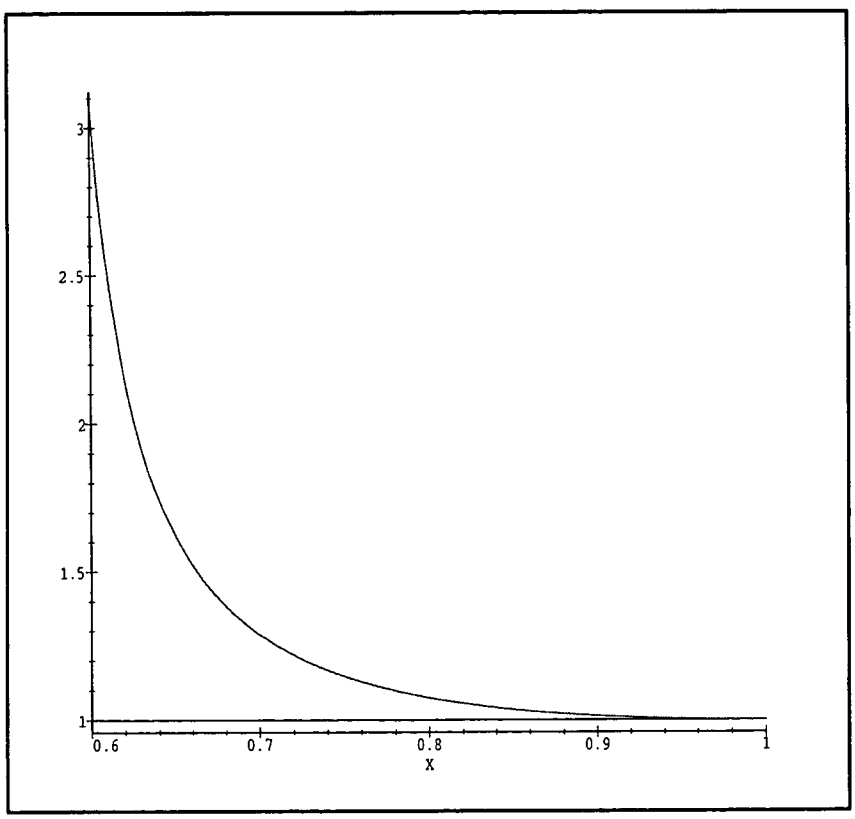

Figure 3.4: A graph of R_C/R_0 vs. $X = R_0/R_{0S}$

the emulsion is to remain metastable then R_0/R_{0S} must be less than 0.778 (where we note that $R_{0B}/R_{0S} \simeq 0.577$).

As can be seen from figure 3.4 as $R_0 \to R_{0S}$ then even very small values of R_C/R_0 will destabilise the emulsion. Writing $R_0 = R_{0S} - \Lambda$ and expanding in terms of Λ we obtain

$$\frac{R_C}{R_0} = 1 + \frac{\Lambda^2}{R_{0S}^2} - \frac{7}{3}\frac{\Lambda^3}{R_{0S}^3} + \frac{21}{4}\frac{\Lambda^4}{R_{0S}^4} + O\left(\frac{\Lambda^5}{r_S^5}\right) \tag{3.17}$$

Hence taking $R_0/R_{0S} = 0.9$ then $\Lambda/R_{0S} = 0.1$ and the emulsion will be unstable if R_C/R_0 is in excess of only $\simeq 1.01$. Since such small variations in droplet size are inevitable, a supposedly metastable emulsion will actually be unstable if R_0 is close to R_{0S}. It is thus clear that Kabalnov's criterion Eq. 3.7 does not quantitatively ensure stability for experimentally realizable emulsions.

In summary, although metastable, near monodisperse emulsions may exist in regime (II), the only reliable criterion for such an emulsion's stability is that it resides in the thermodynamically stable regime (I) (as described previously). This is true even when the emulsion is prepared with a fixed concentration of trapped species, rather than fixed number in each droplet as assumed in sections 3.2 and 3.3.

3.5 Laplace and Osmotic Pressure Balance

We now return to systems in which η is identical for all droplets. In this case the absolute stability requirement, $R_0 \leq R_B$ (Eq. 3.8), is equivalent to requiring that $C(R_0, \eta) \leq C(\infty, 0)$. However, we have for an ideal trapped species

$$C(R, \eta) = C(\infty, 0)\left(1 + \frac{v_b}{k_B T}\left[\frac{2\sigma}{R} - \frac{\eta k_B T}{(4\pi/3)R^3}\right]\right) \tag{3.18}$$

So we see that the absolute stability condition may be simply expressed in terms of the osmotic pressure of trapped species and the Laplace pressure, as

$$\frac{2\sigma}{R} < \frac{\eta k T}{(4\pi/3)R^3} \tag{3.19}$$

or alternatively $2\sigma/k_B T < c_t R$ where $c_t = \eta/V_0$ is the concentration of trapped species in the dispersed phase. This means that if an emulsion is made from a

dispersed phase of fixed c_t, a monodisperse emulsion will be fully stable only if the initial droplet size is sufficiently *large*. (The same applies to the metastability condition of Ref. [12].) This may be a rather unintuitive result; indeed, at fixed number of trapped particles η, as was used to discuss the $f(V,\eta)$ curves, stable emulsions arise only for *small* droplet sizes ($R_0 \leq R_B$). However, for a fixed composition c_t, the value of η depends on R_0; and the important requirement is that the osmotic pressure (which inhibits coarsening) of an initial droplet exceeds its Laplace pressure (which drives it). At given c_t this is true only for large enough droplets.

3.6 Stability of Polydisperse Emulsions

The criterion for full stability, Eq. 3.8 in section 3.2, can be extended to the polydisperse case. Let us first consider the case where the initial state contains droplets with variable sizes V_0, but exactly the same η. This system will again find its equilibrium state at fixed total number of droplets n_0 and fixed volume fraction ϕ, which now obeys

$$\phi = n_0 \overline{V} \tag{3.20}$$

with $\overline{V}$ the mean initial droplet volume. By again ignoring the entropy of mixing of the droplets (treating them as macroscopic objects), we see that the thermodynamic arguments developed in section 3.1 for equilibrium at fixed droplet number apply *without modification* to this type of polydispersity. Therefore, the ultimate behaviour is found simply by substituting $\overline{V}$ for V_0 in our previous discussion. Thus the criterion for full stability in this case is $\overline{V} \leq V_B(\eta)$. It is also clear that in the stable regime the droplet distribution will evolve under the evaporation/condensation dynamics into a monodisperse one, whatever its initial polydispersity. This contrasts with the other regimes, where the final state will again have density n_0 of monodisperse droplets, but of size R_B and in coexis-

tence with an "infinite droplet" containing the excess amount of dispersed phase $(n_0(\overline{V} - V_B))$ not residing in finite droplets.

The situation when η is not the same for all droplets is more complex. To find a stability condition for this case, we consider first a more formal argument which reproduces the above result for a single η. If the emulsion is unstable, we expect that at long times the size distribution will split into a "coarsening part" and a "stable part". As equilibrium is approached, the coarsening part has some average size $\overline{V}_c$ which tends to infinity at long times. This requires that $\epsilon \to 0$, which in turn means that the stable part of the distribution is necessarily monodisperse, and of droplet size $V \to V_B$. (This corresponds to the coexistence condition between finite and an infinite droplet mentioned previously.)

Let n_0, n_s and n_c be respectively the number densities of all the droplets in the system, of those in the "stable part" and of those in the "coarsening part" of the distribution; clearly $n_0 = n_s + n_c$. Then as the system tends to equilibrium, the conservation of ϕ (which we define to include the trapped species) requires

$$n_0\overline{V} = n_s V_B + n_c\overline{V}_c \tag{3.21}$$

and hence

$$n_0(\overline{V} - V_B) = n_c(\overline{V}_c - V_B) \tag{3.22}$$

So if $V_B \geq \overline{V}$, then $0 \geq n_c(\overline{V}_c - V_B)$; but since $\overline{V}_c > V_B$, then $n_c = 0$ and a coarsening part of the distribution cannot exist in this case.

Now we consider the more general situation where there is polydispersity, not only in the initial droplet size, but also in the quantity η of trapped species present in the initial droplets. Let $n(\eta)$, $n_s(\eta)$ and $n_c(\eta)$ be the number densities of droplets which contain η trapped particles in the full distribution, and in its stable and coarsening parts respectively. As the system tends to equilibrium the conservation of ϕ and $n_0 = \int n(\eta)\, d\eta$ now requires

$$\int n(\eta)\overline{V} d\eta = \int n_s(\eta) V_B(\eta) d\eta + \int n_c(\eta)\overline{V}_c(\eta) d\eta \tag{3.23}$$

$$n_s(\eta) + n_c(\eta) = n(\eta) \equiv n_0 p(\eta) \tag{3.24}$$

where $p(\eta)$ is the probability of a given droplet having η trapped particles (which is time-independent). Hence

$$\begin{aligned} n_0 \overline{V} = \; & n_0 \int p(\eta) V_B(\eta) d\eta \\ & + \int n_c(\eta)(\overline{V}_C(\eta) - V_B(\eta)) d\eta \end{aligned} \tag{3.25}$$

which may be rewritten as

$$n_0(\overline{V} - \langle V_B(\eta)\rangle_\eta) = \int n_c(\eta)(\overline{V}_c(\eta) - V_B(\eta)) d\eta \tag{3.26}$$

So if $\overline{V} \leq \langle V_B(\eta)\rangle_\eta$, then

$$0 \geq \int n_c(\eta)(\overline{V}_c(\eta) - V_B(\eta)) d\eta \tag{3.27}$$

but since $\overline{V}_c(\eta) > V_B(\eta)$, then $n_C(\eta) = 0$ for all η, and no coarsening part of the distribution can exist.

In summary, a condition which is sufficient to ensure the full stability of emulsions with an arbitrary initial distribution of sizes V and trapped species η is:

$$\overline{V} \leq \langle V_B(\eta)\rangle_\eta \tag{3.28}$$

where $\overline{V} = \phi/n_0$ and $V_B(\eta)$ is as defined in Eq. 3.8: $V_B(\eta) = (3/4\pi)^{1/2}(\eta k_B T/2\sigma)^{3/2}$.

The assumptions behind this result are:

1. The trapped species has zero solubility in the continuous phase and forms an ideal solution in each droplet.

2. Coalescence is strictly absent.

3. The solubility of the main dispersed-phase species is nonzero (so that diffusion can occur) but small enough that it contributes negligibly to ϕ.

Subject to these assumptions, it is a rigorous result. It is easily established that condition Eq. 3.28 is not only sufficient for full stability but also necessary, in the sense that any distribution which does not satisfy Eq.3.28 can lower its free energy at fixed droplet number by a nucleated (if not a spinodal) coarsening process. As noted in section 3.2 for the monodisperse case, for an emulsion which is only slightly unstable and whose size distribution does not have a tail extending to large droplets, the nucleation time before coarsening begins may be very long. If there is a tail, a long induction time is not expected.

Notice that our rigorous condition Eq. 3.28 involves calculating $\langle V_B(\eta)\rangle_\eta$ by averaging over the probability distribution of the trapped species. This quantity is not the same as $V_B(\langle\eta\rangle)$; indeed for $\alpha \geq 1$ one has the general inequality

$$\int_0^\infty \eta^\alpha p(\eta)d\eta \geq \left(\int_0^\infty \eta p(\eta)d\eta\right)^\alpha \tag{3.29}$$

Since $V_B \sim \eta^{3/2}$ ($\alpha = 3/2$) we find that $\langle V_B(\eta)\rangle_\eta \geq V_B(\langle\eta\rangle)$. Hence the approximate stability requirement $\overline{V} \leq V_B(\langle\eta\rangle)$, based on the *mean* trapped particle number, underestimates the maximum initial droplet size. Accordingly this condition is sufficient, but not necessary, to ensure full stability.

3.7 The Metastable Regime (II)

For a polydisperse system the condition for full stability is clear (see above), whereas that for metastability is less obvious. Even when all droplets have the same η, metastability may depend on the details of the initial droplet size distribution. Certainly, if this has no upper limit (*i.e.*, there is a finite density of droplets above any given size), then the largest droplets will serve as nuclei for coarsening. As a qualitative rule, one can apply the argument of section 3.3 in a mean-field approximation, whereby an anomalously large droplet is considered to be exchanging material with a set of others, which for simplicity we treat as

having a single size $\overline{V}$. This enables a critical radius R_C to be estimated from Eq. 3.9 by replacing Eq. 2.20 for the length scale R_ϵ with

$$R_\epsilon \simeq \left(\frac{3}{4\pi}\right)^{1/3} \left(\frac{\overline{V}_0}{\overline{V}_0^{2/3} - \overline{V}_B^{2/3}}\right) \tag{3.30}$$

As before, if the initial size distribution contains *any* droplets larger than R_C, coarsening can be expected.

We may also make a similar approximation for emulsions formed at fixed concentration of trapped species, replacing R_0 with $\bar{R}_0$ and R_{0B} with $\bar{R}_{0B}$, in section 3.4.

If η varies between droplets, things are still more complicated, since nucleation is likely to involve droplets of larger than average η, as well as larger than average size. Although we still expect three regimes (fully stable, metastable and unstable) corresponding to those discussed in section 3.3 for the monodisperse case, the boundary between the metastable and unstable regimes may have a complicated dependence on the initial distribution of droplets and trapped species. This contrasts with the very simple criterion for full stability, Eq. 3.28 which applies for *arbitrary* initial conditions.

Note that the dynamics we propose for nucleation in the metastable region is peculiar to emulsions. For example, Reiss and Koper [14] discussed the equilibrium state and volume fluctuations of a single drop in a uniform environment with fixed supersaturation. They concluded that for their problem nucleation dynamics were likely to be extremely slow, and deduced a criterion for stability corresponding to that given by Kabalnov et al. [12]. This does not contradict our own conclusions, because Reiss and Koper consider a *single drop* as opposed to a population of droplets. For an emulsion in regime II, only the largest drop present need exceed the nucleation threshold to initiate coarsening, and in many cases a large enough droplet would already be present in the initial droplet size distribution. What is more, in a real emulsion with finite volume fraction, varia-

tions in the local environments experienced by individual droplets will be a source of dynamical fluctuations which may far exceed the purely thermal fluctuations considered in Ref. [14].

In summary, the stability conditions for a single droplet and a population of droplets, are very different. We suspect that even in a nominally monodisperse emulsion, nucleation rates are generally not negligible and hence the only reliable criterion for stability is the one we have given in section 3.6.

3.8 Other Equations of State

The thermodynamic arguments of sections 3.1 and 3.2 generalise readily to an arbitrary equation of state for the trapped species. Indeed, for the case where η is the same in all droplets, one need only replace Eq. 2.6 with,

$$f(V,\eta) = (V/v_b)f_b + 4\pi\sigma(3V/4\pi)^{2/3} + f_t(V,\eta) \tag{3.31}$$

where $f_t(V,\eta)$ is the free energy of η trapped particles in volume V and could include arbitrary interactions between these. If all droplets have the same η, the condition for stability remains that $\overline{V} \leq V_B$ where $V_B(\eta)$ is the droplet size corresponding to the absolute minimum of f'. For such droplets, the osmotic pressure $(-\partial f_t/\partial V)_\eta$ is again in exact balance with the Laplace pressure. The metastability criterion is again that $f'(V,\eta)$ has positive curvature. For the case where η is not the same for all droplets, the full stability criterion is again Eq. 3.28.

A complication arises if the interactions between the trapped species are attractive. Reiss and Koper [14] pointed out that in this case Eq. 2.22 for the droplets growth rate can become negative again for volumes much less than V_B, and hence develop a third, unstable fixed point (consider $U(R)$ becoming negative for $R < R_B$, for case $\epsilon > 0$ shown figure 2.2). They also correctly point out that

such an attraction is likely to cause phase separation within droplets. The latter occurs whenever $f_t(V,\eta)$ has negative curvature (with respect to V at fixed η); the form of $f_t(V,\eta)$ in Eq. 3.31 must then be modified to reflect the internal phase separation, and any negative curvature regions will then be replaced by zero-curvature ones (corresponding to tie lines). In this case, because of the surface tension contribution in Eq. 3.31, there can arise an additional minimum in f' which could lead, for example, to stable bidisperse emulsions for some range of initial conditions. The same can arise without intra-droplet phase separation, if $f_t(V,\eta)$ has a small enough positive curvature for this to be outweighed by the negative contribution from the surface tension term in Eq. 3.31. A detailed discussion of these cases is a possibility for future work.

The above results are sufficient, for example, to deal with the case of a distribution containing trapped salt (where $f_t(V,\eta)$ can be approximated by, say, the Debye Hueckel equation of state [41]) which is of interest in meteorological as well as emulsion stability contexts [30–34, 42].

In the case of repulsive interactions, at least, our stability condition Eq. 3.28 is also easily generalised to a situation in which there is more than one trapped species. Letting η_i be the number of particles of the ith species trapped within a droplet, then the condition for stability generalises to

$$\overline{V} \leq \langle V_B(\eta_1, \eta_2, \ldots)\rangle_{\eta_1,\eta_2,\ldots} \tag{3.32}$$

where $V_B(\eta_1, \eta_2, \ldots)$ is the droplet size corresponding to the absolute minimum of f'. A proof of this generalised stability condition is identical to that given in section 3.6, but with the single variable η replaced by the list of variables $\eta_1, \eta_2, \ldots$, and $V_B(\eta_1, \eta_2, \ldots)$ calculated from the new equation of state.

So far, we have not considered explicitly the role of surfactant (which is usually present to prevent droplet coalescence in emulsions), tacitly assuming that this merely alters the constant value of σ, the surface tension. For a surfactant that is

insoluble in the continuous phase, this surface tension will itself be a function of droplet size. We do not treat this case further, but note that it could be included in Eq. 3.31 by replacing the term in σ with a suitable "surface equation of state" for the trapped surfactant. The same applies to bending energy terms which could be significant for extremely small droplets.

3.9 Slightly Soluble "Trapped" Species

Throughout the above we have treated the trapped species as entirely confined in the emulsion droplets. In this section we briefly consider what happens if this third species is very slightly soluble. (For simplicity we treat η as the same for all droplets.) Our previous classification into regimes I,II and III, though no longer strictly applicable, remains a guide to the resulting behaviour. The discussion that follows is related to that of Kabalnov et al [12].

Recall that for entirely trapped species, the unstable regime (III) is characterised by the evolution of a bimodal distribution of droplet sizes, in which the larger droplets coarsen by the Lifshitz–Slyozov mechanism, while the smaller droplets adopt a size in equilibrium with the larger drops, which approaches V_B as coarsening proceeds. (This scenario is examined in more detail in chapter 4) If the trapped phase is now made slightly soluble, the larger drops will, as before, coarsen at a rate determined by the transport of the majority (more soluble) dispersed phase. However, the small droplets that remain cannot now approach a limiting size, but will themselves evaporate at a much slower rate governed by the transport of the "trapped" species. Therefore, in the unstable regime, a two-stage coarsening is expected. In the fully stable regime (I), on the other hand, the first of these processes (rapid coarsening of the larger droplets) is switched off. The droplet size distribution has a single peak, which in the fully insoluble case will approach a delta function at the initial mean size. However with slight solubility

coarsening will occur via the Lifshitz–Slyozov mechanism, but only at a slower rate controlled by the transport of the less soluble species. The behaviour in the metastable regime (II) is complex [12], possibly characterised by a "crossover" from coarsening controlled by the less soluble component to coarsening controlled by the more soluble component, and we do not pursue it here.

For a slightly soluble trapped species, the best prospect for stability is always to avoid the *rapid* coarsening process associated with the transport of the more soluble dispersed phase component. Since there is always *some* part of the size distribution that coarsens at the slower rate set by the trapped species, the requirement is satisfied so long as the size distribution remains single-peaked with the coarsening rate determined by the rate of diffusive flux of the least soluble (ie "trapped") species. We will now show that a sufficient condition for such behaviour is:

$$\overline{V}(0) \leq V_B(\overline{\eta}(0)) \tag{3.33}$$

where $\overline{\eta}(t)$ is the average number of trapped species in droplets at time t.

We prove the above condition Eq. 3.33 by considering the contrary case of a distribution which consists of both a rapidly coarsening and a quasi-stable part, with the rapid coarsening of the larger drops occurring at a rate determined by the transport of the most soluble component. As $t \to \infty$, the size V_L of the larger droplets becomes large, the supersaturation of the disperse phases will tend to zero, and the smaller drops will tend to sizes $V_B(\eta)$. Here η may now vary among droplets and with time.

The total number of droplets is no longer conserved but becomes time-dependent, and Eq. 3.26 is replaced by

$$n(0)\overline{V}(0) - n(t)\overline{V}_B(t) = \int n_L(\eta, t)(\overline{V}_L(t) - V_B(\eta))d\eta \tag{3.34}$$

where $n_L(\eta, t)$ is the number of droplets at the larger size $V_L(t)$, and $\langle V_B(t)\rangle_\eta$ has

been rewritten as $\overline{V}_B(t)$ for convenience. So if we can ensure that

$$\overline{V}(0) - \frac{n(t)\overline{V}_B(t)}{n(0)} \leq 0 \tag{3.35}$$

then $n_L(\eta, t) = 0$ and the distribution must be single-peaked.

Conservation of the less soluble component requires that

$$n(0)\overline{\eta}(0) = n(t)\overline{\eta}(t) \tag{3.36}$$

or

$$\frac{n(t)\overline{V}_B(t)}{n(0)} = \frac{\overline{\eta}(0)\overline{V}_B(t)}{\overline{\eta}(t)} \tag{3.37}$$

We next note that $V_B(0) = 0$ and assume that $V_B(\eta)$ is convex, as is the case for ideal phases where $V_B \sim \eta^{3/2}$. (This ensures that if $y_2 > y_1$, then $y_1 V_B(y_2) > y_2 V_B(y_1)$.) If so

$$\overline{V}_B(t) \geq V_B(\overline{\eta}(t)) \tag{3.38}$$

and

$$\overline{\eta}(0)\overline{V}_B(t) \geq \overline{\eta}(0)V_B(\overline{\eta}(t)) > \overline{\eta}(t)V_B(\overline{\eta}(0)) \tag{3.39}$$

To obtain the second inequality, we have again used the fact that $V_B(\eta)$ increases faster than linearly with η and also exploited the fact that $\overline{\eta}(t)$ increases with time (the latter follows from the fact that the number of droplets present must decrease as time proceeds). Hence $\overline{\eta}(0)\overline{V}_B(t)/\overline{\eta}(t) > V_B(\overline{\eta}(0))$ and

$$\overline{V}(0) - \frac{n(t)\overline{V}_B(t)}{n(0)} = \overline{V}(0) - \frac{\overline{\eta}(0)\overline{V}_B(t)}{\overline{\eta}(t)} < \overline{V}(0) - V_B(\overline{\eta}(0)) \tag{3.40}$$

So if $\overline{V}(0) \leq V_B(\overline{\eta}(0))$ then $\overline{V}(0) - n(t)\overline{V}_B(t)/n(0) < 0$ and $n_L(\eta, t) = 0$. Hence the distribution may only contain a single peak, and will coarsen at rate determined by the less soluble component.

We note that since $V_B(\overline{\eta}(0)) \leq \overline{V}_B(\eta(0))$, the condition given by Eq. 3.33 is less easily satisfied than our absolute stability condition, Eq. 3.28, which applies for the case of entirely trapped species. We also note, that although this condition is

sufficient, we have been unable to find a necessary condition. In other words, it is possible that some systems will not satisfy Eq. 3.33 but will nonetheless coarsen only slowly. Finally we emphasise that the derivation[§] of Eq. 3.33 requires $V_B(\eta)$ to increase faster than linearly with η; this is valid for ideal mixtures and most other systems (perhaps excluding any in which interactions between the trapped species are attractive; see section 3.8).

3.10 Conclusions

In this chapter, several new results were presented in the quantitative analysis of emulsion stabilisation by trapped species. A rigorous stability condition to prevent coarsening by a diffusive flux of dispersed phase was given (Eq. 3.28), which is valid even for emulsions with polydispersity in droplet size and number of trapped species. It was shown that even if the trapped species is slightly soluble, a condition to prevent coarsening by a flux of the more soluble species will continue to exist (Eq. 3.33). A previously published [12] condition for emulsion stability Eq. 3.7, was shown to correspond to a condition for metastability. Even if satisfying Eq. 3.7, emulsions formed with a fixed concentration of trapped species could require only a minor polydispersity in droplet size to nucleate coarsening: the only reliable criterion for stability is Eq. 3.8. Finally it was noted that similar stability conditions may be calculated for non–ideal trapped species, and merely requires the determination of V_B using the new trapped species equation of state.

[§]This assumes that the volume occupied by a given amount of trapped species is independent of its concentration.

Chapter 4

Coarsening of Unstable Emulsions

4.1 Overview

In the present chapter, long–time asymptotic solutions for the evolution of a continuous size distribution of droplets containing trapped species are determined. This work becomes relevant when the stability criteria presented in chapter 3 are not satisfied.

The late stage behaviour for unstable emulsions involves two populations of droplets: a coarsening part and a stable part. Coarsening is found to be driven by polydispersity in the larger (unstable) droplets, with the smaller (stable) droplets maintaining a size in equilibrium with the supersaturation ϵ. The smaller droplets are found to have no effect on the rate of coarsening, which is determined self consistently by the mechanism of Ostwald ripening in which the average size of drops is able to increase, while a constant volume fraction is maintained by a flux of material from smaller to larger droplets. The only effect of droplets being unable to fully dissolve, instead attaining a small but finite size $\simeq V_B$, is to reduce by V_B per droplet the total volume of disperse phase available to form larger coarsening droplets. This agrees with the result in chapter 3, predicting that if $\overline{V}_0 \leq V_B$

then a distribution of large coarsening droplets cannot exist. In Section 4.4 the treatment is extended to polydisperse η, and confirms the stability condition for polydisperse emulsions Eq. 3.8, derived by a different method in chapter 3.

4.2 The Physics of Coarsening

We consider conditions in which the requirement for stability (Eq. 3.28) is not satisfied, and for simplicity we take the same number of trapped particles η in each droplet. We assume all nucleation events have taken place, and consider the resulting coarsening at late times. This entails small supersaturation ϵ. Throughout this chapter we work in the scaled variables R', R'_B and t' defined in section 2.4.2, with

$$\begin{aligned} R' &\equiv \frac{RkT}{2\sigma v_b} \\ t' &\equiv t\frac{DC(\infty)k^2T^2}{4v_b\sigma^2} \\ {R'_B}^2 &\equiv \frac{3\eta k^3T^3}{32\pi\sigma^3 v_b^2} \end{aligned} \tag{4.1}$$

although the primes will now be omitted for convenience.

In the unstable case, as mentioned in section 2.4.2, the equation for static equilibrium (zero growth) of a given droplet, $U(R,\epsilon) = 0$, has both a stable fixed point close to the balanced droplet size ($R \sim R_B$) and an unstable one at $R \sim 1/\epsilon$. The latter will lead to coarsening. The following arguments will suggest that the presence of the additional, stable fixed point influences the coarsening dynamics only in a rather simple way. At long times, the main role of a population of stable droplets ($R \sim R_B$) is found to effectively exclude a finite proportion of the disperse phase from the coarsening process. The remaining part, whose volume fraction ϕ is effectively reduced, then coarsens almost normally.

To see this, we first expand $U(R,\epsilon)$ for small $R - R_B$ and small ϵ to obtain (in

reduced units)

$$U(R) = \epsilon/R_B - (R - R_B)\left(\frac{2 + \epsilon R_B}{R_B^3}\right) \tag{4.2}$$

with a root $U = 0$ at

$$R_T(t) = R_B + \epsilon(t)\left(\frac{R_B^2}{2}\right) + O(\epsilon^2) \tag{4.3}$$

At late times ϵ will be small and therefore, according to Eq. 4.2, the size of any droplet in the neighbourhood of R_B relaxes exponentially toward $R_T(t)$ with a fixed decay rate $2/R_B^3 + O(\epsilon)$. At long times, this process will be rapid compared with coarsening of droplets of size $R \gg R_B$; hence any non-coarsening part of the droplet distribution comprises an effectively monodisperse population of radius $R_T(t)$ obeying Eq. 4.3. Put differently, $R_T(t)$ is *determined* by ϵ, because the non-coarsening droplets are in local equilibrium with the ambient supersaturation at all times.

Now consider drops with size $R \sim 1/\epsilon$, in the neighbourhood of the second zero of $U(R, \epsilon)$ (this is the unstable fixed point of the growth equation at given ϵ). Expanding $U(R, \epsilon)$ in R about $R = 1/\epsilon$ we find

$$U(R) = (R - 1/\epsilon)\epsilon^3 + R_B^2\epsilon^4 \tag{4.4}$$

with a root

$$R_L(t) = 1/\epsilon - \epsilon R_B^2 \tag{4.5}$$

Accordingly, drops with $R(t) > R_L \sim 1/\epsilon$ will grow, lowering the supersaturation ϵ in the system. As this proceeds, the monodisperse small droplets ($R = R_T(t)$) will shrink slightly to remain in equilibrium with the current supersaturation. If one neglects this last effect, these droplets can play no role, at late times, other than to remove from the coarsening process an amount of material $n_0 V_B$ corresponding to that required to produce a stable monodisperse trapped emulsion in equilibrium with an infinite droplet. The excess material $n_0(V_0 - V_B)$ then becomes concentrated in fewer, larger droplets as coarsening proceeds by (essentially) the usual LSW mechanism. This scenario is confirmed in the following section, where we obtain an asymptotic solution for the coarsening behaviour.

4.3 Asymptotic Analysis

Following LSW [20, 21] we assume a continuous distribution of droplet sizes $n(R,t)$, with $n(R,t)\,dR$ representing the number density of droplets of radius $(R, R+dR)$, at time t. Since droplets of finite size cannot suddenly appear or disappear, the conservation of flux through droplet size space requires [20–22]

$$\frac{\partial n(R,t)}{\partial t} = -\frac{\partial (n(R,t)U(R,\epsilon))}{\partial R} \tag{4.6}$$

Conservation of the volume of disperse–phase species requires that

$$\frac{1}{C(\infty)v_b}\int_0^\infty \frac{4\pi}{3}R^3 n(R,t)dR + \epsilon = \epsilon_0 \tag{4.7}$$

where $\epsilon = (\overline{c}-C(\infty))/C(\infty)$ is the degree of supersaturation and $\epsilon_0 \equiv n_0\overline{V}_0/C(\infty)v_b + \epsilon(0)$.

Taking $R_T(t)$ and $R_L(t)$ as the two roots of $U(R,\epsilon) = 0$, as defined above, we now seek asymptotic solutions of the form

$$n(R,t) = A_T(R_T)f_T(R/R_T) + A_L(R_L)f_L(R/R_L) \tag{4.8}$$

where f_T and f_L are two different scaling functions. That is, we assume (see figure 4.1) that at late times the size distribution splits into two populations, each of fixed shape in terms of an appropriate reduced size variable, and each with some time–dependent amplitude A.

These two distributions are now assumed to *separately* obey Eq.4.6 for conservation of flux through droplet size space. This separation is valid so long as there is no significant range of sizes for which both populations overlap – which is increasingly true at late times. However, the two populations do interact via the supersaturation ϵ. We first solve $U(R_L,\epsilon) = 0$ for $\epsilon(R_L(t))$ to obtain

$$\epsilon = \frac{1}{R_L(t)}\left(1 - \frac{R_B^2}{R_L(t)^2}\right) \tag{4.9}$$

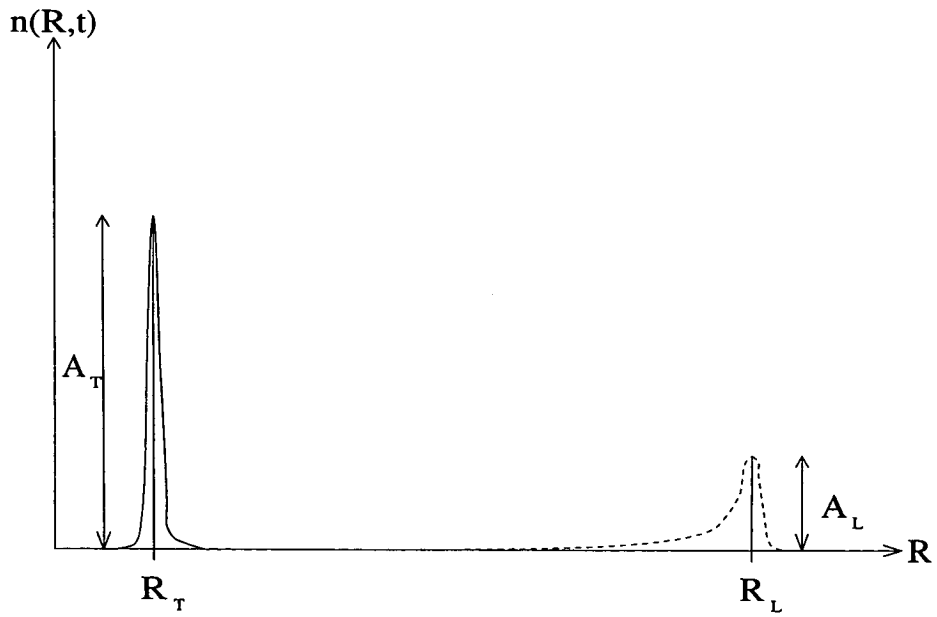

Figure 4.1: Approximating $n(R,t)$ by functions centred on R_T and R_L.

and note that, because of this equation, terms in ϵ and terms in $1/R_L$ are of the same order. In what follows we take the long time limit and therefore write $\epsilon = 1/R_L + O(1/R_L^3)$. We then impose conservation of volume fraction, and of the total number of droplets (n_0), to obtain A_T and A_L. This is done next.

4.3.1 Determination of A_T and A_L

The amplitudes A_T and A_L are determined by the constraints of conservation of volume fraction and conservation of the total number of droplets. We write $n(R,t) = n_T + n_L$, with $n_T = A_T f_T(R/R_T)$ and $n_L = A_L f_L(R/R_L)$. We then define f_T and f_L to be normalised so that $\int_0^\infty f_T(Z_T)dZ_T \equiv 1$ and $\int_0^\infty f_L(Z_L)dZ_L \equiv 1$, where $Z_T \equiv R/R_T$ and $Z_L \equiv R/R_L$. Conservation of total number of droplets then implies

$$A_T R_T + A_L R_L = n_0 \tag{4.10}$$

Defining $\int_0^\infty f_T Z_T^3 dZ_T/C(\infty)v_b \equiv B_{0T}$ and $\int_0^\infty f_L Z_L^3 dZ_L/C(\infty)v_b \equiv B_{0L}$, then

conservation of volume fraction implies

$$\frac{4\pi}{3}(A_T R_T^4(\epsilon) B_{0T} + A_L R_L^4(t) B_{0L}) + \epsilon = \epsilon_0 \tag{4.11}$$

or

$$A_L R_L(t) = \frac{(\epsilon_0 - \epsilon) - B_{0T} A_T (4\pi/3) R_T(\epsilon)^4}{(4\pi/3) B_{0L} R_L(t)^3} \tag{4.12}$$

Substitution into Eq.4.10 for A_T then gives

$$A_T = \frac{n_0}{R_T(\epsilon)} - \frac{(\epsilon_0 - \epsilon) - B_{0T} A_T (4\pi/3) R_T(\epsilon)^4}{(4\pi/3) B_{0L} R_L(t)^3 R_T(\epsilon)} \tag{4.13}$$

which to the order required is,

$$A_T = \frac{n_0}{R_T(\epsilon)} + O\left(\epsilon^3\right) \tag{4.14}$$

So using Eq. 4.14 and Eq. 4.12 we obtain

$$A_L = \frac{(\epsilon_0 - \epsilon) - n_0 B_{0T} (4\pi/3) R_T(\epsilon)^3}{(4\pi/3) B_{0L} R_L(t)^4} \tag{4.15}$$

Substituting Eq. 4.3 for $R_T(\epsilon)$ and Eq. 4.9 for $\epsilon(R_L)$ yields

$$A_L = \frac{\epsilon_0 - n_0 B_{0T} (4\pi/3) R_B^3}{(4\pi/3) B_{0L} R_L(t)^4} - \frac{(1 + (3R_B/2) B_{0T} (4\pi/3) R_B^3)}{(4\pi/3) B_{0L} R_L(t)^5} \tag{4.16}$$

where higher order terms are neglected.

4.3.2 Determination of n_T

We have assumed that $n_T(R,t)$ satisfies (by itself) the continuity equation in droplet size space,

$$\frac{\partial n_T(R,t)}{\partial t} = -\frac{\partial (n_T(R,t) U(R,\epsilon))}{\partial R} \tag{4.17}$$

Writing $n_T(R,t) = A_T f_T(Z_T)$ we obtain

$$\frac{\partial (A_T f_T(Z_T))}{\partial t} = -\frac{\dot{R}_T}{R_T} Z_T A_T \frac{\partial (f_T(Z_T))}{\partial Z_T} + \frac{\partial A_T}{\partial t} f_T(Z_T) \tag{4.18}$$

$R_T(t) = R_B + \epsilon(t)R_B^2/2 + O(\epsilon^2)$, which gives $\dot{R}_T = \dot{\epsilon}(t) + O(\dot{\epsilon}\epsilon)$. Since $\epsilon \sim 1/R_L$, then $\dot{\epsilon} \sim 1/R_L^2 \sim \epsilon^2$ and $\dot{R}_T \sim \epsilon^2$. So $A_T = n_0/R_T + O(\epsilon^3)$, gives $\dot{A}_T = -\dot{R}_T n_0/R_T^2 + O(\dot{\epsilon}\epsilon^2) \sim \epsilon^2$, so that the time dependence of n_T is $O(\epsilon^2)$.

Working at $O(\epsilon)$ we obtain $\frac{\partial}{\partial R}\left(A_T f_T U(R,\epsilon)\right) = 0$, which may be solved to obtain f_T as

$$f_T = \frac{Z_T^4}{\epsilon Z_T^3 - Z_T^2 + R_B^2/R_T^2} \tag{4.19}$$

However since f_T diverges as $Z_T \to \infty$, the solution is not a physically acceptable one.

An alternate but normalisable solution to Eq. 4.17 which is also correct at $O(\epsilon)$ is given by

$$n_T = A_T \delta\left(Z_T - 1\right) \tag{4.20}$$

Noting that $U(R,\epsilon)$ is zero when $R = R_T(t)$ and $Z_T = 1$, then since $\delta(Z_T - 1)$ is zero *except* when $Z_T = 1$, then the right hand side of Eq. 4.17 is identically zero. However since

$$\frac{\partial A_T \delta(Z_T - 1)}{\partial t} = \frac{\dot{R}_T}{R_T} A_T \frac{\partial \delta}{\partial Z_T} + O\left(\epsilon^4\right) \tag{4.21}$$

and $\dot{R}_T \sim \dot{\epsilon} \sim \epsilon^2$, then

$$\frac{\partial A_T \delta(Z_T - 1)}{\partial t} \sim \epsilon^2 \tag{4.22}$$

Hence the solution is correct at order ϵ, with $f_T = \delta(Z_T - 1)$ giving $B_{0T} = 1/C(\infty)v_b$.

This simplifies A_L to

$$A_L = \frac{\epsilon_0 - (n_0(4\pi/3)R_B^3)/(C(\infty)v_b)}{(4\pi/3)B_{0L}R_L(t)^4} - \frac{(1 + (3R_B/2)(4\pi/3)R_B^3)/(C(\infty)v_b)}{(4\pi/3)B_{0L}R_L(t)^5} \tag{4.23}$$

which since Eq. 4.7 has $\epsilon_0 = n_0\overline{V}_0/C(\infty)v_b + O(\epsilon)$, Eq. 4.23 may be written in the alternate form of

$$A_L = \frac{n_0\left(\overline{V_0} - V_B\right)}{C(\infty)v_b(4\pi/3)B_{0L}R_L(t)^4} + O(\epsilon^5) \tag{4.24}$$

4.3.3 Determination of n_L

We have assumed that $n_L(R,t)$ satisfies (by itself) the continuity equation in droplet size space,

$$\frac{\partial n_L(R,t)}{\partial t} = -\frac{\partial (n_L(R,t)U(R,\epsilon))}{\partial R} \tag{4.25}$$

Writing $n_L(R,t) = A_L f_L(Z_L)$ we obtain

$$\frac{\partial (A_L f_L(Z_L))}{\partial t} = -\frac{\dot{R}_L}{R_L} Z_L A_L \frac{\partial (f_L(Z_L))}{\partial Z_L} + \frac{\partial A_L}{\partial t} f_L(Z_L) \tag{4.26}$$

Defining

$$K_1 \equiv \frac{\epsilon_0 - n_0(4\pi/3)R_B^3/C(\infty)v_b}{(4\pi/3)B_{0L}} \tag{4.27}$$

and

$$K_2 \equiv \frac{1 + (3R_B/2)(4\pi/3)R_B^3/C(\infty)v_b}{(4\pi/3)B_{0L}} \tag{4.28}$$

then we find,

$$\frac{\partial A_L}{\partial t} = -4\frac{\dot{R}_L}{R_L} A_L - K_2 \frac{\dot{R}_L}{R_L^6} \tag{4.29}$$

So we obtain

$$\frac{\partial n_L(R,t)}{\partial t} = -A_L \frac{\dot{R}_L}{R_L}\left(4f_L + Z_L \frac{\partial (f_L(Z_L))}{\partial Z_L}\right) - K_2 \frac{\dot{R}_L}{R_L^6} f_L \tag{4.30}$$

We next write $\partial(n_L(R,t)U(R,\epsilon))/\partial R$ in terms of Z_L to obtain Eq. 4.25 in terms of scaled variables as

$$\begin{aligned} \dot{R}_L R_L^2 (4f_L + Z_L \tfrac{\partial (f_L(Z_L))}{\partial Z_L}) + \tfrac{K_2 \dot{R}_L}{R_L^3 A_L} f_L = \; & \left[f_L \left(-\tfrac{1}{Z_L^2} + \tfrac{2}{Z_L^3} - \tfrac{4(R_\alpha/R_L)^2}{Z_L^5} \right) \right. \\ & \left. + \tfrac{\partial (f_L(Z_L))}{\partial Z_L} \left(\tfrac{1}{Z_L} - \tfrac{1}{Z_L^2} + \tfrac{(R_\alpha/R_L)^2}{Z_L^4} \right) \right] \end{aligned} \tag{4.31}$$

Expanding $1/(R_L^3 A_L)$ to lowest order in $1/R_L$ we obtain $K_2 \dot{R}_L / R_L^3 A_L \to K_2 \dot{R}_L R_L$; keeping only the leading terms on the right hand side we are left with

$$\begin{aligned} \dot{R}_L R_L^2 (4f_L + Z_L \tfrac{\partial (f_L(Z_L))}{\partial Z_L}) + K_2 \dot{R}_L R_L f_L = \; & \left[f_L \left(-\tfrac{1}{Z_L^2} + \tfrac{2}{Z_L^3} \right) \right. \\ & \left. + \tfrac{\partial (f_L(Z_L))}{\partial Z_L} \left(\tfrac{1}{Z_L} - \tfrac{1}{Z_L^2} \right) \right] \end{aligned} \tag{4.32}$$

Since the R.H.S. is a constant, then as $t \to \infty$ the L.H.S. must also approach a constant value. Trying $R_L = \Gamma t^\beta$ with Γ a constant, then

$$\dot{R}_L R_L^2 = \beta \Gamma^3 t^{3\beta-1} \tag{4.33}$$

and

$$\dot{R}_L R_L = \beta \Gamma^2 t^{2\beta-1} \tag{4.34}$$

Clearly both will tend to zero if $\beta < 1/3$, which would not correspond to a coarsening state. However if $\beta > 1/3$ then the L.H.S of the equation would diverge at late times. Hence $\beta = 1/3$, and as $t \to \infty$, $\dot{R}_L R_L \to 0$. Writing $\gamma = \Gamma^3/3$ then results in

$$\begin{aligned}\left[4f_L + Z_L \tfrac{\partial(f_L(Z_L))}{\partial Z_L}\right] = \; & \gamma \left[f_L \left(-\tfrac{1}{Z_L^2} + \tfrac{2}{Z_L^3} \right) \right. \\ & \left. + \tfrac{\partial(f_L(Z_L))}{\partial Z_L} \left(\tfrac{1}{Z_L} - \tfrac{1}{Z_L^2} \right) \right] + O(\epsilon)\end{aligned} \tag{4.35}$$

where $Z_L = R/R_L(t)$. This equations is identical to that solved by Bray [22], resulting in the consistency requirement $\gamma = 4/27$, and the solution

$$f_L(Z_L) = \begin{cases} \frac{A Z_L^2 \exp\left(\frac{-3}{3-2Z_L}\right)}{(3+Z_L)^{7/3}(3/2-Z_L)^{11/3}} & 0 \le Z_L < 1.5 \\ 0 & 1.5 \le Z_L \end{cases} \tag{4.36}$$

where A is a constant which is determined by the condition $\int f_L(Z_L) dZ_L = 1$.

The above argument shows that the equation of motion for R_L is exactly the same as in a standard coarsening problem (with no trapped species) [22], to the leading order in small ϵ. Accordingly the solution for $R_L(t)$, which involves seeking a specific γ for which the scaling distribution remains self-consistent in the long-time limit, is also the same. The only difference is in the *amplitude* A_L which, as shown in Eq. 4.23, has to the leading order in ϵ been shifted by a constant amount corresponding to a reduction in ϵ_0. In other words, in the long time limit the large droplets behave *precisely* as they would for an emulsion with no trapped species but with a reduced initial volume fraction determined by Eq. 4.24 as $n_0(V_0 - V_B)$. (Obviously, the latter is assumed positive; otherwise the emulsion is stable and will not coarsen.)

This is perhaps surprising, since according to Eq. 4.3, the decaying supersaturation $\epsilon(t)$ causes the small droplets to give up material at a rate that could perturb $\dot{\epsilon}$ significantly; this might be expected to lead to a slower decay of $\epsilon(t)$ and hence (via Eq. 4.9) of $R_L(t)$. However, this is not a correct argument: for, as mentioned above, the Lifshitz-Slyozov mechanism leads to an autonomous equation for $R_L(t)$ whose time development is then entirely fixed by the self-consistency requirement on γ. Given the behaviour of $R_L(t)$, the ambient supersaturation $\epsilon(t)$ follows directly from Eq. 4.9; the latter in turn dictates the evolution of the size $R_T(t)$ of the small droplets, via Eq. 4.5.

4.4 Polydispersity in Trapped Species

We now consider the effect of polydispersity in η on the asymptotic solutions for the droplet size distribution.

The growth rate for an individual drop is given by

$$U(R, \epsilon, \eta) = \frac{\epsilon}{R} - \frac{1}{R^2} + \frac{R_B^2(\eta)}{R^4} \tag{4.37}$$

and now varies even for droplets of the same size. So $R_T(\eta, t)$ now also varies between droplets. The number density of droplets of size R at time t, $n(R, t)$, is now generalised to the number density of droplets of size R at time t with η trapped particles $n(R, t, \eta)$. We will continue to consider the droplet size distribution as consisting of two peaks.

Before considering the generalisations of conservation of total droplet volume and conservation of total number of droplets, we make the following important assumption:

1. That there are no correlations between a droplet's volume and the number of trapped particles η it contains.

We also continue to assume that:

2. A large droplet's growth is unaffected by the number of trapped species it contains (and hence the large droplets' size distribution is unaffected by variations in the number of trapped species), with the number of trapped species in large droplets assumed negligible in comparison with the quantity of soluble species they contain.

The first assumption allows the droplet size distribution $n(R,t,\eta)$ to be written as $n(R,t,\eta) = n(R,t)p(\eta)$, where $p(\eta)$ is the probability distribution for the number of trapped species in a droplet. The second assumption means that R_L is independent of η, so that the droplet size distribution for the growing droplets becomes

$$n_L = A_L(t) f_L(R/R_L(t))p(\eta) \tag{4.38}$$

We shall assume the small droplet size distribution to be of the form

$$n_T = A_T(t)\delta(R - R_T(\eta,t))p(\eta) \tag{4.39}$$

which we later show to be correct at $O(\epsilon)$.

Conservation of the number of droplets now becomes

$$\begin{aligned} &\int d\eta \int dR A_T(t)\delta(R - R_T)p(\eta) + \\ &\int d\eta \int dZ_L R_L(t) A_L(t) f_L(Z_L)p(\eta) = n_0 \end{aligned} \tag{4.40}$$

which after integrating over R, η, and Z_L as required, gives

$$A_T(t) + A_L(t)R_L(t) = n_0 \tag{4.41}$$

where f_L is normalised as in section 4.3.1. Similarly, integration of conservation of droplet volume over R, η, and Z_L, gives

$$\frac{(4\pi/3)A_T(t)}{C(\infty)v_b}\langle R_T^3(\eta,t)\rangle_\eta + (4\pi/3)A_L(t)R_L^4(t)B_{OL} = \frac{n_0\overline{V}_0}{C(\infty)v_b} + O(\epsilon) \tag{4.42}$$

where we used $n_0\overline{V}_0/v_bC(\infty) = \epsilon_0 + O(\epsilon)$, and $\overline{V}_0$ is the average initial droplet volume. So Eq. 4.42 gives $A_LR_L \sim 1/R_L^3 \sim \epsilon^3$, and Eq. 4.41 becomes

$$A_T = n_0 + O(\epsilon) \tag{4.43}$$

So substitution of Eq. 4.43 into Eq. 4.42, and noting that $R_T(\eta, t) = R_B(\eta) + O(\epsilon)$, we get

$$A_L(t) = \frac{n_0\left(\overline{V}_0 - \overline{V}_B\right)}{C(\infty)v_b(4\pi/3)B_{0L}R_L^4} + O(\epsilon^5) \tag{4.44}$$

where we have written $\overline{V}_B = \langle(4\pi/3)R_B^3\rangle_\eta$.

We continue to assume that both n_T and n_L individually satisfy the continuity equation in droplet size space. Hence for the small droplets we have

$$\frac{\partial n_T}{\partial t} = -\frac{\partial n_T U(R,\epsilon,\eta)}{\partial R} \tag{4.45}$$

and hence

$$\frac{\partial(A_T\delta(R-R_T))}{\partial t} = -A_T\frac{\partial\delta(R-R_T)U(R,\epsilon,\eta)}{\partial R} \tag{4.46}$$

where we have cancelled $p(\eta)$ on either side. Since $U(R,\epsilon,\eta) = 0$ when $R = R_T$, then the right hand side of Eq. 4.46 is identically zero (as in section 4.3.2). Also since $A_T = n_0 + O(\epsilon^3)$, and $\partial\delta(R-R_T)/\partial t = \partial\delta(R-R_T)/\partial(R-R_T)(-\dot{R}_T/R_T) \sim \epsilon^2$, the solution is correct at $O(\epsilon)$.

For the large droplet distribution we have

$$\frac{\partial n_L}{\partial t} = -\frac{\partial n_L U(R,\epsilon,\eta)}{\partial R} \tag{4.47}$$

which integrating over η on both sides gives

$$\frac{\partial A_Lf_L}{\partial t} = -A_L\frac{\partial f_L U(R,\epsilon,\langle R_B^2\rangle_\eta)}{\partial R} \tag{4.48}$$

which may be solved as in section 4.3.3. We note that in the asymptotic solution $\langle R_B^2\rangle_\eta$ is negligible as $R_L \to \infty$ and hence does not appear in the final solution.

Hence we have

$$\begin{aligned} n_T &= n_0\delta(R - R_T(\eta))p(\eta) + O(\epsilon^2) \\ n_L &= A_Lf_L(R/R_L)p(\eta) \end{aligned} \tag{4.49}$$

with A_L given by Eq. 4.44, and f_L, R_L as in section 4.3.3. We note that since R_T is a function of η then if $p(\eta)$ is a continuous function, then n_T will also be a continuous function of η.

Hence the only changes due to polydisperse η are the requirement of

$$n_0\overline{V}_0 > n_0\langle V_B(\eta)\rangle_\eta \tag{4.50}$$

for the existence of n_L (and hence coarsening to occur), and the presence of a *continuous* size distribution of stable, shrunken droplets (for a continuous $p(\eta)$). So as in Eq. 3.28 in chapter 3, we find the condition that if $n_0\overline{V}_0 \leq n_0\langle V_B(\eta)\rangle_\eta$, then $n_L = 0$ and the distribution must be stable.

Finally, we make a few observations regarding the assumption that we may treat a droplet's η_i and initial volume as independent. Since in the long time limit the number of droplets in the shrunken distribution tends to n_0, the assumption will have negligible affect on the calculation of $\langle V_B(\eta)\rangle_\eta$ made using $p(\eta)$. Then since A_L, R_L and $f_L(R/R_L)$ will also be unaffected, the assumption may only affect the dependence of n_T and n_L on η. Hence the qualitative behaviour of the distribution is unaffected by the assumption of uncorrelated η_i and V_i, with the only possible affect being a different distribution of η_i's in the stable and coarsening distribution.

4.5 Conclusions

The dynamics of insufficiently stabilised emulsions containing trapped species are virtually unchanged from those of an emulsion without trapped species. The only effect of the trapped species on the coarsening distribution is to reduce the volume fraction of the growing droplets to $n_0(V_0 - V_B)$, due to the volume fraction of material $\simeq n_0V_B$ contained in the coexisting shrunken droplets. So we recover the stability condition of Eq. 3.8 in chapter 3, that if $V_0 < V_B$ then $n_L = 0$ and

coarsening cannot occur.

Similarly, when there is polydispersity in η, the only affect on coarsening is to reduce the volume fraction of the growing droplets to $n_0(\overline{V}_0 - \langle V_B(\eta)\rangle_\eta)$. Hence if $\overline{V}_0 < \langle V_B(\eta)\rangle_\eta$ then $n_L = 0$ and coarsening cannot occur. So the analysis confirms the result in chapter 3 for the general stability condition Eq. 3.28.

Chapter 5

Applications of Osmotic Stabilisation

5.1 Optimal Sizing of Emulsions

The use of "trapped", or less soluble species to stabilise emulsions is widespread in industry [43]. Such emulsions can be prepared mechanically with various average droplet sizes. Let us assume that any trapped species is dissolved at uniform concentration c_t through the dispersed phase material. As explained in Section 3.5, to form a stable emulsion one must ensure that the initial droplet size is sufficiently *large*. Roughly speaking, this ensures that the typical Laplace pressure $2\sigma/R$ is smaller than the osmotic pressure $c_t k_B T$. (The quantitative version of this, applicable to any initial size distribution, is Eq. 3.28.) Clearly, it is important to resist the temptation to make the initial emulsion too fine (which in ordinary emulsions might be expected to delay coarsening for the maximum possible time). In practice, the need to avoid sedimentation (and perhaps coalescence, which we have neglected) may set an optimal initial size close to, but above, the absolute stability threshold, Eq. 3.28. For the reasons discussed in

Section 3, the weaker "spinodal" condition [12] Eq. 3.7, even for a nominally monodisperse initial state, cannot guarantee stability.

5.1.1 Orders of Magnitude

Trapped species have been used to stabilise both hydrocarbon and fluorocarbon emulsions [29,43]. Such emulsions have surface tensions [29,43] $\sigma \sim 10^{-1}\mathrm{Nm}^{-1}$. As a rough estimate emulsion stability occurs when the osmotic pressure of trapped species exceeds that of the Laplace pressure (see chapter 3 for details, and Eq. 3.28 for the exact condition for stability). Hence a rough estimate of the minimum required quantity of trapped species to stabilise an emulsion may be determined from

$$c_t k_B T \sim \frac{\sigma}{R} \tag{5.1}$$

So letting c_M be the molar concentration of trapped species, and writing the gas constant as R_G, then we may express the above Eq. 5.1 as

$$c_M R_G T \sim \frac{\sigma}{R} \tag{5.2}$$

giving

$$c_M \sim \frac{\sigma}{R_G T R} \tag{5.3}$$

At room temperature $R_G T \sim 10^3\mathrm{J}$, so Fluorocarbon emulsions with droplets of radii $R \sim 10^{-7}\mathrm{m}$ require a minimum $c_M \sim 10^3\mathrm{moles\ m}^{-3} = 1\mathrm{mole}$ per litre, to be stabilised. Similarly Hydrocarbon emulsions with radii $R \sim 10^{-6}\mathrm{m}$ at room temperature require a minimum $c_M \sim 10^2\mathrm{moles\ m}^{-3} = 10^{-1}\mathrm{moles}$ per litre, to be stabilised. We note that both of the required concentrations are small, which is consistent with our assumption in chapter 2 of the trapped species being ideal.

5.2 Reversing the Coarsening Process

Consider a situation where an emulsion is prepared in an unstable state (for example by mechanical agitation) and then starts to coarsen. We now ask what will happen if, after some time interval, a large number of small droplets (containing a trapped species) are added to the emulsion, causing the stability condition $\overline{V}_0 \leq \langle V_B(\eta)\rangle_\eta$ to become satisfied for the system as a whole. According to the arguments of section 3.6, the emulsion is now unconditionally stable. Therefore it will not coarsen further. What is more, for a given total volume fraction ϕ and a given population of trapped species, the final state of the system is the unique one in which droplets of all η have a common chemical potential for the (mobile) disperse–phase species. Thus the addition of the small droplets will not only prevent further coarsening, but will in general cause previously coarsened droplets to *redissolve*. Indeed, if there are no trapped species in the initial unstable droplets, these will evaporate completely, and their material will be entirely absorbed by the added droplets [44].

In principle, the coarsening process can be reversed even when it is complete. For example, a system of small oil-in-water emulsion droplets with trapped species present can, by the evaporation-condensation mechanism, take up oil from an excess bulk phase of pure oil. If the stability condition $\overline{V}_0 \leq \langle V_B(\eta)\rangle_\eta$ is met by the system as a whole*, the bulk phase of oil will disappear entirely (though obviously this process may be slow in practice). Like the rest of our conclusions, this one applies only if both coalescence, and diffusion of the trapped species through the continuous phase, are strictly negligible. With these assumptions, we may minimise the free energy with the constraint of fixed trapped species in each drop; the above result for the equilibrium state follows immediately.

*Where $\overline{V}_0$ has now been defined to include the volume of the bulk phase.

5.3 Formation of Mini-emulsions by Shrinking

"Mini-emulsions", comprised of droplets with radii of between 50 and 150 nm, have many potential uses in industrial and pharmaceutical applications [43]. However their formation by traditional mechanical methods, where droplets are formed by strongly shearing the ingredients, is limited by the high energy required by the process [45], and the difficulty of getting a uniform droplet size. An alternative route is to create an emulsion of relatively large drops (whose size is also more controllable) and then "shrink" them to the required, smaller size. The following describes a non-mechanical method which would allow this to be done.

Consider a situation in which a bulk reservoir of the dispersed-phase species (say, oil), containing trapped species at concentration c_b, is placed in contact with a stable emulsion of oil droplets (in water, say) each containing η molecules of the trapped species (see figure 5.1). This system is then allowed to reach equilibrium under the evaporation-condensation mechanism. (To speed the process, some gentle agitation of the emulsion might be desirable.)

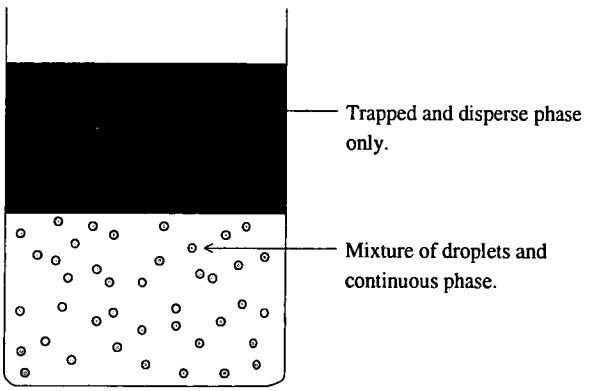

Figure 5.1: Droplets shrink to attain a stable size, which is in equilibrium with an excess bulk phase that also contains a trapped species.

A final state of equilibrium will be reached when the chemical potential of the

dispersed phase species in the emulsion equates to that in the bulk. This requires

$$\Pi_{osm}^{bulk} = \Pi_{osm}^{drop} - \Pi_L \tag{5.4}$$

where $\Pi_{osm}^{bulk,drop}$ are the osmotic pressures of trapped species in the bulk and droplets and Π_L is the Laplace pressure in the droplets. For ideal solutions this condition reads

$$c_b = \frac{\eta}{(4\pi/3)R^3} - \frac{2\sigma}{Rk_BT} \tag{5.5}$$

which is an equation for the final droplet size R. By increasing c_b the final droplet size can be made as small as one wishes: effectively the oil can be "squeezed out" of the emulsion by the osmotic action of the trapped species, now present in the bulk oil phase at higher concentration. (This contrasts with the last example in section 5.2, where a bulk phase, containing no trapped species, could be entirely absorbed by the emulsion droplets.) Once the desired size of mini-emulsion is reached, it can be removed and will remain stable.

Note that, because the trapped species is insoluble in the continuous phase (water in this example), there is no need for a semipermeable membrane to prevent its transfer between the bulk oil phase and the emulsion droplets. Therefore, in practice, a more rapid exchange equilibrium might be reached if the "bulk" oil phase instead took the form of large macroemulsion droplets which can later be separated out easily by sedimentation. Moreover, there is no need for the trapped species in the bulk oil phase and the trapped species in the mini-emulsion droplets, to be identical; so long as both are insoluble in water, the same condition for osmotic equilibrium will apply. Therefore one can "shrink" an emulsion containing an expensive trapped species (such as a fragrance or drug) by contacting it with a cheap polymer solution.

The shrinking process should not only achieve small droplet sizes, but may also allow one to reach concentrations of the trapped phase that would be unattainable by normal means. For example, by making an emulsion of dilute polymer solution and then shrinking the droplets, it may be possible to achieve within each droplet

a highly concentrated polymer solution, too viscous to be dispersed mechanically in its own right.

These ideas may be relevant to various encapsulation technologies. Obviously, the designation of "oil" and "water" in the above is arbitrary and these could be any two phases. We have assumed throughout that coalescence is negligible, which is commonly the case for oil-in-water emulsions so long as they contain a surfactant (typically ionic), to give a surface repulsion between droplets. The presence of the surfactant should not alter our arguments, so long as it is soluble enough in the continuous phase that the surface tension σ does not vary between droplets. In principle, for small enough mini-emulsions, the surfactant could also give rise to significant bending energy terms in the free energy of a droplet, which could be included if required (see section 3.8).

Chapter 6

Effects of Micelles on Emulsion Stability

6.1 Introduction

It is well known that micelles can affect the rate of Ostwald ripening [29,47–52], and it is also well known that micelles can greatly enhance an oil's solubility [2,29], with oil being solubilised *within* micelles [2,46]. Hence a possibility is that micelles may be able to increase the rate of Ostwald ripening by solubilising oil within their cores and acting as *shuttles* to transfer oil between droplets. Since the solubility of disperse phase may have little effect on the rate at which it is transferred by micelles, a mechanism of micelle–mediated oil transfer could destabilise an osmotically stabilised emulsion by transporting the previously trapped species between droplets.

The present chapter considers how micelles shuttling oil between droplets may affect the rate of Ostwald ripening*. We consider both the scenarios where the

*Throughout this chapter, we will denote the disperse phase as "oil" and the continuous phase as "water"; these roles could be reversed.

rate of transfer of oil by micelles is diffusion limited, and when it is reaction limited. In the diffusion limited case we firstly consider coarsening with oil and surfactant exchange only between micelles and droplets, then later we allow oil and surfactant to be exchanged between micelles, modelling the effect by assuming the rate of exchange to be much faster than the rate of diffusion of micelles between droplets. We calculate the effect of micelles on an emulsion droplet's growth rate (and the resulting droplet size distribution), and the rate at which micelles may solubilise an emulsion into oil swollen micelles. We also indicate transient phenomena which may occur early on in the coarsening process.

An outline of the chapter is as follows. Firstly the possible mechanisms by which micelles may solubilise oil are briefly described, but for generality no particular model is adopted, either for the micelles themselves or the mechanism by which they solubilise oil (section 6.2). We next consider coarsening when the rate is limited by the diffusion of micelles between droplets (section 6.3), but without allowing oil and surfactant to be exchanged between micelles. Section 6.3 calculates a droplet's growth rate, and demonstrates that provided micelles may not solubilise all the oil, then the resulting late–time droplet size distribution will be that determined by LSW [20,21]. The rate of diffusion limited solubilisation of oil into previously empty micelles is considered in section 6.4, which considers both the time to solubilise all the oil and the time for micelles to become saturated (and unable to solubilise any more oil). Section 6.4 also discusses transient phenomena which may occur when empty unswollen micelles are added to a dilute emulsion. Section 6.5 considers the effect of a rapid exchange of oil and surfactant molecules between micelles, finding the same qualitative results as when the effect was neglected. Reaction limited coarsening and solubilisation is considered in sections 6.6 and 6.7. Section 6.8 discusses when micelle–mediated coarsening will be important, finding the dominant type of coarsening to be determined by two parameters, enabling a kinetic diagram to be given which indicates which type of coarsening will be dominant for given parameters. A summary and conclusion is

given in section 6.9.

The original motivation for the work in this chapter was to determine the extent to which micelles may destabilise an osmotically stabilised emulsion. However, the current lack of theoretical and experimental results mean that it is not possible to give a clear and definitive answer to this question. Instead the chapter intends to provide a clear and reliable, model–independent, theoretical framework for the effects of micelles on emulsions, so as to enable further experimental and theoretical work to be more clearly and carefully focused. Finally we note that the following work may also apply when coarsening is mediated not by micelles, but by molecules which may bind to disperse phase molecules and subsequently transport them between droplets.

6.2 Mechanisms for Solubilisation

Molecular dynamics simulations [53,54] have suggested three possible mechanisms by which oil may become solubilised within micelles[†].

1. A small amount of the oil drop becomes dissolved in the continuous (water) phase, and then (subsequently) is adsorbed into micelles. A theoretical discussion of the effects of micelles on coarsening of emulsions with oil to micelle transfer by this mechanism, is given by Kabalnov [62].

2. A group of surfactant molecules leave the surface of a droplet, carrying a number of solubilised oil molecules within them. This process is referred to as *budding*. Surfactant is replenished by extra surfactant being adsorbed

[†]A discussion of the effect of an oil molecules geometry on solubilisation rate, along with a summary of solubilisation mechanisms, is given by Coupland et al [46]. A general discussion on solubilisation by micelles is given in "Surfactant Aggregation" by Clint [2].

onto a droplet, either before or after budding has occurred. This is similar to a mechanism which is considered theoretically by Granek et al [55].

3. A micelle collides with a droplets surface, and subsequently solubilises extra oil molecules by incorporating them within the micelle (or alternately a very swollen micelle could lose oil molecules to the droplet), before returning to the continuous phase. Possible evidence for such a mechanism is provided by results of Carroll et al [56–60], and is discussed in Appendix B.

The simulations [53, 54] showed that the solubilisation of oil into micelles by mechanism 1 occurred at a rate comparable with the combined rate of mechanisms 2 and 3. They also found that for small oil molecules the rate of mechanism 1 was higher than the combined rate of mechanisms 2 and 3, but that for larger (less soluble) oil molecules, the opposite was true. So solubilisation of oils with a low solubility will be dominated by mechanisms 2 and 3.

In addition to the above we also note the mechanism in which

4. Surfactant monomer is preferentially oil soluble, with micelles dissociating and surfactant becoming dissolved within oil droplets, lowering a droplets free energy and inducing spontaneous budding. This effect is studied experimentally by Miller et al [61] for surfactants close to their cloud point. The mechanism by which this occurs may also be similar to that described by Granek et al [55].

In the following work we do not consider any specific mechanism, taking the micelle–mediated rate of exchange of oil between droplets as being limited either by the diffusion of micelles to a droplet (diffusion limited), or by the rate at which micelles exchange oil with droplets (reaction limited).

6.3 Diffusion Limited Coarsening: A Simple Model

In the next 3 sections (6.3 to 6.5) we assume that the rate of solubilisation of oil is limited by the rate at which micelles diffuse to a droplet's surface. The model we use also assumes that:

1. Micelles in equilibrium at a droplet's surface will contain a unique number of surfactant molecules S_m, and a unique volume of solubilised oil V_m, both being determined by the given droplet's chemical potential (and hence, radius): $V_m = V_m(R), S_m = S_m(R)$.

2. There are no interactions between micelles, either via coalescence, diffusive interactions, or swelling/deswelling by oil diffusion between micelles. This is an approximation which makes the calculations much easier, although in practice corrections to it will arise.

3. The diffusion field relaxes much more rapidly than the rate at which droplets grow. (This assumption is later shown to be self consistent).

4. The excess chemical potential of oil in droplets is small enough that the volume fraction of oil solubilised in micelles adjacent to a droplet $\phi_m(R)$, may be linearised about that of bulk oil ϕ_m^b.

We take the number of micelles per unit volume which are not in equilibrium with a given droplet, at a distance r from that droplet, as $n_m(r)$. Assumption 1 implies that there exists a unique species of micelle which will be in equilibrium with any given drop, and a population of micelles (the majority, close to the total number of micelles), which are not. If we assume 2 then the number flux of micelles to a droplet of radius R is found by solving a diffusion problem in which micelles diffuse from ∞ to a droplets surface, where they will *react* (via some mechanism)

to produce oil swollen micelles which are in equilibrium with the given drop. So

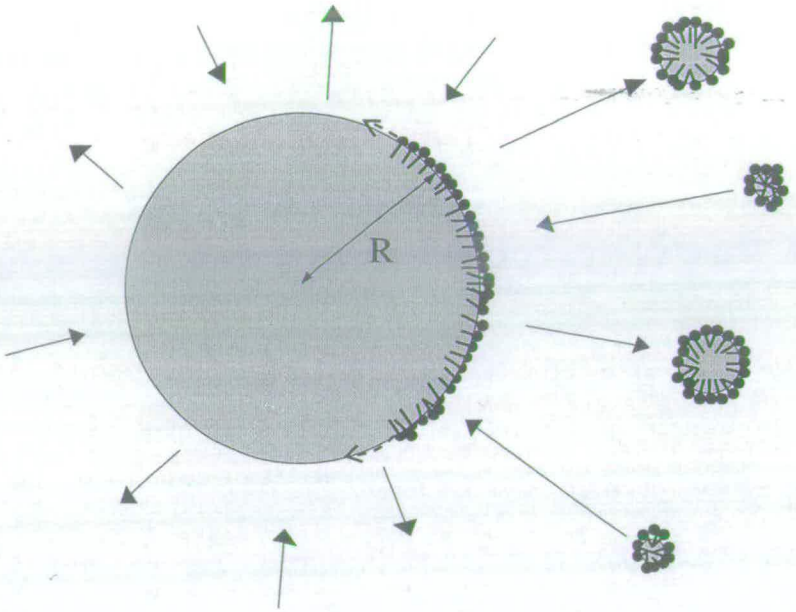

Figure 6.1: Incoming micelles contain the systems average oil/surfactant ratio, where as outgoing micelles contain an oil/surfactant ratio determined by a droplets chemical potential (and hence its radius R).

taking $\overline{n}_m(t)$ as the average number of micelles per unit volume at time t, then by assuming 3 we obtain the flux of incoming micelles (which are not in equilibrium with a given drop) to a droplets surface from

$$\nabla^2 n_m = 0 \tag{6.1}$$

with the boundary conditions

$$n_m(R) = 0 \tag{6.2}$$

$$n_m(\infty) = \overline{n}_m(t) \tag{6.3}$$

where $n_m(\infty) = \overline{n}_m(t)$ because in the system as a whole the fraction of micelles in equilibrium with a *given* drop is negligible, and $n_m(R) = 0$ because micelles adjacent to a droplet are assumed to immediately react with it.

These equations may be solved (by assuming the distribution to be spherically symmetric) to give

$$n_m(r) = \overline{n}_m(t)\left(1 - \frac{R}{r}\right) \tag{6.4}$$

where R is the radius of the drop. Hence the flux of incoming micelles to the surface of a drop is given by

$$J_{in}(R) = D_m \left.\frac{\partial n_m}{\partial r}\right|_R = \frac{D_m}{R}\overline{n}_m(t) \tag{6.5}$$

where $J_{in}(R)$ represents the incoming number flux of micelles per unit area of droplet surface.

The average number of surfactant molecules per micelle is defined as $\overline{S}_m(t)$, so since the total amount of surfactant in the system is constant, we have

$$\overline{n}_m(t)\overline{S}_m(t) = \overline{n}_m(0)\overline{S}_m(0) \tag{6.6}$$

where we neglect any (small) variations in the total surfactant number by adsorption on droplet surfaces. Hence we obtain the flux of micelles to a droplets surface as

$$J_{in} = \frac{D_m}{R}\overline{n}_m(0)\frac{\overline{S}_m(0)}{\overline{S}_m(t)} \tag{6.7}$$

Since (for surfactant to locally be conserved) the total flux of surfactant to a droplet must equal[‡] the total flux of surfactant away from a droplet, we have

$$J_{in}\overline{S}_m(t) = J_{out}S_m(R) \tag{6.8}$$

[‡]Changes in a droplets surface area will require changes in the number of adsorbed surfactant molecules, so surfactant flux is only approximately zero. However it is an approximation valid to terms of order $v_M^{1/3}/R$, where v_M is a molecular volume defined by $v_M \sim V_m/S_m$, with V_m, S_m being the volume of oil and number of surfactant molecules in a given micelle respectively. For example if we consider a typical micelle incident on a drop, then changes in the surface area of the drop are of order V_m/R. Taking a as the molecular area of a single adsorbed surfactant molecule, then we obtain a change in the number of adsorbed surfactant molecules of order V_m/aR, and the fraction of surfactant molecules adsorbed per micelle–droplet interaction to be of order V_m/S_maR. So since $V_m/S_m \sim v_M$, and $v_M^{2/3} \sim a$, then the fraction of surfactant molecules in a micelle which are adsorbed onto the droplets surface would be of order $V_m/S_maR \sim (v_M^{1/3}/R)(v_M^{2/3}/a) \sim v_M^{1/3}/R \ll 1$, and hence negligible.

where J_{out} is the outgoing number flux of micelles per unit area of surface from a droplet, and $S_m(R)$ is the number of surfactant molecules per micelle, for a micelle in equilibrium with a droplet of radius R. Hence we may obtain J_{out} as

$$J_{out} = \frac{D_m}{R}\overline{n}_m(0)\frac{\overline{S}_m(0)}{S_m(R)}. \tag{6.9}$$

Taking the average volume of oil solubilised in a micelle as $\overline{V}_m(t)$, then the rate of change of droplet volume is given by

$$\frac{\partial(4\pi R^3/3)}{\partial t} = 4\pi R^2(J_{in}\overline{V}_m - J_{out}V_m(R)) \tag{6.10}$$

where $V_m(R)$ is the volume of oil solubilised in a micelle in equilibrium with a droplet of radius R. So we obtain dR/dt as

$$\frac{dR}{dt} = \frac{D_m}{R}\overline{n}_m(0)\overline{S}_m(0)\left(\frac{\overline{V}_m(t)}{\overline{S}_m(t)} - \frac{V_m(R)}{S_m(R)}\right) \tag{6.11}$$

Since V_m is the volume of oil solubilised in a swollen micelle, then V_m/S_m is the volume of oil solubilised per surfactant molecule (in such a micelle).

6.3.1 Droplet Growth Rate

Eq. 6.11 may be written as

$$\frac{dR}{dt} = \frac{D_m}{R}(\overline{\phi}_m(t) - \phi_m(R)) \tag{6.12}$$

where $\overline{\phi}_m(t)$ is the total volume fraction of oil solubilised in micelles (and identical to the spatially averaged volume fraction of oil solubilised in micelles), and $\phi_m(R)$ is the volume fraction of oil that would be solubilised in micelles if all the micelles were in equilibrium with a droplet of radius R.

Although Eq. 6.12 is derived rigorously (under assumptions 1 to 3), it is a reasonable form to postulate on purely phenomenological grounds. Assuming the process of micelle absorption to be diffusion limited, then since the relevant length scale and diffusion constant are the droplet radius R, and the micelle diffusion

constant D_m, then one might expect dR/dt to be proportional to D_m/R. Similarly, assuming that the volume fraction of oil solubilised in a micelle from a droplet depends on the chemical potential of oil in that droplet, and that the surfactant is homogeneously distributed[§], then one might expect the average volume of oil flux due to diffusion of micelles to be proportional to $\left(\overline{\phi}_m(t) - \phi_m(R)\right)$. So on the basis of very simple physical arguments we obtain Eq. 6.12 (up to an undetermined constant factor). This suggests that Eq. 6.12 may be valid under more relaxed assumptions than those given in section 6.3.

In terms of the volume fraction of oil that would be present if all micelles were swollen to a size in equilibrium with bulk oil ϕ_m^b, we may write

$$\frac{dR}{dt} = \frac{D_m \phi_m^b}{R}\left(\frac{(\overline{\phi}_m(t) - \phi_m^b)}{\phi_m^b} - \frac{(\phi_m(R) - \phi_m^b)}{\phi_m^b}\right) \tag{6.13}$$

Since the volume fraction of oil that micelles will solubilise from a droplet $\phi_m(R)$ is taken to be approximately equal to ϕ_m^b, we may linearise $\phi_m(R)$ about ϕ_m^b (Assumption 4). In terms of the dimensionless parameter $\Delta\mu(R)/kT$, where $\Delta\mu(R)$ is the chemical potential difference between a droplet of radius R and bulk oil, this gives

$$\phi_m(R) = \phi_m^b\left(1 + \alpha\frac{2\sigma v_b}{kTR}\right) \tag{6.14}$$

where we used $\Delta\mu = 2\sigma v_b/R$, and where α is a dimensionless parameter typically of order 1. The parameter α determines the extent to which micelles will swell/shrink to solubilise more/less oil, as a result of small changes in the oil's chemical potential. The exact value of α will depend on the type of oil, surfactant, and co–surfactant in the system. So Eq. 6.13 now becomes

$$\frac{dR}{dt} = \frac{D_m \phi_m^b}{R}\left(\frac{(\overline{\phi}_m(t) - \phi_m^b)}{\phi_m^b} - \alpha\frac{2\sigma v_b}{kTR}\right) \tag{6.15}$$

Defining $\epsilon(t) \equiv (\overline{\phi}_m(t) - \phi_m^b)/\phi_m^b$, $R' \equiv RkT/\alpha 2\sigma v_b$, and $t' \equiv t\phi_m^b D_m (kT)^2/$

[§]This is a reasonable assumption to make so as to satisfy the steady state requirement of zero net surfactant flux.

$(\alpha 2\sigma v_b)^2$, we obtain the dimensionless droplet growth rate

$$\frac{dR'}{dt'} = \frac{1}{R'}\left(\epsilon(t) - \frac{1}{R'}\right) \tag{6.16}$$

6.3.2 Droplet Size Distribution

Eq. 6.16 is identical in form (but with a different rescaling of variables), to Eq. 2.24, as solved by Bray [22] to obtain the Lifshitz–Slyozov–Wagner (LSW) [20,21] distribution which describes the evolution of a continuous distribution of droplet sizes. Hence provided as $t \to \infty$ the micelles adopt a volume fraction such that $\epsilon(t) \sim 1/\overline{R'}$, where $\overline{R'}$ is a typical droplet size, we obtain the same asymptotic solution for the droplet size distribution as did LSW. So whether oil transport is via diffusion through the continuous phase or via swollen micelles, we may expect the late stage coarsening of the droplet size distribution to be as described by LSW [20,21], but with the rescaling of variables given above.

The asymptotic LSW solution can only apply at later times when micelles are sufficiently swollen that large drops (with lower than average chemical potential) can *compete* with the micelles for absorption of oil. This means that coarsening via micelles and coarsening via oil diffusion through the continuous phase are not entirely the same. When coarsening is via micelles we have at early times $-1 \leq \epsilon(t) < 0$, which contrasts with the scenario where droplets form after a *quench* and $\epsilon \geq 0$ at all times. In fact if there are a sufficiently large number of micelles, then all the oil will be adsorbed into micelles and the asymptotic LSW droplet size distribution will never be observed: instead, all the droplets will be solubilised into micelles. The total solubilisation of oil by micelles is possible since ϕ_m^b may be of the order of the droplets volume fraction ϕ_0. In the scenario considered by LSW, the volume of oil solubilised is of the order of the oil solubility, and negligible in comparison with the oil volume fraction. The solubilisation of oil droplets by micelles, and the initial swelling and saturation

of micelles is considered in section 6.4.

6.3.3 Effect on Ostwald Ripening

To determine the importance of micelle–mediated coarsening, it is necessary to compare it with the rate of coarsening by a flux of dissolved disperse phase alone.

When droplet growth is by micelle–mediated transport alone, the droplet growth rate Eq. 6.15 gives,

$$\frac{dR}{dt} \sim \frac{D_m \phi_m^b \alpha}{R} \left(\frac{2\sigma v_b}{kTR} \right) \tag{6.17}$$

When droplet growth is by flux of dissolved disperse phase then Eq. 2.19 with $\eta = 0$, gives

$$\frac{dR}{dt} \sim \frac{D v_b C(\infty)}{R} \left(\frac{2\sigma v_b}{kTR} \right) \tag{6.18}$$

So defining the volume fraction of dissolved disperse phase as $\phi_{sol}^b \equiv v_b C(\infty)$, we see that whether the effects of micelle–mediated coarsening are important is determined by $\beta \equiv D\phi_{sol}^b / D_m \phi_m^b \alpha$. If $\beta \ll 1$ then micelle mediated effects will dominate, if $\beta \gg 1$ then the affects of micelles will be negligible, and if $\beta \sim 1$ then it is necessary to consider both contributions to the growth rate.

6.4 Rate of Solubilisation

We consider a dilute emulsion of oil droplets into which surfactant is added. The surfactant will rapidly aggregate to form a micellar solution with the concentration of dissolved surfactant molecules being the surfactants' CMC (critical micelle concentration [22]). As micelles encounter droplets they adsorb oil into their cores, a scenario corresponding to section 6.3.2 with $-1 \leq \epsilon(t) < 0$. If all of the oil is solubilised then ϵ remains -ve, however if only part of the oil is solubilised before micelles become saturated then ϵ will become +ve and micelles

may then mediate an oil transfer between droplets. This section calculates the time for total solubilisation of the oil droplets into micelles (given sufficient surfactant), and the time for a net solubilisation of oil into micelles to stop (due to their being saturated).

Since we are interested in the rate at which oil is solubilised into micelles, we now neglect the exchange of oil between droplets and approximate the volume of oil solubilised into a micelle by V_m^b (the volume of oil solubilised by a micelle in equilibrium with bulk oil). So $\phi_m(R)$ is now approximated by ϕ_m^b, and Eq. 6.12 becomes

$$\frac{dR}{dt} = \frac{D_m}{R}\left(\overline{\phi}_m(t) - \phi_m^b\right) \tag{6.19}$$

Since the total oil volume fraction is conserved, we have

$$\overline{\phi}_m(t) + \int_0^\infty n(R,t)\frac{4\pi}{3}R^3 dR = \phi_0 \tag{6.20}$$

where ϕ_0 is the total volume fraction of oil present in the system and $n(R,t)$ is the number density of droplets of radius R at time t. Hence,

$$\frac{d\overline{\phi}_m}{dt} = -\int_0^\infty \frac{\partial n(R,t)}{\partial t}\frac{4\pi}{3}R^3 dR \tag{6.21}$$

which using Eq. 6.19, and the continuity equation

$$\frac{\partial n(R,t)}{\partial t} = -\frac{\partial(n(R,t)dR/dt)}{\partial R} \tag{6.22}$$

gives

$$\frac{d\overline{\phi}_m}{dt} = D_m\left(\phi_m^b - \overline{\phi}_m(t)\right)\int_0^\infty n(R,t)4\pi R dR \tag{6.23}$$

If we take the droplet size distribution as approximately monodisperse and of radius $R(t)$, then we find

$$\frac{d\overline{\phi}_m}{dt} = D_m\left(\phi_m^b - \overline{\phi}_m(t)\right)n_0 4\pi R(t) \tag{6.24}$$

with n_0 the total number of droplets, and now constant. We also obtain,

$$\overline{\phi}_m(t) + n_0\frac{4\pi}{3}R(t)^3 = \phi_0 \tag{6.25}$$

which may be rearranged to give

$$R(t) = R(0)\left(\frac{\phi_0 - \overline{\phi}_m(t)}{\phi_0}\right)^{1/3} \tag{6.26}$$

where we note that $\phi_0 = n_0 \frac{4\pi}{3} R^3(0)$. So in terms of ϕ_0 and $\overline{\phi}_m(t)$, Eq. 6.24 becomes

$$\frac{d\overline{\phi}_m}{dt} = \frac{3D_m\phi_0}{R^2(0)}\left(\phi_m^b - \overline{\phi}_m(t)\right)\left(1 - \frac{\overline{\phi}_m(t)}{\phi_0}\right)^{1/3} \tag{6.27}$$

Finally we define $\mathcal{K} \equiv R^2(0)/3D_m\phi_0$, $x \equiv \overline{\phi}_m/\phi_0$, and $x_0 \equiv \phi_m^b/\phi_0$, to get

$$\frac{dx}{dt} = \frac{1}{\mathcal{K}}(x_0 - x)(1 - x)^{1/3} \tag{6.28}$$

The final volume fraction of oil solubilised into micelles is determined by the smaller of ϕ_m^b and ϕ_0. When total solubilisation of oil is possible, $\overline{\phi}_m(t) = \phi_0$ and $x = 1$.

We may integrate Eq. 6.28 to obtain the time to solubilise a given quantity of oil. In terms of x and x_0 we get[¶],

$$t(x) = \frac{\mathcal{K}}{2(x_0 - 1)^{1/3}} \begin{pmatrix} -\ln\left(\frac{((x_0-1)^{2/3} - (x_0-1)^{1/3}(1-x)^{1/3} + (1-x)^{2/3})}{((x_0-1)^{1/3} + (1-x)^{1/3})^2}\right) \\ -\ln\left(\frac{(1+(x_0-1)^{1/3})^2}{((x_0-1)^{2/3} + (x_0-1)^{1/3} + 1)^2}\right) \\ -2\sqrt{3}\tan^{-1}\left(\frac{2(1-x)^{1/3} - (x_0-1)^{1/3}}{\sqrt{3}(x_0-1)^{1/3}}\right) \\ +2\sqrt{3}\tan^{-1}\left(\frac{2-(x_0-1)^{1/3}}{(x_0-1)^{1/3}\sqrt{3}}\right) \end{pmatrix} \tag{6.29}$$

6.4.1 Solubilisation Time ($x_0 > 1$)

We first consider the case $x_0 > 1$ for which complete solubilisation is possible. This occurs when $x = 1$. Hence the time for complete solubilisation t_{sol}, is given

[¶]Where Maple was used to calculate the integral.

by,

$$t_{sol} = \frac{\mathcal{K}}{2(x_0-1)^{1/3}} \begin{pmatrix} -\ln\left(\frac{(1+(x_0-1)^{1/3})^2}{(x_0-1)^{2/3}+(x_0-1)^{1/3}+1}\right) \\ +\frac{\pi}{\sqrt{3}} \\ -2\sqrt{3}\tan^{-1}\left(\frac{2-(x_0-1)^{1/3}}{(x_0-1)^{1/3}\sqrt{3}}\right) \end{pmatrix} \tag{6.30}$$

Note that all droplets evaporate in finite time; within the model there are no droplets remaining at $t > t_{sol}$. When the total amount of oil which surfactant may solubilise is much larger than the total amount of oil present ($x_0 \gg 1$), then we find,

$$t_{sol} \simeq \frac{\mathcal{K}}{x_0}\left(\frac{3}{2} + \frac{9}{10x_0} + \frac{27}{40x_0^2} + O\left(\frac{1}{x_0^3}\right)\right) \tag{6.31}$$

Figure 6.2 plots[‖] solubilisation time against x_0. As can be seen in the figure,

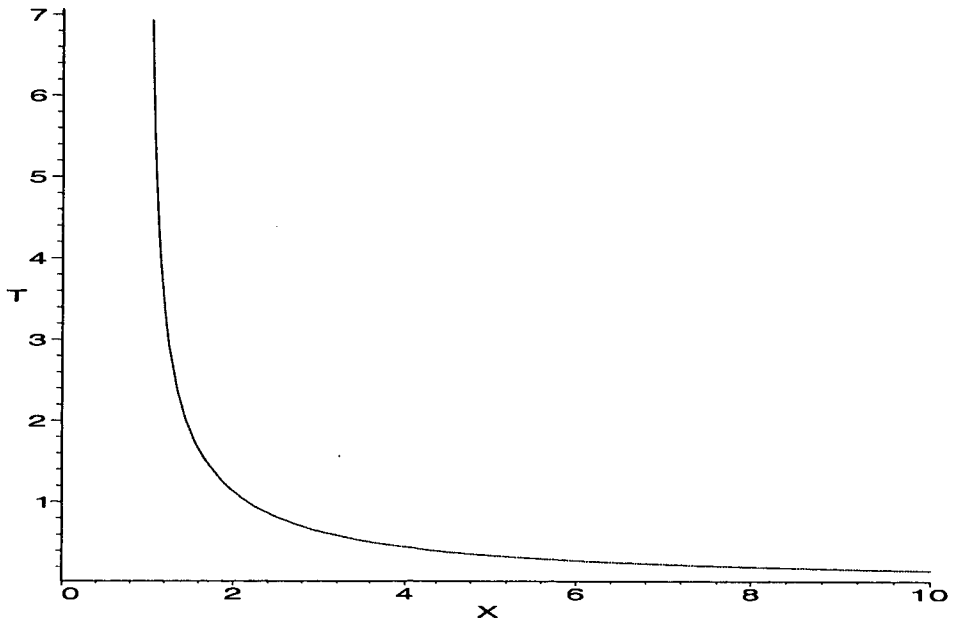

Figure 6.2: Solubilisation time $T \equiv t_{sol}$ against $X \equiv x_0$. The solubilisation time tends to zero as $x_0 \to 0$, and diverges as $x_0 \to 1$ since total solubilisation of oil is not possible for $x_0 \leq 1$. Note that all times are in units $\mathcal{K}$, with $\mathcal{K} \equiv R(0)^2/(3\phi_m^b D_m)$, as previously given in the text.

when $x_0 \to 1$ the solubilisation time diverges. This is because if $x_0 < 1$, then

[‖]The graph was produced using Maple.

not all the oil can be solubilised into micelles. As $x_0 \to \infty$ and the total volume fraction of oil becomes much less than that which may be solubilised in micelles, the solubilisation time tends to zero.

6.4.2 Saturation Time ($x_0 < 1$)

We now turn to the case where $x_0 < 1$ so that micelles saturate before solubilising all the oil. We consider late times when the micelles are nearly saturated with oil. Writing $x = x_0 - \Delta$, then using Eq. 6.28 we find,

$$\frac{d\Delta}{dt} = -\frac{1}{\mathcal{K}}\Delta(1-x_0)^{1/3}\left(1+\frac{\Delta}{1-x_0}\right)^{1/3} \tag{6.32}$$

As $x \to x_0$ and $\Delta \to 0$, we get

$$\frac{d\Delta}{dt} = -\frac{(1-x_0)^{1/3}}{\mathcal{K}}\Delta + O(\Delta^2) \tag{6.33}$$

giving

$$\Delta(t) = \exp\left(\frac{-(1-x_0)^{1/3}}{\mathcal{K}}t\right) \tag{6.34}$$

so that x approaches x_0 at an exponential rate.

Hence although micelles may approach saturation very rapidly, the model suggests that total saturation of the micelles is never quite attained, unlike the total disappearance of droplets described above for $x_0 > 1$. This is for the following reason. When $x_0 > 1$ not all micelles are required to solubilise the oil, but when $x_0 < 1$ total saturation requires *every* micelle to encounter a droplet. So when $x_0 > 1$, as total solubilisation is approached there will remain a significant fraction of micelles which are empty. However when $x_0 < 1$, as total saturation is approached the total number of empty micelles tends to zero, causing the rate of solubilisation to tend to zero, and preventing total saturation from being attained.

6.4.3 Consistency of Steady State Assumption

Solubilisation will occur most rapidly for $x_0 \gg 1$. So if the steady state assumption is reliable for $x_0 \gg 1$, it will be reliable for smaller values of x_0 also. When $x_0 \gg 1$, Eq. 6.31 has

$$t_{sol} \sim \frac{\mathcal{K}}{x_0} \sim \frac{R^2(0)}{D_m} \frac{1}{\phi_m^b} \tag{6.35}$$

Since the time for the micelle diffusion field to relax $t_{relax} \sim R^2(0)/D_m$, we may write

$$t_{sol} \sim \frac{t_{relax}}{\phi_m^b} \tag{6.36}$$

So if $\phi_m^b \sim 1$ then $t_{sol} \sim t_{relax}$ and our assumption of a steady state diffusion profile may no longer be valid, and the corresponding results no longer reliable. For the scenarios considered here however, with ϕ_m^b typically $\sim 10^{-2}$, then $t_{sol} \sim 10^2 t_{relax}$ and the assumption reasonable. We do note however, that if $\phi_m^b \sim 10^{-2}$ and $\phi_0 \ll \phi_m^b$ then we require $\phi_0 \ll 10^{-2}$, ie a very small total volume fraction of oil. For anything more than small ϕ_0, the expression for t_{sol} must be treated with caution.

6.4.4 Transient Phenomena

This section discusses the crossover from absorption of oil by empty micelles, to late–stage coarsening. We continue to consider a system of dilute emulsion droplets into which surfactant is mixed (and forms micelles), at time $t = 0$. We find that there exists a time at which sufficiently large droplets will grow in size, even though there is still a net solubilisation of oil into micelles.

We make the mean field assumption that the average volume fraction of oil in a swollen micelle is determined by the average droplet size. Then defining $\overline{n}_m^e(t)$ as the spatially averaged number of empty micelles (containing no oil), we obtain

the average volume fraction of oil in micelles as

$$\overline{\phi}_m(t) = \left(1 - \frac{\overline{n}_m^e(t)}{\overline{n}_m(t)}\right) \phi_m(\overline{R}) \tag{6.37}$$

Then expanding $\phi_m(\overline{R})$ and $\phi_m(R)$ about ϕ_m^b and substituting into Eq. 6.13 leads to

$$\frac{dR}{dt} = \frac{\phi_m^b D_m}{R}\left(\frac{\alpha'}{\overline{R}} - \frac{\alpha'}{R} - \frac{\overline{n}_m^e(t)}{\overline{n}_m(t)}\left(1 + \frac{\alpha'}{\overline{R}}\right)\right) \tag{6.38}$$

where $\alpha' \equiv \alpha 2\sigma v_b/kT$. The critical radius of droplet above which droplets will grow in size due to a net flux of oil to the droplet, is given by

$$R_c(t) = \frac{\alpha'}{\alpha'/\overline{R} - (\overline{n}_m^e(t)/\overline{n}_m(t))(1 + \alpha'/\overline{R})} \tag{6.39}$$

or infinity, for early times when the above expression would be negative.

The onset of a finite R_c occurs when

$$\frac{\overline{n}_m^e(t)}{\overline{n}_m(t)} = \frac{\alpha'/\overline{R}}{1 + \alpha'/\overline{R}} \simeq \frac{\alpha'}{\overline{R}} + O\left(\frac{\alpha'^2}{\overline{R}^2}\right) \tag{6.40}$$

So there will continue to exist a small but finite fraction of empty micelles, at the time when the largest droplets start to grow in size. The finite fraction of empty micelles will enable a net flux of oil from droplets to micelles to continue even while the largest droplets have started to grow. The continued decrease in $\overline{n}_m^e/\overline{n}_m$ will initially cause R_c to decrease, before it reaches a minimum value and starts increasing, asymptoting to $\overline{R}(t)$ as $t \to \infty$ (see fig. 6.3).

In the above we have considered scenarios where the volume fraction of oil contained in droplets is much larger than the volume fraction of oil micelles may solubilise. Initially, when micelles are empty, they will solubilise oil from droplets and $\overline{\phi}_m(t)$ will be *increasing*. However at later stages when micelles are already swollen, the micelles will exchange oil from smaller to larger droplets, resulting in a growth of average droplet radius and a reduction in the average droplet chemical potential. Since the chemical potential of oil in droplets is now a decreasing function of time, droplets will now (on average) adsorb oil *back* from micelles,

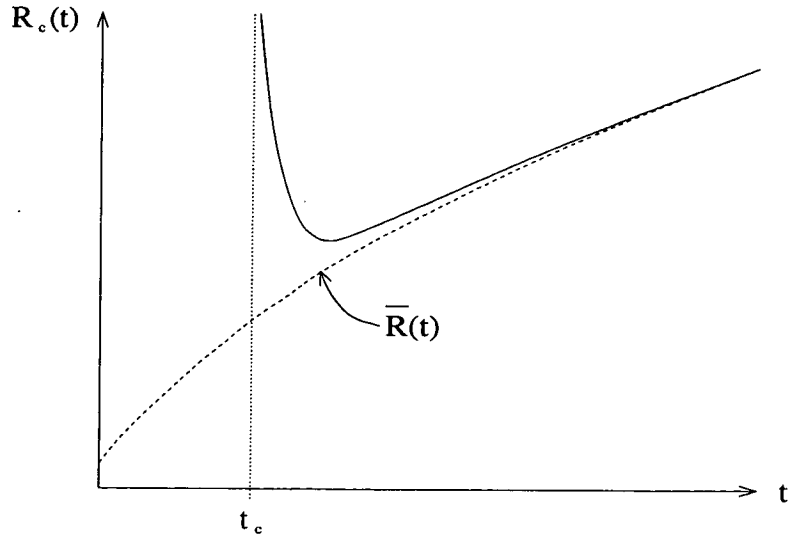

Figure 6.3: Schematic figure, illustrating how the critical radius R_c above which droplets will grow, changes during the early stages of solubilisation. At a critical time t_c, R_c will become finite, before finally asymptoting to the late–time average droplet size $\overline{R}(t)$ determined by LSW [20, 21] (as discussed in section 6.3.2).

resulting in a *decreasing* $\overline{\phi}_m(t)$. Hence at some time a critical radius R_c (above which droplets will grow in size), will start to exist, then gradually decrease in size until attaining a minimum value, before finally asymptoting to the typical droplet size $\overline{R}(t)$. Again, this will mean that there will be a period of time where the largest droplets may grow, even while there remains a net solubilisation of oil into micelles. As before, it is unclear whether this will (significantly) affect the late–stage droplet size distribution, but it would certainly affect the initial droplet size distribution.

These transient phenomena are independent of the specific model proposed above. All that is required is that the oil in micelles may be in equilibrium with the oil in droplets. So models allowing inter–micelle interactions, or which assume differing diffusion/reaction mechanisms, will all exhibit these effects (to a greater or a lesser extent).

6.5 Exchange of Molecules Between Micelles

The present section considers how the exchange of oil and surfactant molecules between micelles in the continuous phase, may affect the rate of micelle–mediated oil transport between droplets. The previous work *neglected* oil and surfactant exchange among micelles, and so is only valid when the rate at which oil and surfactant molecules are transported via micelle diffusion is much *faster* than the rate of oil and surfactant exchange. Now we will study the other extreme, when the rate of oil and surfactant exchange between micelles is rapid compared with rate of oil and surfactant transport via diffusion of the micelles.

Previously in sections 6.3 to 6.4 we assumed that equilibrated micelles would all contain the same number of surfactant and oil molecules. Now we must consider a continuous distribution of micelle compositions, with the number of micelles per unit volume with S_m surfactant and O_m oil molecules, given by $n_m(S_m, O_m, \vec{r}, t)$**. The assumption that surfactant and oil exchange (between micelles) occurs much more rapidly than surfactant and oil is transported by diffusion of micelles, will allow us to assume that locally the micelle distribution $n_m(S_m, O_m, \vec{r}, t)$ adopts the equilibrium micelle distribution $n_m^{eq}(S_m, O_m, n_S(\vec{r}, t), n_O(\vec{r}, t))$ of micelle compositions, determined by $n_S(\vec{r}, t)$ and $n_O(\vec{r}, t)$ the number densities of surfactant and oil molecules. The approach we follow has some similarities to that used to study the diffusion of rod–like micelles, by Cates et al [63].

6.5.1 Calculating Oil and Surfactant Flux

The number of micelles with S_m surfactant and O_m oil molecules per unit volume, $n_m(S_m, O_m, \vec{r}, t)$, may change both by a diffusive flux of micelles (as be-

**The added complication of considering a distribution of micelle compositions is necessary, since oil and/or surfactant will only be exchanged between micelles with differing chemical potentials.

fore) and by exchange of oil and surfactant molecules between micelles. We take $E[S_m, O_m, \{n_m\}]$ as the rate of change in number of micelles with S_m surfactant and O_m oil molecules, by exchange between micelles. Then

$$\frac{\partial n_m(S_m, O_m, \vec{r}, t)}{\partial t} = E[S_m, O_m, \{n_m\}] - \vec{\nabla}.\vec{J}_{diff} \qquad (6.41)$$

where $\vec{J}_{diff}$ is the diffusive flux of micelles, considered below.

We note that $S_m E[S_m, O_m, \{n_m\}]$ is the rate of change in the total number of surfactant molecules in micelles which have S_m surfactant and O_m oil molecules. So if we consider a steady state, then since the number of surfactant molecules is conserved the change in the number of surfactant molecules in micelles per unit volume, by exchange between micelles $\int dO_m \int dS_m S_m E[S_m, O_m, \{n_m\}]$, is zero. Similarly for oil, the change in the total number of oil molecules in micelles per unit volume, by exchange, $\int dO_m O_m \int dS_m E[\ S_m, O_m\ , \{n_m\}]$, is zero. So in a steady state, exchange of molecules between micelles may only alter the micelle distribution.

If we consider the total number densities of surfactant and oil molecules in micelles $n_S(\vec{r}, t) = \int dO_m \int dS_m S_m\ n_m(S_m, O_m, \vec{r}, t)$, $n_O(\vec{r}, t) = \int dS_m \int dO_m O_m\ n_m(S_m, O_m, \vec{r}, t)$, and take the usual expression for a diffusive flux of ideal micellar aggregates $\vec{J}_{diff} = -D_m(S_m, O_m)\ \vec{\nabla}\ n_m(S_m, O_m, \vec{r}, t)$, then in a steady state we require

$$\frac{\partial n_S}{\partial t} = \vec{\nabla}.\int dO_m \int dS_m S_m D_m(S_m, O_m)\vec{\nabla} n_m = 0 \qquad (6.42)$$

and

$$\frac{\partial n_O}{\partial t} = \vec{\nabla}.\int dO_m O_m \int dS_m D_m(S_m, O_m)\vec{\nabla} n_m = 0 \qquad (6.43)$$

Since we consider a rapid exchange of oil and surfactant molecules between micelles, we may now assume a fast relaxation of the micelle distribution, and take $n_m(S_m,\ O_m, \vec{r}, t) = n_m^{eq}(S_m, O_m, n_S(\vec{r}, t), n_O(\vec{r}, t))$. Then expanding about the average number of oil and surfactant molecules per unit volume $\overline{n}_O$ and $\overline{n}_S$

respectively, we get

$$\begin{aligned} n_m(S_m, O_m, \vec{r}, t) = n_m^{eq}(S_m, O_m; \overline{n}_S, \overline{n}_O) \quad & + \frac{\partial n_m^{eq}(S_m, O_m; \overline{n}_S, \overline{n}_O)}{\partial n_S}(n_S - \overline{n}_S) \\ & + \frac{\partial n_m^{eq}(S_m, O_m; \overline{n}_S, \overline{n}_O)}{\partial n_O}(n_O - \overline{n}_O) \end{aligned} \tag{6.44}$$

Substitution into Eqs. 6.42 and 6.43 then gives,

$$\begin{aligned} \frac{\partial n_S}{\partial t} = \quad & \vec{\nabla}.\left[\int dO_m \int dS_m S_m D_m \frac{\partial n_m^{eq}}{\partial n_S}\right] \vec{\nabla} n_S + \\ & \vec{\nabla}.\left[\int dO_m \int dS_m S_m D_m \frac{\partial n_m^{eq}}{\partial n_O}\right] \vec{\nabla} n_O = 0 \end{aligned} \tag{6.45}$$

and

$$\begin{aligned} \frac{\partial n_O}{\partial t} = \quad & \vec{\nabla}.\left[\int dO_m \int dS_m O_m D_m \frac{\partial n_m^{eq}}{\partial n_S}\right] \vec{\nabla} n_S + \\ & \vec{\nabla}.\left[\int dO_m \int dS_m O_m D_m \frac{\partial n_m^{eq}}{\partial n_O}\right] \vec{\nabla} n_O = 0 \end{aligned} \tag{6.46}$$

We now define the total number density of micelles in a neighbourhood where there are n_S surfactant and n_O oil molecules per unit volume; this is given by

$$\int dO_m \int dS_m n_m^{eq}(S_m, O_m; n_S, n_O) \equiv \tilde{n}_m^{eq}(n_S, n_O) \tag{6.47}$$

We also define ratios $f_{S,O}$ as

$$f_{S,O} \equiv \frac{\partial n_m^{eq}(S_m, O_m; \overline{n}_S, \overline{n}_O)}{\partial n_{S,O}} \Big/ \frac{\partial \tilde{n}_m^{eq}(\overline{n}_S, \overline{n}_O)}{\partial n_{S,O}} \tag{6.48}$$

so that $\int dO_m \int dS_m f_{S,O} = 1$. With these definitions we can write

$$\begin{aligned} \frac{\partial n_S}{\partial t} = \quad & \vec{\nabla}.\left[\int dO_m \int dS_m S_m D_m f_S\right] \frac{\partial \tilde{n}_m^{eq}}{\partial n_S} \vec{\nabla} n_S + \\ & \vec{\nabla}.\left[\int dO_m \int dS_m S_m D_m f_O\right] \frac{\partial \tilde{n}_m^{eq}}{\partial n_O} \vec{\nabla} n_O = 0 \end{aligned} \tag{6.49}$$

and

$$\begin{aligned} \frac{\partial n_O}{\partial t} = \quad & \vec{\nabla}.\left[\int dO_m \int dS_m O_m D_m f_S\right] \frac{\partial \tilde{n}_m^{eq}}{\partial n_S} \vec{\nabla} n_S + \\ & \vec{\nabla}.\left[\int dO_m \int dS_m O_m D_m f_O\right] \frac{\partial \tilde{n}_m^{eq}}{\partial n_O} \vec{\nabla} n_O = 0 \end{aligned} \tag{6.50}$$

The form of these equations allows us to define four effective diffusion constants D_{OS}, D_{OO} and D_{SS}, D_{SO}, describing oil / surfactant flux due to surfactant and oil gradients, as

$$D_{SS}, D_{SO} = \left[\int dO_m \int dS_m S_m D_m f_{S,O}\right] \frac{\partial \tilde{n}_m^{eq}}{\partial n_{S,O}} \tag{6.51}$$

$$D_{OS}, D_{OO} = \left[\int dO_m \int dS_m O_m D_m f_{S,O}\right] \frac{\partial \tilde{n}_m^{eq}}{\partial n_{S,O}} \tag{6.52}$$

In matrix notation we have

$$\frac{\partial}{\partial t}\begin{pmatrix} n_S \\ n_O \end{pmatrix} = \vec{\nabla}.\begin{pmatrix} D_{SS} & D_{SO} \\ D_{OS} & D_{OO} \end{pmatrix}\vec{\nabla}\begin{pmatrix} n_S \\ n_O \end{pmatrix} = 0 \tag{6.53}$$

and identifying $\partial n_{S/O}/\partial t = \vec{\nabla}.\vec{J}_{S/O}$ we obtain

$$\begin{pmatrix} \vec{J}_S \\ \vec{J}_O \end{pmatrix} = \begin{pmatrix} D_{SS} & D_{SO} \\ D_{OS} & D_{OO} \end{pmatrix}\vec{\nabla}\begin{pmatrix} n_S \\ n_O \end{pmatrix} \tag{6.54}$$

This is a two component diffusion equation, as one would expect from the fact that (with fast exchange kinetics), n_S and n_O are the only conserved densities.

6.5.2 Steady State Droplet Growth Rate

So we have

$$0 = \vec{\nabla}.\begin{pmatrix} D_{SS} & D_{SO} \\ D_{OS} & D_{OO} \end{pmatrix}\vec{\nabla}\begin{pmatrix} n_S \\ n_O \end{pmatrix} \tag{6.55}$$

which may be solved in spherically symmetric coordinates with an origin at a droplets centre, to give

$$n_S(r) = \overline{n}_S + \frac{R}{r}\left(n_S(R) - \overline{n}_S\right) \tag{6.56}$$

and

$$n_O(r) = \overline{n}_O + \frac{R}{r}\left(n_O(R) - \overline{n}_O\right) \tag{6.57}$$

So we obtain the flux of oil and surfactant molecules to a droplets surface as

$$\vec{J}_O = D_{OS}\frac{n_S(R) - \overline{n}_S}{R} + D_{OO}\frac{n_O(R) - \overline{n}_O}{R} \tag{6.58}$$

and

$$\vec{J}_S = D_{SS}\frac{n_S(R) - \overline{n}_S}{R} + D_{SO}\frac{n_O(R) - \overline{n}_O}{R} \tag{6.59}$$

respectively. If we also assume that there is no net flux of surfactant, so that $J_S = 0$ (ie we again neglect the surfactant which is adsorbed/desorbed from droplets), then we find

$$\vec{J_O} = \left(D_{OO} - \frac{D_{OS}D_{SO}}{D_{SS}}\right)\frac{n_O(R) - \overline{n}_0}{R} \tag{6.60}$$

Which gives

$$\frac{dR}{dt} = \left(D_{OO} - \frac{D_{OS}D_{SO}}{D_{SS}}\right)\frac{\overline{\phi}_m(t) - \phi_m(R)}{R} \tag{6.61}$$

where we note that the volume fraction of oil in micelles is given by $\phi_m(R) = n_O(R)v_b$ and $\overline{\phi}_m(t) = \overline{n}_O(t)v_b$. Eq. 6.61 is entirely analogous to Eq. 6.12, but with D_m replaced by $(D_{OO} - (D_{OS}D_{SO})/D_{SS})$. Hence the results which apply to Eq. 6.12 will also apply to Eq. 6.61.

To recap, we allowed oil and surfactant to be exchanged between micelles, but assumed that it occurs much more rapidly than the rate of diffusion of micelles between droplets. This allowed us to assume an equilibrium micelle distribution, determined by the spatially dependent number densities of oil and surfactant molecules which are present. Then we assumed that we may linearise the distribution about the spatially averaged number densities of surfactant and oil molecules. Finally, as in previous sections, we assumed both a steady state and zero net adsorption/desorption of surfactant onto/from droplets. The result is a droplet growth rate with the same form as Eq. 6.12, but with a different diffusion coefficient. Hence with the above assumptions for oil and surfactant exchange, micelle mediated coarsening appears to be qualitatively unaffected by oil and surfactant exchange between micelles, simply requiring a different diffusion coefficient.

Before considering reaction limited coarsening, it is worth examining the results. Firstly note that $\vec{J_S} = 0$ does not correspond to a zero gradient in surfactant density. In fact for a non–zero oil density gradient, $\vec{J_S} = 0$ is *only* possible with a non–zero surfactant density gradient. Also since $R < \bar{R}$ implies that $n_O(R) - \overline{n}_O > 0$,

then for $\vec{J}_S = 0$ (which corresponds to zero net adsorption/desorption of surfactant from droplets surfaces), we require that $n_S(R) < \overline{n}_S$ so that smaller than average droplets are surrounded by a less than average concentration of surfactant. Furthermore, we would also expect an increased number of oil molecules per micelle in the neighbourhood of smaller drops, so that the smaller surfactant density would be further accentuated to reduce the number density of micelles adjacent to the drop. Hence we expect *smaller* than average drops to be surrounded by a *smaller* concentration of micelles (which will also contain more oil than average, and typically be larger than usual), and *larger* than average drops to have a *larger* concentration micelles (which also contain less oil than average, and will typically be smaller than usual). It might be worth noting that if variations in micelle concentrations are large, the osmotic pressure from micelles may affect the chemical potential of droplets. Under such conditions larger drops will have their chemical potentials increased, and hence the oil concentration gradient will be reduced. Such effects have been ignored throughout this thesis (an assumption which corresponds to assuming negligible variation in the number density of micelles).

It is also interesting to examine the effective diffusion constant $(D_{OO} - (D_{OS} D_{SO})/D_{SS})$. Noting that $O_m \partial n_m^{eq}/\partial n_O \sim n_O/n_O$, $O_m \partial n_m^{eq}/\partial n_S \sim (O_m/S_m) n_S/n_S$, $S_m \partial n_m^{eq}/\partial n_S \sim n_S/n_S$, and $S_m \partial n_m^{eq}/\partial n_O \sim (S_m/O_m) n_O/n_O$, then a very simple estimate gives $D_{OO} \sim D_m$, $D_{SS} \sim D_m$, $D_{OS} \sim (O_m/S_m) D_m$, and $D_{SO} \sim (S_m/O_m) D_m$. So since both $D_{OO} \sim D_m$ and $D_{OS} D_{SO}/D_{SS} \sim D_m$, the effective diffusion constant may be significantly smaller than D_m. In fact depending on the distribution function for micelle composition, there is no apparent reason why the effective diffusion constant need even be positive. A negative diffusion constant would result in larger drops shrinking and small drops growing, leading to the formation of a monodisperse distribution. It is tempting to speculate that a negative effective diffusion constant (which would result in a monodisperse distribution), indicates that a microemulsion will form.

So although the droplet growth rate is the same form as Eq. 6.12, the rate of coarsening may be reduced. In fact since a negative effective diffusion constant appears possible, qualitatively different coarsening behaviour cannot be ruled out. To determine a systems behaviour, we require a sufficiently complex model of micelles to enable calculation of the effective diffusion constant from first principles, this is not considered here.

6.6 Reaction–Limited Coarsening

Here we briefly consider the case when the absorption of oil into micelles is limited not by the rate of diffusion of micelles to droplets, but by the rate at which micelles (already in contact with a droplet), react to solubilise oil. This type of mechanism is proposed by McClements [64] and Carroll et al [56–60], to account for experimental results regarding the solubilisation of oil into non–ionic micelles. Our calculation assumes the following:

- Micelles encounter a droplets surface with a rate proportional to their average concentration, the droplets surface area, and the rate at which they diffuse through a diffusion layer, taken to be of thickness δ_b, the radius of a micelle in equilibrium with bulk oil. This gives an attempt rate, for micelles to react and adsorb/desorb oil.

- A micelle reacts on a fraction χ of its encounters with a droplet. This defines a reaction rate.

- During a successful micelle–droplet encounter, we assume that micelles swell/shrink so as to adsorb/desorb oil, and that the oil contained in the micelle after the collision has the same chemical potential as the oil within the droplet.

Hence J_{in} now represents the flux of micelles which pass through the diffusion layer and also subsequently react with the droplet. So for a diffusion layer of thickness δ_b, J_{in} is given by

$$J_{in} = \frac{D_m \chi}{\delta_b} \overline{n}_m(t) = \frac{D_m \chi}{\delta_b} \overline{n}_m(0) \frac{\overline{S}_m(0)}{\overline{S}_m(t)} \tag{6.62}$$

and (as in section 6.3) *local* conservation of surfactant requires that J_{out}, the flux of equilibrated micelles *away* from the droplet is,

$$J_{out} = \frac{D_m \chi}{\delta_b} \overline{n}_m(0) \frac{\overline{S}_m(0)}{S_m(R)} \tag{6.63}$$

Hence the droplet growth rate (Eq. 6.11) now becomes

$$\frac{dR}{dt} = \frac{D_m \chi}{\delta_b} \overline{n}_m(0) \overline{S}_m(0) \left(\frac{\overline{V}_m(t)}{\overline{S}_m(t)} - \frac{V_m(R)}{S_m(R)} \right) \tag{6.64}$$

and Eq. 6.12 becomes,

$$\frac{dR}{dt} = \frac{D_m \chi}{\delta_b} \left(\overline{\phi}_m(t) - \phi_m(R) \right) \tag{6.65}$$

where $\overline{\phi}_m$ is the average volume fractions of oil solubilised in micelles, and $\phi_m(R)$ is the volume fraction of oil solubilised if all micelles are in equilibrium with a drop of radius R, as before. For comparison with the diffusion limited expression Eq. 6.13, may be written as

$$\frac{dR}{dt} = \frac{\chi \overline{R}}{\delta_b} \frac{D_m \phi_m^b}{\overline{R}} \left(\frac{\overline{\phi}_m(t) - \phi_m^b}{\phi_m^b} - \frac{\phi_m(R) - \phi_m^b}{\phi_m^b} \right) \tag{6.66}$$

Hence the reaction limited growth rate is a factor of $\chi \overline{R}/\delta_b$ times the diffusion limited growth rate, but otherwise of the same form. (For the growth rate to be reaction limited, it must be less than the diffusion limited growth rate. This requires that $\chi \overline{R}/\delta_b$ be less than 1, and χ less than $\delta_b/\overline{R}$.)

We may also proceed in a similar way to section 6.3.1, and define variables $R' \equiv RkT/\alpha 2\sigma v_b$, $\epsilon(t) \equiv (\overline{\phi}_m(t) - \phi_m^b)/\phi_m^b$ and $t' \equiv t\phi_m^b \chi D_m kT/\delta_b \alpha 2\sigma v_b$ to obtain the growth rate as,

$$\frac{dR'}{dt'} = \epsilon(t) - \frac{1}{R'} \tag{6.67}$$

which we use in section 6.6.1.

6.6.1 Reaction Limited Droplet Size Distribution

When all micelles are swollen, we take $\overline{\phi}_m(t)$ to be determined by the average droplet size $\overline{R}$. So $\overline{\phi}_m(t)$ is replaced by $\phi_m(\overline{R})$, and $\epsilon(t)$ becomes $1/\overline{R}'(t)$. So we have

$$\frac{dR'}{dt'} = \frac{1}{\overline{R}'(t')} - \frac{1}{R'} \tag{6.68}$$

Eq.6.68 has the same form of growth rate equation as that studied by Wagner [21], who solved for the time evolution of a continuous distribution of droplet sizes. With a change of constants to account for the different coarsening mechanism (ie via micelles), Wagner's result [21] therefore generalises to give the average droplet size $\langle R \rangle$, as $\langle R \rangle = 8/9R^*(t)$, with $R^*(t)$ given by

$$R^*(t) = R^*(0)\left(1 + \frac{tD_m\chi\phi_m^b kT}{\delta_b \alpha 2\sigma v_b}\right)^{1/2} \tag{6.69}$$

The scaling distribution for the droplet sizes is given in terms of the scaled variable $Z = R/R^*(t)$ as,

$$f(Z) = \frac{8}{3}\frac{Z}{(2-Z)^5}\exp\left(\frac{-3Z}{2-Z}\right)\theta(2-Z) \tag{6.70}$$

As with the diffusion limited case, we find that micelle mediated coarsening in the reaction limited limit is closely related to the standard case of a soluble oil, but with a suitably rescaled diffusion constant which is governed by micelle diffusion rather than that of molecularly solubilised oil.

6.7 Reaction Limited Solubilisation

Following an identical approach to that in section 6.4 we obtain the analogue of Eq. 6.11 for the reaction limited case as

$$\frac{dR}{dt} = \frac{D_m\chi}{\delta_b}\left(\overline{\phi}_m(t) - \phi_m^b\right) \tag{6.71}$$

Since this differs from Eq. 6.19, Eq. 6.23 now becomes

$$\frac{d\overline{\phi}_m}{dt} = \frac{D_m \chi}{\delta_b}\left(\phi_m^b - \overline{\phi}_m(t)\right)\int_0^\infty n(R,t)4\pi R^2 dR \tag{6.72}$$

and the resulting equation for $d\overline{\phi}_m/dt$ now becomes

$$\frac{d\overline{\phi}_m}{dt} = \frac{D_m \chi}{\delta_b}\frac{3\phi_0}{R(0)}\left(\phi_m^b - \overline{\phi}_m(t)\right)\left(1 - \frac{\overline{\phi}_m(t)}{\phi_0}\right)^{2/3} \tag{6.73}$$

We simplify the above equation by writing it in terms of the variables x and x_0 as defined in section 6.4, but with $\mathcal{K}$ now denoting $\mathcal{K} \equiv \frac{R^2(0)}{3\phi_0 D_m}\frac{\delta_b}{\chi R(0)}$, ie a factor of $\frac{\delta_b}{\chi R(0)}$ times that in section 6.4, and obtain

$$\frac{dx}{dt} = \frac{1}{\mathcal{K}}(x_0 - x)(1-x)^{2/3} \tag{6.74}$$

which upon integration[††] gives

$$t(x) = \frac{\mathcal{K}}{2(x_0-1)^{2/3}}\begin{pmatrix} -\ln\left(\frac{((x_0-1)^{1/3}+(1-x)^{1/3})^2}{((x_0-1)^{2/3}-(x_0-1)^{1/3}(1-x)^{1/3}+(1-x)^{2/3})}\right) \\ -\ln\left(\frac{((x_0-1)^{2/3}+(x_0-1)^{1/3}+1)^2}{(1+(x_0-1)^{1/3})^2}\right) \\ -2\sqrt{3}\tan^{-1}\left(\frac{2(1-x)^{1/3}-(x_0-1)^{1/3}}{(x_0-1)^{1/3}\sqrt{3}}\right) \\ +2\sqrt{3}\tan^{-1}\left(\frac{2-(x_0-1)^{1/3}}{(x_0-1)^{1/3}\sqrt{3}}\right) \end{pmatrix} \tag{6.75}$$

6.7.1 Solubilisation Time

Complete solubilisation occurs when $x = 1$. Hence the time for complete solubilisation t_{sol}, is given by,

$$t_{sol} = \frac{\mathcal{K}}{2(x_0-1)^{2/3}}\begin{pmatrix} -\ln\left(\frac{(1+(x_0-1)^{1/3})^2}{((x_0-1)^{2/3}+(x_0-1)^{1/3}+1)^2}\right) \\ +\frac{\pi}{\sqrt{(3)}} \\ +2\sqrt{3}\tan^{-1}\left(\frac{2-(x_0-1)^{1/3}}{(x_0-1)^{1/3}\sqrt{3}}\right) \end{pmatrix} \tag{6.76}$$

[††]The integration was calculated with Maple.

When the total amount of oil which surfactant may solubilise is much larger than the total amount of oil present and $x_0 \gg 1$, then we find,

$$t_{sol} \simeq \frac{\mathcal{K}}{x_0}\left(3 + \frac{9}{4x_0} + \frac{27}{14x_0^2} + O\left(\frac{1}{x_0^3}\right)\right) \tag{6.77}$$

Figure 6.4 plots[‡‡] solubilisation time against x_0. The graphs for solubilisation time

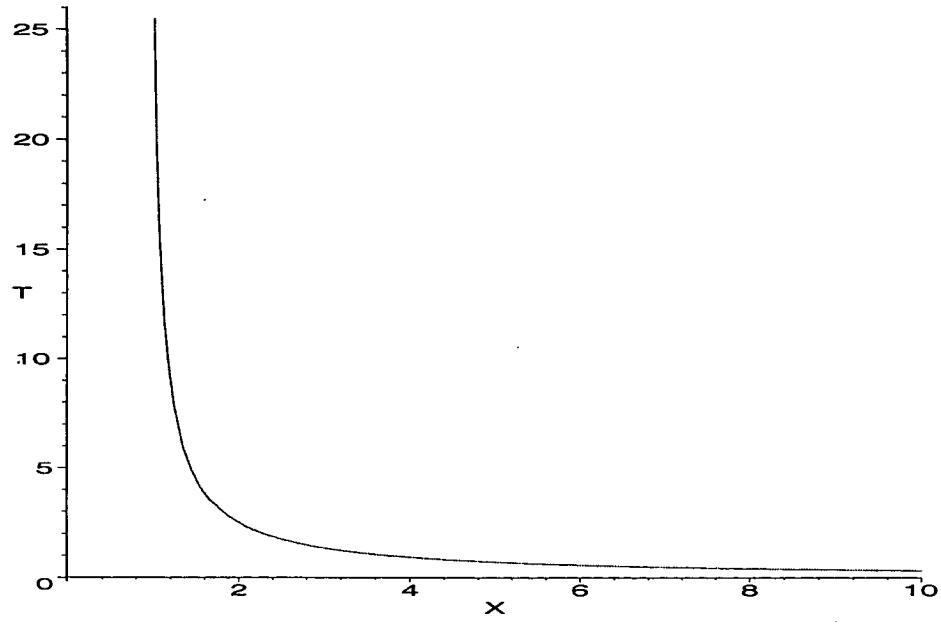

Figure 6.4: Solubilisation time $T \equiv t_{sol}$ against $X \equiv x_0$. The solubilisation time tends to zero as $X \equiv x_0$ becomes large, and diverges as $x_0 \to 1$ since total solubilisation of oil is not possible for $x_0 \leq 1$. Note that all times are in units of $\mathcal{K}$, with $\mathcal{K} \equiv (R^2(0)/3\phi_0 D_m)(\delta_b/\chi R(0))$, as previously given in the text.

are qualitatively the same as those in section 6.4 with t_{sol} diverging as $x_0 \to 1$ as before, and t_{sol} tending to zero as $x_0 \to \infty$.

When $x_0 \gg 1$ then $t_{sol} \sim \mathcal{K}/x_0$, with

$$\frac{\mathcal{K}}{x_0} \sim \frac{\delta_b}{\chi R(0)} \frac{R(0)^2}{D_m} \frac{1}{\phi_0 x_0} \sim \frac{t_{relax}}{\phi_m^b} \frac{\delta_b}{\chi R(0)} \tag{6.78}$$

So the reaction limited solubilisation time is simply a factor of $\delta_b/\chi R(0)$ times the diffusion limited solubilisation time, but otherwise qualitatively of the same form.

[‡‡]The graph was produced using Maple.

For solubilisation to be reaction limited then we require $\chi R(0)/\delta_b$ to be less than 1 (as was also required for the droplet growth rate to be reaction limited). Hence taking $\delta_b \sim 10^{-9}$m and $R(0) \sim 10^{-6}$m, then a reaction limited solubilisation time (or droplet growth rate), requires χ less than $\sim 10^{-3}$.

6.7.2 Saturation Time

As in section 6.4 we write $x = x_0 - \Delta$, then we use Eq. 6.74 to obtain

$$\frac{d\Delta}{dt} = -\frac{1}{\mathcal{K}}\Delta(1-x_0)^{2/3}\left(1+\frac{\Delta}{1-x_0}\right)^{1/3} \tag{6.79}$$

which to lowest order in Δ is virtually identical to the diffusion limited case, but with $(1-x_0)^{1/3}$ replaced by $(1-x_0)^{2/3}$.

6.8 Micelle–Mediated Coarsening?

Whether oil exchange between droplets is mainly due to a diffusive flux of *dissolved oil*, or mediated by *oil–swollen micelles*, is determined by the magnitudes of $\beta \equiv D\phi^b_{sol}/D_m\phi^b_m\alpha$ (previously defined in section 6.3.3) and the reaction rate for micelle–droplet oil exchange χ.

Section 6.6 found that if $\chi > \delta_b/\overline{R}$, then any micelle–mediated coarsening is diffusion limited. Section 6.3.3 found that diffusion limited, micelle mediated effects become important for $\beta \sim 1$, dominating the growth rate for $\beta \ll 1$, but being negligible for $\beta \gg 1$ when coarsening would mainly be due to a flux of dissolved disperse phase. Since both micelle–mediated transport and direct diffusion of dissolved disperse phase can occur simultaneously, there will be a smooth crossover as β passes through 1.

When $\delta_b/\overline{R} > \chi$, then section 6.6 found that any *micelle mediated* coarsening would be reaction limited. Note however that since the reaction limited droplet

growth rate is a factor $\sim \delta_b/\chi\overline{R}$ times the diffusion limited expression, then for micelle mediated growth to be more important than that due to flux of *dissolved disperse phase*, we also require $\chi > \frac{\delta_b}{\overline{R}}\beta$ (and hence β to be small). Since micelle–mediated transport requires both droplet–micelle "reactions" to solubilise oil *and* micelle diffusion to transfer oil between droplets, then micelle–mediated coarsening will be either diffusion *or* reaction limited, with a sharp crossover between the regimes as χ passes through $\delta_b/\overline{R}$. The above results are summarised in figure 6.5.

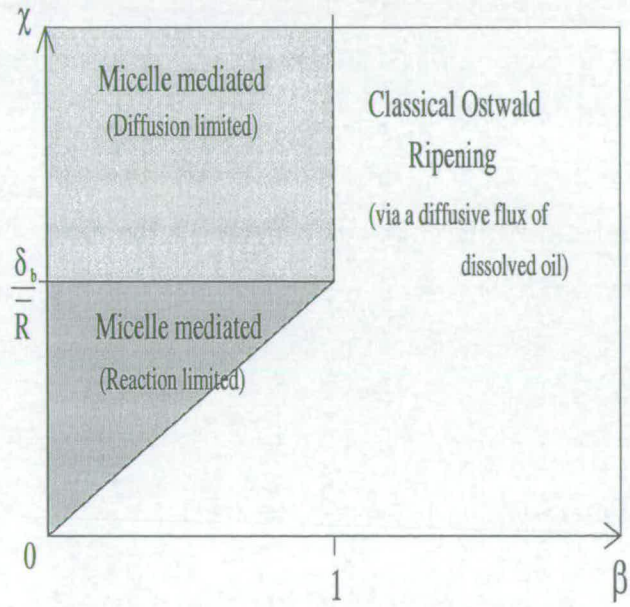

Figure 6.5: Schematic diagram on the (β, χ) plane (with $\beta \equiv D\phi^b_{sol}/D_m\phi^b_m\alpha$), indicating which type of mechanism will transfer the most oil between droplets. Typical orders of magnitude for oil in an aqueous surfactant solution give a maximum value of $\beta \sim 10^{-2}$, hence the reaction rate χ determines the importance of micelle–mediated effects in such systems.

For high molecular weight hydrocarbons (C_9H_{20} to $C_{16}H_{34}$), the addition of sufficient surfactant [62] increases the solubility of oil in an aqueous solution by a factor between 10^4 and 10^5, giving a maximum estimate of $\phi^b_{sol}/\phi^b_m \sim 10^{-4}$. Typically [43, 62] the diffusion constant D for dissolved disperse phase is $D \sim 10^{-9}\mathrm{m}^2\mathrm{s}^{-1}$, and the diffusion constant of micelles D_m is between $10^{-10}\mathrm{m}^2\mathrm{s}^{-1}$ and $10^{-11}\mathrm{m}^2\mathrm{s}^{-1}$.

So taking values for D_m and ϕ^b_{sol}/ϕ^b_m which give the *largest* value of β, and also taking $\alpha \sim 1$, we obtain

$$\beta \sim 10^{-2} \ll 1 \tag{6.80}$$

So given a sufficiently large reaction rate χ, we expect to observe diffusion limited, micelle mediated coarsening. Hence if diffusion limited, micelle mediated coarsening is not observed, it indicates a very low reaction rate χ for micelle–droplet oil exchange, less than of order $\delta_b/\overline{R}$.

Finally, note that when there is exchange of oil and surfactant molecules between micelles the micelle diffusion constant D_m used in β, must be replaced by the effective diffusion constant $(D_{OO} - (D_{OS}D_{SO})/D_{SS})$ defined in section 6.5. Unfortunately the lack of a suitable model for micelles prevents the effective diffusion constant from being calculated. However the simplest estimations (see section 6.5) suggest that the effective diffusion constant may be reduced, so that β will be increased, and micelle mediated effects less likely to be important.

6.9 Conclusions

Simple models for micelle–mediated oil exchange between droplets have been presented and analysed. We have derived droplet growth rates for diffusion limited coarsening (both with and without molecular exchange between micelles), and also for reaction limited coarsening in sections 6.3, 6.5, and 6.6 respectively. The droplet growth rates have enabled us to discuss micelle–mediated coarsening, and indicate the late–time droplet size distributions in sections 6.3.2 and 6.6.1. The rate of solubilisation of an emulsion into oil swollen micelles was considered in sections 6.4 and 6.7, and possible transient phenomena which occur after the initial addition of unswollen micelles to an emulsion, have been described and discussed in section 6.4.4. For a given set of parameters, figure 6.5 indicates whether micelle–mediated coarsening will be important, and whether it will be

diffusion or reaction limited. Section 6.8 considered typical orders of magnitude for an O/W emulsion, and demonstrated that unless there is a very low reaction rate χ, then diffusion–limited, micelle–mediated coarsening will be observed. Hence whether micelles have a significant effect on the coarsening of O/W emulsions is determined by the fraction of encounters χ, with which micelle-droplet interactions result in micelle–droplet oil exchange.

6.9.1 Micelle–Mediated Coarsening

When the micelles present can solubilise only a small part of the oil droplets' total volume fraction, then late–time micelle–mediated oil exchange will be qualitatively the same as classical late–time coarsening. Diffusion–limited coarsening was found to be qualitatively the same as that described by LSW [20, 21], and reaction–limited coarsening was found to be qualitatively the same as that described by Wagner [21].

The late–time diffusion limited coarsening is also qualitatively unaffected by rapid oil and surfactant exchange between micelles (which occurs in addition to micelle–droplet oil exchange). The main effect of allowing oil and surfactant exchange between micelles is to replace the micelle diffusion constant D_m, with an effective diffusion constant, calculable from a suitable model for oil swollen micelles. Whether micelle–mediated coarsening is significantly affected by oil and surfactant exchange between micelles, is determined by the effective diffusion constant. Simple order of magnitude estimates suggest that the effective diffusion constant may be less than D_m, but the exact calculation of an effective diffusion constant is only possible given a suitable model for micelles.

At early times when micelles are initially empty, transient behaviour may be observed. This behaviour is characterised by a growth of the very largest droplets, even while there remains a net flux of oil from droplets to the micellar solution.

The phenomenon is qualitatively the same for all methods of oil exchange between droplets, provided that the system starts with zero solubilised oil volume fraction.

6.9.2 Solubilisation by Micelles

When micelles are sufficient to solubilise all of the oil droplets' volume fraction, then we may obtain expressions for both the diffusion–limited and reaction–limited solubilisation times, Eqs. 6.30 and 6.76 respectively. However, unless both $\phi_m^b \ll 1$ and the oil volume fraction $\phi_0 \ll \phi_m^b$ (which ensures the steady state assumption remains valid), then Eqs. 6.30 and 6.76 must be treated with caution. Whether solubilisation of oil into micelles is diffusion or reaction limited is determined by whether χ is bigger or smaller than $\delta_b/\overline{R}$ respectively.

6.9.3 Can Micelles Destabilise an Emulsion?

So far in this chapter we have disregarded the presence of trapped species. Will micelles destabilise an osmotically stabilised emulsion? Clearly this depends on whether coarsening induced by micelles transporting trapped species can occur much more rapidly than coarsening by a diffusive flux of the (very small) quantity of "trapped" species which would in practice be dissolved in the continuous phase. However, determination of coarsening/solubilisation rates requires (i) knowledge of the reaction mechanism and subsequent reaction rate for solubilisation into micelles, for given types of oil, surfactant and co–surfactant, and (ii) knowledge of how given types of oil, surfactant, and co–surfactant will determine ϕ_m^b the volume fraction of oil that micelles may solubilise. Neither of the above are currently well understood, although they may be determined experimentally. Clearly a combination of careful experimental work, in conjunction with the formation of quantitative theoretical models is required to enable further progress.

Chapter 7

Foams

Foams are all around us. Both you, I, and all multicellular organisms may be considered to be a foam. Open cell foams include all sponge and gel like structures [4], closed cell foams include all cellular structures with solid or liquid walls separating a solid, liquid, or gas phase [4]. Hence any connected space spanning network (with a higher elasticity/shear modulus than the disperse phase), is a foam. Systems and materials in which the opposite is true, such as grains within a continuous gas phase or suspensions in fluid, tend to be described as *granular* matter.

The mechanisms which govern the evolution of the differing foam types may differ dramatically. The evolution of a closed cell foam is typically governed by the rate at which the phase within cells may diffuse through cell walls to cells with lower chemical potential. However in an open cell foam, there are now two connected phases with a network of thickened struts forming via a phase separation firstly into regions of differing densities (which may be considered as closed cells with *thick* cell walls), then by a coarsening of the cell walls to form open cells, and a sponge/gel like structure.

In the following chapters we will restrict our attention to closed cell foams with a

liquid continuous phase separating a gaseous disperse phase (the case of a dense emulsion or liquid–in–liquid foam, is addressed at the end of chapter 9, in section 9.7). Such foams are generally referred to as closed cell liquid foams [4], and have been found to have both many useful applications [5], and to occur in many undesirable circumstances [5]. Hence there has been much theoretical, experimental and computer simulation work on these foams behaviour and stability. For a good general review of closed cell liquid foams see "Foams" in the Kirk–Othmer Encyclopedia of Chemical Technology [5].

In closed cell gas–in–liquid foams (hereafter simply referred to as "foams"), coarsening of foam bubbles and a foam's subsequent destabilisation typically occurs by either [5]

1. *Drainage*: The gravitational segregation of liquid and bubbles.
2. *Film Rupture*: The rupture of cell walls separating adjacent bubbles, leading to the bubbles subsequent coalescence.
3. *Gas Diffusion*: The diffusion of gas (soluble in the continuous phase), from bubbles with a high gas pressure (typically smaller bubbles with higher Laplace pressures), to bubbles with lower gas pressures (typically larger bubbles with lower gas pressures).

Both this and the following chapters restrict their attention to the coarsening and stabilisation of foams which have been stabilised such that coarsening due to either drainage or film rupture, may be neglected. For recent reviews of coarsening in such foams see the review articles by Glazier and Weaire [65], and Stavans [66].

We shall consider the effect of adding an extra species to bubbles, which is highly insoluble in the continuous phase and effectively trapped within bubbles. Such effects were extensively studied in the context of dilute emulsions, in chapters 2–5 (and references within), but only recently been reported in the literature on

foams [67–71] which we will discuss in the following section. Our previous work on emulsions (chapters 2–4) considered emulsions consisting of incompressible liquids, with emulsion droplets taken as being spherical and well–separated.

This chapter firstly reviews previous work on the effects of adding a trapped species within foam bubbles. Then it considers the free energy and chemical potential of foams consisting of compressible gases, but in which bubbles are *dilute* and hence spherical in shape. This is a generalisation of the work on dilute *incompressible* emulsions to dilute *compressible* foam bubbles. The more general case of non–dilute foams in which bubbles press on one another is considered in the following chapter 8, and the exact requirements for stabilisation of foam by trapped species are considered in chapter 9.

Since the insolubility of the trapped species causes the continuous phase to act as a semi–permeable membrane, the pressure of the trapped species may be regarded as an osmotic pressure. Hence we refer to the stabilising effects due to the addition of trapped species as *osmotic stabilisation.*

7.1 A Brief History of Osmotic Stabilisation of Foams

An early case of the stabilising effect of adding a trapped species to foams, was discovered in the oil industry. Falls et al [67], reported experimental evidence of the stabilising effects of adding nitrogen to steam foams used for oil extraction. They analysed the stability of an individual foam bubble and proceeded to derive an expression for the quantity of nitrogen required to stabilise a bubble.

The stabilising effect of nitrogen on foam was also observed in the brewing industry [68, 69]. Parr [68], described how the low solubility of nitrogen allowed the pressurisation of beers which would otherwise have a tendency to form an excessively large and foamy head. Nitrogen's low solubility means that even under

pressure, only a negligibly small quantity of additional nitrogen would dissolve into beer. Hence by adjusting the relative quantities of nitrogen and carbon dioxide, and ensuring the beer is sufficiently agitated on pouring, it is possible to design beers to form the desired size of 'head' after pouring. In addition he noted how the small quantity of dissolved nitrogen resulted in the formation of smaller foam bubbles and a more attractive, creamier, and more stable head. Bamforth [69] observed how even a small mole fraction of Nitrogen could increase the stability of a head, attributing this increased stability to the fact that bubbles which contain nitrogen tend to be smaller in size. He suggested that smaller bubbles have two stabilising effects: (i) the smaller bubbles will take longer to rise and so will accumulate more surface active ingredients; and (ii) a foam formed from smaller bubbles has a larger surface area and the continuous phase liquid will take longer to drain. Neither article mentions the effect of nitrogen on interbubble gas diffusion.

Evidence for the stabilising effect of a trapped species (trapped within foam bubbles), was demonstrated in computer simulations of Weaire and Pageron [70]. They considered 2D disordered foams (or *froths*), in equilibrium with respect to surface tension and pressure. Computer simulations were performed of the foams' evolution, with gas taken to be diffusing between bubbles with a rate proportional to the pressure differences between bubbles. Throughout the simulations they imposed the condition that $\langle P_i \rangle = P$, ie that the average pressure of bubbles was constant.

It was found that very small concentrations of trapped species not only stabilised the foam, but only minor increases in polydispersity of the foam bubbles were required to attain equilibrium. They observed that the effectiveness of the stabilising mechanism arose from the fact that typically, pressure differences between bubbles are small compared with the average pressures in bubbles. Hence they concluded that only small changes in a bubble's gas composition are required

for bubbles to attain equilibrium with one another, and very small quantities of trapped species may stabilise a foam.

Experimental and theoretical evidence for the stabilising effect of a trapped species was presented by Gandolfo and Rosano [71]. They considered the theoretical situation of two bubbles in equilibrium with one another, and how the disproportionation of soluble gas between the bubbles would depend upon the concentration of trapped species they contain. They found that for a sufficient quantity of trapped species, any disproportionation of soluble species between bubbles was small. They concluded that the addition of a sufficient quantity of trapped species would counterbalance Ostwald ripening, and have a stabilising effect on the foam.

Experimentally they also studied how the rate of drainage of a foam is affected by the addition of trapped species. They showed that the addition of trapped species reduced the rate of drainage (a rate which is affected both by gravitational effects and the rate of coarsening of foam bubbles), and found that above a sufficiently high concentration the drainage rates were the same, independent of the additional quantity of trapped species added. This concentration was taken to be a critical concentration above which coarsening via interbubble gas diffusion was prevented, and compared the critical concentration with that found by Kabalnov et al [72] for dilute emulsions. They also considered different ways of fitting the results, and hence the rate limiting mechanisms for the drainage rate.

The desire of a soluble species to mix with and dilute a less soluble species (which remains *trapped* within bubbles) was investigated by Fortes and Deus [73]. They performed both theoretical and experimental work on the kinetics of adsorption of air by a foam consisting of hydrocarbon gas bubbles, in a commercial (Palmolive) shaving cream foam. The work however, was primarily concerned with the adsorption rate of air, and they did not consider the potential of stabilising

foams by the addition of a less soluble species.

This chapter is primarily concerned with obtaining the free energy and chemical potentials of foams consisting of dilute spherical bubbles. We do not consider either the coarsening of unstable foam containing trapped species, or the increases in polydispersity as a stabilised foam attains equilibrium; a start is made on the first of these topics in chapter 10. The rest of this chapter is organised as follows.

Section 7.2 describes the types of foams we consider and the conditions under which they are taken to arise. This enables us to determine the thermodynamic potential required to study foam equilibria, and simplifications which may be made to it for the systems considered here. We then start to generalise the work of chapters 2–3 on dilute *incompressible* emulsions to dilute *compressible* foam bubbles, deriving their free energies and chemical potentials in sections 7.3, 7.4, and 7.5.

7.2 Foam Equilibria

This section describes the types of foam we consider, and the conditions under which we assume them to be formed. We consider the thermodynamic potential relevant to the foams' equilibria, and approximations which may be made to simplify the analysis.

In the following we consider gas–in–liquid foams with bubbles containing a soluble and a trapped gas component, and with a fluid phase maintained at a fixed external pressure which is taken as the atmospheric pressure P. In addition to the trapped and soluble gases within bubbles, there will also be a small quantity of liquid vapour evaporated from the continuous phase. Similarly the continuous liquid phase will contain dissolved (soluble) gas.

The foam constitutes a closed system at pressure P and temperature T, containing a fixed number of liquid and gas molecules. Hence the equilibrium state is obtained by minimising the system's Gibbs free energy at a fixed number of bubbles and soluble gas molecules.

The Gibbs free energy of the foam may be written as

$$G = F_c + \sum_i F_i + \sigma \sum_i A_i + P\left(V_c + \sum_i V_i\right) \tag{7.1}$$

where F_c, F_i are the Helmholtz free energies of the continuous phase and the gases in the ith disperse phase bubble respectively, V_c is the volume of the continuous phase, and V_i, A_i are the volume and area of the ith disperse phase gas bubble.

We now make the following reasonable approximations. Since we expect variations in bubbles pressures to be small compared with the actual gas pressure within foam bubbles, we take variations in the quantity of gas dissolved in the continuous phase as negligible, and hence variations in the free energy of the continuous phase due to dissolved gas as negligible*. We also restrict ourselves to systems in which only a very small fraction of the liquid molecules evaporate into the gas phase (eg at 25 degrees Celsius, and 1 atmosphere, the vapour pressure of water is $\sim 3 \times 10^{-2}$ atmospheres [75] and negligible compared with those of the added gases), and we assume that we may neglect changes in the free energy due to liquid vapour. Finally, we take the continuous liquid phase to be incompressible.

Armed with these arguments, we assume that

1. Changes in the free energy of the continuous phase are negligible, so that the continuous phases free energy may be regarded as constant and unchanging.

*Since we consider systems in which a very small fraction of gas dissolves into the continuous phase (eg at 1 atmosphere and room temperature $\simeq$ 3.3 grams of CO_2 dissolves in 1000 grams of water [74]), changes in the free energy of the continuous phase due to the dissolved gas may be entirely negligible.

2. To calculate the free energy of the disperse phase gas bubbles, we need only consider the trapped and soluble gases, and the bubbles' interfacial energy†.

3. Changes in the system's volume are due to changes in the volume of bubbles.

To obtain the equilibrium state of the foam, we need only consider the minimisation of those contributions to the Gibbs free energy which are neither constant or negligible. So we need only consider the minimisation of the Gibbs free energy of bubbles containing soluble and trapped gas, ie to minimise

$$G_d = \sum_i F_i^s + F_i^T + \sigma A_i + PV_i \tag{7.2}$$

where G_d is the approximate Gibbs free energy of the disperse phase, F_i^s and F_i^T are the Helmholtz free energies of soluble and trapped gases respectively (assumed to be noninteracting). G_d may also be written as $G_d = \sum_i G_i$, where $G_i = F_i^s + F_i^T + \sigma A_i + PV_i$ and is the Gibbs free energy of the ith bubble.

7.3 The Helmholtz Free Energy of Dilute Ideal Gases

We treat the Helmholtz free energy per molecule as composed of a local part f, due to local molecular properties and interactions, and an entropy of mixing. The Helmholtz free energy of a bulk quantity of ideal gas consisting of N_b disperse phase molecules in a volume V_b is then given by [76]

$$F_b = N_b f_b + N_b kT \left[\ln\left(\frac{N_b v_b}{V_b}\right) - 1\right] \tag{7.3}$$

where $v_b \equiv (h^2/2\pi mkT)$ and has the dimensions of volume, with h being Planck's constant, m the molecular mass, T the temperature, and the subscript b is to remind us that we consider a bulk quantity of gas.

†We take the surface tension as constant and independent of bubble area.

7.4 Gibbs Free Energy of a Bulk Gas Phase

The Gibbs free energy of a bulk gas phase without trapped species is given by

$$G_b = F_b^s + \sigma A_b + PV_b \tag{7.4}$$

where F_b^s is the Helmholtz free energy of the soluble gas, A_b is the interfacial area of the bulk gas phase, and V_b is the volume of the bulk gas phase. Using Eq. 7.3 we obtain

$$\begin{aligned} G_b = \; & f_b^s N_b^s + kT N_b^s \left[\ln\left(\tfrac{N_b^s v_b^s}{V_b}\right) - 1\right] + \\ & \sigma A_b + PV_b \end{aligned} \tag{7.5}$$

where N_b^s is the number of molecules of soluble gas, and f_b^s, v_b^s are as defined in section 7.3 but for the soluble gas.

Writing the partial pressure of the soluble species as P_b^s, then since the gas phase only contains soluble molecules, equilibrium between the continuous and gas phases requires $P = P_b^s$. This requirement that $P = P_b^s$ is later referred to as a requirement for *mechanical equilibrium*, since were $P \neq P_b^s$ then mechanical work could be done as the interface moves until $P = P_b^s$.

The chemical potential of the soluble gas may be obtained from $\mu_b = (\partial G_b / \partial N_b^s)_{T,P}$, with the chemical potential of the soluble gas in the bulk phase denoted by μ_b, we find

$$\mu_b = f_b^s + kT \ln\left(\frac{N_b^s v_b^s}{V_b}\right) \tag{7.6}$$

where we used the ideal gas equation $P_b^s = N_b^s kT / V_b^s$, $P = P_b^s$, and noted that a bulk phase will have a flat interface with $(\partial A_b / \partial N_b)_{T,P} = 0$.

7.5 Gibbs Free Energy of Dilute (Spherical) Bubbles

We now consider the free energy of bubbles which contain both soluble and trapped gas molecules. The foam bubbles are considered to be sufficiently dilute that bubbles are spherical in shape. Then a bubble of disperse phase of volume V_i and area A_i, has a contribution to the systems Gibbs free energy given by

$$G_i = F_i^s + F_i^T + \sigma A_i + PV_i \tag{7.7}$$

Noting that the increased pressure within a bubble will only affect the densities of the gases, we may use the Helmholtz free energy for bulk phases (Eq. 7.3) to obtain the Helmholtz free energies of the soluble and the trapped gases, so

$$\begin{aligned} G_i = \; & f_b^s N_i^s + kTN_i^s \left[\ln\left(\tfrac{N_i^s v_b^s}{V_i}\right) - 1\right] \\ & f_b^T N_i^T + kTN_i^T \left[\ln\left(\tfrac{N_i^T v_b^T}{V_i}\right) - 1\right] \\ & +\sigma A_i + PV_i \end{aligned} \tag{7.8}$$

where N_i^s and N_i^T are the number of soluble and trapped molecules in the disperse phase bubble.

The addition of extra soluble gas molecules to a bubble will result in an increased internal pressure, and subsequent changes in its volume and interfacial area. Since the volume and area of a spherical bubble are not independent, when calculating a bubble's chemical potential we need only consider changes in volume and the number of soluble species it contains. So denoting the soluble disperse phase's chemical potential by μ_i, and using the ideal gas law for the soluble and trapped species respectively, we find

$$\mu_i = \left(\frac{\partial G_i}{\partial N_i^s}\right)_{T,P,V_i} + \left(\frac{\partial V_i}{\partial N_i^s}\right)_{T,P} \left(\frac{\partial G_i}{\partial V_i}\right)_{T,P,N_i^s} \tag{7.9}$$

with

$$\left(\frac{\partial G_i}{\partial N_i^s}\right)_{T,P,V_i} = f_i^s + kT \ln\left(\frac{N_i^s v_b^s}{V_i}\right) \tag{7.10}$$

and

$$\left(\frac{\partial G_i}{\partial V_i}\right)_{T,P,N_i^s} = P + P_i^G - P_i^s - P_i^T \tag{7.11}$$

where P_i^s, P_i^T are the partial pressures of the soluble and trapped gases respectively, and $P_i^G = \sigma(\partial A_i/\partial V_i)$ is a pressure determined by a bubble's spherical geometry. We note that P_i^G for a spherical 3D bubble is identical to its Laplace pressure, but for the benefit of later chapters we keep P_i^G and the Laplace pressure as distinct from one another.

We now assume that a bubbles volume adjusts rapidly compared with flux of soluble disperse phase, and take $(\partial G_i/\partial V_i)_{T,P,N_i^s} = 0$. This corresponds to the requirement of *mechanical equilibrium*, with the pressure inside a bubble being balanced by the combination of external pressure and the additional geometric (or Laplace, for a spherical bubble) pressure due to surface tension[‡]. So taking $(\partial G_i/\partial V_i)_{T,P,N_i^s} = 0$, and noting that for a spherical bubble of radius R_i, $P_i^G = 2\sigma/R_i$, we find

$$P_i^s + P_i^T = P + \frac{2\sigma}{R_i} \tag{7.12}$$

which is the well known Laplace equation [39]. So we obtain the chemical potential as

$$\mu_i = f_i^s + kT \ln\left(\frac{N_i^s v_b^s}{V_i}\right) \tag{7.13}$$

This differs from Eq. 7.6, since N_i^s/V_i depends on both the soluble and the trapped species; it is not equal to the same ratio evaluated in a bulk gas phase.

The ideal gas equation for the bubble's soluble gas has

$$\frac{P_i^s}{kT} = \frac{N_i^s}{V_i} \tag{7.14}$$

So we may use Eqs. 7.12, 7.13, and 7.14, to get

$$\mu_i = f_i^s + kT \ln\left(\frac{v_i^s}{kT}(P + \frac{2\sigma}{R_i} - P_i^T)\right) \tag{7.15}$$

[‡]This also corresponds to minimising the free energy at a fixed number of soluble gas molecules in a bubble (approximately true over short times), which is accomplished by minimising G by changing the only free variable, the bubble's volume.

Since we are interested in how the trapped species and the bubble geometry alter the chemical potential from that of the bulk gas phase, we consider $\Delta\mu_i \equiv \mu_i - \mu_b$ and rearrange to get

$$\Delta\mu_i = kT \ln\left(1 + \frac{\frac{2\sigma}{R} - P_i^T}{P}\right) \tag{7.16}$$

(where we also used $\frac{P}{kT} = \frac{P_b^s}{kT} = \frac{N_b^s}{V_b}$ in Eq. 7.6).

Provided $(\frac{2\sigma}{R_i} - P_i^T)/P \ll 1$ then we may expand Eq. 7.16, which to $O((\frac{2\sigma}{R_i} - P_i^T)/P)$ gives

$$\Delta\mu_i = \frac{kT}{P}\left(\frac{2\sigma}{R_i} - P_i^T\right) \tag{7.17}$$

We now define a volume per molecule the ith gas bubble by $v_i \equiv V_i/(N_i^s + N_i^T)$, and also write the partial pressure of the trapped species as $P_i^T = N_i^T kT/(4\pi R_i^3/3)$. Then using the bubble's ideal gas equation $(P + \frac{2\sigma}{R_i})/kT = (N_i^s + N_i^T)/V_i$, and continuing to work to $O(\frac{2\sigma}{R_i}/P)$ we obtain

$$\Delta\mu_i = \left(\frac{2\sigma}{R_i} - \frac{N_i^T kT}{(4\pi/3)R_i^3}\right) v_i \tag{7.18}$$

The assumption of $\frac{2\sigma}{R_i}/P \ll 1$, corresponds to taking bubbles as effectively incompressible (in that although coarsening may exchange volume between bubbles, the total bubble volume will remain constant). Hence the resemblance of Eq. 7.18 to Eq. 2.10 in chapter 3 for a spherical incompressible emulsion droplet, ie

$$\Delta\mu_i = \left(\frac{2\sigma}{R_i} - \frac{\eta kT}{(4\pi/3)R_i^3}\right) v_b \tag{7.19}$$

with η being the number of trapped species in the emulsion droplet, and v_b being the volume per molecule of the bulk *liquid* disperse phase.

Chapter 8

Non–Dilute Foams

This chapter considers non-dilute foams in which bubbles press against one another and are no longer spherical in shape. To help clarify the degree to which bubbles press on one another, we will follow the approach of Princen et al [77–79] and consider the compression of a dilute foam by a piston with a semi–permeable membrane. Although the liquid phase may flow freely through the semi–permeable membrane, bubbles may not and hence exert an osmotic pressure Π on the piston. Hence we may form a non–dilute foam by an osmotic compression of a previously dilute foam.

The main subject of this chapter is how pressures within bubbles are affected by the osmotic pressure Π. In the dilute case bubbles were able to locally minimise their surface area by adopting a spherical shape, while under atmospheric pressure P. Hence 3D bubble pressures were given simply by $P_i = P + 2\sigma/R_i$, where $2\sigma/R_i = \sigma(\partial A_i/\partial V_i)$, and is the Laplace pressure of a spherical bubble. Now however the osmotic pressure Π exerts a pressure on bubbles, causing them to distort and increase their surface area.

The chapter starts by discussing the interaction between bubble membranes in section 8.1, and section 8.2 motivates the suggestion that a bubble's pressure may

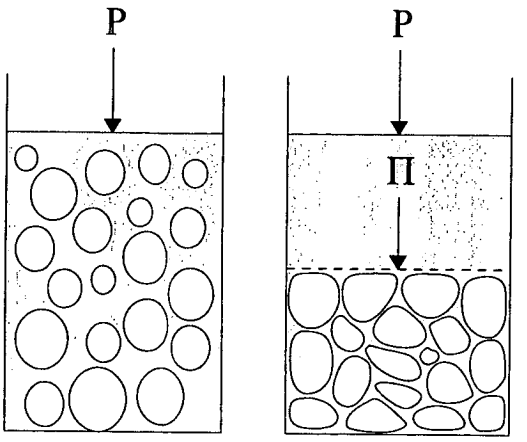

Figure 8.1: Formation of a non–dilute foam by the osmotic compression of a dilute foam, with an applied osmotic pressure Π.

be expressed as $P_i = P + \Pi + P_i^G$, with $P_i^G \ll \Pi$ and analogous to the Laplace pressure of a spherical bubble. We support and clarify the discussion in section 8.3 by carefully considering observations of dry 2D foams, before presenting a simple monodisperse 2D model in section 8.4 for which we exactly calculate bubble pressures and confirm that $P_i = P + \Pi + P_i^G$ as previously proposed. Section 8.5 considers when the arguments will generalise to polydisperse systems, and presents two simple examples of highly polydisperse systems which demonstrate that our proposed equation for bubble pressures cannot *always* be correct. After outlining the conditions under which we expect $P_i = P + \Pi + P_i^G$ to be valid, we then consider an argument in section 8.6 which enables us to determine the order of magnitude of $\langle P_i^G \rangle$.

Motivated by the previous sections we then define in section 8.7 the "geometric pressure" as $P_i^G \equiv P_i - P - \Pi$, and suggest a form for P_i^G. Since bubbles' pressure differences determine the rate of coarsening, then since $P_i - P_j = P_i^G - P_j^G$, differences in bubbles' geometric pressures will determine the rate of coarsening of a foam. Finally we consider some further consequences of our discussion, deriving the analogy of Von Neumann's law when bubbles contain trapped species in section 8.8, and propose a model for bubble arrangements in section 8.9 to

explain the experimental observations of Durian et al [86,87].

8.1 Role of the Disjoining Pressure

In a very wet foam with a large volume fraction of liquid, bubbles will *locally* minimise their free energies by adopting a spherical shape. However, foams with small volume fractions of liquid consist of bubbles in contact with one another, and the bubbles are distorted from their ideal spherical shape. In the limit of a totally dry foam, 3D bubbles will form polyhedral bubbles (but with curved interfacial faces), and monodisperse 2D foams will form hexagonal bubbles. Dry foams can be obtained from wet foams by lowering the volume fraction of the continuous phase either by compressing the foam with a semipermeable membrane through which only continuous phase may pass, or by increasing the bubbles' volume fraction by lowering the system's pressure P so that bubbles may expand and press against one another.

Similarly, compressed emulsions are emulsions consisting of incompressible liquid droplets, pressed together by the action of a semipermeable membrane through which only continuous phase may pass, to result in touching, non–spherical emulsion drops.

Both dry foams and compressed emulsions consist of bubbles/droplets of disperse phase, pressed together so that the majority of the continuous phase resides in the Plateau borders which border the bubble–bubble faces. Hence a typical bubble's interface consists of gently curved faces which border adjacent bubbles, and highly curved regions at Plateau borders (see figure 8.2). If we consider the concentration of the disperse phase dissolved within plateau borders, we find it should be higher than that above the flattened bubble interfaces. This would result in a continual flux of disperse phase, evaporating at the plateau borders and then subsequently

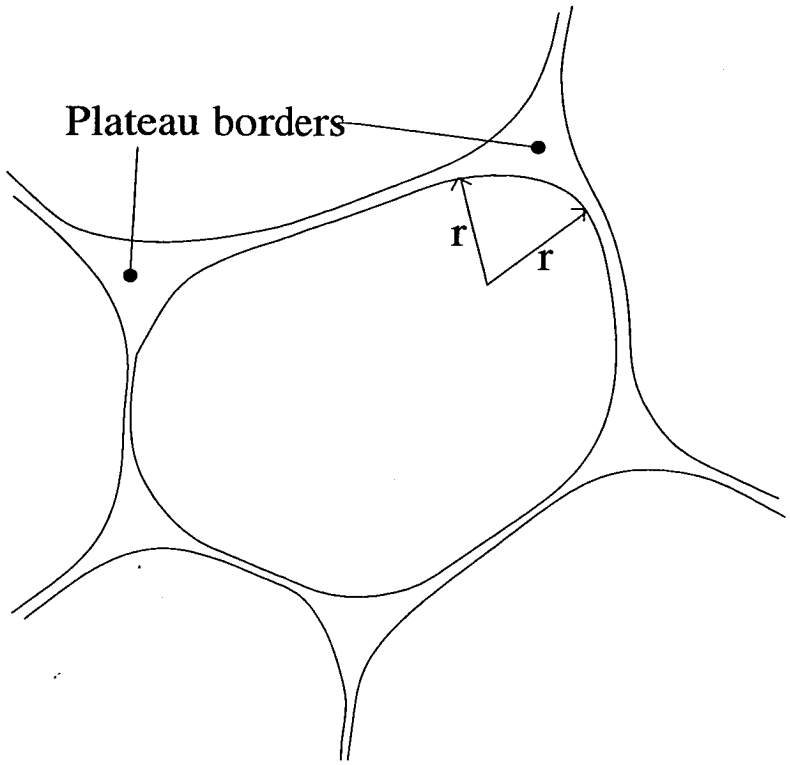

Figure 8.2: Non–dilute *dry* foams consist of bubbles pressing on one another with gently curved adjacent bubble faces, and regions of high curvature ("Plateau borders") in which the majority of continuous phase resides.

being readsorbed at the flattened faces. Since thermal equilibrium forbids the presence of cyclical steady states, we can deduce the existence of an extra force which increases the chemical potential of solubilised disperse phase in the liquid films separating the flattened interfaces. The extra "disjoining" force is directly or indirectly due to the intermolecular interactions between adjacent bubble faces (and their ion clouds, in the case of double layer forces), and must increase the chemical potential of solubilised disperse phase in the flattened films so that at equilibrium, there is zero flux.

Buzza and Cates [80], considered the contribution of the double layer forces to an *emulsion* droplets free energy. They found that for typical emulsions with radii = 50μm, ionic concentration (in the continuous phase) = 0.1M, surface

tension $10 \times 10^{-3}\mathrm{Jm}^{-2}$, and surface charge density $0.2\mathrm{Cm}^{-2}$, that the potential effectively acted as a 'hard wall', with the contribution to a droplets free energy being negligible compared with that due to surface tension between the disperse and continuous phases. Hence although in an emulsion the double layer forces provide the mechanism by which equilibrium is maintained, we may neglect their contribution to an emulsion droplets free energy.

The air water surface tension is $\sim 10 \times 10^{-3}\mathrm{Jm}^{-2}$, and foams typically use similar surfactants to emulsions (eg SDS [5]) while typically also containing electrolytes [5]. Hence we shall take the double layers contribution to the free energy of a *foam* stabilised by ionic surfactants as being negligible. The interaction between nonionic surfactants is even shorter ranged than that between ionic surfactants. So the potential between nonionic surfactant membranes is even more like a hard wall than the potential for ionic surfactants. Hence we also take the contribution to a bubble's free energy due to the interaction between nonionic surfactants, as negligible compared with the surface tension between the disperse and continuous phases. So in all that follows we assume that the disjoining pressure only indirectly affects a bubble's free energy, by increasing its internal pressure and distorting its shape with an associated increase its surface area. The above assumptions will be used in all that follows. Next we provide a simple calculation for the chemical potential within foam bubbles.

Consider an element of volume within a gas bubble. Within such a volume, the gases chemical potential is determined solely by its pressure. So if we treat the gas as ideal, and apply the Gibbs–Duhem relation at fixed T to the ith bubble, then we have [39],

$$N_i^s d\mu_i^s = V_i dP_i^s \tag{8.1}$$

which may be integrated using the ideal gas equation $P_i^s V_i = N_i^s kT$, to obtain the soluble species chemical potential as

$$\mu_i^s = \mu_b^s + kT \ln\left(\frac{P_i^s}{P_b^s}\right) \tag{8.2}$$

Since a bulk gas bubble must experience a pressure P for dilute foams or $\tilde{P} \equiv P + \Pi$ for non–dilute foams (see figure 8.3), then $P_b^s = \tilde{P}$ and we have

$$\mu_i^s = \mu_b^s + kT \ln\left(\frac{P_i^s}{\tilde{P}}\right) \tag{8.3}$$

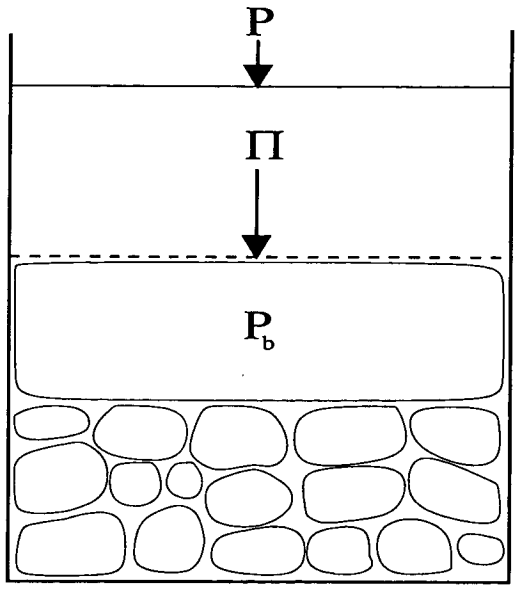

Figure 8.3: The increase in pressure of a bulk gas due to interfacial tension is negligible, so the pressure of a bulk gas will balance (and hence equal) $P + \Pi$.

8.2 'Softness Simplifies'

When considering the effect of compressing a foam or emulsion, the softness of the system may result in drastic simplifications.

For example, if we consider compressing the system with a semipermeable membrane, the *soft* previously spherical bubbles will distort in shape and the continuous phase will flow so that the additional pressure is evenly distributed amongst bubbles/droplets. This contrasts with granular materials for example, in which compressive forces vary with position, with a compressive stress typically being

distributed along lines which percolate from the top (where the pressure is applied), to the bottom of the structure [81,82]. Were the grains to become 'soft', then the grains would distort and distribute the stress tangentially to the previous 'stress lines', resulting in the stress becoming increasingly uniform as grains become increasingly soft.

In the simplest scenario of 2D, monodisperse foams/emulsions, the bubbles would be compressed into monodisperse hexagons (with 'rounded' corners), and equal internal pressures. However, compression of a general polydisperse foam will result in bubbles deforming into various different geometries, depending on properties of both the bubble itself and those of its neighbours. Hence a given bubble will have a pressure which depends not only on its volume (as for spherical bubbles), but on the arrangement and pressures of *all* of its adjacent neighbours.

The above discussion may be clarified by noting that bubble interfaces which press on one another must do so with a radius of curvature of the order of $1/R$ (where R is the radius of a bubble with the same volume in an uncompressed state). Hence pressure differences between bubbles will be of the order of σ/R, so that as Π and bubbles' pressures are increased, the increase *must* occur homogeneously throughout the foam.

So in a sufficiently soft and monodisperse system in which all bubbles are compressed and pressing on one another, we expect the osmotic pressure Π to be fairly evenly distributed between bubbles. In addition we expect a further increase in bubbles' pressures due to interfacial tension, and expect a contribution to a bubble's pressure of P_i^G, which is analogous to the Laplace pressure of a spherical bubble. Hence we expect that a bubble's pressure P_i may be written as

$$P_i = P + \Pi + P_i^G \tag{8.4}$$

which for a dilute uncompressed 3D bubble of radius R_i is

$$P_i = P + P_i^G \tag{8.5}$$

with $P_i^G = 2\sigma/R_i$, and for a bulk gas bubble in a compressed foam would require

$$P_b = P + \Pi \tag{8.6}$$

as emphasised in figure 8.3.

Eq. 8.4 also enable us to clarify what we mean by a 'soft' system. If bubbles are to become highly distorted we require $\Pi \gg P_i^G$, so in a soft foam all bubbles will have

$$\Pi \gg P_i^G \tag{8.7}$$

We note that generally we will not know what P_i^G is, nor will it always be well defined. The definition of P_i^G is clarified later, and a specific example where P_i^G is exactly determined is given in section 8.4.

8.3 Case Study: *Dry* 2D Foam

To clarify and support the above arguments we shall carefully consider some observations of dry 2D foams.

There is a popular misconception that in a dry 2D foam (with negligible liquid volume fraction), 3 edges meet at a vertice with angle $2\pi/3$. This is an increasingly good approximation as foams become increasingly dry, but never strictly correct (for the physically correct scenario of small though non–zero water content).

We may prove the assertion is false by noting the following:

1. If 3 edges meet at $2\pi/3$, then the 3 meeting bubbles must have the same radius of curvature r at the plateau border (by geometry, see figure 8.4).

2. Since a bubble's total pressure P_i is given by $P_i = \sigma/r_i + P$, then any given bubble must have the same radius of curvature r_i at *all* of its vertices.

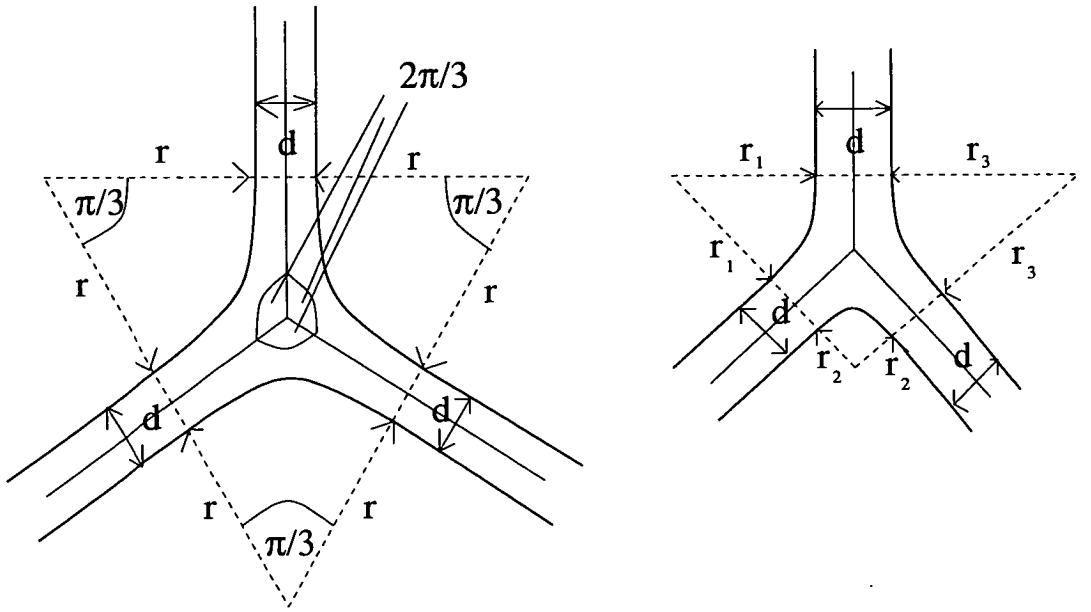

Figure 8.4: Diagram on left of figure shows how if edges meet at $2\pi/3$, then bubbles have equal radii of curvature at their plateau borders. Diagram on right of figure shows how differing radii at bubble plateau borders lead to edges no longer meeting with angle $2\pi/3$.

Then 1 and 2 together imply that all bubbles have the same $r_i = r$, and hence that all bubbles must have the same pressure! However since coarsening occurs and is due to pressure differences (chemical potential differences) between bubbles, then the assertion that bubble edges meet with an angle of *exactly* $2\pi/3$ must be false.

Nonetheless, the observation that to a very good approximation edges meet with angle $2\pi/3$ in turn implies that differences in pressure between bubbles must be small and much less than $P_i = P + \sigma/r_i$, where r_i is the radius of curvature of a bubbles plateau border. We make the following observations which are increasingly true as a foam becomes increasingly dry:

1. $\sigma/r_i \gg \sigma/R_i$, so there is a large increase in bubbles' internal pressures (due to Π) above those of equivalent bubbles in a dilute (uncompressed) foam.

2. $P_i \simeq P_j$, so that the increase in bubble pressure is evenly distributed.

3. The relatively small curvature of adjacent bubble faces means that pressure differences between bubbles ΔP_{ij} are of order σ/R_i, where R_i is of order the square root of the average bubble area.

4. The angles between bubble edges (defined by extrapolating bubble edges until they meet within a Plateau border), tend to $2\pi/3$.

In addition we note that $P_i \gg \Delta P_{ij}$ means that variations in the area per gas molecule are of order $\Delta P_{ij}/P_i \ll 1$ (where we assume the gas is ideal). So if we consider coarsening of a dry 2D foam by interbubble gas diffusion, we may treat the gas as if it were incompressible.

We may compare the above observations with our qualitative discussion in section 8.2, which for a dry (soft) foam would suggest we write $P_i = P + \Pi + P_i^G$, with $\Pi \gg P_i^G$. Hence by our definition of a "soft" foam $\Pi \gg P_i^G$, so that $P_i \simeq P_j \simeq P + \Pi$ (as in item 2). Since $P_i = P + \Pi + P^G$ leads to $\Delta P_{ij} = P_i^G - P_j^G$, then if we assume $P_i^G \sim \sigma/R_i$, we immediately have $\Pi \gg P_i^G \sim \sigma/R_i$ (as in item 2), and $\Delta P_{ij} \sim \sigma/R_i$ (as in item 3). So comparisons with a dry 2D foam are consistent with our qualitative discussion in section 8.2, and are also consistent with the hypothesis of $P_i^G \sim \sigma/R_i$ (which we might expect if P_i^G is truly analogous to the Laplace pressure of a dilute, spherical bubble). We note that since dry 3D foams have fourfold vertices with faces meeting with an internal angle of 109.47 degrees [65], we expect similar arguments to the above to also apply to dry 3D foams.

In the next section we consider a simple model of a monodisperse 2D foam, for which we may *exactly* calculate Π and P_i^G.

8.4 A Simple 2D Model

We consider a monodisperse, incompressible, 2D foam, in which bubbles are compressed by an osmotic pressure Π. Since the bubbles are monodisperse, they will form an hexagonal array of bubbles which are distorted into approximately hexagonal shapes but with rounded corners (see figure 8.5). We take the surface tension to be constant, and neglect any (presumed small) interaction energies arising from the disjoining pressure between bubble interfaces*. For simplicity the separation between adjacent bubbles is taken to be negligible (ie zero). A schematic picture of the foam is given in figure 8.5.

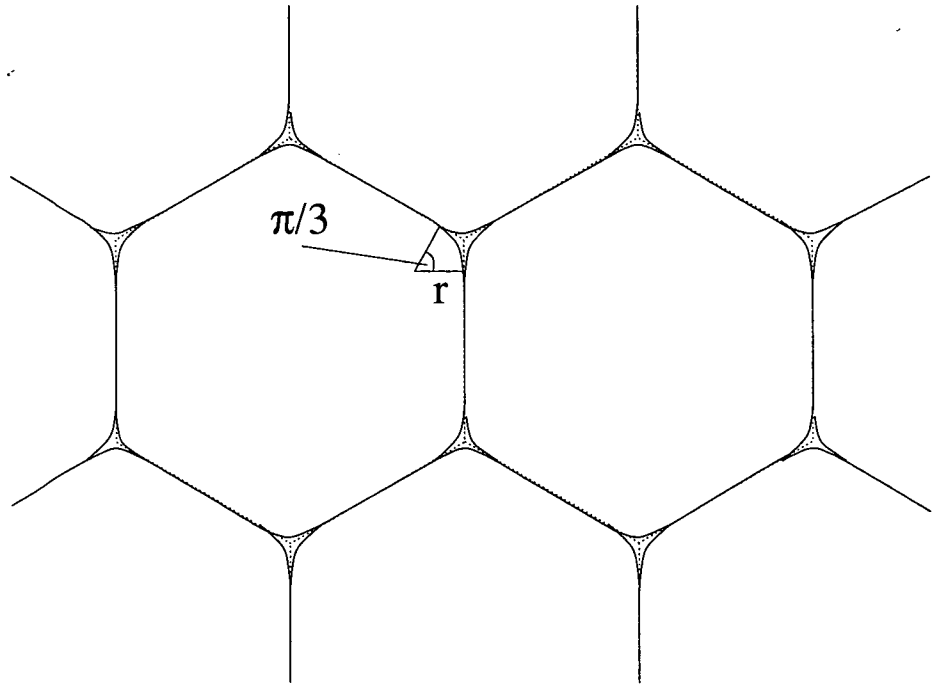

Figure 8.5: We consider a model of a 2D foam which consists of bubbles of the same size which form a hexagonal array. Since bubbles are equivalent they have the same pressures and hence radii of curvature at their Plateau borders.

Since the bubbles are taken to be incompressible (for small changes in their interfacial area), then in an infinitesimal compression the osmotic pressure Π

*See section 8.1 for details.

does work by removal of liquid continuous phase from bubbles' Plateau borders. So writing the area of liquid in the system as A_l^{sys}, the interfacial length within the system as L^{sys}, and the total area of bubbles in the system as A_i^{sys}, then we have

$$\Pi dA_l^{sys} = -\sigma \left(\frac{\partial L^{sys}}{\partial A_l^{sys}} \right)_{A_i^{sys}} dA_l^{sys} \tag{8.8}$$

For the monodisperse, hexagonal system of bubbles studied we may associate an area of liquid A_{li} with each bubble, with A_{li} given as the sum of one third of the volume of liquid at each of its Plateau borders. Then since the system is monodisperse we have $A_{li} = A_{lj}$ and $A_i = A_j$ so that

$$\Pi \sum_i dA_{li} = -\sigma \sum_i \left(\frac{\partial L_i}{\partial A_{li}} \right)_{A_i} dA_{li} \tag{8.9}$$

gives

$$\Pi = -\sigma \left(\frac{\partial L_i}{\partial A_{li}} \right)_{A_i} \tag{8.10}$$

where A_i, L_i are the area and interfacial length of the ith bubble respectively.

As discussed in section 8.2 we expect a bubbles pressure to be given by $P_i = P + \Pi + P_i^G$, with P_i^G being an additional increase in bubble pressure, typically due to interfacial tension and analogous to a dilute bubble's Laplace pressure. So by analogy with the Laplace pressure we postulate an additional pressure due to surface tension, calculated for an isotropic growth[†] at fixed liquid area. So for the monodisperse system considered here we postulate

$$P^G = P_i^G = \sigma \left(\frac{\partial L_i}{\partial A_i} \right)_{A_l} \tag{8.11}$$

with $(\partial L_i/\partial A_i)_{A_l}$ calculated for an isotropic expansion, and with $P_i^G = P^G$ the same for all bubbles (since the system is monodisperse). Since for an isotropic expansion P^G will depend on a bubbles geometry, generally we refer to P^G as a bubble's "geometric" pressure.

[†]The symmetry of the hexagonal system suggests we consider an isotropic expansion.

The postulated geometric pressure for a nearly hexagonal bubble is calculated next, in section 8.4.1. Then in section 8.4.2 we provide an exact calculation for the systems osmotic pressure, and find that the pressure increase within a bubble (above atmospheric pressure) is given *exactly* by the sum of the osmotic pressure Π and the proposed geometric pressure P^G. This is an entirely rigorous result, exact for the system studied (shown in figure 8.5). The result confirms our physical arguments, while also (as a corollary) providing an exact expression for the osmotic pressure in terms of the radius of curvature of the rounded corners of the hexagonal bubbles (or equivalently the volume of liquid in the osmotically compressed foam). It also clarifies and confirms the existence of an additional pressure due to interfacial tension, which for the system studied is proportional to the rate of change in interfacial area with increase in bubble area, for an isotropic expansion at *fixed* liquid content (ie, fixed radius of curvature of plateau borders).

8.4.1 The Geometric Pressure of a Nearly Hexagonal Bubble

We consider nearly hexagonal bubbles, and use the definition of P^G postulated in Eq. 8.11. Since P^G is calculated at a fixed volume of liquid per bubble, it must be calculated at a fixed radius of curvature at the Plateau borders (since each of a bubble's Plateau borders are equivalent, and of a fixed total number). Hence we may write Eq. 8.11 as

$$P^G = \sigma \left(\frac{\partial L}{\partial l}\right)_r \left(\frac{\partial l}{\partial A}\right)_r \tag{8.12}$$

where l is the length of the flat bubble–bubble faces, and where since bubbles are equivalent we've ignored the subscripts on L_i and A_i.

In appendix C we obtain the exact expressions for the interfacial length, and area of a nearly hexagonal bubble as

$$L = 6l + 2\pi r \tag{8.13}$$

and

$$A = \pi r^2 + 6lr + \frac{3\sqrt{3}}{2} l^2 \tag{8.14}$$

respectively. So we obtain

$$\left(\frac{\partial L}{\partial l}\right)_r = 6 \tag{8.15}$$

and

$$\left(\frac{\partial l}{\partial A}\right)_r = \frac{1}{6r + 3\sqrt{3}l} \tag{8.16}$$

which gives

$$P^G = \frac{6\sigma}{6r + 3\sqrt{3}l} \tag{8.17}$$

Using Eq. 8.14 we obtain

$$l = \frac{-6r + \sqrt{36r^2 + 6\sqrt{3}(A - \pi r^2)}}{3\sqrt{3}} \tag{8.18}$$

where we note that we've taken l as the physically correct, positive solution for l from Eq. 8.14. So substituting Eq. 8.18 into 8.17, gives after some algebra

$$P^G = \frac{6\sigma}{\sqrt{36r^2 + 6\sqrt{3}(A - \pi r^2)}} \tag{8.19}$$

which we shall use in the following section.

We note that P^G may also be written as

$$P^G = \frac{\sqrt{2\sqrt{3}}\sigma}{\sqrt{A + A_l}} \tag{8.20}$$

with

$$A_l = \left(2\sqrt{3} - \pi\right) r^2 \tag{8.21}$$

which equals the area of liquid continuous phase associated with a bubble (this is shown to be the case in the following section 8.4.2).

8.4.2 Exact Calculation of the Osmotic Pressure

The osmotic pressure is given by Eq. 8.10 as[‡]

$$\Pi = -\sigma \left(\frac{\partial L}{\partial A_l} \right)_A \tag{8.22}$$

where since bubbles are equivalent we continue to ignore the subscripts on L_i, V_{li}, and A_i. The total area of a bubble is conserved during an osmotic compression, so that a bubble's radius of curvature at its plateau borders r and the length of a flat interface between itself and an adjacent bubble l are not independent of one another. Hence since the volume of liquid in the plateau border is given in terms of bubbles' radii of curvature r at the Plateau border, we may write Eq. 8.22 as

$$\Pi = -\sigma \left(\frac{\partial L}{\partial r} \right)_A \left(\frac{\partial r}{\partial A_l} \right)_A \tag{8.23}$$

We may calculate the volume of liquid at a plateau border in terms of r. From figure 8.6 we see that the area of liquid within the plateau border is given by

$$A_{pb} = \sqrt{3} r^2 - \frac{1}{2} \pi r^2 \tag{8.24}$$

So since each bubble has 6 vertices (for an hexagonal packing), and each vertex is shared between 3 neighbours, we have a total volume of liquid per bubble of

$$A_l = \frac{1}{3} 6 \left(\sqrt{3} r^2 - \frac{1}{2} \pi r^2 \right) = r^2 \left(2\sqrt{3} - \pi \right) \tag{8.25}$$

and hence obtain

$$\frac{\partial r}{\partial A_l} = \frac{\sqrt{3}}{r(12 - 2\pi\sqrt{3})} \tag{8.26}$$

[‡]We note that an equivalent calculation was done by Princen [77–79], for the osmotic pressure of monodisperse, *cylindrical*, emulsion droplets. Princen's calculation gives the osmotic pressure in terms of the volume fraction of droplets, and the volume fraction of close packed cylindrical droplets. However Princen [77–79] does not interpret the osmotic pressure in terms of a bubbles pressure P_i and its geometric pressure P_i^G as we will do here. Appendix D confirms that the two calculations for the osmotic pressure give the same result.

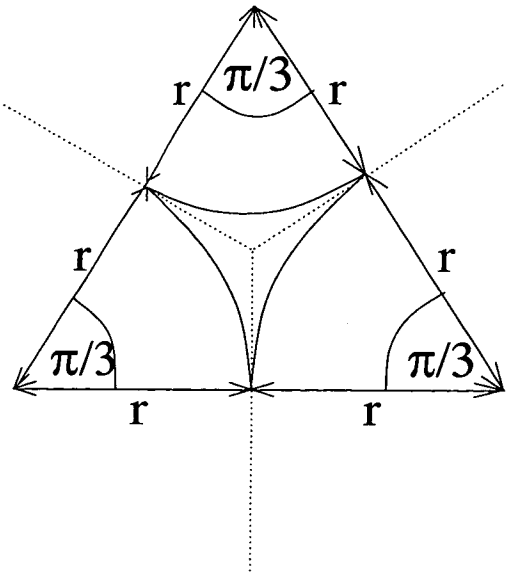

Figure 8.6: Each Plateau border has 3 adjacent bubbles, each with radius of curvature r at the Plateau border. Hence the radii of the 3 bubbles form an equilateral triangle which encloses the Plateau border.

where we have multiplied numerator and denominator by $\sqrt{3}$ for clarity of presentation in the following.

Eq. 8.18 gives l in terms of r and A, with

$$l = \frac{-6r + \sqrt{36r^2 + 6\sqrt{3}(A - \pi r^2)}}{3\sqrt{3}} \tag{8.27}$$

Substituting Eq. 8.18 into 8.13, and differentiating, leads after some algebra to

$$\left(\frac{\partial L}{\partial r}\right)_A = \frac{(2\pi\sqrt{3} - 12)}{\sqrt{3}} \left(1 - \frac{6r}{\sqrt{36r^2 + 6\sqrt{3}(A - \pi r^2)}}\right) \tag{8.28}$$

Hence using Eqs. 8.23, 8.26, and 8.28 we obtain

$$\Pi = \frac{\sigma}{r} - \frac{6\sigma}{\sqrt{36r^2 + 6\sqrt{3}(A - \pi r^2)}} \tag{8.29}$$

which comparing the last part of Eq. 8.29 with Eq. 8.19, enables us to write

$$\Pi = \frac{\sigma}{r} - P^G \tag{8.30}$$

If we consider a bubbles plateau border, then we find that the total pressure P_i within a bubble must satisfy

$$P_i = P + \frac{\sigma}{r} \tag{8.31}$$

where P is the atmospheric pressure. So using Eq. 8.29, gives

$$P_i = P + \Pi + P^G \tag{8.32}$$

Hence after the osmotic compression of a monodisperse array of 2D bubbles, their internal pressure is increased above that of atmospheric pressure by an amount given by a sum of the applied osmotic pressure Π and their geometric pressure P^G.

The exact result Eq. 8.32 confirms our physical argument for the pressure in a bubble following osmotic compression. The result also confirms our hypothesis for the system studied, that the geometric pressure must be calculated for an isotropic expansion at a fixed radius of the plateau borders r.

It is interesting to note the behaviour of Eq. 8.19 for P^G, which has

$$P^G = \frac{6\sigma}{\sqrt{36r^2 + 6\sqrt{3}(A - \pi r^2)}} \tag{8.33}$$

In the dilute limit $A \to \pi r^2$ and hence $P^G \to \frac{\sigma}{r} = \sqrt{\pi}\sigma/\sqrt{A}$, and in the dry limit $r^2/A \to 0$ and hence $P^G \to \sqrt{2\sqrt{3}}\sigma/\sqrt{A}$. So since $\sqrt{\pi}/\sqrt{2\sqrt{3}} \simeq 1.05$, we find the surprising result that P^G is approximately the same for dilute bubbles as it is for compressed bubbles, regardless of the magnitude of Π.

8.5 Polydisperse systems

We now consider more carefully the requirements for us to be able to write even for polydisperse foams that,

$$P_i = P + \Pi + P_i^G \tag{8.34}$$

and to also have

$$P_i^G \ll P_i \tag{8.35}$$

Clearly for the above equation and conditions to apply, it requires that all bubbles will experience an osmotic pressure that results in all bubbles having a pressure of the same order of magnitude. For the packing of monodisperse 2D foam bubbles, the homogeneity of the system resulted in all bubbles experiencing the same osmotic pressure, and the hexagonal structure of monodisperse bubbles ensured all bubbles had the same pressure.

There are two main factors which determine whether the above will generalise, these are:

1. The degree of compression. This is determined by the competition between the osmotic pressure trying to distort bubbles, and their geometric pressure. If the system is soft with $\Pi \gg \sigma/R_i$, with R_i^2 of the order of typical bubble area, then the system will be highly compressed and plateau borders will be small (and the foam fairly dry).

2. The degree of polydispersity. At very high polydispersity this may enable sufficiently small bubbles to be uncompressed, by residing *within* the plateau borders between larger bubbles (see figure 8.7).

If the system is sufficiently monodisperse, and sufficiently compressed that no bubbles may reside in an uncompressed state, then all bubbles will experience an osmotic compression. If plateau borders are sufficiently small in comparison with bubble sizes (ie, if the foam is fairly *dry*), then requirements for mechanical equilibrium impose increasingly accurate restrictions on the angles with which bubble edges and faces must meet. For example a 2D foam will have edges meeting with angle $\simeq 2\pi/3$, an approximation which becomes increasingly good as the foam becomes drier. A foam in which edges meet with an *exactly* fixed angle (eg $2\pi/3$ for a dry foam), would have bubbles with *exactly* equal radii of curvature

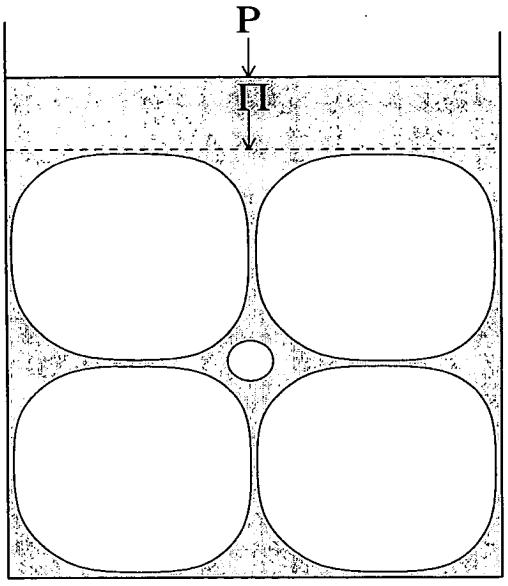

Figure 8.7: A foam in which polydispersity is too large and osmotic pressure too small may have bubbles which do not experience the osmotic pressure Π. Such bubbles would have a pressure $P_i = P + P_i^G$, as opposed to $P_i = P + \Pi + P_i^G$ as proposed above.

at their Plateau borders, and hence equal bubble pressures. Finally, noting that the curvatures between adjacent bubbles must remain $\sim 1/R_i \ll 1/r_i$, then as a foam becomes increasingly dry the pressures within bubbles become increasingly equal, and pressure differences increasingly small. Hence our expression of $P_i = P + \Pi + P_i^G$, with $P_i^G \ll P_i$, will become increasingly accurate as foams become increasingly dry.

We emphasise that bubbles' pressure differences are of the order of P_i^G, and that $\Delta P_{ij} \sim \sigma/R_i$ suggests that $P_i^G \sim \sigma/R_i$ as opposed to the much greater Laplace pressure at Plateau borders of the order of σ/r_i. Next in section 8.6 we will provide an argument for $\langle P^G \rangle \sim \sigma/\bar{R}$, a result which suggests that we may define $P_i^G \equiv \Gamma_i \sigma / V_i^{-1/D}$ with D the bubble's dimension, and have $\Gamma \sim 1$.

Finally we note that in a weakly compressed foam of arbitrary polydispersity, $P_i = P + \Pi + P_i^G$ will not generally hold, and that for a given Π even the *volume* of the foam will depend on the arrangement of bubbles within the foam. This is

proven in figure 8.8 by a similar argument to that in figure 8.7. In the foam on

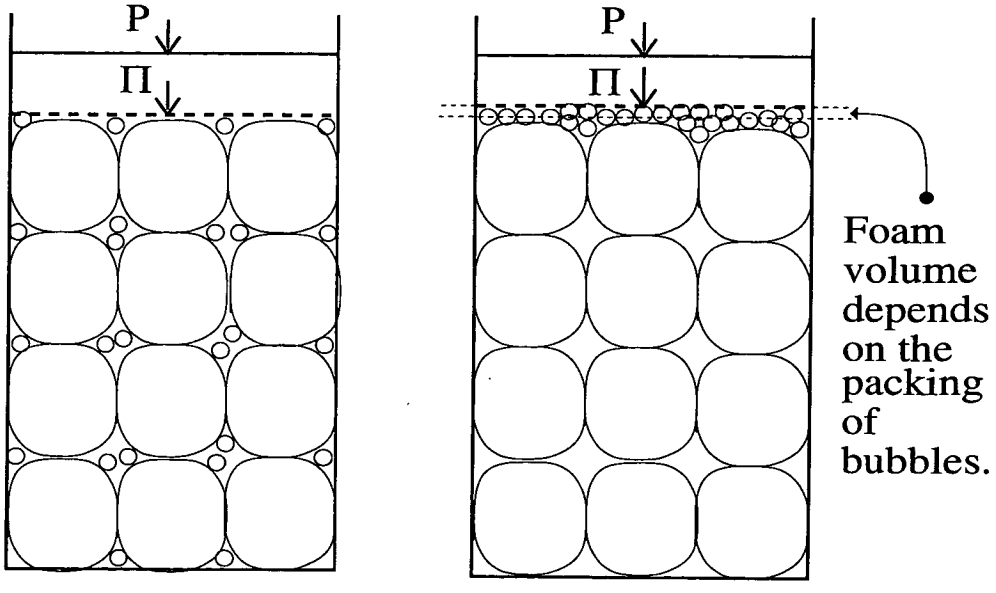

Figure 8.8: At a given osmotic compression Π, the volume occupied by a weakly compressed polydisperse foam will depend on the way in which bubbles are arranged. This is emphasised by the foams on the left and right of the figure, which both contain the same bubbles but whose different bubble arrangements result in their occupying different volumes.

the left of figure 8.8 smaller bubbles are uncompressed and reside within Plateau borders, so that the volume of the foam is determined by the volume fraction of the larger bubbles alone. However in the foam on the right of figure 8.8, the smaller bubbles are all at the top of the foam and under compression, and contribute to a *larger* foam volume. Hence at a given osmotic pressure Π both a foams volume and its bubbles' pressures, may in general depend on the particular way in which bubbles are arranged.

8.6 Alternate Approach: Force Balance

Here we consider a different approach for the calculation of Π and P^G which will enable us to obtain the order of magnitude for P^G when bubble sizes are

polydisperse. We shall firstly apply the method to the model for a monodisperse 2D foam described in section 8.4, and confirm the previous results. We note that the method has much in common with one used previously by Princen [77, 78], and is valid for both compressible and incompressible systems.

Imagine a semipermeable membrane with a shape which follows the top surface of a line of hexagonal bubbles (see figure 8.9), so that bubbles remain hexagonal in

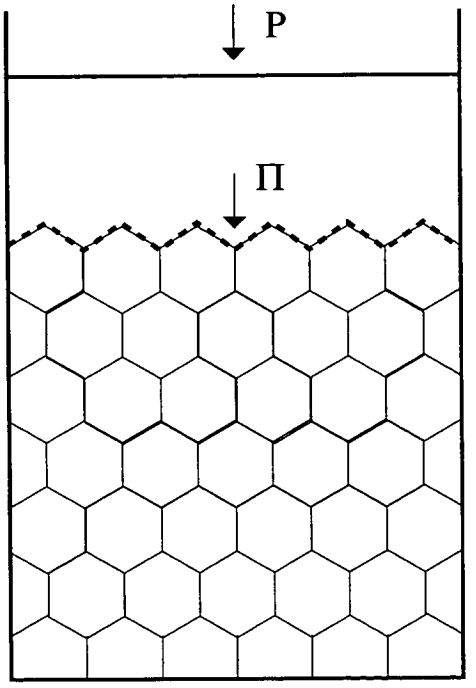

Figure 8.9: We imagine a semipermeable membrane with a shape that maintains the hexagonal bubble structure. For example you could imagine a soft membrane initially between bubble layers, which subsequently hardens and enables you to remove the bubble layers above the membrane while maintaining a pressure Π on the bubbles below the hardened membrane. We may also apply the same thought experiment when bubbles are polydisperse in size and shape.

shape. Then since the membrane doesn't move, the total force on the membrane due to $(\Pi + P)$ must balance the total force on the membrane acting from below. If we consider a typical bubble adjacent to the membrane (see figure 8.10), then for the forces above and below to balance we require[§]

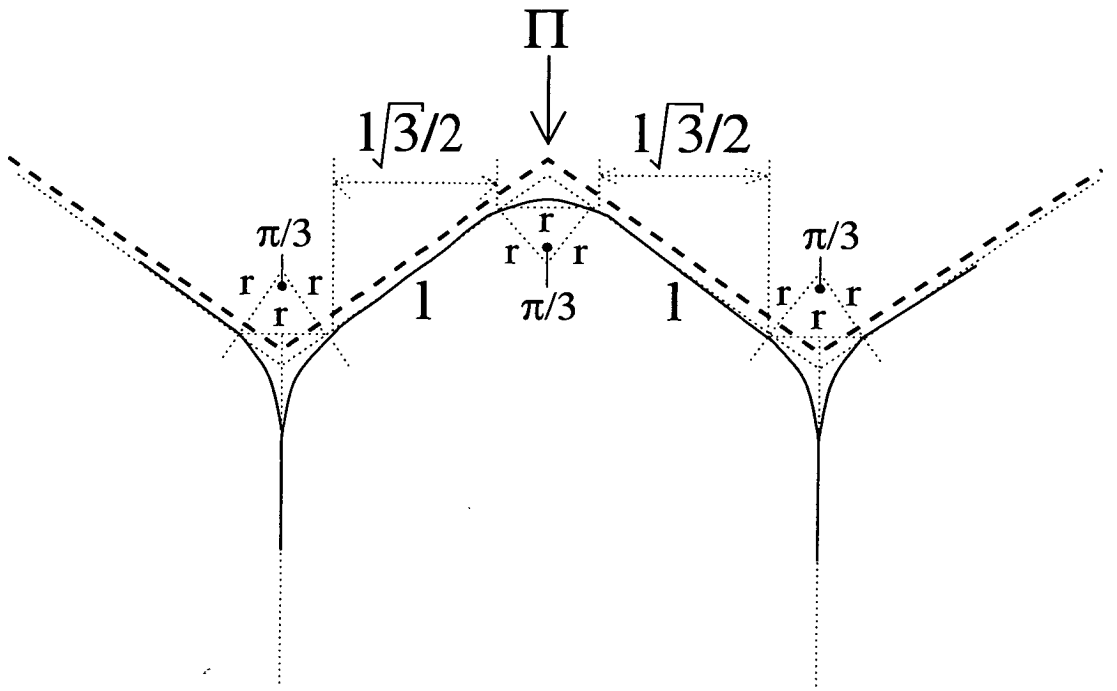

Figure 8.10: The pressure acting from below the membrane is P at the Plateau borders, and P_i where the bubble presses on the membrane. The force exerted upwards on the membrane is the pressure multiplied by distance over which it acts, projected onto the horizontal axis.

$$2P_i\frac{l\sqrt{3}}{2} + P2r = (\Pi + P)\left(2\frac{l\sqrt{3}}{2} + 2r\right) \tag{8.36}$$

Writing $P_i = P + \sigma/r$ and rearranging, we obtain

$$\Pi = \frac{\sigma}{r} - \frac{6\sigma}{3\sqrt{3}l + 6r} \tag{8.37}$$

which comparison with Eq. 8.17 gives

$$\Pi = \frac{\sigma}{r} - P^G \tag{8.38}$$

as before. Note that since the method may be applied to compressible systems, both P_i and P^G for the monodisperse 2D model will remain the same for both compressible and incompressible bubbles.

[§]Where the force acting is pressure multiplied by distance over which it acts, projected onto the horizontal axis.

We now generalise the argument to a polydisperse system. The projections of the bubble faces and plateau borders onto the horizontal axis are written as $l_i^{P_i}$ and l_i^P respectively. Then considering a suitably shaped membrane, force balance requires

$$\langle P_i l_i^{P_i} \rangle_i + P\langle l_i^P \rangle_i = (\Pi + P)\left(\langle l_i^{P_i} \rangle_i + \langle l_i^P \rangle_i\right) \tag{8.39}$$

So writing $P_i = P + \sigma/r_i$ and restricting ourselves to fairly dry foams with $r_i \simeq r_j$, then $\langle l_i^{P_i}/r_i \rangle_i \simeq \langle l_i^{P_i} \rangle_i / r$ where $r \equiv \langle r_i \rangle_i$, and we can obtain

$$\Pi \simeq \frac{\sigma}{r} - \frac{\sigma}{r} \frac{\langle l_i^P \rangle_i}{\langle l_i^{P_i} \rangle_i + \langle l_i^P \rangle_i} \tag{8.40}$$

Now we note that since $l_i^P \sim r$ and $l_i^{P_i} \sim \bar{R}$, where $\bar{R} \equiv \langle \sqrt{A}/\pi \rangle_i$, then

$$\Pi \sim \frac{\sigma}{r} - \frac{\sigma}{\bar{R}} \tag{8.41}$$

so that if $P_i^G \equiv P_i - P - \Pi$ then $\langle P_i^G \rangle \sim \sigma/\bar{R}$.

In 3D the same argument but with projected areas $\langle A_i^P \rangle \sim \bar{R} \times r$, and $\langle A_i^{P_i} \rangle \sim \bar{R}^2$ leads to

$$\Pi \sim \frac{\sigma}{r} - \frac{\sigma}{\bar{R}} \tag{8.42}$$

which for $P_i^G = P_i - P - \Pi$ gives

$$\langle P_i^G \rangle \sim \sigma/\bar{R} \tag{8.43}$$

Finally we note that in higher dimensions the equivalent argument will continue to give $\langle P_i^G \rangle \sim \sigma/\bar{R}$.

8.7 Definition and Estimation of P^G

Motivated by the previous sections we now define

$$P_i^G \equiv P_i - P - \Pi \tag{8.44}$$

a definition involving no approximations, but which does allow arbitrary variations in bubbles' P_i^G's. Writing P_i^T and P_i^s as the partial pressures of the soluble and trapped phase respectively, then the above definition of P^G gives

$$P_i^s = P + \Pi + P_i^G - P_i^T \tag{8.45}$$

So using Eq. 8.45 and Eq. 8.3 for the chemical potential of soluble disperse phase in a bubble, we obtain the chemical potential of soluble species as

$$\Delta\mu_i = kT \ln\left(1 + \frac{P_i^G - P_i^T}{\tilde{P}}\right) \tag{8.46}$$

with $\tilde{P} \equiv P + \Pi$, as usual.

Since $\Delta P_{ij} \sim \sigma/R_i$ and $\langle P^G \rangle \sim \sigma/\bar{R}$, we also expect that $P_i^G \sim \sigma/R_i$. So for a bubble in $\mathcal{D}$ dimensions of volume V_i, we define Γ_i such that

$$P_i^G \equiv \Gamma_i \frac{\sigma}{V_i^{1/\mathcal{D}}} \tag{8.47}$$

and expect $\Gamma_i \sim 1$, and hence expect $\langle \Gamma_i \rangle \sim 1$ also.

For example our model 2D foam had P^G given by Eq. 8.20 as

$$P^G = \frac{\sqrt{2\sqrt{3}}\sigma}{\sqrt{A + A_l}} \tag{8.48}$$

which after some algebra may be written,

$$P^G = \frac{\sqrt{2\sqrt{3}}\sigma}{\sqrt{A}}\sqrt{1 - \frac{A_l}{A + A_l}} \tag{8.49}$$

So writing

$$\Gamma = \sqrt{2\sqrt{3}}\sqrt{1 - \frac{A_l}{A + A_l}} \tag{8.50}$$

then $P^G = \Gamma\sigma/\sqrt{A}$. For a fairly dry foam with $A_l \ll A$, $\Gamma \simeq \sqrt{2\sqrt{3}}$ and hence of order 1, and if the foam is entirely dry then $\Gamma = \sqrt{2\sqrt{3}}$ exactly. If we write A and A_l in terms of r and l, we obtain

$$\Gamma = 3^{1/4}\sqrt{2}\left(1 - \frac{1}{3}\left(\frac{r}{l}\right)^2\left(\frac{4 - 2\pi/\sqrt{3}}{1 + (4/\sqrt{3})(r/l) + (4/3)(r^2/l^2)}\right)\right)^{1/2} \tag{8.51}$$

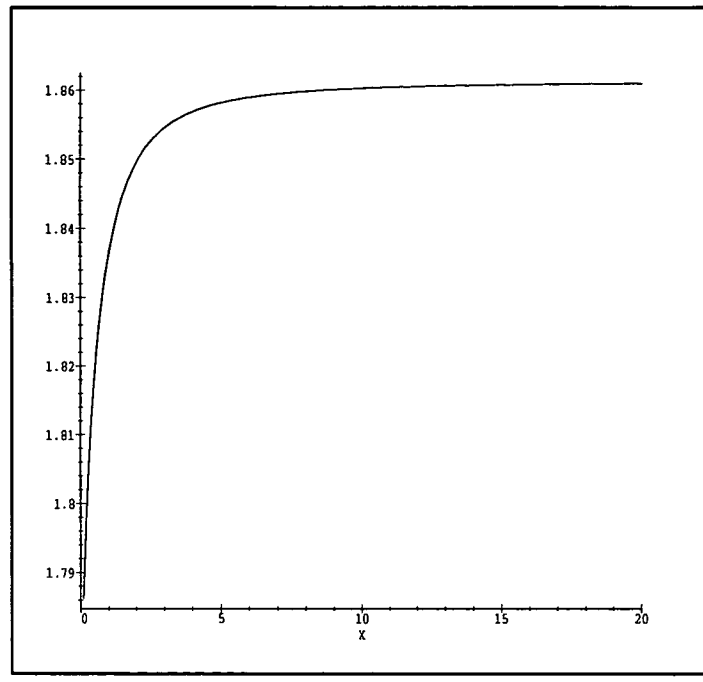

Figure 8.11: Variation of Γ (vertical axis), from $\sqrt{\pi}$ to $\sqrt{2\sqrt{3}}$, with $X \equiv l/r$. Increasing X corresponds to the bubble becoming increasingly dry, and $X \to 0$ corresponds to the bubble becoming circular in shape.

which is graphed in figure 8.11. Hence although Γ varies with the geometry of the bubbles (ie osmotic pressure Π), it always remains of order 1.

Chapter 9 considers the possibilities and requirements for the osmotic stabilisation of foams. It contains exact results for dilute foams and monodisperse 2D foams (or equivalently 2D emulsions), and contains a careful investigation of the requirements for stability of a reasonably monodisperse and dry foam.

Before considering stability requirements, we will end this chapter by exploring some of the consequences of $P_i^G \equiv P_i - P - \Pi$, and $\langle P^G \rangle \sim \sigma/\bar{R}$.

8.8 Relationship to Von Neumann's Law

Von Neumann's law applies to dry, incompressible 2D foams in which bubble–bubble interfaces meet with angles of $2\pi/3$. It assumes that the flux between two bubbles is proportional to the pressure differences between them, and measures exactly how deformations due to a bubble's environment result in pressure differences and fluxes. For a more thorough derivation of Von Neumann's law see the review article by Glazier [65], for example.

As noted in section 8.3 when a foam of gas bubbles is referred to as *incompressible*, it effectively means that $P_i^G \ll \tilde{P}$ so that although gas volume may be exchanged between bubbles the *total* gas volume remains constant. Hence to treat a foam as effectively incompressible we take $P_i^G \ll \tilde{P}$, and expand Eq. 8.46 to get

$$\frac{\Delta\mu_i}{kT} = \frac{P_i^G - P_i^T}{\tilde{P}} \tag{8.52}$$

for the ith bubble. If we consider the differences in chemical potential between two bubbles $\Delta\mu_{ij}$ and rearrange, we obtain

$$(P_i^G - P_i^T) - (P_j^G - P_j^T) = \tilde{P}\frac{\Delta\mu_{ij}}{kT} \tag{8.53}$$

which using $P_i^s + P_i^T = \tilde{P} + P_i^G$ becomes

$$P_i^s - P_j^s = \tilde{P}\frac{\Delta\mu_{ij}}{kT} \tag{8.54}$$

Since the fluxes of the disperse phase are proportional to the differences in chemical potential between bubbles, the assumption for incompressibility results in fluxes being proportional to the partial pressure differences of the soluble disperse phase component. So for incompressible gases we find that the assumption of gas fluxes being proportional to the pressure differences between bubbles (Von–Neumann), is equivalent to the assumption that fluxes are proportional to the chemical potential differences between bubbles.

Von Neumann only considered a single soluble gas, and mechanical equilibrium between bubbles then requires $\sigma c_{ij} = P_i^s - P_j^s$, where c_{ij} is the curvature of the bubbles face. Since he also took the total flux of disperse phase between bubbles as proportional to the length l_{ij} of the bubble–bubble interface he found the rate of bubble growth as

$$\frac{dA_i}{dt} = -K \sum_j \sigma c_{ij} l_{ij} = -K \sum_j (P_i^s - P_j^s) l_{ij} \tag{8.55}$$

where A_i is a 2D bubbles area, and K is a diffusion constant. Noting that $P_i^s = \tilde{P} + P_i^G$, and performing an integral around the bubble i, leads to

$$\frac{dA_i}{dt} = \frac{K\sigma\pi}{3}(n-6) = K \sum_j (P_j^G - P_i^G) l_{ij} \tag{8.56}$$

where n is the number of neighbours of a bubble. Hence the rate of growth of a bubble as determined by Von Neumann's law is directly related to the differences in geometric pressures between bubbles.

If we now consider when trapped species are present, then the condition for mechanical equilibrium becomes that $\sigma c_{ij} = (P_i^s + P_i^T) - (P_j^s + P_j^T)$ so since the flux between bubbles remains proportional to the partial pressure of the soluble species we now find the total flux into a bubble as

$$\frac{dA_i}{dt} = -K \sum_j (P_i^s - P_j^s) l_{ij} = \frac{K\sigma\pi}{3}(n-6) + K \sum_j (P_i^T - P_j^T) l_{ij} \tag{8.57}$$

Hence when we consider the inclusion of trapped species we find that it is possible to have zero flux of disperse phase with $n \neq 6$. This contrasts with Von Neumann's original conclusion (without trapped species), that growth or shrinkage of a bubble is entirely determined by its number of sides.

We note that the derivation of the above expression Eq. 8.57, did not require any approximations or assumptions about P_i^G. Hence Eq. 8.57 is an exact result.

8.9 Bubble Rearrangements

Neighbour switching (so called T1) bubble rearrangements have been observed in coarsening foams, both by experiment [83,84] and computer simulations [85]. Experiments by Glazier et al [83,84], revealed that $\simeq 50\%$ of all changes in bubble topology were due to T1 processes. Hertdle and Aref [85] reported the results of simulations in which they found the ratio of T1 to T2 processes (where T2 processes refer to bubble's sides being lost as a result of a bubble disappearing), being 3:2, ie for every 2 sides a bubble lost by another bubble disappearing, 3 were lost by T1 side switching processes.

Although T1 bubble rearrangements have been suggested to be solely due to bubbles disappearing, experiments by Durian et al [86,87] show that this is not the case. Durian et al [86,87] used diffusing wave spectroscopy to study the coarsening of a non–dilute foam with $92 \pm 1\%$ volume of bubbles. They observed coarsening with average bubble diameter $d \sim t^{1/2}$, as well as localised bubble rearrangements. They found the rate of rearrangements per unit volume $\mathcal{R}$, to vary as $\mathcal{R} \sim t^{-2\pm0.2}$. The rearrangements were attributed to changes in packing conditions of the bubbles due to coarsening, with bubbles rearranging to reduce local stresses.

The result shows that the rearrangements were not directly due to bubbles disappearing, which for self similar coarsening in which the number of bubbles varies as $\sim t^{-3/2}$ would predict bubble rearrangement to occur with frequency $\sim t^{-5/2}$, and a rearrangement rate per unit volume of $\mathcal{R} \sim t^{-4}$.

Hence bubble rearrangements have been observed to occur in foams, and to do so without the need for bubbles to disappear. Next we will suggest a physical mechanism to cause bubble rearrangements, and find that the rate of rearrangements predicted by $\langle P^G \rangle \sim \sigma/\bar{R}$ agrees with that observed experimentally.

8.9.1 A Mechanism for Bubble Rearrangements

We suggest here that rearrangements are necessary for coarsening, and occur continually.

We note that coarsening will result in stress inhomogeneities throughout the foam, and propose that these stresses (of the order of bubbles geometric pressures) require bubble rearrangements to maintain equilibrium. We propose that when stress inhomogeneities exceed a typical yield stress of the order of σ/b, with b a constant length scale relevant to rearrangements[¶], then rearrangements are likely to occur. So since the number of bubbles per unit volume $\sim 1/\bar{V}$, then taking the rate of rearrangement per unit volume $\mathcal{R}$ as proportional to the ratio of the systems average geometric pressure[‖] and σ/b gives

$$\mathcal{R} \sim \frac{1}{\bar{V}} \frac{\langle P^G \rangle}{\sigma/b} \tag{8.58}$$

which using Eq. 8.43 for $\langle P^G \rangle \sim \sigma/\bar{R}$, becomes

$$\mathcal{R} \sim \frac{b}{\bar{V}^{(\mathcal{D}+1)/\mathcal{D}}} \tag{8.59}$$

So for a 3D foam of average radius $\bar{R}$ we have

$$\mathcal{R} \sim \frac{b}{\bar{R}^4} \tag{8.60}$$

Durian et al [86,87] found $\bar{R} \sim t^{1/2}$ for a 3D foam, hence we get the rate of rearrangements per unit volume to be

$$\mathcal{R} \sim \frac{1}{t^2} \tag{8.61}$$

as was observed by Durian et al [86,87].

[¶]It is noted that there are two important length scales in the problem, the radius of curvature of Plateau borders and the typical curvature of bubble–bubble faces R. Since the following argument is invalid for $b \sim R$, it is tempting to suggest that $b \sim r$, and that the order of magnitude of the yield stress is determined by the volume fraction of liquid in the system.

[‖]Equivalent to assuming fluctuations in P_i^G about the mean, are of order $\langle P_i^G \rangle$.

Hence the simple mechanism of bubble rearrangements to relieve coarsening induced stresses, plus the result of $\langle P^G \rangle \sim \sigma/\bar{R}$, is sufficient to explain the rate of bubble rearrangements observed by Durian et al [86,87] (given their coarsening rate $\bar{R} \sim t^{1/2}$).

For the above mechanism, rearrangements are likely to occur for excessive variations in P_i^G. So if the mechanism proposed above *is* correct, then it will prevent excessive variations in P_i^G about the mean value. Hence the apparent correctness of the mechanism suggests $P_i^G \simeq \langle P^G \rangle$, as a reasonable approximation. This will be used in subsequent chapters.

8.10 Conclusions

We have considered how the pressure within foam bubbles is affected by an osmotic compression Π. We contrasted foams with granular material, and suggested that foams become increasingly similar to homogeneous matter when strongly compressed, but more similar to granular matter when only slightly compressed. Hence although determining the pressures within foam bubbles is a complex packing and stress distribution problem, we suggest that sufficiently compressed foam should be sufficiently homogeneous to be described by Eqs. 8.4 and 8.7 with $P_i = P + \Pi + P_i^G$, and $P_i^G \ll \Pi$.

Eqs. 8.4 and 8.7 were confirmed for dry 2D foams in section 8.3, by a careful study which also suggested that $P_i^G \sim \sigma/R_i$. Eqs. 8.4 and 8.7 were also confirmed in section 8.4 for the model of a monodisperse 2D foam, by an exact calculation which gave $P_i^G = \sqrt{2\sqrt{3}}\sigma/\sqrt{A + A_l} \sim \sigma/R$. For the model in section 8.4 the ratio of P^G for entirely dry bubbles and P^G for entirely dilute bubbles was 1.05, so that P^G is approximately the same regardless of Π. This is important since differences between bubbles' pressures determine the rate of coarsening; so an

assumption that coarsening is driven by bubbles' Laplace pressures would, even in the concentrated case, give the wrong order of magnitude for pressure differences (σ/r instead of σ/R).

Section 8.5 demonstrated that Eqs. 8.4 and 8.7 would fail if the foam was too polydisperse and insufficiently compressed, and emphasised their validity is restricted to sufficiently compressed and monodisperse foams. A calculation which considered the balance of forces between Π, bubbles' pressures, and the pressure in bubbles' Plateau borders P, reconfirmed the correctness of $P_i^G = \sqrt{2\sqrt{3}}\sigma/\sqrt{A + A_l}$ for the model in section 8.4, and also gave the general result that $\langle P_i^G \rangle_i \sim \sigma/\bar{R}$. We noted that the calculation applies to both compressible and incompressible systems, so that the results for the *incompressible* monodisperse 2D model also apply when bubbles are *compressible*.

We defined $P_i^G \equiv P_i - P + \Pi$ in section 8.7, where we also propose in Eq. 8.47 that we may define Γ_i by $P_i^G \equiv \Gamma_i \sigma / V_i^{1/\mathcal{D}}$, and expect $\Gamma_i \sim 1$. In section 8.8 we related our definition of P^G to Von Neumann's law for the coarsening of dry 2D foams, and also indicated how the law is altered by the presence of trapped molecules within bubbles.

The final section 8.9 suggested a mechanism for bubble rearrangements which explains the experimental observations of Durian et al [86, 87]. Provided the mechanism *is* correct, then it also implies that $P_i^G \simeq \langle P_i^G \rangle$ is a reasonable approximation.

Given the evidence presented in this chapter, we finally propose the ansatz that a sufficiently compressed and monodisperse foam will satisfy Eqs. 8.4 ($P_i = P + \Pi + P_i^G$), 8.7 ($\Pi \gg P_i^G$), and 8.47 ($P_i^G \equiv \Gamma_i \frac{\sigma}{V_i^{1/\mathcal{D}}}$). The ansatz will be used in section 9.5 of chapter 9, to investigate the requirements for the stabilisation of sufficiently compressed and monodisperse foams.

Chapter 9

Stabilisation of Foams

This chapter uses the results of chapters 7 and 8 to discuss the requirements for osmotic stabilisation of foams. Section 9.1 considers the requirements for foam bubbles to coexist with a bulk gas phase, and emphasises that bubbles will coexist with a bulk gas at some (hopefully calculable) coexistence size. Section 9.2 uses bubbles' coexistence sizes (compositions) to derive a general stability condition. Unfortunately the stability condition is not always calculable, however it is calculated for dilute foams in Section 9.3, and Section 9.4 calculates the condition for the model of monodisperse 2D foams previously described in chapter 8. In chapter 8 we suggested that we may write $P_i^G = \Gamma_i \sigma / V_i^{1/\mathcal{D}}$; this is used in section 9.5 to carefully investigate the requirements for us to always be able to osmotically stabilise a sufficiently dry, polydisperse foam. Finally section 9.6 provides a bound on the quantity of soluble gas beyond which an osmotically compressed foam must be *unstable*.

9.1 Coexistence Size/Composition

Let us assume that coarsening does take place. Thus we consider a distribution of coarsening foam bubbles, in which the largest growing bubbles dilute the trapped species within, to the extent that $\mu_i \to \mu_b$ and $\Delta\mu_i \to 0$. The smaller bubbles will shrink until they are sufficiently enriched in trapped species that their chemical potential equals that of the larger bubbles. Hence as $t \to \infty$ and $\Delta\mu_i \to 0$, the smaller bubbles will tend to a size/composition such that $\Delta\mu_i = 0$, and

$$0 = kT \ln\left(1 + \frac{P_i^G - P_i^T}{P}\right) \tag{9.1}$$

which is satisfied when

$$P_i^G = P_i^T \tag{9.2}$$

Hence, since the surface tension is the cause of coarsening, once the effects of surface tension (represented by $P_i^G \sim \sigma/R_i$, and *not* Laplace pressure σ/r_i), are counteracted by a sufficient pressure of trapped species, bubbles can then coexist with a bulk quantity of soluble gas.

For the dilute foams considered in chapter 7 and the model 2D foam considered in chapter 8, the condition $P_i^G = P_i^T$ will determine a bubble's coexistence size V_i^B (or A_i^B in 2D). The calculation and estimation of coexistence sizes is considered in sections 9.3, 9.4, and 9.5.

We note that at coexistence, compressed foam bubbles have a pressure of soluble species $P_i^s = P_b^s = \tilde{P}$, and hence the ideal gas law has $\tilde{P} = N_i^{sB} kT/V_i^B$ (or equivalently $\tilde{P} = N_i^{sB} kT/A_i^B$ in 2D). So since $P_i^s = \tilde{P}$, we may easily obtain the number of soluble gas molecules in coexisting bubbles from

$$N_i^{sB} = \frac{\tilde{P}}{kT} V_i^B \tag{9.3}$$

or the equivalent expression for a 2D or $\mathcal{D}$ dimensional foam. Similarly if foams are not subject to an osmotic compression then

$$N_i^{sB} = \frac{P}{kT} V_i^B \tag{9.4}$$

These results may be compared with those for incompressible emulsions; taking the volume per *liquid* disperse phase molecule as v_b, these have $N_i^s = (1/v_b)V_i^B$, compared with $N_i^s = (\tilde{P}/kT)V_i^B$ for the compressible foam bubble.

9.2 A Condition for Stability

We next use conservation of the total number of gas molecules and total number of bubbles, to derive a criterion to ensure the formation of a stable distribution of foam bubbles. We consider the bubble size distribution to be composed of two parts, one part in which coarsening occurs with some bubbles growing at the expensé of other bubbles shrinking (referred to as the 'coarsening' part of the distribution), and another part consisting of bubbles shrunken to a stable size at which they may coexist with the coarsening bubbles (referred to as the 'stable' part of the distribution). We find that for sufficiently concentrated initial bubble compositions the assumption of the bubble distribution having a coarsening part is inconsistent, enabling us to derive a stability criterion for foams. These arguments parallel those of section 3.6 in chapter 3 for dilute emulsions.

We take n_b^0, n_b^S, and n_b^C as the number densities of bubbles in the system, in the stable part of the distribution (containing shrunken bubbles), and in the coarsening part of the distribution respectively. Conservation of bubbles gives

$$n_b^0 = n_b^S + n_b^C \tag{9.5}$$

where we note that n_b^S and n_b^C may be time–dependent.

N_i^{sB}, the number of soluble species with which a bubble will coexist with a bulk gas phase, is determined by $P_i^G = P_i^T$. However since relations between P_i^G and V_i may vary during coarsening (due to changes in bubbles' environments, and coarsening of bubbles), we take N_i^{sB} as time–dependent. We define the following

- $\bar{N}^{s0} \equiv \langle N_i^s(t) \rangle_i$: The average number of soluble molecules per bubble. This is *time independent.*

- $\bar{N}^{sB}(t)$: The average number of soluble molecules per bubble when coexisting with a bulk gas phase. Since $n_b^C/n_b^0 \to 0$ as coarsening proceeds, then $n_b^S \to n_b^0$, and hence the average number of soluble molecules in the shrunken bubble distribution tends to $\bar{N}^{sB}(t)$.

- $\bar{N}^{sC}(t)$: The average number of soluble molecules per bubble, in the larger bubbles of the coarsening distribution, at time t.

So as a coarsening foam tends towards an equilibrium state, conservation of the number of soluble molecules requires,

$$n_b^0 \bar{N}^{s0} = n_b^S \bar{N}^{sB}(t) + n_b^C \bar{N}^{sC}(t) \tag{9.6}$$

Combining Eqs. 9.5 and 9.6, we obtain,

$$n_b^0 \left(\bar{N}^{s0} - \bar{N}^{sB}(t) \right) = n_b^C \left(\bar{N}^{sC}(t) - \bar{N}^{sB}(t) \right) \tag{9.7}$$

so provided that we can guarantee that,

$$\bar{N}^{sB}(t) \geq \bar{N}^{s0} \tag{9.8}$$

then Eq. 9.7 requires $0 \geq n_b^C(\bar{N}^{sC}(t) - \bar{N}^{sB}(t))$, and since the larger, coarsening bubbles have $\bar{N}^{sC}(t) > \bar{N}^{sB}(t)$, then $n_b^C = 0$ and the foam must be stable against coarsening. We note that since $\bar{N}^{sB}(t)$ depends on $P_i^G(t)$, whose relation to V_i may not always be known, the derivation of an exact stability condition is not always possible. However, the above condition enables us to clearly investigate the requirements for stability. This is done in sections 9.3, 9.4, and 9.5 below.

9.3 Dilute Bubbles

Dilute foams have $P_i^G = \frac{2\sigma}{R_i}$ for 3D foam bubbles (and $P_i^G = \sigma/R_i$ for 2D foam bubbles). So a 3D bubble's coexistence size is determined from

$$\frac{2\sigma}{R_i^B} = \frac{N_i^T kT}{\frac{4\pi}{3} R_i^{B3}} \tag{9.9}$$

giving

$$R_i^B = \sqrt{\frac{3}{4\pi}} \sqrt{\frac{N_i^T kT}{2\sigma}} \tag{9.10}$$

and hence

$$V_i^B = \sqrt{\frac{3}{4\pi}} \left(\frac{N_i^T kT}{2\sigma} \right)^{3/2} \tag{9.11}$$

This volume is identical to the coexistence size of a dilute incompressible emulsion droplet,

$$V_i^B = \left(\frac{\eta_i kT}{2\sigma} \right)^{3/2} \sqrt{\frac{3}{4\pi}} \tag{9.12}$$

in which σ remains the surface tension and η_i is the number of trapped species (see chapter 3 for details). The exact correspondence is because the trapped species are treated as ideal, both when the majority disperse phase is an incompressible fluid (chapter 3) or an ideal gas (as here).

So substituting Eq. 9.11 into Eq. 9.4 we obtain the number of soluble gas molecules in shrunken bubbles as

$$N_i^{sB} = \frac{P}{kT} \sqrt{\frac{3}{4\pi}} \left(\frac{N_i^T kT}{2\sigma} \right)^{3/2} \tag{9.13}$$

and hence

$$\bar{N}^{sB} = \frac{P}{kT} \sqrt{\frac{3}{4\pi}} \left(\frac{kT}{2\sigma} \right)^{3/2} \langle N_i^{T3/2} \rangle_i \tag{9.14}$$

So if the dilute foams are formed with $\bar{N}^{s0} < \bar{N}^{sB}$, then the foam will be stable.

Similarly a dilute 2D foam has

$$A_i^B = \frac{1}{\pi} \left(\frac{N_i^T kT}{\sigma} \right)^2 \tag{9.15}$$

and is stable if $\bar{N}^{s0} < \bar{N}^{sB}$, with

$$\bar{N}^{sB} = \frac{P}{kT}\left(\frac{1}{\pi}\right)\left(\frac{kT}{\sigma}\right)^2 \langle N_i^{T\,2}\rangle_i \tag{9.16}$$

9.4 Monodisperse, 2D Model

For our 2D model Eq. 8.20 gives

$$P^G = \frac{\sqrt{2\sqrt{3}\sigma}}{\sqrt{A + A_l}} \tag{9.17}$$

So a coexistence size is determined from $P^G(A^B) = N^T kT/A^B$, requiring that

$$A^{B2} - \left(\frac{N^T kT}{\sigma}\right)^2 \frac{A^B}{2\sqrt{3}} - \left(\frac{N^T kT}{\sigma}\right)^2 \frac{A^l}{2\sqrt{3}} = 0 \tag{9.18}$$

which has a physical (positive) solution of

$$A^B = \left(\frac{N^T kT}{\sigma}\right)^2 \frac{1}{2\sqrt{3}}\left(\frac{1 + \sqrt{1 + 4A_l \frac{2\sqrt{3}\sigma^2}{N^{T2}(kT)^2}}}{2}\right) \tag{9.19}$$

So an entirely dry foam with hexagonal bubbles has

$$A_H^B = \left(\frac{N^T kT}{\sigma}\right)^2 \frac{1}{4\sqrt{3}} \tag{9.20}$$

and we may alternately write

$$A^B = A_H^B\left(1 + \frac{\sqrt{1 + \frac{4A_l}{A_H^B}}}{2}\right) \tag{9.21}$$

from which we may obtain the number of trapped species at coexistence from $N^{sB} = \frac{\tilde{P}}{kT}A^B$.

So if we have $N^{s0} < N^{sB}$, with

$$N^{sB} = \frac{\tilde{P}}{kT}A_H^B\left(1 + \frac{\sqrt{1 + \frac{4A_l}{A_H^B}}}{2}\right) \tag{9.22}$$

then the foam will be stable.

9.5 Sufficiently Dry Foams

In chapter 8 we defined $P_i^G \equiv P_i - P - \Pi$, and noted that for sufficiently dry foams that $P_i^G \ll \Pi$. We also suggested that for sufficiently dry foams we may write

$$P_i^G = \Gamma_i \frac{\sigma}{V_i^{1/\mathcal{D}}} \tag{9.23}$$

with $\Gamma_i \sim 1$ and $\mathcal{D}$ the bubbles dimension. We note that although our model of a monodisperse 2D foam had Γ dependent on bubble area A, for reasonably dry foams it remained of order 1 and tended to $\sqrt{2\sqrt{3}}$ as the foam became increasingly dry. Hence we calculate an approximate coexistence size by assuming Γ_i is independent of bubble size. This gives

$$V_i^B = \left(\frac{N_i^T kT}{\sigma \Gamma_i}\right)^{\mathcal{D}/(\mathcal{D}-1)} \tag{9.24}$$

and

$$N_i^B = \frac{\tilde{P}}{kT}\left(\frac{N_i^T kT}{\sigma \Gamma_i}\right)^{\mathcal{D}/(\mathcal{D}-1)} \tag{9.25}$$

Given the above equation for a bubbles coexistence size, we are now able to more carefully consider the requirements for foam stability.

9.5.1 Requirements for Stability

We proceed by examining the form of $\bar{N}_i^{sB}(t)$, the number of soluble species per bubble below which a stable foam is ensured. Noting that $\bar{N}_i^{sB}(t) = \langle N_i^{sB}(t)\rangle_i$, we write it out in full to obtain,

$$\langle N_i^{sB}(t)\rangle_i = \frac{\tilde{P}}{kT}\left(\frac{kT}{\sigma}\right)^{\mathcal{D}/(\mathcal{D}-1)} \left\langle \left(\frac{N_i^T}{\Gamma_i}\right)^{\mathcal{D}/(\mathcal{D}-1)} \right\rangle_i \tag{9.26}$$

We note that $\mathcal{D} \geq 2$ so that

$$\left\langle \left(\frac{1}{\Gamma_i}\right)^{\mathcal{D}/(\mathcal{D}-1)} \right\rangle_i \geq \frac{1}{\langle \Gamma_i \rangle_i^{\mathcal{D}/(\mathcal{D}-1)}} \tag{9.27}$$

So provided that Γ_i and N_i^T are uncorrelated, then

$$\langle N_i^{sB}(t)\rangle_i \geq \frac{\tilde{P}}{kT}\left(\frac{kT}{\sigma}\right)^{\mathcal{D}/(\mathcal{D}-1)} \frac{\langle {N_i^T}^{\mathcal{D}/(\mathcal{D}-1)}\rangle_i}{\langle\Gamma_i\rangle_i^{\mathcal{D}/(\mathcal{D}-1)}} \tag{9.28}$$

In chapter 8 we found that $\langle P^G\rangle \sim \sigma/\bar{R}$, which suggests $\bar{\Gamma}$ is of order a constant $\bar{\Gamma}_C$. Then since

$$\langle N_i^{sB}(t)\rangle_i \geq \frac{\tilde{P}}{kT}\left(\frac{kT}{\sigma}\right)^{\mathcal{D}/(\mathcal{D}-1)} \frac{\langle {N_i^T}^{\mathcal{D}/(\mathcal{D}-1)}\rangle_i}{\bar{\Gamma}_C^{\mathcal{D}/(\mathcal{D}-1)}} \tag{9.29}$$

a foam formed with an initial number of soluble species $\bar{N}^{s0}$ such that

$$\frac{\tilde{P}}{kT}\left(\frac{kT}{\sigma}\right)^{\mathcal{D}/(\mathcal{D}-1)} \frac{\langle {N_i^T}^{\mathcal{D}/(\mathcal{D}-1)}\rangle_i}{\bar{\Gamma}_C^{\mathcal{D}/(\mathcal{D}-1)}} \geq \bar{N}^{s0} \tag{9.30}$$

will be stable. Similarly if $\bar{\Gamma}$ is bounded by $\bar{\Gamma}_{max}$, then a foam formed with

$$\frac{\tilde{P}}{kT}\left(\frac{kT}{\sigma}\right)^{\mathcal{D}/(\mathcal{D}-1)} \frac{\langle {N_i^T}^{\mathcal{D}/(\mathcal{D}-1)}\rangle_i}{\bar{\Gamma}_{max}^{\mathcal{D}/(\mathcal{D}-1)}} \geq \bar{N}^{s0} \tag{9.31}$$

will be stable. Alternately, if $\bar{\Gamma}$ is a decreasing function of time, then we would have $\bar{\Gamma}(0) \geq \bar{\Gamma}(t)$ and hence $1/\bar{\Gamma}(t)^{\mathcal{D}/(\mathcal{D}-1)} \geq 1/\bar{\Gamma}(0)^{\mathcal{D}/(\mathcal{D}-1)}$, so provided

$$\frac{\tilde{P}}{kT}\left(\frac{kT}{\sigma}\right)^{\mathcal{D}/(\mathcal{D}-1)} \frac{\langle {N_i^T}^{\mathcal{D}/(\mathcal{D}-1)}\rangle_i}{\bar{\Gamma}(0)^{\mathcal{D}/(\mathcal{D}-1)}} \geq \bar{N}^{s0} \tag{9.32}$$

then we could again guarantee a stable foam. In contrast to the above cases, if $\bar{\Gamma}$ *increases* without bound, then so also would $\bar{N}^{sB}(t)$ *decrease* without bound, and a stability condition would never strictly exist. So in summary, the only way a stability condition could fail to exist is if $\bar{\Gamma}$ can increase in time *without bound.*

We note that coarsening occurs with a constant average volume of liquid in Plateau borders, so as coarsening proceeds bubbles will become increasingly dry. Hence we might expect $\bar{\Gamma}$ to increase with time. However in our model of a monodisperse 2D foam Γ tends to a constant value of $\sqrt{2\sqrt{3}}$ as the foam became increasingly dry, suggesting that $\bar{\Gamma}$ may be bounded in a similar way. Also if $\bar{\Gamma}$ were to increase in time without bound then either our discussion of bubble rearrangements in chapter 8 is incorrect, or Γ_i and R_i are correlated in a very

specific way (with $\langle \Gamma_i/R_i \rangle \sim 1/\langle R_i \rangle$ required to ensure $\langle P^G \rangle \sim \sigma/\langle R \rangle$). Hence although there is evidence to suggest $\bar{\Gamma}$ is either constant or bounded, there is no reason to believe that $\bar{\Gamma}$ may increase *without bound.* Hence current results suggest it should be possible to osmotically stabilise any reasonably dry foam.

In Appendix E we consider whether there exist stability conditions to prevent coarsening by a flux of the more soluble species alone, when the "trapped" species is slightly soluble. We find that provided there exists a stability condition when the trapped species is entirely insoluble, then there will also exist a corresponding condition which is sufficient to prevent coarsening by a flux of the more soluble species alone. The resulting condition is given in Appendix E.

9.6 A Lower Bound on Stability Requirements

Generally the geometric pressures of bubbles are not known, however we consider here a particular mode of growth by which a foam may lower its free energy (by separating into a foam of smaller bubbles coexisting with a bulk gas phase), in which the geometric pressure is well defined. We do not consider exactly how such growth may be accomplished within a real foam, but are merely interested (at this point) in obtaining a requirement for the *thermodynamic* instability of a foam.

We imagine a simultaneous change in volume of *all* the bubbles by an amount $dV_i = \alpha V_i$. Hence the foam changes in volume in a similar way to "blowing up" or "reducing" a picture on a photocopier, but at fixed liquid content. For such growth P^G is well defined as $P^G = \sigma(\partial A_i/\partial V_i)_{A_{li}}$ for an isotropic growth (or shrinkage) at fixed liquid volume.

Since a spherical bubble has the minimum surface area to volume ratio, then for the growth described above $P_i^G \geq 2\sigma/R_i$, with $R_i \equiv (\frac{3}{4\pi}V_i)^{1/3}$. Hence an

osmotically compressed foam will need smaller bubble volumes to coexist with a bulk gas phase (so as to have the higher pressure of trapped species required by $P_i^G = P_i^T$), than will a foam with the same bubbles diluted and spherical in shape, but under an *atmospheric* pressure $(P + \Pi)$ (see figure 9.1). So the quantity of

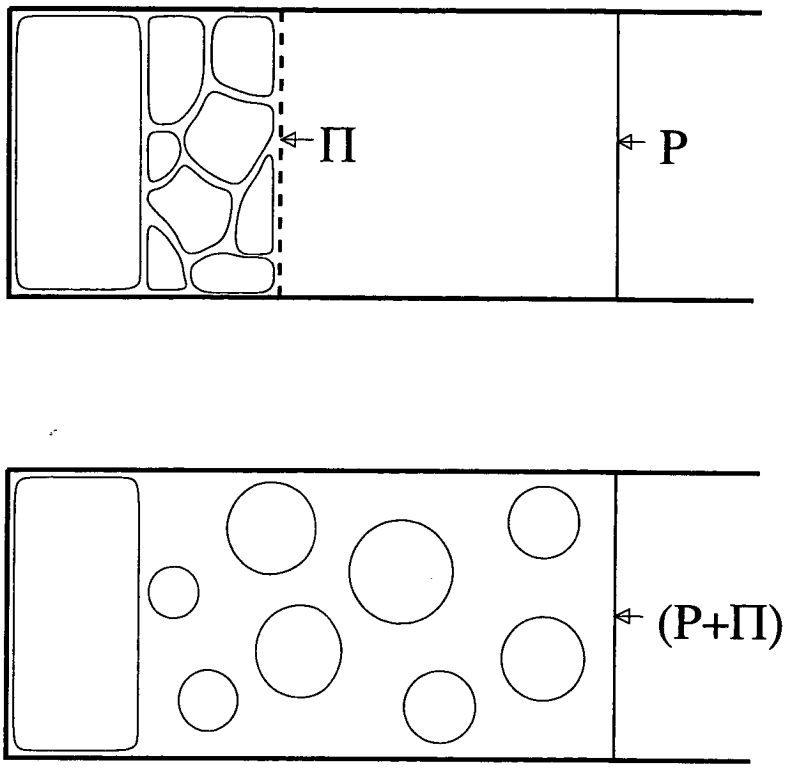

Figure 9.1: The mode of growth described in the text emphasises that the compressed bubbles coexisting with a bulk gas phase in (i), require a higher pressures of trapped species (and hence smaller volumes), than the coexisting bubbles in (ii). Hence the quantity of soluble gas in the coexisting bubbles in (ii), gives an upper bound for the *maximum* quantity of soluble gas in the compressed bubbles in (i).

soluble gas in dilute spherical bubbles which coexist with a bulk gas phase under *atmospheric* pressure $P + \Pi$, provides an upper bound on the *maximum* quantity of soluble gas in bubbles under *osmotic* pressure Π and *atmospheric* pressure P, which coexist with a bulk gas phase. Hence the stability condition for the *maximum* quantity of soluble gas in an osmotically stabilised foam of spherical bubbles at *atmospheric* pressure $\tilde{P} = P + \Pi$, imposes an upper bound on the *maximum* quantity of soluble gas in an osmotically stabilised, compressed foam,

under *atmospheric* pressure P and *osmotic* pressure Π. So replacing P with $\tilde{P} = P + \Pi$ in Eq. 9.14 gives,

$$\bar{N}^{sB} = \frac{\tilde{P}}{kT}\sqrt{\frac{3}{4\pi}}\left(\frac{kT}{2\sigma}\right)^{3/2}\langle N_i^{T\,3/2}\rangle_i \tag{9.33}$$

so a compressed foam with $\bar{N}^{s0} > \bar{N}^{sB}$ is unstable to the mode of growth considered above, and hence unstable.

Noting that $\bar{N}^{sB}$ calculated at P is less that $\bar{N}^{sB}$ calculated at $\tilde{P}$, then the above result implies that a compressed foam will become unstable at a lower $\bar{N}^{s0}$ than when it is uncompressed ($\Pi = 0$). Hence we find that a compressed foam is less stable (in the sense described above), than it is when uncompressed and dilute.

It is wörth emphasising again that the above result is a purely thermodynamic one, and does not rule out the possibility of local stabilising effects (such as a lack of bubble rearrangements), resulting in stable foams which would be unstable according to the above criterion.

9.7 Compressed Emulsions

We note that from chapter 3 the coexistence size for a dilute incompressible emulsion* is attained when

$$P_i^G = P_i^T \tag{9.34}$$

with P_i^G being the Laplace pressure of a spherical drop, and P_i^T the osmotic pressure of the trapped species.

We now consider compressed emulsions, in which droplets are in contact with one another and become distorted in shape. Since the typical increase in the

*Where *incompressible* refers to the incompressibility of the liquids in the emulsions, and an emulsion is *compressed* by a semipermeable membrane through which continuous phase may pass but not emulsion droplets (which become distorted in shape).

bubbles free energies due to the disjoining pressures between adjacent droplets is negligible [80], the stability condition remains the same, but with the distorted bubble geometry causing P_i^G to differ from that of an equivalent, but spherical drop. The arguments in chapter 8 for $P_i = P + \Pi + P^G$ and P_i^G, are unchanged for incompressible foams, and hence also apply equally well to incompressible emulsions. Since the trapped species are considered to be dilute and ideal, the osmotic pressure of the trapped species is $P_i^T = N_i^T kT/V_i$, where we have now written N_i^T in place of η.

Finally we conclude that all the results in this chapter will apply to compressed emulsions, but with $\tilde{P}/kT$ replaced by $1/v_b$ (with v_b the volume per molecule of liquid disperse phase), and a dry foam corresponding to a highly compressed emulsion.

9.8 Conclusions

Using the results of chapters 7 and 8, we have derived exact stability conditions for dilute foams and our model of monodisperse 2D foams. We have also used the results of chapter 8 to investigate the requirements for a sufficiently compressed and monodisperse foam to be able to be stabilised.

Section 9.6 emphasised that the compression of a previously dilute foam will make it less thermodynamically stable, and gave a requirement for instability (valid in the absence of local stabilising effects such as a lack of bubble rearrangements). However, our investigations in section 9.5 combined with results in chapter 8 and the results for 2D monodisperse foams, *all* suggest that stabilisation of sufficiently compressed and monodisperse foam should be possible. More importantly the requirements for stability are determined by $P_i^T = P_i^G$, with results in chapter 8 having $P_i^G \sim \sigma/R_i$. So although one might have expected osmotic stabilisation

to require the pressure of trapped molecules to balance the Laplace pressure at bubbles' Plateau borders (which is determined by Π and may be arbitrarily large), in actuality our results find the requirement for stability to be relatively unaffected by compression. As a rough estimate, the minimum required P_i^T for stability will have $P_i^T \sim \sigma/R_i$, which for $\sigma \sim 10^{-1}\mathrm{Nm}^{-1}$ and $R_i \sim 10^{-6}\mathrm{m}$ requires $P_i^T \sim 10^5\mathrm{Nm}^{-2} \sim P$, the same order of magnitude as atmospheric pressure.

Chapter 10

Coarsening of Unstable Foams

10.1 Coarsening of Foams: Qualitative Behaviour

We now consider the coarsening of unstable, non–dilute foams. We note that previous work on coarsening of dilute emulsions in chapter 4 also applies to dilute foams, but with a different constant prefactor in the droplet/bubble growth rate Eq. 2.22. Here we will concentrate on non–dilute foams in which bubbles impinge on one another and are distorted from their otherwise spherical shape.

As was the case for dilute emulsions, the trapped species will again prevent bubbles from entirely disappearing. The resulting foam morphology and the coarsening kinetics will be strongly affected by two main factors,

1. **The excess volume fraction of disperse phase:** Defined as the total volume fraction that at equilibrium would form a bulk gas phase, which would coexist with the smaller shrunken bubbles.

2. **Rate of bubble rearrangements:** The ease and rate with which bubbles may rearrange to allow larger bubbles to grow or shrink.

We will consider each of these next.

10.1.1 The Excess Volume Fraction of Disperse Phase

It is useful to classify systems by their total excess volume fraction of disperse phase, which controls the expected late–stage morphology in a coarsening system:

1. **No excess volume fraction:** The foam is stable.

2. **Very low excess volume fractions (figure 10.1):** The larger bubbles become surrounded by a sea of shrunken bubbles, with the competitive coarsening between larger bubbles occurring by a gas flux through the sea of smaller bubbles.

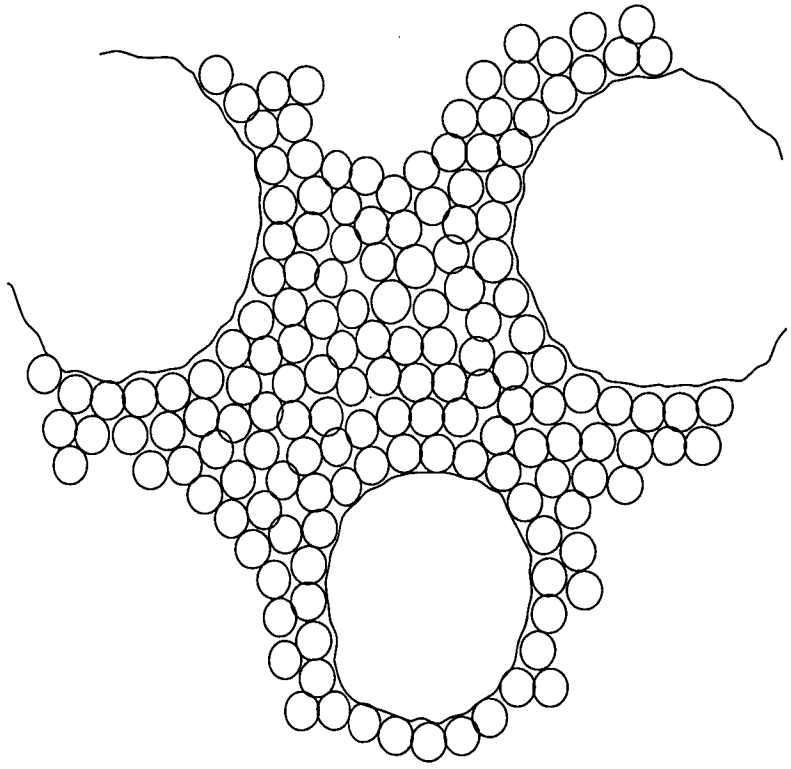

Figure 10.1: Low excess volume fractions, in which grown bubbles become surrounded by a 'sea' of smaller shrunken bubbles.

3. **Very high excess volume fraction (figure 10.2):** Resulting in a structure with larger bubbles being *decorated* by collections of smaller bubbles at their *corners/vertices*, with their *faces* impinging on other large bubbles. The structure may be similar to that of a slightly wet foam in which Von-Neumann's law is violated by the presence of plateau borders at bubble vertices.

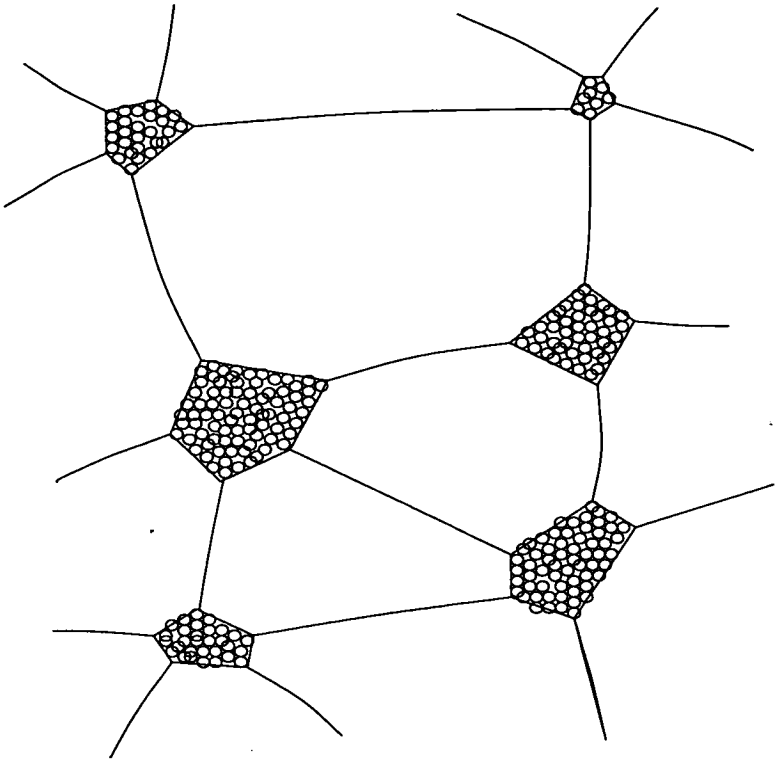

Figure 10.2: High excess volume fractions, in which grown bubbles impinge on one another with smaller shrunken bubbles decorating their vertices.

4. **Intermediate volume fractions (figure 10.3):** Includes structures between both of the above extremes. A sufficiently large volume fraction to prevent any kind of mean-field treatment of the coarsening, but sufficiently low volume fraction that bubbles may become separated by strings or collections of smaller bubbles.

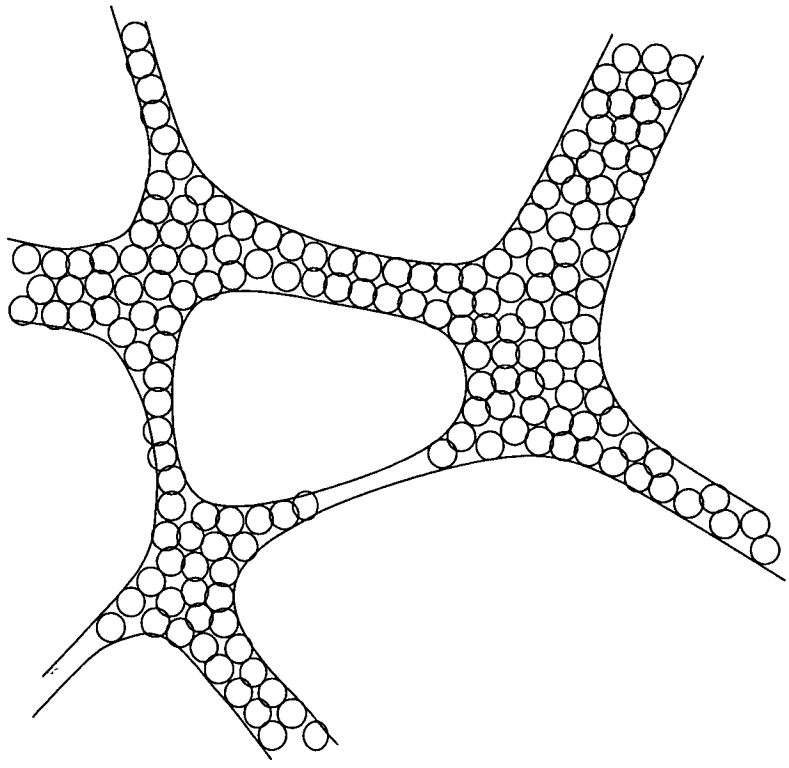

Figure 10.3: Intermediate volume fractions, in which grown bubbles are typically surrounded by small numbers of shrunken bubbles.

The first scenario of a low excess volume fraction appears most accessible to analytical techniques, since the sea of smaller bubbles may allow a mean–field like treatment analogous to that of LSW [20,21]. This scenario will be considered in later sections.

10.1.2 Rate of Bubble Rearrangements

When the excess volume fraction is small, then the coarsening of the larger bubbles will require rearrangements of the smaller bubbles so as to prevent the build up of excess strains which we expect would halt coarsening.

We suggest 4 scenarios, whose applicability will depend on the ease with which bubbles can rearrange.

1. **Inviscid rearrangements:** Bubble rearrangements can occur easily, and have no direct effect on coarsening.

2. **Viscous rearrangements:** Bubbles can rearrange, but resist doing so and hence slow the rate of coarsening. The resistance to rearrangement is taken to be from the shear in the liquid layer separating bubbles' faces, as bubbles slide past one another.

3. **No rearrangements (elastic medium):** Bubbles grow into an effectively elastic medium, which eventually may prevent them from coarsening further. This would presumably be the case if T1 neighbour switching processes were entirely suppressed.

4. **Elasto–plastic rearrangements:** There is a maximum yield strain beyond which rearrangements occur, but below which the surrounding shrunken bubbles behave as an elastic medium.

We might expect the scenarios from $1 \rightarrow 3$, to become more applicable as foams become increasingly dry. For example, we might expect rearrangements in a sufficiently wet foam to occur easily, but rearrangements in a very dry foam to occur rarely or not at all.

We might also expect a crossover between the types of coarsening we observe. Since *both* rearrangements and diffusion of disperse phase are required for coarsening to occur, we would expect coarsening to proceed with a rate determined by the *slowest* process. This contrasts with phase separation in a binary fluid for example, where the observed coarsening is that occurring by the *fastest* process (with diffusive coarsening dominating at early times, viscous hydrodynamic coarsening dominating at intermediate times, and inertial hydrodynamic coarsening dominating at late times [22]). A foam in which coarsening could rapidly occur may initially be limited by viscous forces which would determine the rate

of coarsening, then later as coarsening slowed viscous forces would become negligible, and coarsening diffusion–limited.

In following sections we will consider coarsening of a small excess volume fraction. Firstly we consider the scenario of 'inviscid' rearrangements with zero dissipation as bubbles rearrange (section 10.2.2). Next in section 10.3 we calculate the order of magnitude of growth rates by considering *the rates of dissipation* when rearrangements are inviscid (section 10.3.2), and 'viscous', where the sea of bubbles acts as a viscous fluid in section 10.3.3. The effects of having no rearrangements are considered in section 10.4, and elastoplastic rearrangements which occur at strains in excess of a system's yield strain are considered in section 10.5. We will briefly consider higher excess volume fractions in section 10.6.

10.2 A Simple Mean–Field Model

We will firstly present a simple mean–field model for coarsening of a small excess volume fraction of disperse phase.

10.2.1 System Studied

We take the larger coarsening bubbles to be surrounded by a 'sea' of smaller shrunken bubbles (see figure 10.1). Coarsening then occurs by a competitive exchange of disperse phase between the grown bubbles, with the gas flux being mediated by the sea of smaller bubbles.

For simplicity we will restrict ourselves to 3D incompressible foams, with a small excess volume fraction of disperse phase. In addition we make the following assumptions, which should be true at late times:

1. The larger bubbles are approximately spherical with radius R_i and a geometric pressure $P_i^G \simeq \frac{2\sigma}{R_i}$, and shrunken bubbles have an approximately constant size $V_B \equiv \frac{4\pi}{3}{R_B}^3$, with $R_B \ll R_i$.

2. The larger bubbles have a negligible partial pressure of trapped species, so that $P_i^s \simeq \tilde{P} + \frac{2\sigma}{R_i}$.

3. We may describe the average pressure of soluble gas in a shrunken bubble at a distance r from the centre of a grown bubble by $P^s(r,t)$ (ie we are effectively coarse–graining over bubbles at distance r).

4. As $r \to \infty$, there is a well established mean pressure of soluble gas in shrunken bubbles $P^s(\infty,t)$.

Finally we also assume:

5. Bubble rearrangements are inviscid, so that bubble growth is solely determined by the rate at which soluble gas fluxes through the bubble interfaces in the 'sea' of smaller bubbles.

These assumptions allow us to develop a number of mean–field arguments to determine the coarsening of foams.

10.2.2 Mean–Field Model

We consider shrunken bubbles at a distance r from the centre of the larger bubble, and which have an average pressure of soluble gas $P^s(r,t)$. We consider the flux of gas from bubbles at radius r to adjacent bubbles at radius $(r + R^B)$, see figure 10.4. We follow the approach of Von Neumann (for comparison see Glazier [65]), and take the flux of gas between bubbles as proportional to both the pressure differences of soluble gas between bubbles, and the surface area through which

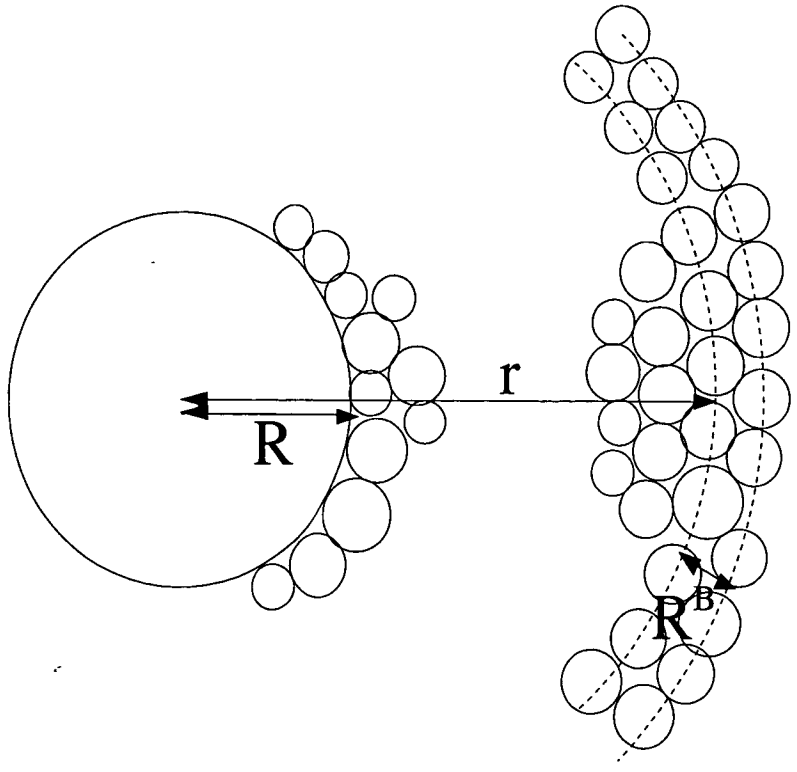

Figure 10.4: We consider grown bubbles with $R \gg R^B$, and shrunken bubbles at a distance r from the centre of large bubbles to have an average pressure of soluble gas $P^s(r,t)$.

the gas may pass. So defining a diffusion constant K in an analogous way to that of Von Neumann (so that K would be the same in 2D, as in Von Neumann's definition), we have an average volume flux of gas from bubbles at r to bubbles at $(r + R^B)$ given by

$$\mathbf{J}_V(r,t) = K4\pi r^2 \left(P^s(r,t) - P^s(r+R^B,t)\right)\hat{\mathbf{r}} \tag{10.1}$$

Since $R \gg R^B$ we may write this as

$$\mathbf{J}_V(r,t) = -K4\pi r^2 R^B \frac{\partial P^s(r,t)}{\partial r}\hat{\mathbf{r}} \tag{10.2}$$

So solving for a steady state gas flux with $\nabla.\mathbf{J} = 0$ we have

$$P^s(r,t) = \frac{R(P^s(R) - P^s(\infty))}{r} + P^s(\infty) \tag{10.3}$$

and

$$\mathbf{J}_V(R,t) = K4\pi R^2 R^B \frac{P^s(R) - P^s(\infty,t)}{R}\hat{\mathbf{r}} \tag{10.4}$$

Hence we obtain a droplet growth rate as

$$\frac{dR}{dt} = \frac{KR^B}{R}\left(\Delta P^s(\infty,t) - \frac{2\sigma}{R}\right) \tag{10.5}$$

where we have written $\Delta P^s(\infty,t) = P^s(\infty,t) - \tilde{P}$, and used $P^s(R) = \tilde{P} + \frac{2\sigma}{R}$. Since we consider an incompressible system we may define a volume per molecule by $v_g \equiv \frac{kT}{\tilde{P}}$, the volume per molecule when in equilibrium with a bulk gas. So with a little algebra we may write

$$\frac{dR}{dt} = \frac{K\tilde{P}R_B}{R}\left(\epsilon - \frac{2\sigma v_g}{kTR}\right) \tag{10.6}$$

where we have $\epsilon \equiv (P^s(\infty,t) - \tilde{P})/\tilde{P}$. Here we can see that K defines a growth rate per unit pressure.

The above Eq. 10.6 may be compared with the droplet growth rate of a dilute foam (which for incompressible foams is obtained by replacing v_b with v_g in Eq. 2.22), and is

$$\frac{dR}{dt} = \frac{Dv_gC(\infty)}{R}\left(\epsilon - \frac{2\sigma v_g}{kTR}\right) \tag{10.7}$$

with D being the standard diffusion constant for the flux of dissolved gas through the continuous phase, and $C(\infty)$ is the concentration of dissolved gas in the continuous phase when in contact with a bulk phase of gas (a bubble with infinite radius). Hence we find that if bubble rearrangements are inviscid, then the coarsening of a small excess of disperse phase is equivalent to the coarsening of dilute gas bubbles, but with D replaced by an effective diffusion constant D_{eff} defined as,

$$D_{eff} \equiv \frac{K\tilde{P}R_B}{v_gC(\infty)} \tag{10.8}$$

We may calculate K in terms of $\tilde{P}$, $C(\infty)$, v_g, D and the separation between bubbles d. This is done in Appendix F and gives

$$K = \frac{Dv_gC(\infty)}{\tilde{P}d} \tag{10.9}$$

So the growth rate may also be written as

$$\frac{dR}{dt} = \left(\frac{R_B}{d}\right)\left(\frac{Dv_gC(\infty)}{R}\right)\left(\epsilon - \frac{2\sigma v_g}{kTR}\right) \tag{10.10}$$

which is a factor R_B/d greater than the growth rate for dilute foam bubbles in liquid only. Since $d \ll R_B$ the volume fraction of liquid separating bubbles is $\sim R_B^2 d/(R_B+d)^3 \sim \frac{d}{R_B}$. So writing $\phi_{int} \sim \frac{d}{R_B}$ for the volume fraction of liquid in interfaces separating bubbles (which does not include the liquid in the Plateau borders), then we find the growth rate is increased by a factor of $1/\phi_{int}$. As $\phi_{int} \to 1$ we regain the expression for coarsening of dilute foam bubbles in liquid only.

For comparison with an expression derived later in section 10.3.2, note that Eq. 10.10 has

$$\dot{R} \sim \frac{R_B}{d}\frac{Dv_g C(\infty)}{R}\frac{\sigma v_g}{RkT} \tag{10.11}$$

which may be written as

$$\dot{R}R^2 \sim \frac{R_B}{d}\frac{Dv_g^2 C(\infty)\sigma}{kT} \tag{10.12}$$

10.3 Rate–Limiting Mechanisms

The present section considers the orders of magnitude for the rate of dissipation and bubble growth, when bubble growth is limited by the diffusion of disperse phase between bubbles (inviscid rearrangements, section 10.3.2), or by the rate at which shrunken bubbles rearrange (viscous rearrangements, section 10.3.3) respectively. Firstly sections 10.3.1–10.3.3 will calculate the rate of dissipation due to rearrangements or diffusive flux, and equate it with the rate of decrease in the free energy to determine the order of magnitude of droplet growth rate for each presumed rate–limiting mechanism. Then section 10.3.4 compares the dissipation rates, so as to determine when each of the rate limiting mechanisms would apply.

As an example of the method we firstly use it to derive the coarsening rate in the traditional LSW [20, 21] scenario of a vanishingly small volume fraction of

bubbles in a liquid (without trapped species). In this scenario dissipation is from the *diffusion resistance* of the dissolved disperse phase which diffuses between bubbles.

10.3.1 LSW Coarsening of Bubbles

Firstly we determine the average velocity of the dissolved disperse phase as it moves through the continuous phase near a drop. Since we consider the system to be in a steady state with an approximately constant concentration of dissolved disperse–phase molecules, we may treat the number of dissolved disperse–phase molecules as effectively conserved. Conservation of dissolved disperse–phase within the continuous phase requires that $\vec{\nabla}.[\vec{u}(\vec{r})c(\vec{r})] = 0$, with $\vec{u}$ the average velocity of dissolved disperse phase, and $c(\vec{r})$ the concentration of dissolved disperse phase at a position relative to the centre of a bubble*. Taking the average velocity of dissolved disperse phase to be in a radial direction, then in spherical coordinates $\vec{\nabla}.[\vec{u}(\vec{r})c(\vec{r})] = 0$ becomes $\frac{1}{r^2}\partial(u_r(r)c(r)r^2)/\partial r = 0$, which may be solved to give

$$u_r(r)c(r)r^2 = \mathcal{C} \tag{10.13}$$

with $u_r(r)$ the radial velocity component, and $\mathcal{C}$ being the total rate of flux of dissolved disperse phase molecules away from (u_r positive), or towards (u_r negative), a drop. Since at a droplets surface we have a total rate of flux of dissolved disperse phase molecules of $4\pi R^2\dot{R}/v_g$, then $\mathcal{C} = 4\pi\frac{R^2\dot{R}}{v_g}$. So we find

$$u_r(r) = 4\pi\frac{R^2\dot{R}}{v_g}\frac{1}{c(r)r^2} \tag{10.14}$$

In the following we will drop the subscript on u_r, instead taking all velocities to be in a radial direction. Incompressible foams have $\sigma/R \ll P$, so $c(r) \sim C(\infty)$,

*This is equivalent to writing the flux of disperse phase $\vec{J}(\vec{r})$ as $\vec{J}(\vec{r}) = \vec{u}(\vec{r})c(\vec{r})$, so that in a steady state the diffusion equation $\partial c(\vec{r})/\partial t = -D\vec{\nabla}.\vec{J}(\vec{r})$ becomes $\vec{\nabla}.\vec{J}(\vec{r}) = 0$, which requires $\vec{\nabla}.[\vec{u}(\vec{r})c(\vec{r})] = 0$.

ie that above a 'bulk' gas phase. So we have

$$u(r) \sim \frac{R^2\dot{R}}{v_g C(\infty)}\frac{1}{r^2} \tag{10.15}$$

Knowing the order of magnitude for the average velocity of dissolved molecules, we may now estimate the total rate of dissipation arising from the net flux of material between drops.

The total number of dissolved molecules within spheres of radii r and $r + dr$ is of order $r^2 drc(r) \sim r^2 drC(\infty)$. The average dissipation rate per molecule at r is $\zeta u(r)^2$, where ζ is the viscous drag coefficient on a molecule of disperse phase moving through the liquid. Hence the total dissipation arising from diffusion to a drop is of order $\int_R^\infty r^2 drC(\infty)\zeta u(r)^2$. Using the relation [88] $\zeta = kT/D$, Eq. 10.15, and integrating, gives the rate of dissipation $T\dot{S}$ as

$$T\dot{S} \sim \frac{kT}{DC(\infty)v_g^2}\dot{R}^2 R^3 \tag{10.16}$$

The transfer of material between droplets occurs so as to reduce their free energy, the rate of reduction of which equals the rate of dissipation. The reduction in free energy per particle transferred is of the order of the difference in the droplets chemical potentials and is of order $\sim \frac{\sigma v_g}{R}$. Hence since the total flux of material to a drop is $\sim \frac{R^2\dot{R}}{v_g}$ the rate of reduction in the free energy must be of order

$$\frac{R^2\dot{R}}{v_g}\frac{\sigma v_g}{R} \sim \sigma R\dot{R} \tag{10.17}$$

that is, of the order of the rate of change of a droplets surface energy.

Equating expressions 10.17 and 10.16 gives

$$\sigma R\dot{R} \sim \frac{kT}{DC(\infty)v_g^2}\dot{R}^2 R^3 \tag{10.18}$$

which may be rearranged to give

$$R^2\dot{R} \sim \frac{Dv_g^2 C(\infty)\sigma}{kT} \tag{10.19}$$

as is found by the traditional analysis of LSW [20, 21] for dilute *droplets* (as opposed to bubbles), in a continuous phase.

10.3.2 Inviscid Rearrangements

When bubble rearrangements are inviscid the above argument may be modified to give the rate of dissipation and growth rate for bubbles growing within a *sea* of smaller shrunken bubbles, as considered in section 10.2.2's mean–field model. Given the rate of bubble growth $\dot{R}$, and continuing to treat the foam as incompressible, then in a steady state we continue to obtain the flux of dissolved disperse phase through the *liquid* within bubble–bubble interfaces as

$$u(r) \sim \frac{R^2\dot{R}}{v_g C(\infty)} \frac{1}{r^2} \tag{10.20}$$

as in Eq. 10.15 in the previous section 10.3.1. The rate of dissipation per molecule dissolved in the liquid films will remain as $\zeta u(r)^2$, so the only other required change is to only integrate over disperse phase in the liquid interfaces. Hence the integral is reduced by a factor d/R_B, and integrating we obtain

$$T\dot{S} \sim \frac{d}{R_B} \frac{kT}{DC(\infty)v_g^2} \dot{R}^2 R^3 \tag{10.21}$$

and hence a growth rate which satisfies

$$\dot{R}R^2 \sim \frac{R_B}{d} \frac{Dv_g^2 C(\infty)\sigma}{kT} \tag{10.22}$$

a result in agreement with Eq. 10.12, obtained by the more accurate calculation in section 10.2.2.

Next we consider viscous bubble rearrangements, in which bubbles slide past one another dissipating energy via the viscous stresses which occur in the liquid separating the bubbles.

10.3.3 Viscous Rearrangements

We take the shrunken bubbles to be sufficiently concentrated that they press against one another, with the repulsive disjoining pressure between bubble membranes maintaining touching faces at a distance d from one another.

We consider growing bubbles to be sufficiently dilute that flow due to bubble growth is approximately radially outward from the bubble. Restricting ourselves to 3D foams, and taking $\vec{u}(\vec{r})$ as the velocity of the liquid and shrunken-bubble fluid, then incompressibility of the fluid requires that $\vec{\nabla}.\vec{u}(\vec{r}) = 0$, so that in spherical coordinates

$$0 = \frac{\partial(u_r r^2)}{\partial r} \tag{10.23}$$

Hence for a growing bubble of radius R, growing with velocity $\dot{R}$, we find

$$u_r(r) = \frac{R^2\dot{R}}{r^2} \tag{10.24}$$

In all that follows we again drop the subscript on u_r, and take all fluid velocities to be in a radial direction.

Consider two touching bubbles at radial distances r and $r + R_B$ respectively. The differing velocities at r and $r + R_B$ will mean that bubbles must rearrange, and slide past one another. For $r \gg R_B$ the relative velocity of the bubbles is $\simeq \frac{\partial u(r)}{\partial r} R_B$. The shear rate of the fluid between bubbles (separated by a distance d), is of the order of the relative bubble velocities divided by their separation distance d. Hence we obtain a viscous stress due to the relative bubble motion as

$$\eta \frac{1}{d}\left(\frac{\partial u(r)}{\partial r} R_B\right) \sim \eta \frac{R_B}{d}\frac{\partial u(r)}{\partial r} \tag{10.25}$$

where η is the viscosity of the liquid continuous phase.

Since the viscous stress is only present in the continuous phase between bubbles, the viscous dissipation per unit volume is proportional to the volume fraction of continuous phase in the 'sea' of shrunken bubbles which for small liquid volume fractions is of order d/R_B.

So we may obtain the total dissipation rate due to a bubble growing as

$$T\dot{S} \sim \int_R^\infty r^2 dr \frac{d}{R_B}\eta\left(\frac{R_B}{d}\frac{\partial u(r)}{\partial r}\right)^2 \tag{10.26}$$

which using Eq. 10.24 and integrating, gives

$$T\dot{S} \sim \frac{\eta R_B}{d} R\dot{R}^2 \tag{10.27}$$

As in the previous calculations (sections 10.3.1 and 10.3.2), the rate of decrease in the free energy due to changes in the surface area of a growing droplet, is of order $\sigma R\dot{R}$. Hence we find that

$$\sigma R\dot{R} \sim \frac{\eta R_B}{d} R\dot{R}^2 \tag{10.28}$$

which may be rearranged to give

$$\dot{R} \sim \frac{\sigma}{\eta} \frac{d}{R_B} \tag{10.29}$$

and hence a linear rate of droplet growth. The expression may also be written as

$$\frac{\eta \dot{R}}{d} \sim \frac{\sigma}{R_B} \tag{10.30}$$

which states that the viscous stress is of the same order of magnitude as the smaller bubble's geometric pressure.

We note that the argument above does not apply to the coarsening of emulsion droplets in an ordinary (structureless) fluid, for the following reason. Coarsening requires both fluid to be displaced and disperse phase to diffuse to the drop. The finite molecular volume of the dissolved disperse phase requires that there be a backflow of fluid past a dissolved disperse phase molecule as it diffuses towards a drop. Once the disperse phase molecule reaches the drop it is incorporated into the droplet with an increase in the droplets volume. Hence there is no additional displacement of fluid required by droplet growth, with the displacement of fluid occurring continually as backflow past the diffusing dissolved phase. Since the backflow required by the diffusing solvent is accounted for by the Stokes–Einstein relation, coarsening would occur as described by the traditional LSW analysis [20, 21]. A generalisation of the argument to an emulsion droplet, would only apply to a scenario of a droplet being *inflated* by a needle and syringe, for example[†].

[†]Because the volume of a gas molecule in a bubble is much larger than its volume when dissolved in solution, the argument given *does* apply to coarsening of dilute foam bubbles in

So when coarsening is occurring into a 'sea' of bubbles/droplets, the *structure* of the liquid–bubble fluid requires rearrangements for coarsening to occur, with an associated extra dissipation of energy. In contrast when coarsening occurs into a structureless fluid, fluid is displaced by the diffusion of solvent with a dissipation in energy already accounted for by the Stokes–Einstein relation for the diffusant.

10.3.4 Viscous or Diffusion Limited Growth?

The growth rates (Eqs. 10.22 and 10.29) derived for viscous and inviscid rearrangements correspond to growth rates which are limited by the rate of viscous dissipation and the rate of diffusive flux respectively. Here we attempt to find out when each of the scenarios will apply.

Since both rearrangements and diffusion are necessary for bubble growth, bubble growth will be limited by the *greatest* source of dissipation and will occur with the *slowest* of the possible growth rates. Hence if we consider the ratio $T\dot{S}_{DL}/T\dot{S}_{VL}$ of the dissipation rates by diffusion and viscous rearrangements respectively, then when $T\dot{S}_{DL}/T\dot{S}_{VL} > 1$ coarsening will be diffusion limited and when $T\dot{S}_{DL}/T\dot{S}_{VL} < 1$ coarsening will be limited by viscous dissipation.

The dissipation rates are given by Eqs. 10.21 and 10.27 respectively: $T\dot{S}_{DL} \sim \frac{d}{R_B}\frac{kT}{DC(\infty)v_g^2}\dot{R}^2R^3$ and $T\dot{S}_{VL} \sim \frac{\eta R_B}{d}\dot{R}^2R$. So we obtain

$$\frac{T\dot{S}_{DL}}{T\dot{S}_{VL}} \sim \left(\frac{d}{R_B}\right)^2 \frac{kT}{DC(\infty)v_g^2\eta}R^2 \tag{10.31}$$

This may be written in terms of a molar concentration C_M, the molar volume

a structureless fluid. A simple order of magnitude estimate gives $T\dot{S} \sim \eta R\dot{R}^2$ and $\dot{R} \sim \eta$, so that the rate of dissipation is no longer increased by a factor of R_B/d. The following section 10.3.4 will demonstrate that at room temperature and atmospheric pressure, viscous limited coarsening is unlikely to be observed even in a non–dilute foam/emulsion, so at room temperature and atmospheric pressure the reduced dissipation of a structureless fluid makes viscous limited coarsening even *less* likely to be observed.

v_{Mg} of gas in bubbles at pressure $\tilde{P}$, and the gas constant R_G as

$$\frac{T\dot{S}_{DL}}{T\dot{S}_{VL}} \sim \left(\frac{d}{R_B}\right)^2 \frac{R_G T}{DC_M(\infty)v_{Mg}^2\eta} R^2 \tag{10.32}$$

We take $R_G T \sim 10^3$J, $D \sim 10^{-9}\mathrm{m}^2 s^{-1}$, $C_M(\infty) \sim 10^2\mathrm{m}^{-3}$, $v_{Mg} \sim 10^{-2}\mathrm{m}^3$, and $\eta \sim 10^{-3}\mathrm{Nm}^{-2}\mathrm{s}$, (as we might expect for a soluble gas of CO_2 and a liquid phase of water for example[‡]). Then considering $R \sim 10^{-6}$m, gives

$$\frac{T\dot{S}_{DL}}{T\dot{S}_{VL}} \sim 10^5 \left(\frac{d}{R_B}\right)^2 \tag{10.33}$$

So if R is $R \sim 10^{-6}$m, then viscous–dissipation will be observed for d/R_B smaller than $10^{-2.5}$.

So at room temperature and atmospheric pressure, given sufficiently small bubbles, low liquid volume fraction, and high liquid viscosity for Eq. 10.32 to be less than 1, then viscous limited growth may be observed with $\bar{R} \sim t$. However, such systems appear difficult to form and hence are likely to be uncommon, so coarsening will typically be diffusion limited[§].

Viscous limited coarsening is more likely to be observed in low pressure/high temperature systems in which the volume per gas molecule in bubbles $v_g = kT/\tilde{P}$, is large. In such systems a given diffusive flux of disperse phase between bubbles will require a larger displacement of fluid than an equivalent system at atmospheric pressure, and hence the rate of viscous dissipation will be increased relative to that of diffusion–limited dissipation. For example, if the pressure is reduced by a factor of 100, then v_g^2 is increased by a factor of 10^4, so that viscous limited growth merely requires that $d/R_B < \sqrt{10}$.

[‡]For a list of order of magnitude of constants, and further explanation see Appendix G.

[§]It is interesting to note that the viscous limited and diffusion limited growth laws may be predicted (up to a constant prefactor), by the most naive order of magnitude arguments applied to the phase ordering kinetics of binary fluids (see "Theory of Phase Ordering Kinetics" by A.J. Bray [22], page 375). Such arguments *do not* however enable the correct prediction of when each regime will apply, which is determined by the structure of the shrunken–bubble fluid.

10.4 No Rearrangements: Elastic Energy

Next we consider the behaviour of a bubble within a 'sea' of smaller shrunken bubbles, in which bubble rearrangements are not allowed to occur. The growth or shrinkage of such a bubble will deform the surrounding bubbles, and hence increase their interfacial energies. By estimating the increase in elastic energy associated with a bubbles growth or shrinkage, we are able to show that stability against coarsening may be recovered, even when the quantity of trapped species is insufficient to osmotically stabilise the foam.

For definiteness we imagine a system which has undergone sufficient coarsening that we have an idealised scenario of *grown* bubbles in a sea of smaller shrunken bubbles. We take this initial state to be *unstrained* elastically, and consider whether further coarsening can occur. Such a scenario could have arisen by coarsening from an initial configuration in which the larger chemical potential differences would provide a stronger driving force for coarsening, forcing plastic rearrangement (this is considered explicitly in section 10.5 below). Alternately such a system could occur by an osmotic compression of a previously dilute, partially coarsened foam.

10.4.1 Small Deformations

Firstly we consider small deformations. Treating bubbles as incompressible, a large bubble's growth by an amount ΔR will displace an element of the fluid at an initial distance r_0 from the centre of the bubble (see figure 10.5), by

$$\Delta u(r_0) = \frac{R_0^2 \Delta R}{r_0^2} \tag{10.34}$$

where R_0 is the bubble's original size, and $R_0 \gg \Delta R$. So taking the shrunken bubbles to have size of order R_B, then a shrunken bubble at a distance r_0 will

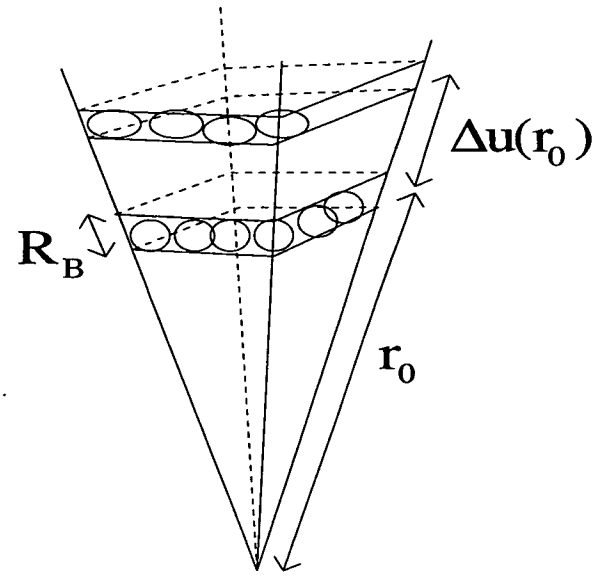

Figure 10.5: In the absence of rearrangements, bubble growth results in an increase in the shrunken bubbles' interfacial area.

experience an extension/contraction by a distance H, with

$$H = \Delta u(r_0 + R_B) - \Delta u(r_0) \simeq \frac{R_0^2 \Delta R}{r_0^2}\left(\frac{1}{(1+R_B/r_0)^2} - 1\right) \tag{10.35}$$

so since $r_0 > R_0 \gg R_B$, then expanding in R_B/R_0 gives

$$H \simeq -2R_B \frac{R_0^2 \Delta R}{r_0^3} \tag{10.36}$$

Next we consider the energy of extending or contracting along one axis of a single shrunken bubble such that its length would be increased from R_B to $R_B + H$. If we restrict ourselves to relatively small strains (or distances far from a growing/shrinking bubble), then we may expand the associated increase in energy ΔE_1 in terms of a power series in H,

$$\Delta E_1 = \sigma\left(\alpha_1 H + \alpha_2 H^2 + O(H^3)\right) \tag{10.37}$$

Since we consider an initially unstrained state with spherical shrunken-bubbles, then symmetry requires that both +ve and −ve values of H will increase ΔE_1 by the same amount. So to lowest order

$$\Delta E_1 = \sigma\left(\alpha_2 H^2\right) \sim \sigma H^2 \tag{10.38}$$

So using Eq. 10.36 for H, we find the bubbles interfacial energy changes by

$$\Delta E_1 \sim \sigma \frac{R_B^2 R_0^4 \Delta R^2}{r_0^6} \tag{10.39}$$

where we have ignored a factor of 4.

Initially we have of order $r_0^2 dr_0/R_B^3$ shrunken bubbles between spheres at r_0 and r_0+dr_0. So the total change in elastic energy due to a bubbles growth or shrinking is

$$\Delta E \sim \sigma \int_{R_0}^{\infty} \left(\frac{r_0^2 dr_0}{R_B^3}\right) \left(\frac{R_B^2 R_0^4 \Delta R^2}{r_0^6}\right) \tag{10.40}$$

which upon integration gives

$$\Delta E \sim \sigma \frac{R_0}{R_B} (R - R_0)^2 \tag{10.41}$$

where we have written $\Delta R = R - R_0$.

Following a similar approach to that described by Pippard [90], we now imagine a piston connected to a reservoir of gas, which holds a grown bubble at constant pressure P_i. Then considering a reversible fluctuation in bubble volume by dV, the work done by the bubble $P_i dV$, equals the sum of the work done against $P + \Pi$, the increase in the bubble's interfacial energy σA, and the increase in ΔE. So we have

$$P_i dV \sim \left(P + \Pi + \frac{\partial(\sigma A)}{\partial V} + \frac{\partial(\Delta E)}{\partial V}\right) dV \tag{10.42}$$

hence

$$P_i \sim P + \Pi + \frac{\sigma}{R_i} + \frac{\partial(\Delta E)}{\partial V} \tag{10.43}$$

Differentiating Eq. 10.41 for ΔE then gives

$$P_i \sim P + \Pi + \frac{\sigma}{R} + \frac{R_0}{R_B}\frac{\sigma}{R}\left(1 - \frac{R_0}{R}\right) \tag{10.44}$$

If we look at the above Eq. 10.44 we see that P_i will initially increase until R exceeds R_0, then later decrease with $P_i \to P + \Pi$ as $R \to \infty$. Hence if a drop was to grow to an infinite (bulk) size, then it would have $P_b = P + \Pi$ as

when rearrangements are allowed. The initial increase in P_i before R exceeds R_0 (or decrease in P_i, for R dropping below R_0), could prevent coarsening from occurring. However if a sufficiently large droplet is nucleated, then it will coarsen to form a bulk gas phase.

In summary, the above calculation *suggests* that an absence of bubble rearrangements could result in a long lived metastable state, but that any subsequent nucleation of a sufficiently large drop would allow coarsening to continue.

10.4.2 Larger Deformations

The previous calculation was only valid for small strains in which $\Delta R \ll R_0$. We now improve the previous calculation by exactly calculating the displacement of a bubble layer, and then expanding in $(R^3 - R_0^3)/r_0^3$, which for large r_0 is a valid expansion even for large deformations. Although the resulting expression applies both to expansions and contractions of a bubble, for ease of presentation we will refer to a bubble's growth.

We continue to consider a layer of bubbles, and make the observation that bubble growth will require any given layer to move so as leave a volume equal to the change in the larger bubble's volume, which is $\frac{4\pi}{3}(R^3 - R_0^3)$. So for a layer with an initial inner radius of r_0 it must expand to a radius r such that

$$r^3 - r_0^3 = R^3 - R_0^3 \tag{10.45}$$

so as to make way for the larger bubble's growth[¶]. Hence we obtain a bubble layer's new position $r(r_0)$ as

$$r(r_0) = \left(r_0^3 + R^3 - R_0^3\right)^{1/3} \tag{10.46}$$

[¶]We continue to implicitly assume the bubbles are incompressible.

The extension H of bubbles in a layer with initial inner radius r_0 is

$$H = \Delta u(r_0 + R_B) - \Delta u(r_0) \tag{10.47}$$

So using $\Delta u(r_0) = r(r_0) - r_0$ and $\Delta u(r_0 + R_B) = r(r_0 + R_B) - (r_0 + R_B)$, we obtain

$$H = (r(r_0 + R_B) - r(r_0)) - R_B \tag{10.48}$$

Using Eq. 10.46 we may expand in terms of R_B/r_0, which to lowest order gives

$$H \simeq R_B \left(\frac{r_0^2}{r^2} - 1 \right) \tag{10.49}$$

If we again use Eq. 10.46, then for small strains or large distances r_0 from a bubble we may expand in terms of $(R^3 - R_0^3)/r_0^3$, to obtain

$$H \simeq -\frac{2}{3} R_B \left(\frac{R^3 - R_0^3}{r_0^3} \right) + O\left(\frac{R^3 - R_0^3}{r_0^3} \right)^2 \tag{10.50}$$

We note that if $\Delta R \equiv (R - R_0) \ll R_0$, then we could further expand the above equation to obtain

$$H \sim -\left(\frac{2 R_B R_0^2 \Delta R}{r_0^3} \right) \tag{10.51}$$

as before. However if we continue to take $\Delta E_1 \sim \sigma H^2$, and integrate our new expression for $H(r_0)$ then we get

$$\Delta E \sim \sigma \int_{R_0}^{\infty} \frac{r_0^2 dr_0}{R_B^3} H^2 \sim \frac{\sigma}{R_B} \frac{(R^3 - R_0^3)^2}{R_0^3} \tag{10.52}$$

So that $\Delta E \sim R^6$, as opposed to $\Delta E \sim R^2$ as in our previous calculation.

The result $\Delta E \sim R^6$ clearly indicates that in the absence of bubble rearrangements the elastic energy due to bubble deformations will prevent coarsening and stabilise the system. This is emphasised by using Eqs. 10.52 and 10.43 to obtain a bubble's pressure as

$$P_i \sim P + \Pi + \frac{\sigma}{R} + \frac{\sigma}{R_B} \frac{R^3 - R_0^3}{R_0^3} \tag{10.53}$$

which becomes increasingly large for increasingly large or small deviations in R from R_0. Since an increase in a bubble's pressure corresponds to an increase in the chemical potential of the gas molecules it contains, coarsening will not occur.

In the calculation of ΔE we used $\Delta E_1 \sim \sigma H^2$, an approximation strictly only valid for large r_0 or sufficiently small strains. So the above result is correct for small strains and approximate for larger strains. If strains are very large we might expect rearrangements to occur in a plastic manner. Hence we next consider the effect of a finite yield strain above which rearrangements occur, and below which the medium behaves elastically.

10.5 Finite Yield Strain

We now consider the following simple model: the system may only support a maximum finite yield strain y^*, above which rearrangements will occur. We take

$$y^* \sim H^*/R_B \tag{10.54}$$

with H^* the maximum extension/contraction of bubbles before rearrangements occur.

In the absence of rearrangements Eq. 10.50 gives

$$H \sim R_B|R^3 - R_0^3|/r_0^3 \tag{10.55}$$

so that H^* implicitly defines a radius r_0^* within which rearrangements occur, but beyond which the medium behaves elastically. So rearranging Eq. 10.55, we may define $r_0^* \equiv \frac{R_B}{H^*}(|R^3 - R_0^3|)$, which since $H^* \sim y^* R_B$ gives

$$r_0^{*3} \sim \frac{|R^3 - R_0^3|}{y^*} \tag{10.56}$$

For a plastic region to exist around a bubble, we require $r_0^* > R$, so that Eq. 10.56 requires

$$\left|R^3 - R_0^3\right| > y^* R^3 \tag{10.57}$$

So if $R > R_0$ then we require

$$R > R^{*+} \equiv \frac{R_0}{(1-y^*)^{1/3}} \tag{10.58}$$

for a plastic region to exist, and if $R < R_0$ then we require

$$R < R^{*-} \equiv \frac{R_0}{(1+y^*)^{1/3}} \tag{10.59}$$

So we find that the existence of a plastic region will require a sufficient nucleation in droplet size R above R^{*+} or below R^{*-}, with the magnitude of R^{*+} and R^{*-} determined by the yield strain y^*. Large yield strains will require a large nucleation event, where as small yield strains will require only a small nucleation event.

If we take deformations within the plastic region to be of order H^*, then we may calculate the elastic energy as

$$\Delta E \sim \sigma \int_{R_0}^{r_0^*} \frac{r_0^2 dr_0}{R_B^3} H^{*2} + \sigma \int_{r_0^*}^{\infty} \frac{r_0^2 dr_0}{R_B^3} H(r_0)^2 \tag{10.60}$$

giving

$$\Delta E \sim y^* \frac{\sigma}{R_B} \left(\left| R^3 - R_0^3 \right| - y^* R_0^3 \right) + y^* \frac{\sigma}{R_B} \left| R^3 - R_0^3 \right| \tag{10.61}$$

where we note that since $y^* < \left| R^3 - R_0^3 \right| / R_0^3$, the left hand term is positive. So using Eq. 10.43 we get

$$P_i \sim P + \Pi + \frac{\sigma}{R_i} + \begin{cases} \frac{\sigma}{R_B} \frac{R^3 - R_0^3}{R_0^3} & R^{*-} < R < R^{*+} \\ y^* \frac{\sigma}{R_B} \frac{R^3 - R_0^3}{\left| R^3 - R_0^3 \right|} & R < R^{*-} \text{ or } R^{*+} < R \end{cases} \tag{10.62}$$

So that a bulk gas would now have

$$P_b \sim P + \Pi + y^* \frac{\sigma}{R_B} \tag{10.63}$$

So will the foam be stable? This may be answered by considering whether a sufficiently large nucleated bubble will shrink in size again, or start to coarsen. If all sizes of a nucleated bubble will shrink in size again then the system must be stable, otherwise the system will be metastable. The largest possible nucleated bubble with the lowest possible chemical potential obtainable by an increase in bubble size will have pressure P_b. So if the average bubble pressure has $\bar{P} < P_b$

then the bubble will shrink again, but if $\bar{P} > P_b$ then the drop will continue to grow in size[‖]. Since we consider the system as initially unstrained with $R = R_0$, then

$$\bar{P} \sim P + \Pi + \frac{\sigma}{R_0} \tag{10.64}$$

Comparing Eq. 10.64 with Eq. 10.63, then for instability we require $\bar{P} > P_b$, and hence

$$\frac{\sigma}{R_0} > \frac{y^* \sigma}{R_B} \tag{10.65}$$

which requires $y^* < R_B/R_0$. Hence since $R_B \ll R_0$, then unless $y^* \ll 1$, the system will be stable.

So given a sufficiently small y^*, the stability of the system will depend on how it is prepared. For example, if we consider a foam formed by the osmotic compression of a dilute partially coarsened foam, then a sufficiently coarsened foam may have R_0 large enough that $y^* > R_B/R_0$ and be stable, but if R_0 is too small then we can have $y^* < R_B/R_0$ and coarsening can occur[**].

10.6 Higher Volume Fractions

The above concludes the discussion of coarsening mechanisms with small excess volume fraction (figure 10.1). We briefly give some simple order of magnitude estimates for coarsening rates at higher excess volume fractions.

[‖]Note that the grown bubbles are taken to be sufficiently large that we may neglect the pressure of trapped species within them.

[**]Although the radius at which shrunken bubbles coexist with grown bubbles depends on the radius of the larger bubbles R_0, it remains of order R_B, and the above estimations remain valid.

10.6.1 High Excess Volume Fractions

At high excess volume fractions the grown bubbles will be in contact with one another, with shrunken bubbles *decorating* grown bubbles' vertices (see figure 10.2). If we describe a grown bubble's size by an effective radius R, then we expect its geometric pressure to be of order σ/R. Since the grown bubbles are in contact with one another, growth occurs by gas diffusing through a single bubble wall. So defining a diffusion constant K as in section 10.2.2, then we have

$$\frac{d(\bar{R}^3)}{dt} \sim K\bar{R}^2\Delta P \tag{10.66}$$

where ΔP is the pressure difference between bubbles and $\Delta P \sim \sigma/R$. Hence we have

$$\bar{R}\dot{\bar{R}} \sim K\sigma \tag{10.67}$$

and

$$\bar{R} \sim (K\sigma t)^{1/2} \tag{10.68}$$

We note that using $K = Dv_gC(\infty)/\tilde{P}d$ (see Appendix F), and $\tilde{P} = kT/v_g$, we alternately have

$$\bar{R} \sim \left(\frac{Dv_g^2C(\infty)\sigma}{dkT}\right)^{1/2} t^{1/2} \tag{10.69}$$

10.6.2 Intermediate Volume Fractions

We consider volume fractions which are sufficiently low that grown bubbles do not directly press on one another, but sufficiently high that they would not generally be considered as dilute. Then if we take the excess volume fraction as ϕ_{ex}, then the volume fraction of shrunken bubbles is of order $\sim 1 - \phi_{ex}$. The number of grown bubbles per unit volume is of order $\phi_{ex}/\bar{R}^3$, so the *thickness* of the layer of shrunken bubbles separating grown bubbles d', satisfies $d'\bar{R}^2\phi_{ex}/\bar{R}^3 \sim 1 - \phi_{ex}$. Hence

$$d' \sim \bar{R}\left(\frac{1-\phi_{ex}}{\phi_{ex}}\right) \tag{10.70}$$

So gas flux will pass through of order $d'/R_B \sim (\bar{R}/R_B)(1-\phi_{ex})/\phi_{ex}$ layers. There will be a pressure gradient in the shrunken bubbles of order $(R_B/d')\Delta P$, so if we assume coarsening is diffusion limited (ie treat rearrangements as inviscid), the rate of bubble growth will be

$$\frac{d(\bar{R}^3)}{dt} \sim K\bar{R}^2\left(\frac{R_B}{d'}\right)\Delta P \tag{10.71}$$

which using equation 10.70 gives

$$\dot{\bar{R}}\bar{R}^2 \sim K\sigma R_B \frac{\phi_{ex}}{1-\phi_{ex}} \tag{10.72}$$

So also using $K = Dv_gC(\infty)/\tilde{P}d$ (see Appendix F), and $\tilde{P} = kT/v_g$, we have

$$\dot{\bar{R}}\bar{R}^2 \sim \frac{R_B}{d}\frac{Dv_g^2C(\infty)\sigma}{kT}\left(\frac{\phi_{ex}}{1-\phi_{ex}}\right)^{1/3} t^{1/3} \tag{10.73}$$

ie a growth rate which is a factor of $\phi_{ex}/(1-\phi_{ex})$ times that when ϕ_{ex} was negligible. So we find that the increase in bubble separation d' during bubble growth is sufficient to restore the coarsening from a $t^{1/2}$ to a $t^{1/3}$ time dependence.

10.7 Conclusions

The qualitative features of an unstable, coarsening foam, will be determined by the excess volume fraction of gas ϕ_{ex} which at equilibrium forms a bulk gas phase. Typical foam morphologies for low, high, and medium ϕ_{ex} are suggested in figures 10.1, 10.2, and 10.3 respectively.

At low excess volume fractions, viscous limited coarsening will be found in systems with sufficiently small bubbles, low liquid volume fractions, and high enough liquid viscosities that the ratio in Eq. 10.32 is less than 1. Viscous limited growth is easily distinguished from diffusion limited growth by its linear growth rate in time. At room temperature and atmospheric pressure however, such systems appear difficult to form and hence will be uncommon, so that under such conditions

coarsening will typically be diffusion limited. Viscous limited coarsening is more likely to be observed in low pressure/high temperature systems, in which the increased volume per gas molecule in bubbles $v_g = kT/\tilde{P}$, requires a much greater displacement of fluid (and hence dissipation), for a given flux of gas.

Hence for low excess volume fractions at room temperature and atmospheric pressure, we generally expect to observe diffusion limited coarsening, with a $t^{1/3}$ growth law as in the traditional LSW scenario [20,21]. In such cases the only effect of the shrunken bubbles on the growth rate is to require the diffusion constant for dissolved disperse phase in liquid D, to be multiplied by a factor R_B/d to account for the reduced volume fraction of liquid that the disperse phase need diffuse through between coarsening bubbles.

We found in section 10.4.2 that in the absence of bubble rearrangements, elastic strains which oppose bubble growth will stabilise the foam. When there is a finite yield strain above which rearrangements occur, then a bulk gas phase formed by coarsening will have a higher pressure and chemical potential than when rearrangements occur easily. As a rough estimate, if the yield strain y^* is sufficiently large that $y^* > R_B/R_0$ then the foam will be stable, but if $y^* < R_B/R_0$ then coarsening may occur. For example considering foams formed by the osmotic compression of dilute partially coarsened foam, then a sufficiently coarsened foam with sufficiently large bubbles may have $y^* > R_B/R_0$ and be stable, but if R_0 is too small then we may have $y^* < R_B/R_0$ and coarsening may occur.

We briefly discussed higher excess volume fractions, finding at very high ϕ_{ex} (see figure 10.2) droplet growth to have $\bar{R} \sim t^{1/2}$, as would also typically be found in dry foams without trapped species. However provided grown bubbles do not directly press on one another then the shrunken bubbles cause the number of liquid bubble–bubble interfaces between bubbles to increase as coarsening proceeds, resulting in $\bar{R} \sim t^{1/3}$. The growth rate was also found to be a factor of $\phi_{ex}/(1-\phi_{ex})$ times the equivalent expression for $\phi_{ex} \ll 1$.

Hence we find that when trapped species are present and result in coexisting shrunken bubbles, then unless ϕ_{ex} is sufficiently high that bubbles press on one another, then coarsening is typically more similar to coarsening of dilute emulsions, with $\bar{R} \sim t^{1/3}$ as opposed to dry foams with $\bar{R} \sim t^{1/2}$.

Chapter 11

Conclusions

11.1 Stabilisation Against Ostwald Ripening

Several new results were presented in the quantitative analysis of emulsion stabilisation by trapped species. A rigorous stability condition to prevent coarsening by a diffusive flux of dispersed phase was given (Eq.3.28), which is valid even for emulsions with polydispersity in droplet size and number of trapped species. It was shown that even if the trapped species is slightly soluble, a condition to prevent coarsening by a flux of the more soluble species will continue to exist (Eq.3.33). A previously published [12] condition for emulsion stability Eq. 3.7, was shown to correspond to a condition for metastability. Even if satisfying Eq. 3.7, emulsions formed with a fixed concentration of trapped species could require only a minor polydispersity in droplet size to nucleate coarsening: the only reliable criterion for stability is Eq. 3.8. Finally it was noted that similar stability conditions may be calculated for non–ideal trapped species, and merely requires the determination of V_B using the new trapped species equation of state.

Hence further work on stabilisation of dilute foams and emulsions may now focus on determining the coexistence size V_B for various non–ideal trapped species, be

they within the drop, on the droplets surface, or even forming a gel network. Perhaps more interesting would be to study the phase diagram of droplets/bubbles containing more exotic trapped species; such a diagram may for example indicate possibilities of stable bimodal distributions (eg an elastic membrane which limits growth, and a trapped species preventing shrinkage).

Turning to the case of foams, we gave careful arguments and emphasised existing experimental results which suggest that bubble pressures in sufficiently compressed and monodisperse foam may be written as $P_i = P + \Pi + P_i^G$, with $P_i^G \sim \sigma/R_i$. Since a bulk gas has $P_b = P + \Pi$, then the stabilisation of such a foam requires bubbles to have $P_i^T \geq P_i^G \sim \sigma/R_i$. So the pressure of trapped species required to stabilise a foam is of order σ/R_i as opposed to the much higher Laplace pressure across films at the Plateau borders σ/r_i. This indicates that the requirements for stabilisation are approximately independent of the osmotic pressure Π, instead primarily determined by bubble size as for dilute foams and emulsions. These results are confirmed for a model of monodisperse 2D foam, for which the ratio of P^G for an entirely dry foam and an entirely dilute foam is merely 1.05. Hence the required stability conditions Eqs. 9.16 and 9.22 are extremely similar, with N^{sB} for dilute bubbles having a prefactor of $1/\pi$ compared with a prefactor of $1/2\sqrt{3}$ for entirely dry bubbles. So for the monodisperse 2D model, the maximum number of soluble molecules in stable bubbles N^{sB} is never less than 90% of that for the entirely dilute foam, regardless of the magnitude of Π.

We note also the extra stabilisation mechanism due to the elastic energy of bubble deformations which is required if bubbles are unable to easily rearrange. Such elastic energies need not exist in foams without trapped species since such foams may coarsen by exchange of volume and bubble disappearance alone. In the absence of bubble rearrangements it was demonstrated in chapter 10 that a foam will be stable. When there is a finite yield strain above which rearrangements

occur, then the system's stability was shown to be determined by the systems yield strain y^*, and the grown bubbles' sizes (taken to be of order R_0). As a rough estimate, if $y^* > R_B/R_0$ then the foam will be stable, but if $y^* < R_B/R_0$ then coarsening may occur.

Finally we note that the results in chapter 3 for the dependence of bubbles' pressures on osmotic pressure Π apply equally to non–dilute emulsions, as does the requirement for coexistence with a bulk gas, that $P_i^G = P_i^T$. Hence the requirements for stability calculated and discussed in chapter 9 also apply to osmotically compressed emulsions.

11.2 Coarsening of Foams and Emulsions

It was found that the coarsening of dilute, insufficiently stabilised emulsions and foams would proceed as when no trapped species were present, but with a reduction in the volume fraction of the growing bubbles due to the volume fraction now residing in coexisting shrunken droplets. This was surprising since coexisting bubbles continue to shrink as coarsening proceeds, and hence continue to supply material to growing bubbles; however the quantity of material they supplied was found to be negligible. As a corollary the calculations also reconfirmed the stability requirement Eq. 3.28, found by an alternate method in chapter 9.

Order of magnitude calculations were given for the coarsening of non–dilute incompressible foams. It was found that at low excess volume fractions coarsening could be "viscous limited" with $\bar{R} \sim t$, and "diffusion limited" with $\bar{R} \sim t^{1/3}$. However at room temperature and atmospheric pressure, viscous limited coarsening requires a combination of sufficiently small bubble sizes, low liquid volume fraction, and high liquid viscosity, which will be difficult to realise and hence uncommon. In general at room temperature and atmospheric pressure it was found

that unless bubbles directly impinge on one another, then coarsening will typically occur with $\bar{R} \sim t^{1/3}$. This was surprising since non–dilute foams without trapped species generally coarsen with $\bar{R} \sim t^{1/2}$, where as $\bar{R} \sim t^{1/3}$ is typically observed in dilute emulsions. Viscous limited coarsening is most likely to be observed in low pressure/high temperature systems, in which the increased volume per gas molecule in bubbles $v_g = kT/\tilde{P}$, requires a much greater displacement of fluid (and hence dissipation), for a given flux of gas.

The coarsening of insufficiently stabilised non–dilute foams is likely to result in many interesting foam morphologies. This would be interesting to investigate both experimentally and by computer simulations, and may help to clarify previous questions regarding whether or not a foam can always be stabilised.

11.3 Effect of Micelles

It was shown that whether micelles may significantly affect emulsion behaviour is determined by the type of micelle (surfactant and co–surfactant), the type of oil, and the mechanism by which solubilisation occurs. Micelles can destabilise an osmotically stabilised emulsion, but not *necessarily* any more rapidly than would normally occur by a slow flux of the small quantity of trapped species which in practice dissolves in the continuous phase.

Further work is required to indicate the mechanisms by which solubilisation occurs, how oil becomes solubilised within micelles and the resulting distribution of micelle compositions, and how the above are affected by different types of oil, surfactant and co–surfactant. These questions are relevant not only to emulsions, but to detergency, biological mechanisms, and selective adsorption of oils for example. Work is also required to investigate whether similar effects may be observed for molecules which may bind to disperse phase molecules and subse-

quently transport them between droplets.

11.4 Possible Applications

A common characteristic of the results in this thesis is their potential applicability. The work on stabilisation of emulsions and foams provides exact and approximate criterion respectively, for the formulation of stable emulsions and foams. Such work is relevant to the formulation of stable fluorocarbon blood substitutes [43] and stable beer foam [68, 69], for example. Although such specific results are of direct interest in themselves, it it the understanding of the physical mechanisms behind the results which are of more importance.

For example, the understanding that an osmotic pressure of trapped species could counteract the effects of surface tension led to the suggestions in chapter 5 of novel methods for reversing the coarsening process, and for shrinking emulsion droplets to form "miniemulsions". Similarly the work of chapter 10 suggests that a rapid compression of a dilute partially coarsened foam (or equivalently emulsion), could in the absence of bubble rearrangements lead to the formation of a stable foam.

Since the microscopic mechanisms by which micelles may solubilise and transport molecules between droplets is currently not well understood, chapter 6 provides few specific results. However the work is able to indicate the relationship between rate limiting processes and coarsening behaviour, and should enable further work to be carefully focused.

Given a better understanding of the above topics it is possible to speculate on some further applications. For example, a better understanding of micelles could lead to novel applications such as using micelles to tune the rate of drug delivery from multiple emulsions, for selective solubilisation of oils and molecules, or for selective exchange of molecules between droplets, cells, or vesicles stabilised by

certain surfactants or containing certain molecules. Similarly it is also possible to suggest how osmotic effects may be used for the controlled formation of multiple emulsions by swelling preformed vesicles, or conversely for the controlled formation of vesicles by shrinking multiple emulsion droplets (which could also result in complex multi–compartment vesicles, or "microfoams").

Appendix A

Table of Notation

Ch. 2: Emulsions

R,V	Radius R and volume V of a droplet.
f_b	Local part of the Helmholtz free energy per molecule in bulk disperse phase, due to local molecular interactions and properties.
σ	Surface tension
$f(R,\eta)$	Free energy of a droplet of radius R containing η trapped species.
F	Helmholtz free energy of an emulsion.
F_c	Helmholtz free energy of the continuous phase of an emulsion.
P	Pressure within a droplet. In later chapters on Foams, P becomes the atmospheric pressure, and P_i the pressure within a bubble.
P_b	Pressure in a bulk quantity of disperse phase.
μ	Chemical potential of a droplet.
μ_b	Chemical potential of a bulk quantity of disperse phase.
v_b	Volume per molecule of bulk disperse phase.
$\Delta\mu$	$\equiv \mu - \mu_b$.

η	Number of trapped species in a droplet.
v_b^η	Volume per molecule of trapped species.
k	Boltzmanns constant.
T	Temperature.
R_i,V_i,η_i	Radius, volume, and number of trapped species in the ith droplet.
C	Concentration of dissolved disperse phase.
μ_c	Chemical potential of dissolved disperse phase.
μ_{c0}	A reference value for the chemical potential of dissolved disperse phase.
$C(\infty)$	Concentration of dissolved disperse phase adjacent to a bulk phase.
$C(R)$	Concentration of dissolved disperse phase adjacent to a droplet of radius R.
$c(r)$	Concentration of dissolved disperse phase at a distance r from a droplets centre. So $c(r)$ is spatially dependent, unlike C, $C(\infty)$, and $C(R)$.
$\bar{c}$	Average concentration of dissolved disperse phase.
ϵ	$\equiv \frac{\bar{c}-C(\infty)}{C(\infty)}$.
D	Diffusion constant of dissolved disperse phase.
R_ϵ	$\equiv \frac{2\sigma v_b}{\epsilon kT}$.
R_B	$\equiv \left(\frac{3\eta kT}{8\pi\sigma}\right)^{1/2}$.
R',t',R'_B	Dimensionless variables for dimensionless droplet growth rate. They are defined as $R' \equiv RkT/(2\sigma v_b)$, $t' \equiv tDC(\infty)k^2T^2/(4v_b\sigma^2)$, and $R'_B \equiv 3\eta k^3T^3/(32\pi\sigma^3 v_b^2)$.
$U(R',\epsilon)$	Dimensionless droplet growth rate.

Ch. 3: Formation of Stable Emulsions

$n(V)$	Number density of droplets of volume V.
f'	Free energy of a droplet, in which the constant and linear terms in V have been removed.
F'	Free energy density of an emulsion, in which the linear and constant terms in V have been removed.
n_0	Initial number density of droplets.
ϕ	Volume fraction of disperse phase.
$\overline{V}$	Average droplet volume.
λ	Compositional variable used in an analogy with binary phase equilibrium.
$v(\lambda)$	Volume of phase with composition λ.
V_B,R_B	Volume and radius of a droplet (containing trapped species), at which it will coexist with a bulk phase.
V_S,R_S	Volume and radius at the spinodal point of f'. Is also the size at which the chemical potential of a droplet containing ideal trapped species is a maximum.
R_0	Initial droplet radius.
R_C	Critical size above which a droplet will become unstable and start to grow.
$\Delta\mu_R$	Chemical potential difference between a single large drop and a bulk phase.
$\Delta\mu_r$	Chemical potential difference between monodisperse, metastable small drops, and a bulk phase.
R_{0B}	Size at which smaller metastable–drops may coexist with a bulk phase.
R_{0S}	Spinodal size of the metastable smaller drops.
η_R	Number of trapped species in the single larger drop of radius R.
Λ	$\equiv R_0 - R_{0S}$.

c_t	Initial concentration of trapped species in disperse phase.
n_s	Number density of shrunken drops in the "stable" part of the droplet size distribution.
n_c	Number density of drops in the "coarsening" part of the droplet size distribution.
$\overline{V}_c$	The average volume of droplets in the coarsening part of the droplet size distibution.
$p(\eta)$	Probability of having η trapped molecules in a bubble.
$f_t(V,\eta)$	Free energy of η trapped molecules in a droplet of volume V.
η_1,η_2,..	Number of trapped molecules of species 1,2,..
$\overline{\eta}(t)$	Average number of trapped species in droplets at time t.

Ch. 4: Coarsening of Unstable Emulsions

$R_T(t)$	Radius with which shrunken droplets coexist with coarsening droplets, defined by the smaller root of $U(R,\epsilon)=0$.
$R_L(t)$	The typical radius of droplets in the coarsening part of the droplet size distribution which is of order $1/\epsilon$, and defined by the larger root of $U(R,\epsilon)=0$.
n_T,n_L	Number densities of droplets with radii of order R_T and R_L respectively.
f_T,A_T	f_T is a scaling function with order of magnitude 1, and A_T is the amplitude required for $A_T f_T = n_T$.
f_L,A_L	f_L is a scaling function with order of magnitude 1, and A_L is the amplitude required for $A_L f_L = n_L$.
Z_T,Z_L	$Z_T \equiv R/R_T$, and $Z_L \equiv R/R_L$.
B_{0T}	$\equiv \int_0^\infty f_T Z_T^3 dZ_T / C(\infty) v_b$.
B_{0L}	$\equiv \int_0^\infty f_L Z_L^3 dZ_L / C(\infty) v_b$.
$\delta(Z_T-1)$	Dirac delta function, non–zero at $Z_T=1$.
K_1	$\equiv (\epsilon_0 - n_0(4\pi/3)R_B^3/C(\infty)v_b)/(4\pi/3)B_{0L}$
K_2	$\equiv (1+(3R_B/2)(4\pi/3)R_B^3/C(\infty)v_b)/(4\pi/3)B_{0L}$
$\delta(R-R_T)$	Dirac delta function, non–zero at $R=R_T$.

Ch. 5: Applications of Osmotic Stabilisation

c_M	Molar concentration of trapped species.
R_G	Ideal gas constant.

Ch. 6: Effects of Micelles on Emulsion Stability

$V_m(R)$	Volume of oil solubilised within a micelle in equilibrium with a droplet of radius R.
$S_m(R)$	Number of surfactant molecules in a micelle in equilibrium with a droplet of radius R.
$n_m(r)$	Number density of micelles at a distance r from a given droplets center.
$\overline{n}_m(t)$	Average number density of micelles at time t.
J_{in}	Flux of micelles towards a given droplet per unit time.
J_{out}	Flux of micelles away from a given droplet per unit time.
$\overline{S}_m(t)$	Average number of surfactant molecules per micelle at time t.
$\overline{V}_m(t)$	Average volume of solubilised oil per micelle at time t.
D_m	Diffusion constant of micelles.
$n(R,t)$	Number density of droplets of radius R at time t.
n_0	Total droplet number density.
$\phi_m(R)$	Volume fraction of oil solubilised in micelles adjacent to (and in equilibrium with), a droplet of radius R.
$\overline{\phi}_m(t)$	Average volume fraction of oil solubilised within micelles at time t.
ϕ_m^b	Volume fraction of oil solubilised in micelles in equilibrium with bulk oil.
ϕ_{sol}^b	$\equiv v_b C(\infty)$, (Volume fraction of dissolved oil in equilibrium with bulk oil).
ϕ_0	Total volume fraction of oil in the system (including that in emulsion droplets and that in micelles).

α	Typically of order 1, α determines the extent to which micelles swell/shrink to solubilise more/less oil as a result of small changes in the oil's chemical potential. The exact value of α is determined by the type of oil, surfactant, and co–surfactant in the system.
β	$\equiv D\phi^b_{sol}/D_m\phi^b_m$.
$\overline{n}^e_m$	Average number of "empty" micelles (containing no oil).
x	$\equiv \overline{\phi}_m/\phi_0$
x_0	$\equiv \phi^b_m/\phi_0$
$\mathcal{K}$	$\mathcal{K} \equiv R^2(0)/3\phi^b_m D_m$ for diffusion–limited solubilisation, and $\mathcal{K} \equiv (\delta_b/\chi R(0))(R^2(0)/3\phi^b_m D_m)$ for reaction limited solubilisation.
t_{sol}	Time for micelles to solubilise *all* the oil (where possible).
t_{relax}	Time for the micelle diffusion field to relax.
$E[S_m, O_m, n]$	Rate of change in the number of micelles with S_m surfactant molecules and O_m oil molecules, by exchange of molecules between micelles.
$n_m(S_m, O_m, \vec{r}, t)$	Number density distribution for micelles with S_m surfactant molecules and O_m oil molecules, at position $\vec{r}$ relative to a droplet's center, at time t.
$n_S(\vec{r}, t)$	Number density of surfactant molecules at position $\vec{r}$ relative to a droplet's center, at time t.
$n_O(\vec{r}, t)$	Number density of oil molecules at position $\vec{r}$ relative to a droplet's center, at time t.
$n^{eq}_m(S_m, O_m, n_S, n_O)$	Equilibrium number density distribution for micelles with S_m surfactant molecules and O_m oil molecules, for given number densities of oil and surfactant molecules.
$\tilde{n}^{eq}_m(n_S, n_O)$	Total number of micelles in an equilibrium micelle distribution, given number densities of n_S surfactant and n_O oil molecules.

D_{SS},D_{SO},	Effective diffusion constants for oil and surfactant flux.
D_{SO},D_{OO}	(Required to describe oil and surfactant flux when there's molecular exchange between micelles.)
$f_{S,O}$	Distribution functions for the number of oil and surfactant molecules in micelles, of order of magnitude of 1. (Dependent on the number densities of oil and surfactant molecules.)
$\vec{J}_S$	Surfactant flux rate.
$\vec{J}_O$	Oil flux rate.
δ_b	Thickness of diffusion layer. (Through which micelles must diffuse to interact with a droplet).
χ	Fraction of encounters with which a micelle *reacts* with a droplet to exchange oil and/or surfactant.

Ch. 7: Foams

P_i	Pressure of gas in bubble i.
P_i^s	Pressure of soluble gas in bubble i.
P_i^T	Pressure of trapped gas in bubble i.
P	Atmospheric pressure. (Previously P was the pressure within an emulsion droplet).
T	Temperature.
k	Boltzmanns constant.
G	Gibbs free energy of a dilute foam.
F_c	Helmholtz free energy of continuous phase in a dilute foam.
F_i	Helmholtz free energy of gas in the ith bubble.
F_i^s	Helmholtz free energy of soluble gas in the ith bubble.
F_i^T	Helmholtz free energy of trapped gas in the ith bubble.
A_i, V_i	Surface area and volume of the ith bubble.
V_c	Volume of continuous phase in a dilute foam.
σ	Surface tension.
G_i	The ith bubble's contribution to the Gibbs free energy.
G_d	$\equiv \sum_i G_i$. The total contribution of bubbles' free energies to the systems free energy.
N_b^s	Number of soluble molecules in bulk disperse phase.
V_b	Volume of bulk disperse phase.
f_b	*Local* contribution to the Helmholtz free energy per molecule in a bulk gas, due to molecular properties of the gas.
v_b	$\equiv h^2/2\pi mkT$ and is of order of a molecular volume, with h Plancks constant, m the molecular mass (of a gas molecule), and T the temperature.
F_b^s	Helmholtz free energy of a bulk quantity of soluble gas.
f_b^s, f_b^T	f_b, but for soluble and trapped gas respectively.
v_b^s, v_b^T	v_b, but for soluble and trapped gas respectively.

P_b^s Pressure of soluble gas in a bulk gas phase (which since a bulk gas formed by coarsening will have a negligible concentration of trapped species, equals the pressure of the bulk gas phase).

μ_b Chemical potential of bulk gas.

F_i^s Helmholtz free energy of soluble gas molecules in the ith bubble.

F_i^T Helmholtz free energy of trapped gas molecules in the ith bubble.

N_i^s Number of soluble gas molecules in the ith bubble.

N_i^T Number of trapped gas molecules in the ith bubble.

μ_i Chemical potential of the ith bubble.

P_i^G "Geometric" pressure of the ith bubble, analogous to the Laplace pressure of a spherical bubble (see main text for details).

f_i^s, f_i^T *Local* contribution to the Helmholtz free energy per molecule of soluble and trapped gas respectively, due to molecular properties of the gases.

$\Delta\mu_i$ $\equiv \mu_i - \mu_b$.

v_i $\equiv V_i/(N_i^s + N_i^T)$, average volume per gas molecule in bubble i. (Gases are considered to be ideal gases).

Ch. 8: Non–Dilute Foams

Π Osmotic pressure, applied so that foam bubbles press against one another and become distorted from their previously spherical shape.

$\tilde{P}$ $\equiv P + \Pi$.

N_M Total number of moles of gas in the foam.

R_G The ideal gas constant.

ΔP_{ij} $\equiv P_i - P_j$.

A_l^{sys} Total area of liquid in a 2D foam.

L^{sys} Total interfacial length in a 2D foam.

A_i^{sys} Total area of bubbles in a 2D foam.

A_{li} Area of liquid associated with the ith bubble.

A_l A_{li} in a monodisperse foam.

A_i, L_i Area and interfacial length of the ith bubble.

A, L Area and interfacial length of bubbles in a monodisperse foam.

l Length of the flat bubble–bubble interface in a monodisperse 2D foam.

r_i Radius of curvature at the ith bubbles Plateau border.

r Radius of curvature at a Plateau border in a monodisperse system.

A_{pb} Area of liquid at a Plateau border in the model of a monodisperse 2D foam.

$l_i^{P_i}$ The projection of a 2D bubble face onto the horizontal axis (not including the portion of bubble face residing at the bubble's Plateau borders.

l_i^P The projection of a 2D bubble's Plateau borders onto the horizontal axis.

$\mathcal{D}$ The dimension of the foam.

Γ_i Defined by $\Gamma_i \sigma V_i^{-1/\mathcal{D}} \equiv P_i^G$, and expected to be of order 1 for sufficiently compressed and monodisperse foams.

Ch. 9: Stabilisation of Foams

V_i^B Volume with which bubble i will coexist with a bulk gas phase.

A_i^B Area with which bubble i (for 2D foams) will coexist with a bulk gas phase.

R_i^B Radius with which bubble i will coexist with a bulk gas phase.

N_i^{sB} Number of soluble gas molecules in bubble i, when it is coexisting with a bulk gas phase.

n_b^0 Number density of bubbles in the system.

n_b^S Number density of bubbles in the stable shrunken–bubbles.

n_b^C Number density of bubbles in the coarsening bubbles.

$\bar{N}^{s0}$ Average number of soluble molecules in bubbles (which is constant).

$\bar{\Gamma}_c$ Postulated value to which $\bar{\Gamma}$ may tend towards.

$\bar{\Gamma}_{max}$ Postulated maximum value of $\bar{\Gamma}$.

Ch. 10: Coarsening of Unstable Foams

r	Distance from the center of a grown bubble.
$P^s(r,t)$	Average pressure of soluble gas in shrunken bubbles at distance r from the center of a grown bubble, at time t.
R_B	Radius of shrunken bubbles.
$\vec{J}_V$	Volume flux of soluble gas from bubbles at r to bubbles at $(r+R_B)$.
K	A diffusion constant defined in a way analogous to the diffusion constant defined by Von Neumann in deriving his droplet growth rate for dry 2D foams. Has units of length per unit pressure. (See text for details and references).
ϵ	$\equiv (P^s(\infty,t)-\tilde{P})/\tilde{P}$.
$\vec{u}(\vec{r})$	The average velocity of dissolved disperse phase at position $\vec{r}$ relative to the center of a droplet.
$u_r(r)$	The solution in spherical coordinates for the radial component of $\vec{u}(\vec{r})$ relative to the center of a droplet.
$c(r)$	The concentration of dissolved disperse phase at distance r from the center of a bubble.
ζ	Coeffecient of viscous drag.
$\dot{S}$	Rate of change of entropy.
d	Distance between adjacent bubble faces.
η	Continuous–phase liquid's viscosity.
$\dot{S}_{DL}$	Rate of change of entropy when coarsening is "diffusion limited".
$\dot{S}_{VL}$	Rate of change of entropy when coarsening is "viscous limited".
C_M	Molar concentration of gas in bubbles.
v_{Mg}	Molar volume of gas in bubbles.
r_0	Initial distance from the centre of a grown bubble.
$\Delta u(r_0)$	Distance moved by a layer of bubbles initially at r_0, due to a larger bubble growing or shrinking.

R_0	Initial radius of a grown bubble.
ΔR	$\equiv R - R_0$.
$H(r_0)$	Extension or contraction of a layer of bubbles initially at r_0.
$\Delta E_1(H)$	Change in energy of a shrunken bubble due to an extension or contraction by H.
ΔE	Change in energy of the sea of shrunken bubbles, due to a larger bubble growing or shrinking.
y^*	Maximum yield strain.
H^*	Maximum extension/contraction before rearrangments occur.
r_o^*	Radius within which rearrangements occur.
R^{*+}	Radius *above* which a droplet must grow, before a plastic region is nucleated.
R^{*-}	Radius *below* which a droplet must grow, before a plastic region is nucleated.
d'	The typical distance between grown bubbles is given by d', and d'/R_B gives the typical number of shrunken bubbles between two grown bubbles.

Appendix B

Solubilisation of Oil by Non–Ionic Micelles

A number of papers authored and co–authored by B.J. Carroll [56–60], studied the solubilisation of oil by nonionic surfactants. They used a drop–on–fibre technique [56], to study the rate of solubilisation of the drop and how it was affected by the temperature, oil composition and surfactant concentration.

The drop–on–fibre technique [56], studies the time evolution of a droplet on a fibre, by measuring how the distance between the droplets surface which is furthest from the fibre, varies in time.

Above the CMC it was found that the rate of solubilisation was proportional to the concentration of surfactant, and hence (since the concentration is above the CMC), the concentration of micelles. Measurements of how the rate varied with temperature were found to be linear on an Arrhenius plot (log(rate) vs. $1/T$), suggesting a reaction limited mechanism. Since the rate was proportional to the concentration of micelles, the rate limiting step would appear to be the solubilisation of oil into micelles. The Arrhenius plots gave the same activation energies for different types of oil (typically C_nH_{2n}; $n = 8 - 16$), suggesting that

the oil is incorporated directly into micelles without passing through the continuous phase (since differing oil solubility would result in differing rates). Hence Carroll et al [56–60] proposed an adsorption/budding mechanism where oil is solubilised by the budding of oil swollen micelles from the O/W droplet interface. Since the rate of solubilisation was proportional to the concentration of micelles, the rate limiting step was taken to be the supply of surfactant to the O/W interface (as opposed to the rate of budding of oil swollen micelles). Assuming that only surfactant monomers are able to adsorb at an O/W interface, Carroll et al [56–60] concluded that the rate limiting step must be the dissociation of micelles to provide extra surfactant monomers and replenish the O/W interface with surfactant. The rate limiting step being micelle dissociation, is consistent both with the rate being proportional to surfactant concentration, and their observation of a divergent increase in the solubilisation rate close to the surfactants cloud point temperature.

To summarise, Carroll et al [56–60] concluded that in the systems they studied, the solubilisation of oil by non–ionic surfactants (typically $C_{12}E_{5/6}$), was a reaction limited process, with the rate limiting step being the dissociation of micelles to replenish the O/W interface with surfactant monomers.

Although the mechanism suggested by Carroll et al appears consistent, a simpler one would be that solubilisation is a reaction limited process in which oil adsorption resulted from sufficiently energetic collisions of micelles with a droplets surface (mechanism 3 in Section 6.2). This would result in a reaction limited process with a linear behaviour on an Arrhenius plot, and also would predict an increased solubilisation rate proportional to the micelle concentration due to the increased frequency of micelle collisions with a droplets surface. Hence the work of Carroll et al provides evidence for mechanism 3 described in Section 6.2.

Appendix C

Geometry of Monodisperse, 2D Bubbles

The area of the hexagon is six times the area of the equilateral triangles of which it is composed (see figure C.1). The area of each triangle is $(l/2)h$, with

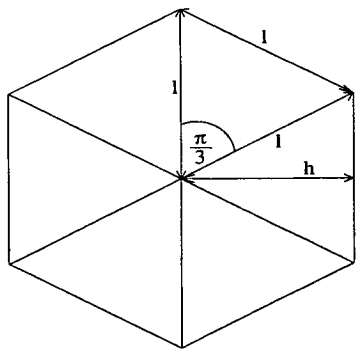

Figure C.1: Hexagonal foam bubble of side length l.

$h = l\sin(\pi/3)$, since each triangle has interior angles of $\pi/3$. Hence noting that $\sin(\pi/3) = \sqrt{3}/2$, we obtain the area of a hexagon as

$$A = \frac{3\sqrt{3}}{2}l^2 \tag{C.1}$$

Its interfacial length is simply given by

$$L = 6l \tag{C.2}$$

We describe a nearly hexagonal bubble in terms of the length of the flattened faces l, and the radius of curvature of the plateau border r (see figure C.2). Then

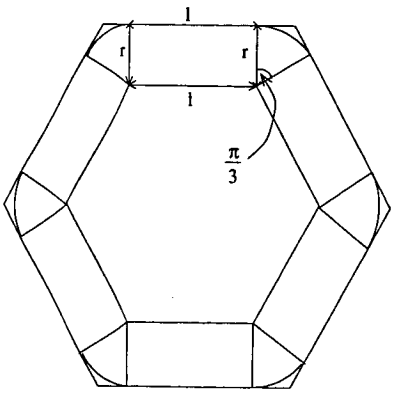

Figure C.2: Nearly hexagonal foam bubble with flat sides of length l, and radii of curvature r.

the area of a nearly hexagonal bubble is given by the sum of six sections of a circle, each of angle $\pi/3$ and radius r, plus six rectangles of length l and height r, plus the area of a hexagon of side length l. So a nearly hexagonal bubbles area is given by

$$A = \pi r^2 + 6lr + \frac{3\sqrt{3}}{2}l^2 \tag{C.3}$$

and its surface length by

$$L = 6l + 2\pi r \tag{C.4}$$

Appendix D

Osmotic Pressure: Princen's Calculation

The osmotic pressure of monodisperse, cylindrical emulsion droplets was calculated by Princen. Princen calculated the osmotic pressure firstly by considering the requirements for the semipermeable membrane to be in equilibrium, with the forces acting from above and below the membrane balanced; then later by considering the increase in interfacial energy as continuous phase is removed [78,79].

For the monodisperse, cylindrical emulsion droplets Princen found

$$\Pi = \frac{\sigma}{R}\left(\frac{\phi}{\phi_0}\right)^{1/2}\left[\left(\frac{1-\phi_0}{1-\phi}\right)^{1/2} - 1\right] \tag{D.1}$$

with ϕ the volume fraction of emulsion droplets, ϕ_0 the volume fraction of close packed emulsion droplets, and R the radius of a close packed cylindrical emulsion droplet. The removal of liquid at fixed droplet length results in the droplets cross section (perpendicular to its length), becoming increasingly hexagonal in shape. Hence the osmotic pressure calculated by Princen should equal that calculated in Section 8.4.2.

Buzza and Cates [80] noted that

$$\frac{a}{R} = \frac{2}{\sqrt{3}} \left(\frac{\phi_0}{\phi} \right)^{1/2} \tag{D.2}$$

and

$$\frac{r}{R} = \left(\frac{\phi_0}{1-\phi_0} \right)^{1/2} \left(\frac{1-\phi}{\phi} \right)^{1/2} \tag{D.3}$$

with a and r as in figure D.1. Using Eqs. D.2, D.3, and D.1 we obtain

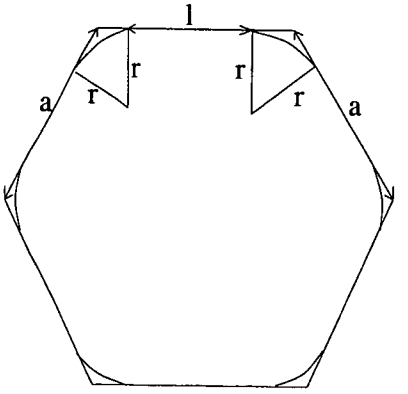

Figure D.1: The lengths a, r, and l, are as shown in the above diagram.

$$\Pi = \frac{\sigma}{r} - \frac{2\sigma}{\sqrt{3}a} \tag{D.4}$$

So noting that $a = l + 2r/\sqrt{3}$ we obtain

$$\Pi = \frac{\sigma}{r} - \frac{6\sigma}{6r + 3\sqrt{3}l} \tag{D.5}$$

So Eq. 8.17 gives

$$\Pi = \frac{\sigma}{r} - P^G \tag{D.6}$$

as in Section 8.4.2.

Appendix E

Slightly Soluble 'Trapped' Species

If we consider the previously trapped species as being slightly soluble, then conservation of bubble number is slowly violated*. Eq. 9.5 must then be generalised to

$$n_b(t) = n_b^S(t) + n_b^C(t) \tag{E.1}$$

with Eq. 9.7 becoming

$$n_b(0)\bar{N}^{s0} - n_b(t)\bar{N}^{sB}(t) = n_b^C(t)\left(\bar{N}^{sC}(t) - \bar{N}^{sB}(t)\right) \tag{E.2}$$

So stability is ensured if

$$n_b(0)\bar{N}^{s0} - n_b(t)\bar{N}^{sB}(t) \leq 0 \tag{E.3}$$

an expression equivalent to the requirement that

$$\bar{N}^{s0} - \frac{n_b(t)}{n_b(0)}\bar{N}^{sB}(t) \leq 0 \tag{E.4}$$

Since the total number of previously 'trapped' species is also conserved, we have

$$n_b(0)\bar{N}^T(0) = n_b(t)\bar{N}^T(t) \tag{E.5}$$

*The derivation in this section is closely related to that given in chapter 3.9.

where $\bar{N}^T(t) = \langle N_i^T(t) \rangle_i$, and is the average number of the (previously) 'trapped' species in bubbles at time t (where we again neglect any of the previously 'trapped' species which may dissolve in the continuous phase). So Eq. E.4 may be rewritten as

$$\bar{N}^{s0} - \bar{N}^T(0)\frac{\bar{N}^{sB}(t)}{\bar{N}^T(t)} \leq 0 \tag{E.6}$$

We define

$$N_{max}^{sB}(\bar{N}^T(t)) \equiv \frac{\tilde{P}}{kT}\left(\frac{kT}{\sigma}\right)^{D/(D-1)} \frac{\bar{N}^T(t)^{D/(D-1)}}{\bar{\Gamma}_C^{D/(D-1)}} \tag{E.7}$$

with $\bar{\Gamma}_C$ corresponding to the constant, maximum or initial value ($\bar{\Gamma}(0)$) of $\bar{\Gamma}$, depending on the behaviour of $\bar{\Gamma}$ in the system studied and the corresponding stability condition for entirely trapped species. Noting that for $D \geq 2$ then $\langle N_i^T \rangle^{D/(D-1)} \leq \langle N_i^{T\,D/(D-1)} \rangle$, so that Eq. 9.29 will ensure that

$$N_{max}^{sB}(\bar{N}^T(t)) \leq \bar{N}^{sB}(t) \tag{E.8}$$

Since $\bar{N}^T(t)$ increases in time, and since $N_{max}^{sB}(\bar{N}^T)$ increases faster than linearly with $\bar{N}^T$, then

$$\frac{N_{max}^{sB}(\bar{N}^T(0))}{\bar{N}^T(0)} < \frac{N_{max}^{sB}(\bar{N}^T(t))}{\bar{N}^T(t)} \tag{E.9}$$

so that

$$\bar{N}^{s0} - \bar{N}^T(0)\frac{\bar{N}^{sB}(t)}{\bar{N}^T(t)} \leq \bar{N}^{s0} - \bar{N}^T(0)\frac{N_{max}^{sB}(\bar{N}^T(t))}{\bar{N}^T(t)} < \bar{N}^{s0} - N_{max}^{sB}(\bar{N}^T(0)) \tag{E.10}$$

Hence provided that

$$\bar{N}^{s0} < N_{max}^{sB}(\bar{N}^T(0)) \tag{E.11}$$

then $\bar{N}^{s0} < \bar{N}^T(0)(\bar{N}^{sB}(t)/\bar{N}^T(t))$, so that $n_b^C(t) = 0$, and the distribution will coarsen at the slower rate determined by the less soluble, previously considered 'trapped' species.

Appendix F

Calculating the Diffusion Constant K

We obtain K by first calculating the rate of diffusive flux of gas through a liquid membrane and then comparing it with the corresponding equation using K.

We consider a liquid membrane of thickness d with gas pressures P_1 and P_2 on either side (see figure F.1). The differing pressures result in differing dissolved concentrations of gas in the surface of liquid adjacent to the relevant gas bubble. The dissolved concentration of gas is given by

$$C_1 = C(\infty)e^{\frac{\Delta\mu_1}{kT}} \tag{F.1}$$

where $\Delta\mu_1$ is the difference in chemical potential between gas in bubble 1 and gas in a bulk gas phase, and $C(\infty)$ is the concentration of dissolved gas adjacent to a bulk gas phase. So using $\Delta\mu_1 = kT\ln\left(1+\frac{P_1^G}{\tilde{P}}\right)$ we obtain a concentration difference of

$$C_1 - C_2 = C(\infty)\left(\frac{P_1^G - P_2^G}{\tilde{P}}\right) = C(\infty)\frac{\Delta P_{12}}{\tilde{P}} \tag{F.2}$$

Since we will have a concentration gradient $(C_1 - C_2)/d$, the flux rate per unit

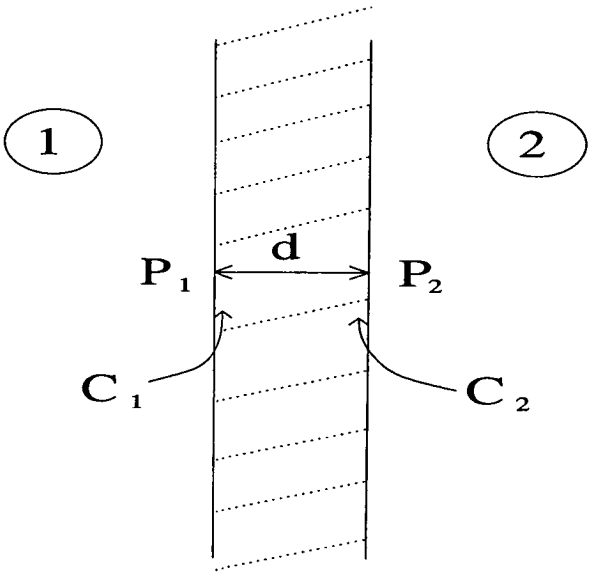

Figure F.1: A liquid interface of thickness d separating bubbles 1 and 2 from one another. Differing pressures in the bubbles will result in differing concentrations of dissolved gas adjacent to the bubble interfaces, resulting in dissolved gas diffusing down any concentration gradients and hence being transferred between bubbles.

area per unit time will be

$$\frac{C_1 - C_2}{d} D = \frac{C(\infty) D}{\tilde{P} d} \Delta P_{12} \tag{F.3}$$

from which we obtain a volume flux per unit area per unit time as

$$K \Delta P_{12} = \frac{v_g C(\infty) D}{\tilde{P} d} \Delta P_{12} \tag{F.4}$$

where v_g is the volume per molecule of gas in the gas phase. Hence we obtain

$$K = \frac{v_g C(\infty) D}{\tilde{P} d} \tag{F.5}$$

Appendix G

Foam Constants

We list here the orders of magnitude for important constants relevant to foam behaviour.

$D \sim 10^{-9}$ m^{2}s^{-1}	Diffusion constant for small molecules in solution [89].
$\sigma \sim 10^{-1}$Nm^{-1}	Surface tension of Water–Air or Water–Oil interface (with surfactant).
$\tilde{P} \sim 10^{5}$Nm^{-2}	Atmospheric pressure [89].
$R \sim 10^{-6} - 10^{-8}$m	Radius of emulsion drops.
$R \sim 10^{-2} - 10^{-7}$m	Radius of foam bubbles.
$kT \sim 10^{-21}$J & $RT \sim 10^{3}$J	Thermal energy [89].
$\eta \sim 10^{-3}$Nsm^{-2}	Viscosity of water [89].
$\rho \sim 10^{3}$kgm^{-3}	Density of water [89].

G.1 Solubility of CO_2

3.3gms of Carbon Dioxide will dissolve in 1000gms of water [89], so since the relative molecular mass of CO_2 is 44, and 1000gms of water is one litre, we have 3.3/44 moles of dissolved CO_2 per litre. Since there are 10^3 litres of water in a m^3 of water we must have $3.3/44 \times 10^3$ moles of dissolved CO_2 in a m^3 of water. Hence we have a molar concentration for CO_2 in water of

$$c_M \sim 0.1 \times 10^3 \sim 10^2 \text{moles m}^{-3} \tag{G.1}$$

G.2 Molar Volume of CO_2 at Atmospheric Pressure

Since $v_g = \frac{V}{N}$ then using the ideal gas law we have $v_g = \frac{V}{N} = \frac{kT}{P}$. So we also have a molar volume $v_{Mg} = \frac{RT}{P}$, which using the values given above gives

$$v_{Mg} \sim \frac{10^3}{10^5} \sim 10^{-2}\text{m}^3 \tag{G.2}$$

Appendix H

Publications

Webster, A.J. ; Cates M.E. "Stabilisation of Emulsions by Trapped Species" *Langmuir* **1998** *14*, 2068-2079.

Webster, A.J. ; Cates M.E. "Coarsening and Osmotic Stabilisation of (Polydisperse) Foams and Dense Emulsions" submitted to *Langmuir* April **2000**

Bibliography

[1] *"Food Emulsions"* ed. Friberg, S.E. ; Larsson, K. **1997** Marcel Dekker, Inc., New York.

[2] Clint, J.H. *"Surfactant Aggregation"* **1992**, Blackie & Son, London.

[3] Ratke, L. *"Low–Gravity Fluid Dynamics and Transport Phenomena"* **1990** p 661. Washington DC: Am. Inst. Aeronaut. Astronaut.

[4] Weaire, D. ; Fortes, M.A. *Advances in Physics* **1994** *43*, 685–738.

[5] Durian, D. J.; Weitz, D. A. *"Foams"*, in Kirk–Othmer Encyclopedia of Chemical Technology, 4th edition, ed. by Kroschwitz, J.I. (Wiley, New York) **1994** *11*, p783–805.

[6] Atkins, P. W. *"Physical Chemistry"* **1994** p973. Oxford : Oxford University Press.

[7] Higuchi, W.I. ; Misra, J. *J. Pharm. Sci.* **1962** *51*, 459.

[8] Hallworth, G.W. ; Carless, J. *"Theory and Practice of Emulsion Technology"* **1976** (A.L. Smith, Ed.), Academic Press, London/New York. p305.

[9] Davis, S.S. ; Smith, A. *"Theory and Practice of Emulsion Technology"* **1976** (A.L. Smith, Ed.), Academic Press, London/New York. p325.

[10] Davis, S.S. ; Round, H.P. ; Purewal, T.S. *J. Coll. Int. Sci.* **1980** *80*, No. 2, 508.

[11] Kabalnov, A.S. ; Pertsov, A.V. ; Shchukin, E.D. *J. Coll. Int. Sci.* **1987** *118*, No. 2, 590.

[12] Kabalnov, A.S. ; Pertsov, A.V. ; Shchukin, E.D. *Colloids. Surf.* **1987** *24*, 19–32.

[13] Kabalnov, A.S. ; Pertsov, A.V. ; Shchukin, E.D. *J. Coll. Int. Sci.* **1989** *138*, No. 1, 98.

[14] Reiss, H. ; Koper, J.M. *J. Phys. Chem.* **1995** *99*, 7837–7844.

[15] Webster, A.J. ; Cates, M.E. *Langmuir* **1998** *14*, 2068–2079.

[16] Webster, A.J. ; Cates, M.E. submitted to *Langmuir* April **2000**.

[17] Ostwald, W. *Z. Phys. Chem.* (leipzig) **1900** *34*, 295.

[18] Thomson, W. (Lord Kelvin), *Proc. Roy. Soc.* (Edinburgh) **1871** *7*, 63.

[19] LaMer, V.K. ; Gruen, R. *Trans. Faraday Soc.* **1952** *48*, 410.

[20] Lifshitz, I.M. ; Slyozov, V.V. *Phys. Chem. Solids.* **1961** *19* 35–50.

[21] Wagner, C. *Z. Elektrochemie* **1961** *65*, 581–591.

[22] Bray, A.J. *J. Adv. Phys.* **1994**, *43*, 357–459.

[23] Voorhees, P.W. *Annu. Rev. Mater. Sci.* **1992**, *22*, 197–215.

[24] Marqusee, J.A. ; Ross, J. *J. Chem. Phys.* **1983** *79*, 373.

[25] Voorhees, P.W. *J. Stat. Phys.* **1985** *38*, 231.

[26] Fradkov, V.E. ; Glicksman, M.E. ; Marsh, S.P. *Phys. Rev. E* **1996** *53*, No. 4, pt B, 3925–3932.

[27] Marsh, S.P. ; Glicksman, M.E. *Acta Materialia* **1996** *44*, No. 9, 3761–3771.

[28] Kabalnov, A *Current Opinion in Colloid & Interface Science* **1998** *3*, p270–275.

[29] Taylor, P. *Adv. Colloid Interface Sci.* **1998** *75*, p107–163.

[30] Kohler, H. *Geofys. Pub. Krestiania* **1921** *1*, 1.

[31] Kohler, H. *Geofys. Pub. Krestiania* **1921** *2*, 6.

[32] Kohler, H. *Nova Acta Refiae Soc. Sci. Ups.* **1950** *14*, 9.

[33] Kulmala, M. ; Laaksonen, A. ; Charlson, R.J.; Korhonen, P. *Nature* **1997** *388*, 336.

[34] Kulmala, M. ; Laaksonen, A. ; Charlson, R.J.; Korhonen, P. preprint: *"Modification of the Kohler equation to include soluble trace gases and slightly soluble substances"*.

[35] Doherty, R.D. *"Encyclopedia of material science and technology"* **1986** *5*, 3354–3355.

[36] Cahn, R.W. ; Haasen, P. ; Kramer, E.J. *"Materials science and technology"* **1992** *7*, Sec. 8.7, 360–367, Sec. 9.4.3, 425–428.

[37] Kuehmann, C.J. ; Voorhees, P.W. *Metall. Trans. A* **1996** *27A*, 937–943.

[38] Buscall, R. ; Davis, S.S. ; Potts, D.C. *Colloid Polym. Sci.* **1979** *257*, 636.

[39] Rowlinson, J.S. ; Widom, B. *"Molecular Theory of Capillarity "* **1989** Oxford University Press, Walton Street, Oxford.

[40] DeHoff, R.T. *"Thermodynamics in Materials Science"*; McGraw Hill: New York, **1992**, p 228.

[41] Kubo, R. *"Statistical Mechanics"*; North–Holland: Amsterdam, **1965**, p 310.

[42] Defay, A. ; Prigogine, I. ; Bellemans, A. ; Everett, D.H. *"Surface Tension and Adsorption"* ; Longmans Green and Co: London, **1966** ; p265.

[43] Kabalnov, A.S.; Shchukin, E.D. *Adv. Coll. Int. Sci.* **1992**, *38*, 69.

[44] The similar effect of *recondensation* of more soluble emulsion droplets onto less soluble droplets, is described by Pertsov, A.; Kabalnov, A.S.; Kumacheva, E.E. *Kolloidnyi Zh.* **1988**, *50*, 616.

[45] Taylor, P.; Ottewill, R.H. *Progr. Colloid Polym.. Sci.* **1994**, *97*, 199.

[46] Coupland, J.N. ; Weiss, J. ; Lovy, A. ; McClements, D.J. ; *Journal of Food Science*, **1996**, *61*, p1114.

[47] McClements, D.J. ; Dungan, S.R. ; German, J.B. ; Kinsella, J.E. *Food Hydrocolloids* **1992** *6*, No. 5, 415–422.

[48] McClements, D.J. ; Dungan, S.R. *J. Phys. Chem.* **1993** *97*, 7304–7308.

[49] McClements, D.J. ; Dungan, S.R. ; German, J.B. ; Kinsella, J.E. *Colloids and Surfaces A* **1993** *81*, 203–210.

[50] McClements, D.J. ; Dungan, S.R. *Colloids and Surfaces A* **1995** *104*, 127–135.

[51] Weiss, J. ; Coupland, J.N. ; McClements, D.J. *J. Phys. Chem.* **1996** *100*, 1066–1071.

[52] Weiss, J. ; Coupland, J.N. ; Brathwaite, D. ; McClements, D.J. *Colloids and Surfaces A* **1997** *121*, 53–60.

[53] Esselink, K. ; Hilbers P.A.J. ; van Os, N.M. ; Smit, B. ; Karaborni, S. *Colloids and Surfaces A: Physiochem. Eng. Aspects* **1994**, *91*, 155–167.

[54] Karaborni, S. ; van Os, N.M. ; Esselink, K. ; Hilbers P.A.J. *Langmuir* **1993**, *9*, 1179–1183.

[55] Granek, R. ; Ball, R.C. ; Cates, M.E. *J.Phys II France* **1993** *3*, pgs 829–849.

[56] Carroll, B.J. *J. Coll. Int. Sci.* **1981** *79*, p126.

[57] Carroll, B.J.; O'Rourke, B.G.C.; Ward, A.J.I. *J. Pharm. Pharmacol.* **1982** *34*, 287–292.

[58] Donegan, A.C.; Ward, A.J.I. ; Carroll, B.J. *J. Pharm. Pharmacol.* **1986** *39*, 45–47.

[59] O'Rourke, B.G.C.; Ward, A.J.I.; Carroll, B.J. *J. Pharm. Pharmacol.* **1987** *39*, 865–870.

[60] Carroll, B.J.; Doyle, P.J. *J. Pharm. Pharmacol.* **1988** *40*, 229–232.

[61] Miller, C.A. ; Raney, H.R. *Colloids Surfaces A: Physicochem. Eng. Aspects* **1993** *74*, pp 169–215.

[62] Kabalnov, A.S. *Langmuir* **1994**, *10*, 680–684.

[63] Cates, M.E.; Marques, C.M.; Bouchaud, J.P. *J. Chem. Phys.* **1991** *94*, pp8529–8536.

[64] McClements, D.J.; Dungan, S.R. *Colloids Surfaces A: Physicochem. Eng. Aspects* **1995** *104*, pp 127–135.

[65] Glazier, J.A. ; Weaire, D. *J. Phys. Condens. Matter* **1992** *4* p1867–1894.

[66] Stavans, J. *Rep. Prog. Phys.* **1993** *56* p733–789.

[67] Falls, A. H.; Lawson, J. B.; Hirasaki, G. J. *J. Pet. Technol.* **1988** p95

[68] Parr, D. *Physics World* **1989** *September*, p21

[69] Bamforth, C. W. *"Food Colloids"* **1989** ed. Bee, R.D.; Richmond, P. ; Mingins, J. (London: Royal Society of Chemistry) p48.

[70] Weaire, D. ; Pageron, V. *Philos. Mag. Lett.* **1990** *62*, No. 2, 417–421.

[71] Gandolfo, F. G. ; Rosano, H. L. *J. Coll. Int. Sci.* **1997** *194* 31–36.

[72] Kabalnov, A.S. ; Weers, J. G. ; Arlauskas, R. A.; Tarara, T. E. *Langmuir* **1995** *11* p2966.

[73] Fortes, M. A. *J. Coll. Int. Sci.* **1995** *176* 248–255.

[74] Forsythe, W.E. *"Smithsonian Physical Tables"*, pub. Smithsonian Institute, **1954**, p358.

[75] *"American Institute of Physics handbook"*, coordinating Ed. Gray, D. E., pub. M^{c}Graw Hill, **1972**, p**4**-304.

[76] Gupta, M.C. *"Statistical Thermodynamics"* **1990** John Wiley & sons.

[77] Princen, H.M. *J. Coll. Int. Sci.* **1979** *71*, No. 1, p55–66.

[78] Princen, H.M. *Langmuir* **1986** *2*, No. 4, p519–524.

[79] Princen, H.M. *Langmuir* **1988** *4*, No. 1, p164–169.

[80] Buzza, D.M.A.; Cates, M.E. *Langmuir* **1993** *9*, 2264–2269.

[81] Radjai, F. ; Wolf, D.E. ; Jean, M. ; Moreau, J–J. *Phys. Rev. Lett.* **1998** *80*, No. 1, 61–64.

[82] Cates, M.E. ; Wittmer, J.P. ; Bouchaud, J–P. ; Claudin, P. *Phys. Rev. Lett.* **1998** *81*, No. 9, 1841–1844.

[83] Glazier, J.A.; Gross, S.P.; Stavans, J. *Phys. Rev. A* **1987** *36*, No. 1, 306–312.

[84] Stavans, J.; Glazier, J.A.; *Phys. Rev. Lett.* **1989** *62*, No. 11, 1318–1321.

[85] Hertdle, T.; Aref, H. *J. Fluid Mech.* **1992** *241*, 233–260.

[86] Durian, D.J.; Weitz, D.A.; Pine, D.J. *Phys. Rev. A* **1991** *44*, No 12, R7902–R7905.

[87] Durian, D.J.; *Current Opinion in Colloid & Interface Science* **1997** *2*, 615–621.

[88] Reif, F. *"Fundamentals of Statistical and Thermal Physics"* **1985** International Edition, McGraw–Hill Co–Singapore, p567.

[89] *"CRC Handbook of Chemistry and Physics"*, 74th edition, **1993** CRC press, inc., Ed. DL Lide.

[90] Pippard, A. B. *"The Elements of Classical Thermodynamics"* **1964** Cambridge University Press, Cambridge, UK. p84.